UNIVERSITY OF SOUTHAMPTON

FACULTY OF SOCIAL, HUMAN AND MATHEMATICAL SCIENCES

Academic Unit of Geography and Environment

Monitoring decadal land cover and crop production in Iraq using time series remote sensing data

by

Sarchil Hama Qader

Thesis for the degree of Philosophy

September 2016

UNIVERSITY OF SOUTHAMPTON

ABSTRACT

FACULTY OF SOCIAL, HUMAN AND MATHEMATICAL SCIENCES

Geography and Environment

Thesis for the degree of Doctor of Philosophy

MONITORING DECADAL LAND COVER AND CROP PRDUCTION IN IRAQ USING TIME SERIES REMOTE SENSING DATA

Sarchil Hama Qader

Iraq contains the Great Mesopotamian alluvial plain of the Euphrates and Tigris rivers. Its regional vegetation phenological patterns are worthy of investigation because relatively little is known about the phenology of semi-arid environments, and because their inter-annual variation is expected to be driven by uncertain rainfall and varied topography. In addition, in Iraq accurate discrimination of different vegetation types using Earth observation data is challenging due to their similar spectral responses and reliable ground information about croplands and natural vegetation in such regions is generally scarce. Furthermore, inter-annual variation in climatic factors (such as rainfall) and anthropogenic factors (such as civil war) pose a major risk to crop production and in turn, food security in Iraq. Therefore, this research aimed to i) assess and map the spatial variation in key land surface phenology (LSP) parameters over the last decade and their relation with elevation, ii) develop a phenology-based classification approach using support vector machines for the assessment of space-time distribution of the dominant vegetation land cover (VLC) types, iii) evaluate the potential of Moderate Resolution Imaging Spectroradiometer MODIS-derived measures of greenness and productivity, and information related to the phenology of crops to estimate crop production and yield in the arid and semi-arid regions like Iraq.

Across all Iraq, a large spatiotemporal variation in the LSP parameters such as start of the season (SOS), end of the season (EOS) and length of the season (LOS) were observed. These variations are explained by the spatial distribution of rainfall and temperature as a function of elevation. A positive coefficient of determination was observed for SOS and EOS with elevation for all major land cover types. In particular, raising the elevation by 500m leads to a delay in EOS by

around 22 or more days in all vegetation types. In addition, the dominant vegetation land cover (VLC) types resulted from the phenology-based classification have a strong similarity with the expected land cover types over the region. The classification approach produced satisfactory classification accuracies (generally > 85%, with relatively high Kappa coefficients >0.86) among the dominant VLC types of Iraq. In terms of regional accuracy assessment and areal agreement with ground crop area data, the VLC classification outperformed the global MODIS land cover dataset. This research also showed that the 2008 drought, the most extreme event during the last decade in Iraq. Despite testing several methodological approaches, it was not possible to forecast crop yield at the governorate level over Iraq, mainly due to ground data quality and a coarse spatial resolution. However, more precise estimates of crop production were possible over the region. The result of the current research implies that the date of the maximum vegetation index (VI) offered the most accurate forecast of crop production. The date of MODIS normalized difference vegetation index (NDVI) was the most accurate predictor of crop production in Iraq with an average R^2=0.70 compared to the date of MODIS enhanced vegetation index (EVI) (Avg R^2=0.68) and a net primary productivity (NPP) (Avg R^2=0.66) using the leave-one-year-out approach. The research indicated that remote sensing indices could characterize and forecast crop production more accurately than simple cropping area, which was treated as a null model or benchmark against which to evaluate the proposed approach. The results also point to the implementation of crop forecasting models in arid and semi-arid environments, which have utility in relation to tackling food insecurity.

Contents

List of Tables

List of Figures

DECLARATION OF AUTHORSHIP

I, Sarchil Qader, declare that this thesis and the work presented in it are my own and has been generated by me as the result of my own original research.

Monitoring decadal land cover and crop production in Iraq using time series remote sensing data

I confirm that:

1. This work was done wholly or mainly while in candidature for a research degree at this University;
2. Where any part of this thesis has previously been submitted for a degree or any other qualification at this University or any other institution, this has been clearly stated;
3. Where I have consulted the published work of others, this is always clearly attributed;
4. Where I have quoted from the work of others, the source is always given. With the exception of such quotations, this thesis is entirely my own work;
5. I have acknowledged all main sources of help;
6. Where the thesis is based on work done by myself jointly with others, I have made clear exactly what was done by others and what I have contributed myself;
7. Parts of this work have been published as:

Qader, S. H., Atkinson, P. M., & Dash, J. (2015). Spatiotemporal variation in the terrestrial vegetation phenology of Iraq and its relation with elevation. International Journal of Applied Earth Observation and Geoinformation, 41, 107-117.

Qader, S. H., Dash, J., & Atkinson, P. M. (2015). Classification of vegetation type in Iraq using satellite-based phenological parameters. IEEE Journal of Selected Topics in Applied Earth Observation and Remote Sensing, 9(1), 414-424.

QADER, S. H., DASH, J. & ATKINSON, P. M. (submitted). Forecasting wheat and barley crop production in arid and semi-arid regions using remotely sensed primary productivity and crop phenology: a case study in Iraq. ISPRS Journal of Photogrammetry and Remote Sensing.

Conference oral Presentations:

Qader, S. H., Dash, J., & Atkinson, P. M. (2014). Crop area estimation in Iraq based on satellite derived phenological metrics and the influence of war and drought. Presented at 20th International Congress of Biometeorology, Cleveland, Ohio, USA.

Qader, S. H., Atkinson, P. M., & Dash, J. (2015). Decadal dominant vegetation land cover classification in Iraq based on satellite derived phenological parameters. Presented at RSPSoc, NCEO and CEOI-ST Joint Annual Conference 2015, Southampton, UK.

Qader, S. H., Atkinson, P. M., & Dash, J. (2015). Analysing the impact of natural and anthropogenic stresses on crop production in Iraq using time series of remote sensing data. Presented at Remote Sensing for Agriculture, Ecosystems, and Hydrology Conference (SPIE Remote Sensing), Toulouse, France.

Signed: .....

Date: .....

Acknowledgements

Firstly, I would like to express my deepest gratitude to the Ministry of Higher Education and Scientific Research-Kurdistan Regional Government (KRG) Human Capacity Development Programme (HCDP), for providing me the scholarship and financial support during my study.

I also would like to express my sincere gratitude to my supervisors: Dr Jadunandan Dash and Professor Peter M. Atkinson, for continuous support of my PhD research, for their motivation, immense knowledge and enthusiasm. Their guidance and cooperation for the past several years are invaluable and expanded my knowledge enormously in the field.

A very special thanks goes out to my family, my father, mother, sisters and brothers for their constant encouragement and support throughout my study to achieve this goal. I would like to thank Julio Pastor, who as a good friend and colleague was always willing to help and give his best suggestion.

Last but not the least; I would like to thank my friends and colleagues at the University of Sulaimani, Faculty of Agriculture Science, Soil and Water Science Department for their facility and support.

Definitions and abbreviations

ASA: Arid and Semi-Arid

AVHRR: Advances Very High Resolution Radiometers

COSIT: Central Organization for Statistics and Information Technology

CPPI: Crop Proportion Phenology Index

DT: Decision Tree

ELLA: Evidence and Lessons from Latin America

EOS: End of Season

ETM^{+}: Enhanced Thematic Mapper Plus

EVI: Enhanced Vegetation Index

FAO: Food Agriculture Organization

FEWSNET: Famine Early Warning System Network

GDP: Gross Domestic Product

GPP: Gross Primary Productivity

GYURI: General Yield Unified References Index

HMM: Hidden Markov Model

IFAD: International Fund for Agriculture Development

IGBP: International Geosphere and Biosphere Programme

LAI: Leaf Area Index

LOS: Length of Season

LP DAAC: Land Processes Distributed Active Archive Centre

LSP: Land Surface Phenology

LULC: Land Use Land Cover

MAE: Mean Absolute Error

MBE: Mean Bias Error

MERIS: Medium-Spectral Resolution, Imaging Spectrometer

MODIS: Moderate Resolution Imaging Spectroradiometer

MOWI: Ministry of Water and Irrigation

MSS: Multispectral Scanner System

NDVI: Normalized Difference Vegetation Index

NDWI: Normalized Difference Water Index

NOAA: National Oceanic and Atmospheric Administration

NPP: Net Primary Productivity

PDSI: Palmer Drought Severity Index

QA: Quality Assurance

RBF: Radial Basis Function

RMSE: Root Mean Square Error

SAFY: Simple Algorithm for Yield Estimation

SOS: Start of Season

SPI: Standard Precipitation Index

SPOT VGT : Satellite Pour l'Observation de la Terre Vegetation

SRTM: Shuttle Radar Topography Mission dataset

STD: Slandered Deviation

SVM: Support Vector Machine

TM: Thematic Mapper

UNDP: United Nations Development Programme

UNEP: United Nations Environment Programme

UNIC: United Nations Information Centre

UNSO: United Nations Statistical Office

USAID: United States Agency International Development

USDA FAS: United States Department of Agriculture Foreign Agriculture Service

VI: Vegetation Index

VLC: Vegetation Land Cover

WDRVI: Wide Dynamic Range Vegetation Index

WFP: World Food Programme

Chapter 1: **Introduction**

Agriculture is the world's largest industry which employs over one billion people and makes more than 1.3 trillion dollars' worth of food annually (WWF 2016). The agricultural sector does not contribute a large part of global gross domestic product (GDP) but it is a vital component due to the fact that around one-third of the world's population gains its livelihood from agriculture with the major part in Asia (FAO, 2013). Agriculture can make on average 29% of the GDP and employs 65% of the labour force on country basis (World Bank, 2008). Global expectations of rising population and demand for food have insisted to look at the global and regional food production seriously. In addition, many economic crises and food insecurities have posed major risk on sustainable food production.

Generally, global agriculture may face several challenges in the future such as providing an extra food for global population growth (global food security), decreasing global poverty rate and sustainable natural resource management. Meeting these challenges will need to generate a set of technologies, wise policy and easy access to international and domestic markets for farmers. The world population is expected to increase to around 9 billion people in 2050 (FAO, 2013). Recent studies have claimed that the world requires 70 to 100% more food by 2050 to meet the growing demand (FAO, 2009a; World Bank, 2008; Royal Society of London, 2009). To cope with these challenges, areas under agriculture was expanded which have been a major driver of deforestation and other decimating habitats, biodiversity and ecological destruction (Millennium Ecosystem Assessment 2005). Therefore, unsustainable farming practice to increase the production could threat the global environment and biodiversity.

War and conflict are among the major drivers of damage to the economy and spread of disease, leading to forced emigration, refugee populations, a collapse of social trust and severe food insecurity (WFP, 2011). In addition, war and political conflicts can affect the land use practices, particularly agriculture in a country and in turn could affect the availability of food grain and food security of a country. Therefore, the evaluation and analysis of the factors which are making a region's food insecure is an important case in the world. For instance, there are more than 870 million people undernourished in (2010-2012) in the world (FAO, 2012). Many reasons are involved into this: which include economic crises, high food price, region of political instability and climate change. In fact, the main factors of more than 35% of food emergencies from 1992 to 2003 were economic

issues and conflict; in contrast, this value was 15% in the period between 1986 and 1991 (FAO, 2003a). However, conflict was the main cause of more than of half of countries were undernourishment in the period of 1990s (FAO, 2003b).

On the other hand, throughout the human history, natural disasters such as drought, floods and storms have played a major role in hindering agriculture growth and economic cost. Since the 1950s, the economic losses by all natural disasters have increased by 14 fold (World Disaster Report, 2001). Drought occurs nearly in all climatic zones and describes as a slow onset natural disaster and creeping phenomenon. Drought has been defined in different ways in respect to different aspects as it affects different part of society in various ways. Tucker and Choudhury (1987), and Wilhite and Glantze (1985) defined drought as a distinct period which receives lower than average precipitation, as a result it has a significant impact on vegetation growth. In addition, agriculture drought take places when there is inadequate soil moisture to meet the needs of a specific crop at a specific time, resulting in crop failure (American Meteorological Society, 2004). It is therefore important to understand the impact of drought on food production to plan for adequate food stock to ensure food security.

Iraq has been established as one of the oldest agricultural countries in the world. For instance, according to Meyers (1997), the village that called Jarmo, situated in Iraqi Kurdistan Region, has been the oldest known agricultural and pastoral community in the world, dated back to the seventh millennium (BCE). Looking into the history indicated that in the past agriculture was the primary economic activity of the people of old Mesopotamia and modern day in Iraq, since the beginning of recorded time. For instance, agriculture played a crucial role in the country's major economic activity in the 1920s, but its contribution the gross domestic product (GDP) fell from 42% in 1981 to 18% in 1990 (Jaradat, 2002). Although agriculture is no longer have a significant contribution of the country's economy, it is a vital component of GDP (Schnepf 2004). This sector declined considerably again during the last few decades due to some unfavourable factors from both natural and anthropogenic impacts. For example, the contribution of agriculture in GDP had dropped from around 9% in 2002 to 4% in 2008 (FAO, 2009) mainly due to drought; however, this value was increased to nearly 12% in 2010 because of some recent policy improvements in this sector (USAID, 2010).

Over last decade, crop production in Iraq has been subjected to a sequence of major turbulences, both natural and anthropogenic leading to push the country toward regional food insecurity. For instance, Iraq had been involved in a war

'Post-Gulf' mainly to oppose the previous regime. Due to the political instability and fear for the life during the war many farmers were unable to grow the crop. In some places, the military activity and building military encampment encroached up on agriculture land. In addition to the war, due to its geographical location, the region is affected by irregularities in precipitation resulting in frequent occurrence of drought (Al-Timimi, and Al-Jiboori). Both these factors made the region vulnerable to sustained food production. Therefore, timely and comprehensive method is highly required to monitor the outcome of those factors on land use/land cover (LULC) changes and crop production during last decade.

Remote sensing has been used widely in both agriculture and agronomy. The monitoring of agricultural activity is challenging due to the very large area that requires repeated coverage; thus, the employment of remote sensing is vital (FAO, 2011). Agricultural production is predictable based on monitoring of the seasonal patterns of the growth phase of crops. Moreover, those seasonal patterns (and, thus, agricultural production) are driven by several factors such as climatic variables, the physical landscape and agricultural management. These factors are subject to large changes in time and space. Therefore, timely agricultural monitoring through the growth season via remote sensing is needed.

Globally there are various applications of remote sensing in the agricultural sector, related to food production, aiming to provide reasonable spatial and temporal data. These applications have been seen in different context like increasing production would be the global challenges of the agriculture sector which may have an impact on the environment. The current study will attempt to use three remote sensing applications in agriculture sector in Iraq. All three applications are aimed to support decision making in order to improve the regional production and improve regional food security. Three different applications have been selected such as land surface phenology, crop mapping and crop area estimation, and yield estimation due to the fact these areas have been subjected to a sequence of major turbulences during last decade, and on the country level they have not been assessed yet. The unreliability of the country's official statistical data (USDA FAS 2008) and difficulties with access to the country due to security problems mean that remote sensing is the only viable method to map the country's land cover types and estimate and forecast crop yield across the country.

In general, phenology has a long tradition in agriculture. The extracted knowledge of the vegetation phenology can be used as a surrogate of climate change (Menzel et al. 2006). The data can be used to accurate identification LULC change, and identifying, mapping and estimating area of various land cover types, particularly crop (Newstrom et al. 1994; Gu at al. 2010; Clerici et al. 2012; Lupo at al. 2007). In addition, crop phenological observation can also play an essential role in process that is relevant to estimate crop yield (Bolton and Friedl, 2013; Funk and Budde, 2009; Sakamoto et al. 2013). Moreover, LSP information can help to improve agricultural management such as fertilization and irrigation through aiming to establish a suitable relationship between the timing of plant growth phases and carbohydrate consumption (Garcia-Tejero et al., 2010; Menke and Trlica 1981; Mooney and Billings, 1960). Therefore, the current study mainly relied on vegetation related phenology information to derive land cover classification and crop production estimation.

This thesis **monitors decadal land cover and crop production in Iraq using time series remote sensing data**. Chapter 1 provided a general introduction of the work that included the importance of agriculture on a broad scale, then looking down into Iraq and why Iraq has been selected for the current study. In addition, the importance of remote sensing to monitor agriculture activity, particularly crop including crop mapping and crop yield forecasting via related vegetation phenology information. Specifically, this work aimed to:

1- Map and assess the spatial variation in key land surface phenology (LSP) parameters across Iraq over the last decade and explore their relation with elevation (as a surrogate of temperature and precipitation).
2- Develop and apply a phenology-based approach for the assessment of dominant vegetation land cover (VLC) types in Iraq, particularly croplands from 2002 to 2012.
3- Evaluate the potential of MODIS-derived measures of greenness and productivity, and information related to the phenology of crops to estimate crop production and yield in the arid and semi-arid regions like Iraq

Chapter 2 will be mainly split into three sections. Section 2.1 will provide a general description of food insecurity. In addition, short introduction of the arid and semi-arid regions in term of climatic, location, crop area, and crop production, in particular the contribution of these regions in the world food production will be highlighted. This section also addresses the food insecurity in

arid and semi-arid regions in the world and why it is important to evaluate these vulnerable regions in term of crop production. Furthermore, the impact of the main drivers such as rainfall, temperature, population growth and conflict on the regional food insecurity in these regions will be explained. Section 2.2 focuses on using remote sensing data for several applications such as classification, crop condition and yield forecasting. This section also discusses different methodological approaches for such applications and validation of the space observation results with *in situ* data. Section 2.3 provides a historical data of wheat and barley in term of harvested area and production in past 50 years in Iraq. Chapter 3 to 5 embody three analysis chapter which will be conducted in three individual papers. Chapter 3 (research paper one) highlights the spatiotemporal variation of dominant vegetation types phenology such as croplands, grasslands and shrublands in Iraq and their relation with elevation. Chapter 4 (research paper two) focuses on using several phenological parameters to develop a phenology-based classification that can derive an accurate vegetation land cover types for Iraq during last decade. In chapter five (research paper three) several remote sensing based methodological approaches will be tested to estimate and forecast crop yield/production at the governorate level using different remotely sensed indices. Chapter 6 provides combine discussion of the research findings for the papers generated in this work and assessing the main uncertainties and variations with several suggestions for the future studies. Final chapter (Chapter 7) highlights the most important conclusions derived from this thesis.

Chapter 2: **Food insecurity in arid to semi-arid regions**

Throughout the history of civilisation, the foremost concern of human societies has been to ensure that people have access to adequate food to survive and, in the present day, to lead a healthy and active life. More than 30 definitions of the term "food security" have been proposed in previous studies (Maxwell and Smith 1992). The most common definition of the term was made by the Food and Agriculture Organization (FAO): "Food security is a situation that exists when all people at all times have physical, social, and economic access to sufficient, safe, nutritious food that meets their dietary needs and food preference for an active and healthy life" (FAO 2001). The definition can be divided into three main components: food availability, food access and food consumption. Availability refers to adequate quantities of food available on a regular basis; access refers to having enough resources to acquire satisfactory foods for a nutritious diet; consumption refers to adequate utilization depended on knowledge of basic nutrition of the food content and the ability of the body to use it effectively. The concept of the food availability will be more explored in the context of estimation methodology and controlling factor in the arid and semi-arid regions.

Food availability is determined by a combination local food production and food imports. The food availability dimension of food security encloses issues of global and regional food supply, and reminds us the simple question whether enough food is available to feed our population efficiently. The import part includes many aids from different aspects, which cannot be measured easily due to constant trade and personal business to import food in various ways in some regions. In addition, these aids are not on a regular basis and mainly occur in a time of natural disasters and catastrophes. Therefore, the local production will be mostly a target of our evaluation due to the fact that in many arid and semi-arid regions, the local food productions can still be accounted as the main source of food.

Grain crops and vegetables are the main component of the home food production. One of the first priorities of the earliest settler's communities arriving in a place to obtain food was crop growing. According to recent FAO statistics, more than 1.5 billion ha (around 12% of the world's total land area) was dedicated to crop production in 2013 (FAO 2013). To meet the basic calorific requirement

of humans per day per capita, requires around 219 kg of grain annually (Palm et al. 2010). “The world now produces enough food to feed its population. The problem is not simply technical. It is a political and social problem. It is a problem of access to food supplies, of distribution, and of entitlement. Above all, it is a problem of political will” (Shaw 2007). Many people in arid and semi-arid regions rely directly on agriculture for their basic source of food, and any negative impacts on crop productivity can lead to overall food shortages at the local level. Therefore, comprehensive information about grain crop production of region or country will lead us to know how the food secure or insecure of that region or country is and provides better base for making policy.

Arid regions can be described as areas where the ratio of mean annual rainfall to mean annual potential evapotranspiration ranges between 0.05 to 0.020 and semi-arid regions as those where the ratio varies between 0.2 and 0.5 (UNEP 1992). Arid regions occur within rainfall zones of 0-300 mm, with inter-annual variability of 50-100%, whereas semi-arid regions occur within rainfall zones 300-600 mm, with inter-annual variability of 25-50% (Barakat 2009; IFAD 2000). Arid and semi-arid regions, situated in the tropical and sub-tropical zones of the world, cover around 30% of the global total land and are inhabited by around 20% of the total world’s population (Sivakumar 2005). At the continental level, arid and semi-arid regions are home to around 23% of the total population of Asia, 24% in Africa, 11% in Europe, 6% in Australia and Oceania, and 17% in the Americas and the Caribbean (UNDP/UNSO 1997). Arid and semi-arid regions are highly vulnerable to disruption of local grain crop production due to climatic fluctuations, which cause such regions to have unstable annual crop production such that food insecurity is always present and famine is a constant risk.

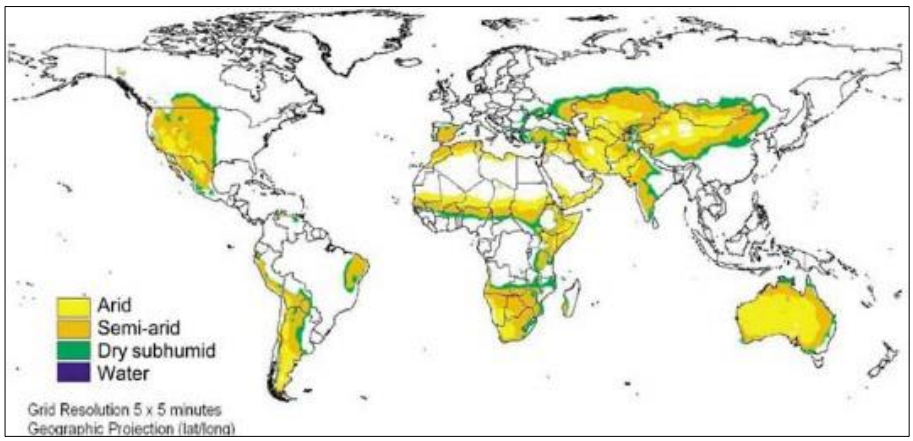

Figure 2-1 Global distribution of arid and semi-arid regions (FAO 2002).

Drylands, refer to arid, semi-arid and dry sub-humid area, have a ratio of average annual precipitation to potential evapotranspiration of less than 0.65 (UNEP 1992). In drylands, food security is essential in the global fight against hunger, as drylands is the home for 60% of the world's food insecure population and more than 80% of the rural population in this region is reliant on livestock and agriculture for both food and income (ELLA 2011). It was also reported that drylands are accommodating around 40% of the world population where over half of the world's livestock are grown (UNIC 2011). Therefore, a sustainable agricultural monitoring system is highly required to provide comprehensive information to exile these risks in drylands where arid and semi-arid region are part of them.

2.1 Main Drivers of food insecurity in arid and semi-arid regions

2.1.1 Precipitation

In part, due to the likelihood of unfavourable climatic events across many regions around the world, local communities are often food insecure and at risk of famine. Environmental conditions have a direct impact on food availability. For example, weather extremes such as droughts and flood and sudden climatic changes can negatively affect the storage and distribution of food (Haile 2005; Wheeler and von Braun 2013). Biophysically, crop production is affected by climatic variables such as temperature and precipitation. However, their effect on agricultural production varies across the globe, in some regions positive and negative in others. In arid and semi-arid regions, the amount and pattern of rainfall are among the most important factors that affect cropping systems, since rainfall is marginal and erratic, exacerbated by large runoff and evaporation losses, which can constrain crop production. In these regions, rainfall patterns are unpredictable and highly variable in time, amount, duration and space, and are subject to large fluctuations. Thus, water is the leading factor affecting agricultural and biological activities in these areas. For example, historically, lack of rainfall has been a major cause of famines and food shortages in Ethiopia (Bewket 2009). Time-series data on rainfall and crop production from 1994 to 2003 indicated that sorghum production had the largest inter-annual variability, as it is cultivated in arid and semi-arid parts of the country. Simple linear

correlation and standardized multiple-regression analyses were conducted to show the correlation of precipitation and temperature with grain yields in Lebanon, in which barley grain yield was correlated positively with precipitation (r=0.70), and the rainfall distribution index (r=0.71), but negatively with temperature (Yau and Ryan 2013). Most case studies suggested that in arid and semi-arid regions, fluctuation in crop production is closely linked to variability in rainfall, which may cause food insecurity. However, this might vary with the types of crops cultivated, types and characteristics of soil, and climatic condition of a given area.

2.1.2 Temperature

Temperature, and particularly increasing trends in temperature, is another main constraint on crop production in arid and semi-arid regions. On a regional basis, strong warming trends have been observed around the world since 1980, especially in the Middle East, northern half of China, Japan and Europe (Gourdji et al. 2013). The output from 23 global climate models reveals that there is a 90% chance that growing season temperature will exceed the most extreme seasonal temperature record in the tropics and subtropics by the end of 21st century (Battisti and Naylor 2009). In the arid and semi-arid regions of Asia, the projected area-averaged annual mean warming is expected to be 1.6 ± 0.2°C in the 2020s and rising up to 4.6 ± 0.4°C by 2080 (Sivakumar, 2005). This will add further pressure on crop production, as crop ecologists found that for each 1°C increase in temperature above the optimum during the growing season grain yields will decline by 10% (Brown 2006). A study also revealed that changes in climate such as increasing temperature and reducing levels and distribution of rainfall are more likely to lead to a decline in yields of wheat, maize, rice and other food crops in the semi-arid regions of the world (Lobell et al. 2009). Therefore, besides production reduction in response to global warming, rising temperature may affect all aspects of the hydrological cycle resulting in the frequent occurrence of severe droughts in arid and semi-arid regions.

A great challenge to crop production and food price stability is global warming and it's resultant of severe drought events. Increasing aridity, more frequent and intense meteorological drought, and extended periods without precipitation are common components of future climatic projections for many arid and semi-arid regions (Seager et al. 2007). For example, the 2009 drought in California's San Joaquin Valley affected of 285,000 acres of land resulting in loss of around

10000 jobs, and $340 million in revenue (Howitt et al 2011), the same event also caused a reduction of 20% in the value of irrigated agriculture in Australia (Kirby et al. 2012). In 2000 and 2001, drought posed significant social and economic issues in central Asia especially in Tajikistan, Turkmenistan and Uzbekistan where only in Tajikistan, for example, the direct economic cost of agricultural production was estimated at around 5% of national GDP (World Bank, 2006). The recent drought in 2008-2009 also caused sizeable declines in crop yields which cost $1-2 billion and affected over 435,000 farmers in Turkey as well as reducing by 45% the total wheat production in Iraq compared to the previous year (Table 2.1) (USDA FAS, 2008). Therefore, agriculture and related sectors in arid and semi-arid regions have been challenged by drought and its frequency, which can eliminate or reduce food production, and adversely affect food prices, market access, trade, employment and farm income (FAO, 2013b).

Regional Wheat Production (Million Tons)

Country	2007/08	2008/09	Change From Last Year	Percent Change
Afghanistan	3.80	1.50	-2.30	-60.53%
Azerbaijan	1.43	1.60	0.18	12.28%
Iran	15.00	10.00	-5.00	-33.33%
Iraq	2.34	1.30	-1.04	-44.52%
Israel	0.15	0.06	-0.09	-58.62%
Jordan	0.04	0.02	-0.02	-50.00%
Pakistan	23.30	21.50	-1.80	-7.73%
Syria	4.00	2.00	-2.00	-50.00%
Tajikistan	0.53	0.40	-0.13	-24.53%
Turkmenistan	1.60	1.20	-0.40	-25.00%
Uzbekistan	6.20	6.00	-0.20	-3.23%
Total	**58.38**	**45.58**	**-12.80**	**-21.93%**

Table 2.1 The impact of drought on the regional wheat production (million tons) (USDA FAS, 2008).

2.1.3 Population growth

Of seven people around the world, one is chronically hungry. The recent FAO report indicated that around 850 million people are estimated to be chronically undernourished in 2012-2014 in the world (FAO, IFAD and WFP, 2014). The report also stated that Asia has the largest number of undernourished, and Sub-Saharan Africa has the highest prevalence of undernourishment (one in four people). One of the reasons could be rapid global population growth, particularly in arid and

semi-arid regions, which has caused a considerable increase in demand for agricultural lands and a growing consumption of food. The world's population living in arid and semi-arid regions was estimated at around 15% of the global population (841 million), of which about 524 million live in semi-arid regions. Arid and semi-arid regions have the most rapid population growth in the world, which has led to dense habitation of these regions in recent decades (Barakat, 2009). This rapid population growth, with increasing demand for food is a major driver of land conversion. For example, 70% of tropical forests, 70% of Mediterranean forests and 60% of temperate broadleaved forests have been converted to agricultural/grazing land (Millennium Ecosystem Assessment 2005). Thus, rapid population growth in arid and semi-arid regions has the potential to cause regional food insecurity, producing an environment in which people cannot guarantee both physical and economic access to adequate food to fulfil their needs. This, in turn, may make these regions politically unstable.

2.1.4 War/conflict

The causes and consequences of conflict might induce food insecurity. Food availability can be reduced because of conflict by influencing agricultural production through demolition of agricultural assets and infrastructure (FAO, 2000; Deininger and Castagnini 2006). In the 21st century, food security in developing countries has been impacted by the exclusive phenomenon of civil war (Hendrix and Brinkman, 2013), and the fact that a relationship exists between both chronic food insecurity and civil war with poverty (Collier et al. 2003), because food insecurity can be fuelled by conflict itself. Experience from other world regions reveals that Arabic countries in transition such as Egypt, Tunisia, Yemen, and Libya are at a high risk of entering extended phases of conflict (Maystadt et al. 2014). The analysis also showed that among these countries, at the macro dimension of food security, Libya performed well (due to its oil wealth), but the remaining the countries will need to focus on macro food security, whereas only Tunisia showed a relative good performance at the household level food security. The recent conflict and drought in Syria led to a large reduction in winter cereal cropped area in 2013/2014 of around 21% lower than the planned level, maintained a significant food price inflation, and raised the number of displaced people from 4.25 million to 6.5 million in July 2013, with more than 2.7 million refugees registered in nearby countries of the region (FAO, 2014). Therefore, the previous examples and many other researchers suggest that

shocks to regional security due to extreme conflict events may increase regional food insecurity.

In addition to previous factors, there are many other drivers which may push the region toward food insecurity such as farming background, water scarcity, corruption, pests and livestock disease.

2.2 Monitoring crop by remote sensing

To meet a reasonable regional food security, the previous mentioned drivers have to be monitored and updated to target a sustainable food production. One of the most crucial technical options for regional food insecurity mitigation in agriculture is improving cropland management and timely monitoring of yield to provide robust data to be prepared for any unfavourable events. In this regard, the traditional method relied on the classical field based statistical data collection both on the regional and sub-regional level. Agricultural production has different characteristics which are different to other sectors such as large area, high spatial variation, different environmental condition, and substantial intra-annual and inter-annual seasonal variation. Due to these properties, consistent survey and traditional monitoring approach are not adequate to provide an accurate and low cost agricultural statistical data set to fulfil the agricultural production and management needs in time. Furthermore, subjectivity in sampling and data collection and lack of spatial distribution are the most common issues of the existing sample survey approaches.

Land surface can be monitored periodicity, macroscopically and economically through remotely sensed data. Remote sensing can provide numerous opportunities in the field of crop monitoring and management. In addition there has been increased interest in using space based observation due to the ability to offer crop information with greater spatial coverage, potentially at the global scale with high degree of availability. Providing timely comprehensive crop information by remotely sensed data can provide key information to help decision maker act to mitigate food insecurity. Here, three main applications of remote sensing in crop monitoring such as crop area estimation and identification, crop condition, and crop yield estimation will be explored.

2.2.1 Crop area estimation and identification

Prior information on cropped area plays crucial role in different applications ranging from economy, environment to policy (Wardlow et al. 2007). As the world population is growing rapidly, more food and irrigation water is required. Crop type maps are among the crucial datasets in yield estimation because it is needed by policy makers in the global food market (Doraiswamy et al. 2004; Thenkabail et al. 2009). Due to rapid agricultural development and scarcity in water resources, irrigation water management and planning face several challenges. Meanwhile, crop classification can facilitate irrigation timing and water planning (Xie et al. 2007; El-Magd and Tanton 2003). In this regard, remote sensing data can offer and facilitate crop type identification and area estimation due to mainly large spatial coverage and frequent revisiting. For instance, Gallego (2006) reported the evaluation of three activities to estimate crop area which was conducted in Monitoring Agriculture ResourceS (MARS) project; i) combining ground survey and satellite image to generate regional crop inventories, ii) ignore the ground survey and estimate a rapid crop area change and iv) stratification of a large resample of points by photo-interpretation on areal orthophotos for Eurostat's LUCAS 2006 survey. The results indicated that the third activity outperformed the other two. Regarding to the attempt of using the remote sensing data and ignoring the ground survey, the effort did not reach the cost efficiency at that time. However, the author deduced that as more improved sensors are generating, the future cost efficiency might change a swell.

With development of remote sensing technology, land cover classification estimation using remote sensing based approaches have become widely used over last few decades particularly in crop area estimation. According to Gallego (2008), the timing of estimating crop area or advance area prediction is based on following factors; i) the spatial differences in sowing practice, ii) the time after sowing a crop can be exposed by remote sensor, iii) spatial and temporal properties of remote sensors, iv) regional crop calendar, v) an appropriate date when the crop can be identified in the field, vi) time required for ground data collection and vii) time required to process the ground data. However, lack of quality in ground data is still one of the key issue to achieve a better classification accuracy. Although, many efforts have been made in methodological improvement and potential of remote sensing for estimating land cover area, still quality of ground survey is crucial. Instead, high spatial resolution imageries are sometimes replaced for ground surveys if the regions have time, budget and

access restrictions. However, less success was mostly observed for these efforts. For instance, less encouraging results were revealed when Gallego (2006) and Narciso et al. 2008 attempted to avoid or minimize ground data collection substituting by high spatial resolution imagery.

2.2.1.1 Classification

For the purpose of the classification, single date imagery and multi-temporal imagery (time series) have been used to identify or classify crop. Reducing the number of the images to be acquired and less processing requirement are the main advantages of the single date classification. The object-oriented classification, with a single date of Polarimetric Synthetic Aperture Radar (POLSAR) imagery in North-eastern Ontario, Canada, was able to classify five crop types with an overall accuracy of 95% and Kappa of 0.93 (Jiao et al. 2014). In Tavakkoli et al. (2006) noticed that classification accuracy is strongly based on acquisition date and land use type, for instance each crop can be distinct on some images better than on other, on the other hand extracting some crops is sufficient in each image than other crops. In the semi-arid region, Thiruvengadachari, (1981) demonstrated that croplands irrigated by surface water could be discriminated visually from those irrigated by ground water in a single Landsat image, however discriminating of different crop types is much harder. In addition, Masialeti et al. (2010) and Wardlow et al (2007) claimed that crop mapping using single date image is a real challenge as most of the time overlapped signature of various crops exist in a same date. Therefore, in arid and semi-arid regions, single date capture remotely sensed data might be insufficient to track large temporal variability and frequent spatial land cover changes among vegetation types.

Due to the spatio-temporal variation in cropping area in arid and semi-arid regions because of climatic variability and crop rotation practices, researchers promote the use of time-series data in these regions. First, at different phenological stages, time-series data can be selectively analysed to provide more useful vegetation spectral information, whereas this information is limited in single date imagery (Singh and Glenn 2009; Key et al. 2001). Second, temporal analysis of crops can aid in the discrimination of various crop classes based on differences in their growth patterns. Third, multi-temporal data may increase the quality of the imagery as the Sun angle changes with the season, which affects surface reflectance (Song and Woodcock 2003). Fourth, time-series data have the potential to provide a larger number of predictor variables which can suit machine learning classification approaches, thus, providing greater class accuracy

(Pal and Mather 2005; Ham et al. 2005). Extracting data from Landsat TM and ETM$^+$ sensors were employed in comparison between Hidden Markov Model (HMM) and single date image for classifying various crops over state of Sao Paulo, Brazil and the result showed a great achievement of HMM model by increasing the accuracy from 58% to 86% (Leite et al. 2011). The percentage difference between maximum NDVI and minimum NDVI was extracted from time-series data to differentiate crop area from non-crop areas in central Arizona (Zheng et al 2015). Then, a support vector machine (SVM), a machine learning classifier, was employed to discriminate various crop types in a complex cropping system in the region. The result showed an overall accuracy of >86% for crop classes and the study demonstrated that multi-temporal Landsat data are capable of monitoring cropping pattern and crop types over time in arid and semi-arid regions. The hierarchical classification approach using MODIS 250 m NDVI data was used to produce large-area crop mapping over the U. S. Central Great Plains (Wardlow and Egbert, 2008). The classes were: a) crop/non-crop, b) general crop types, c) specific summer crop types, and d) irrigated/non-irrigated crops, with incorporation a series of quantitative and qualitative evaluations, the overall map quality and misclassified area were assessed. The crop maps generally had classification accuracy more than 80% and at the state level, the crop patterns classified were consistence with general cropping pattern across Kansas. In addition, for the most classes, the classified crop areas were usually within 1-5% of the USDA reported area.

Remote sensing data can estimate and predict crop area in advance and the result has relatively good agreement with the ground data. In Rio Grande do Sul state, Brazil, MODIS crop detection algorithm (MCDA) using temporal profile of MODIS EVI was developed to estimate soybean crop area in December, using images from the sowing period, and March, using images from sowing and maximum crop development (Gusso et al. 2012). The coefficients of determination ranged from 0.91 to 0.95 were observed in comparison between results were obtained from MCDA and official statistics. Unsupervised *k-means* approach was employed to compute the integrated difference of two consecutive MODIS EVI images (one-month part) for three EVI threshold cut-offs at monthly breaks from April to October in order to estimate total winter crop area in Queensland, Australia (Potgieter et al. 2010). The highest pixel accuracy was observed for July with percent correctly classified for all thresholds of 94% and 98% for 2003 and 2005, respectively. The results also indicated that early estimation of crop area using multi-temporal approach could be confidently predicted at least one to two

months prior to harvest. At the same area, the rigour of the harmonic analysis of time series (HANTS) and early season metric produced high accuracy, 4 months prior to harvest, at pixel and regional level with percent errors of -8.6% and -26% for the 2005 and 2006 (Potgieter et al. 2011).

Over the past decade, research on land cover classification has involved the use of vegetation phenological information to discriminate between land cover types. Several phenological parameters, extracted from temporal profile of Landsat data, have been proved considerable in discriminating between corn, wheat, soybean and barley (Badhwar et al. 1982; Crist and Malila 1980). An innovative technique of harmonic analysis was proposed by Jakubauskas et al. (2002) to identify crop type from amplitude and phases of decomposed of Fourier component. The technique was applied to NDVI time series data from AVHRR and the result indicated its usefulness in detecting LULC changes during planting and harvesting. In terms of the comparison, a phenological based classification to map crop type was compared to the traditional maximum likelihood classifier and the result showed a great advantage of the former approach (Zhong et al. 2011). Although, discriminating cultivated and non-cultivated areas in arid and semi-arid regions of northern Asia is challenging due to mainly their similar seasonal change, several phenological parameters extracted from MODIS-NDVI can be employed to detect cultivated area in these regions (Enkhzaya and Tateishi 2011). In addition, multi-temporal time series analysis was used to estimate post-harvest total and specific crop area in related to crop phenology attributes using different fitting procedures (Potgieter et al 2013; Gongalton and Green 2009; Potgieter et al 2010, 2007). Time series MODIS-NDVI was used to extract key parameters to discriminate crop types over northern China (Zhang et al. 2008). The result showed a well correlation between area estimated by MODIS and the statistics at county level. A relatively high agreement regional LULC classification was obtained using phenological based classification approach in Upper Pangani River Basin, Eastern Africa, comparing to available detailed datasets for the region (Table 2.1). Son et al (2014) reported a close relationship between MODIS-derived rice area and rice area statistics ($R^2 \geq 0.89$) from 2001 to 2012 using phenology based classification in Mekong Delta, Vietnam. There were, however, slightly overestimated areas, with a relative error in area (REA) from 0.9-15.9% (Table 2.2). To sum up, having the knowledge of what kind of crop is going to be grown in the country will help a region financially, as this information will lead the region to have a pre-plan for importing and exporting of food product.

Table 2.2 Comparison of land use land cover classification using phenological variability MODIS vegetation with other sources of datasets such as Irrigation survey was done by the irrigation department, Ministry of Water and Irrigation (MOWI, 2009) and the surface areas of the water bodies (IUCN, 2003; PBWO/IUCN (2008) in Upper Pangani River Basin, Eastern Africa (Kiptala et al. 2012).

S/No.	Classification	Present study (ha)	Other sources (ha)	% Agreement	Source
1	Total irrigated area	129406	95823	74	MOWI (2009)
2	Irrigated sugarcane	8919	8480	95	MOWI (2009)
3	Water bodies	10525	7555-18800	72-179	IUCN (2003), PBWO/IUCN (2008)

Table 2.3 Results of regression analysis and the relative error in area (REA) between the MODIS-derived rice area and the rice area statistics, REA=(MOD-RAS)/RAS*100, where RAS= rice area statistics, MOD=MODIS-derived rice area (Son et al. 2014).

Year	*R2*	RAS (km^2)	MOD (km^2)	REA (%)
2001	0.90	3792	4393.4	15.9
2002	0.89	3834.8	4356.1	13.6
2003	0.89	3787.3	4136	9.2
2004	0.92	3815.7	4246.2	11.3
2005	0.95	3826.3	4095.6	7
2006	0.95	3773.9	4138.2	9.7
2007	0.96	3683.1	4060.2	10.2
2008	0.96	3858.9	4047.7	4.9
2009	0.97	3863.9	4121.2	6.7
2010	0.94	3945.9	4051.4	2.7
2011	0.94	4089.3	4126.3	0.9
2012	0.94	4181.3	4248.5	1.6

2.2.2 Crop condition

Monitoring crop condition, health, and seasonal progress are also essential in securing regional crop production. Wang et al. (2010) stated that one of the most crucial methods of yield estimation and food security is monitoring crop growth condition. The traditional approach of crop growth condition in the field, as a surrogate of the crop health, was limited in time and labour, and was subjected to many factors. Remote sensing for evaluating crop condition is relied on the relationship between multispectral reflectance, photosynthesis, temperature of crop canopy and evapotranspiration (Seelan et al. 2003). Four main necessities for remote sensing systems such as high temporal resolution, spatial resolution

of 5-25 m, combining agronomic and meteorological data into an intelligent system and quick data delivery were suggested by Bauer (1985) for farm management. Hatfield and Pinter (1993) stated that thermal infrared obtained from aircraft or satellite platform has the potential to provide a clue on crop related to frost, water stress, insect and disease.

A wide range of commercial crops might be affected by plant diseases and pests, which pose a major risk to final crop production. Globally, at least 10% of food production is lost because of plant disease (FAO 2000; Christou and Twyman 2004). This can be controlled in time if disease and pest are timely monitored and dealt locally. In this regard, the information of disease infected area is required as early and precisely as possible. The traditional approach of monitoring crop growth condition in the field, as a surrogate of crop health, is time and labour intensive, and the results are subject to many factors. Remote sensing data can supply relatively low cost data over wide spatial coverage of the area which is infected by disease and pest. In last two decades, many remote sensing based methods were developed to monitor crop condition in different countries and most common methods such as image classification method (Li et al. 2001; Li 2002), direct monitoring method through remote sensing indices (Wang 1991; Liu and Zhang 1997), crop growth profile monitoring method (Zhang and Wu 2004), same period comparing method (Zhao 2002; Zhang and Wu 2004) and crop growing models method (Xie and Kiniry 2002). Hyperspectral data were obtained for winter wheat using field spectroradimeter to evaluate severity of yellow rust disease and both techniques of the partial least square (PLS) and multiple linear regression (MLR) were employed to assess the suitability of the bands and develop the spectral model (Krishna et al. 2014). The result revealed that an accurate delineation and detection of yellow rust disease can be obtained through the developed model. Near-infrared reflectance spectroscopy (NIRS) was used to investigate early diagnosis of strip rust and leaf rust in incubation period and disease period (Li et al. 2013). The results depicted that the identification rate of training sets was 97% and the identification of testing sets was 96% using distinguished partial least square (DPLS) model. The physiological variables such as vegetation water content (VWC) and dry matter were obtained from MODIS normalized difference water index (NDWI) and NDVI to assess crop condition over the Yellow River, China (Yi et al. 2007). In general, NDWI was found to have great potential for VWC and soil moisture change monitoring. Combined analysis between NDWI and VWC indicated that wheat was under water stress at the end of the growing season in 2006, which was supported by ground experiment.

Fine spatial and temporal resolution remotely sensed data have been demonstrated for crop condition monitoring, assessing crop damage in flood areas (Zhang et al. 2013), assessing crop condition in relation to soil moisture (Bolten et al. 2010), and monitoring crop condition in extreme events such as drought (Krishna et al. 2009). In addition, good progress has been made in estimation of crop phenological parameters which can facilitate crop condition assessment resulting may provide more precise agricultural decision support (Doraiswamy et al. 2004; Sakamoto et al. 2005). Meng and Wu (2008) stated that having the crop condition information in pre-harvest stage can help to indicate potential food shortages and surpluses, and related wise policy making-decision. A crop suitability index was used to show that cropland suitability was at good level, and an overall gradual improvement in cropland quality during the period was observed but in some regions, the cropland quality had worsened over the period mainly due to government policies and population growth. Besides detecting the problems related to crop condition through the growing season, the success of treatments can also be monitored. Nevertheless, identifying and observing crop health and damage needs fine spatial, multi-spectral and multi-temporal imagery.

2.2.3 Yield estimation

The need to model and forecast crop yield in arid and semi-arid regions is increasing in parallel with recent and projected changes in land use and climate, and with recent crises in food security occurring mainly because of rapid global population growth (Antônio et al. 2009). Forecasting crop yield and production are essential for agricultural and economic stability of the region and are vital to sustaining global food security. Farmers, policy-makers, investors and hedgers need accurate and timely information on crop quality and supply. This information will also help governors to ensure a strategic contingency plan to redistribute food during times of crisis. It is important to consider which spatial, temporal and spectral resolutions meet the requirements. For example, medium to coarse spatial resolution satellite sensor data are commonly used in crop early warning systems by many aid organizations such as FAO to mitigate food insecurity (Hielkema, and Snijders 1994). In the context global agricultural observation, the group on earth observation ‘s Global Agricultural Monitoring (GEOGLAM) provides timely and accurate forecasts of agriculture production and yield at national, regional and global scales through the use of Earth Observations (EO) for which satellite and ground-based observation are included (GEO 2011;

Whitcraft 2015). GEOGLAM covers four main cereal crops (wheat, rice, maize and soy) within the main agricultural producing regions of the AMIS countries (G20+7). In contrast, fine spatial and moderate temporal resolution imagery is required if the study aims are localized at the farm level. In addition, Dadhwall and Ray (2000) stated that in managing large agricultural areas, forecasting crop yield is essential, and to achieve this remotely sensed data are required. This could be more efficient for a region where yield data are either unreliable or non-existent, often the case in war affected countries.

The advantage of using remote sensing data in crop yield assessment can be divided into two main parts. Firstly, it can estimate crop yield at the sub-region/region/global scale which could be useful for inaccessible countries in the world where data are not available or not in a good quality. Secondly, yield can be forecasted by remotely sensed data with supplying a precise, scientific and independent forecast of crops' yield in advance during the crop growing season to predict any unfavourable events. The possibility of involving remote sensing approaches to estimate crop yield and production have been demonstrated in many studies (Singh et al. 2002; Funk and Budde 2009; Ren et al. 2008; Dadhwall and Ray 2000; Tennakoon et al. 1992; Chang et al. 2005). In addition, as an action against the recent food price instability and to improve information on food supplies by international community, lunching satellite monitoring observation system in various regions of the world was proposed in the G20 Agriculture Minister meeting held in Paris (Becker-Reshef et al. 2010a).

In some countries, weather data have been used to monitor and forecast crop production (Andarzian et al. 2008; Liu and Kogan 2002; Paul et al. 2013; de Wit and Boogaard 2001). Missing data, a lack of continuity in weather data and the sparse spatial distribution of ground weather stations for a large diverse crop area limit the utility of these approaches (Liu and Kogan 2002; Dadhwall and Ray 2000; de Wit and Boogaard 2001). At the same time, to predict yield before harvesting, several empirical simulation crop models with incorporation of remotely sensed data have been developed and established. Examples of crop simulation models includes World Food Studies (WOFOST) (Vandiepen et al. 1989), Simulateur mulTIdisciplinaire pour les Cultures Standard (STICS) (Brisson et al. 1998) and Crop Systems Simulation (CROPSYST) (Van Evert and Campbell, 1994).

2.2.3.1 **Modelling (empirical)**

The most widely used approach to forecast crop yield is empirical regression-based models. In these models, crop yield is correlated to some selected predictors such as vegetation indices (VIs) obtained from remote sensing data and meteorological monitoring. The assumption behind regression-based models is that photosynthetic activity, extracted from spectral Vis, is correlated with eventual yield (Becker-Reshef et al. 2010). Thus, any positive or negative impact on the crop growing season (photosynthetically active biomass) is likely to result in a corresponding impact on the final crop yield. A linear regression model was established by Hamar et al (1996) to estimate wheat and corn yield at a regional level based on vegetation indices derived from Landsat MSS data. A strong relationship between wheat yield and integrated NDVI over entire growing season, and with late season NDVI variables was observed at region and farms scale in Montana for the years 1989-1997 (Labus et al. 2002). Ren et al. (2008) found the highest correlation between the spatial accumulation of MODIS-NDVI, at 40 days ahead of harvest time of winter wheat, and regional winter wheat production in Shandong, China. Similarly, spatial cumulative of SPOT NDVI has shown to have suitable prediction capability of 20 and 30 days before harvest for the short and long maize crop cycle in Kenya (Rojas, 2007). Normalized Difference Water Index (NDWI) and two-band variant of the Enhanced Vegetation Index were employed to predict the U. S. crop yield, and showed that including crop phenology related information improved model prediction, and the best time to predict crop yield were 65-75 days and 80 days after the MODIS derived green up for maize and soybean, respectively (Bolton and Friedl 2013). The fact that statistical regression remote sensing-based approaches are relied on the empirical relationship between satellites derived vegetation index and historical yield data, thus this relationship is typically localized and cannot be extended to other areas easily (Moriondo et al. 2007; Doraiswamy et al. 2003). However, their limited data requirements and simplicity to practice led them to be still most preferred approaches in crop estimation and forecasting.

Different approaches with incorporation of phenological-based remotely sensed data have been developed to estimate and forecast crop production. For instance, a corn yield estimation model using time series MODIS Wide Dynamic Range Vegetation Index (WDRVI) was developed by incorporating crop phenology detection approach (Sakamoto et al. 2013). The study found that the smoothed MODIS WDRVI (α=0.1), taken at 7-10 days before the MODIS deriving silking

stage, accurately estimated corn grain yield as well as observed the spatial patterns of corn yield all over the U. S. from 2000 to 2011. In north India, phenological parameters such as length of the season and start of the season, extracted from MODIS data, were used to measure the vulnerability of, and yield falls in, the wheat crop to extreme heat events (Lobell et al. 2012). In addition, many organization monitoring systems have employed the land surface phenology (LSP) information as an essential key component to assess the food security. For instance, NDVI as a surrogate of vegetation activity is used in the Famine Early Warning System Network (FEWSNET) as a part of integrated early warning system for food security (Ross et al. 2009). Furthermore, MODIS data with incorporation of county level data from United States Department of Agriculture (USDA) were employed to develop empirical models forecasting maize and soybean yield in the USA (Bolton and Friedl 2013). The results indicated that the model performance was significantly improved within and across year with inclusion of crop phenology information extracted from MODIS.

The remote sensing based approaches have been proved suitable for estimating and forecasting crop yield at different scales by comparing to ground or other official statistics data. For instance, Ferencz et al. (2004) presented two methods for estimating the yield of different crops in Hungary from satellite remote sensing data. A new vegetation index General Yield Unified References Index (GYURI) was used for the first method using double-Gaussian curve to NOAA AVHRR and other method was investigated by only using NOAA AVHRR county level yield data. The R^2=0.75 was obtained for the correlation between GYURI and the field level yield data. In the second method, the county level yield and the deduced vegetation index, GYURRI, were examined for eight various crops over eight years where high correlations were observed (R^2=84.6-87.2). An advance version of the method was developed by Bognar et al. (2011) to forecast corn and wheat, several weeks before harvest, in Hungary from 1996 to 2000. The difference between forecasted and reported yield data for wheat and corn were not more than 5%, except in 1997 where the absolute error is around 8%. At the provincial level in Italy, correlation coefficient equal to 0.77-0.73 were obtain between observed and simulated wheat yield, with corresponding root mean square errors (RSME) of 0.47 and 0.44 Mg/ha for Grosseto and Foggia, respectively (Moriondo et al. 2007). At regional scale, Ren et al. (2008) proposed a method of winter wheat yield estimation using MODIS-NDVI data. To validate the method, the results were compared to the ground data and the errors of the agro-climatic models. The results revealed that the relative errors of the predicted

yield using MODIS-NDVI are between 4.62% and 5.40% and that measured RMSE was 214.16 kg/ha lower than the RMSE (233.35 kg/ha) of agro-climatic models. An approach for predicting rice crop yield was developed in Vietnamese Mekong Delta using MODIS enhanced vegetation index (EVI) and leaf area index (LAI) (Son et al. 2013). Ten sampling districts were used to evaluate the robustness of the model by comparisons between predicted yield and crop yield statistics in 2006 and 2007. The results in 2006 revealed that better predictions were obtained for the spring winter crop (RMSE= 10.18%, mean absolute error (MAE) =8.44%, mean biased error (MBE) =0.9%) compared with the autumn summer crop (RMSE= 17.65%, MAE=14.06%, MBE=3.52%). In 2007, the spring winter crop yielded better results (RMSE= 10.56%, MAE=9.14%, MBE=3.68%) compared with the autumn summer crop (RMSE= 17%, MAE=12.69%, MBE=2.31%). Three different approaches: fine-resolution remote sensing imagery, the agro-meteorological Simple Algorithm For Yield (SAFY) model and the combination of both were evaluated to forecast crop yield in the semi-arid, low productivity regions of North Africa (Chahbi et al. 2014). The result indicated a greater accuracy using fine-resolution remote sensing imagery over others with a root mean square error equal to 8.5 and 1160kg ha-1 between the predicted and ground measured data. The regression-based models were built using MODIS-derived vegetation and production indices to predict summer crop yield in semi-arid irrigated ecosystems within the conflict-affected country of Syria (Jaafar and Ahmed 2015). The research reported a significant correlation ($p<0.05$) between the predicted and reported summer crop yield and demonstrated the potential of the approach to forecast crop yields during conflict years where reported data could be questionable.Therefore, remote sensing based methods are generally robust, accurate and stable for predicting yield at county, region and country level.

Remote sensing-based approaches to estimate and forecast crop yield also have some limitations which might not be able to achieve a high accuracy required in agricultural monitoring. One of the main issues for any based on satellite reflectance measurement is persistence of cloud cover during crop growing season which may prevent an accurate crop estimation or forecasting (Lobell et al. 2003). Space observation remotely sensed data, such as satellite derived vegetation indices, can provide a crop growth signal over the crop growing season. This information can be used as an estimation of crop condition and crop yield rather than directly its size, health and weight (Allen et al. 2002). In addition, other limitations are related to the sensor attributes including limited

spectral range, low frequent visit, and coarse spatial resolution (Moran et al. 1997).

Lack of the study with incorporation of remote sensing data in the arid and semi-arid regions pose many challenges for local farmers and decision makers to establish a proper policy to avert food insecurity. The necessity for surrogating and modelling crop yield in arid and semi-arid regions is increasing parallel to the vast changes in land use and climate with recent occurrence of crisis in food security mainly because of rapid global population growth (Antônio et al. 2009). In managing large agricultural land, estimating of its crop yield is very essential (Hutchinson 1991), to achieve this involving remotely sensed data is the best option (Dadhwall and Ray 2000). Satellite imagery data are potential tool for crop acreage and biomass production assessments in arid and semi-arid regions due to their ability to offer reasonable spatial and temporal knowledge's of various vegetation in these conditions (Teixeira et al. 2009). The design of operational tool which has the ability to provide regional estimate of crop production may maintain the regional food security. For instance, water scarcity is one of the series problems in arid and semi-arid regions which restricted the crop production. Quantifying crop production at regional level could help to simplify the observation of crop water use and irrigation efficiency. In the context of semi-arid regions, low productivity areas in North Africa, three approaches such as high resolution remote sensing data, the agro-meteorological Simple Algorithm for Yield Estimation (SAFY) model, and combination of remotely sensed data with SAFY model were evaluated to estimate the dynamic and yields of cereal (Chahbi et al. 2014). For wheat and barley, a strong correlation coefficient ($R^2 > 0.6$) was observed between NDVI, pre-time before the maximum growth (April), and grain and straw.

2.3 Smoothing remote sensing time series data

The use of remote sensing time series for crop and vegetation monitoring often needs a number of processing steps that include the temporal smoothing of the cloud-impacted remote sensing signal. This is mainly because the reflected light waves that satellite sensors detect coming from vegetation on the Earth's surface can be altered or blocked by a variety of phenomena, which produce noise in the raw data. To address this issue, raw data are processed using techniques that

filter out noise and produce a clearer, more representative data set. Various methods have been employed in smoothing out noise from remote sensing time series data. They include Discrete Fourier Transformation (DFT) (Wagenseil and Samimi, 2006), best index slope extraction (BISE) (Viovy et al., 1992), the double logistic model (Zhang et al., 2004), Savitzky–Golay (S-G) (Chen et al., 2004) and asymmetric Gaussian model (Jönsson and Eklundh, 2004). These approaches all have their advantages and drawbacks which are also reliant on the frequency of cloud contamination and seasonal variability of vegetation indices in the time series (Atkinson et al. 2012). BISE was compared to maximum value compositing (MVC) and concluded that BISI was performed better in terms of de-noising (Viovy et al., 1992). DFT, BISE and S-G were highlighted as effective techniques for constructing high quality NDVI (Chen et al., 2004). The S-G, changing-weight filter (CW) and the Whittaker smoother (WS) techniques revealed better performance in comparison to other tested techniques (Geng et al. 2014).

Any complex vegetation temporal profile can be decomposed through DFT into a series of sinusoids of various frequency. Individual sinusoids and their frequencies can be combined into a complex waveform for which noise has been removed. In the current work, DFT is targeted to be employed as it has minimal user interactions (only require to decide the number of harmonics to reconstruct the time series) and have been implemented successfully to many regional to global remote sensing time series data (Dash et al. 2010, Los et al. 2000). Recently, Atkinson et al. (2012) compared several models including Fourier analysis, and the asymmetric Gaussian, double logistic and Whittaker filter models in terms of their ability to fit a smooth time-series of a vegetation index such as to capture SOS (Atkinson et al. 2012). Several tests were applied including the root mean square error, Akaike information criterion and Bayesian information criterion and indicated that Fourier analysis is superior to other tested techniques.

The DFT is given by:

$$F_{(\omega)} = \frac{1}{N}\sum_{t=0}^{N-1} VI(t) * e^{-\frac{2\pi u x}{T}} \qquad (1)$$

Where VI(*t*) is the input vegetation index value at time *t* in the time series, *u* is the number of Fourier components, *t* is the composite number, *T* is the length of time period (number of composite), and here *T* is equal to *N*.

The effect of data smoothing on the time series for (a) crop, (b) shrub and (c) grass is depicted in Figure 2-2. The FT was able to capture the broad phenological pattern and major variation throughout a phenological cycle. Crop land cover type has the highest NDVI value around 0.5 and more, whereas the NDVI value is slightly lower for grass and much lower for shrub. It can be seen in the figure that there are number of missing data and this increases toward the very high altitude area in the region due to mainly cloud cover and snow. These were removed by the data cleaning operation. The final smoothed curve was constructed from the first five harmonics of the DFT.

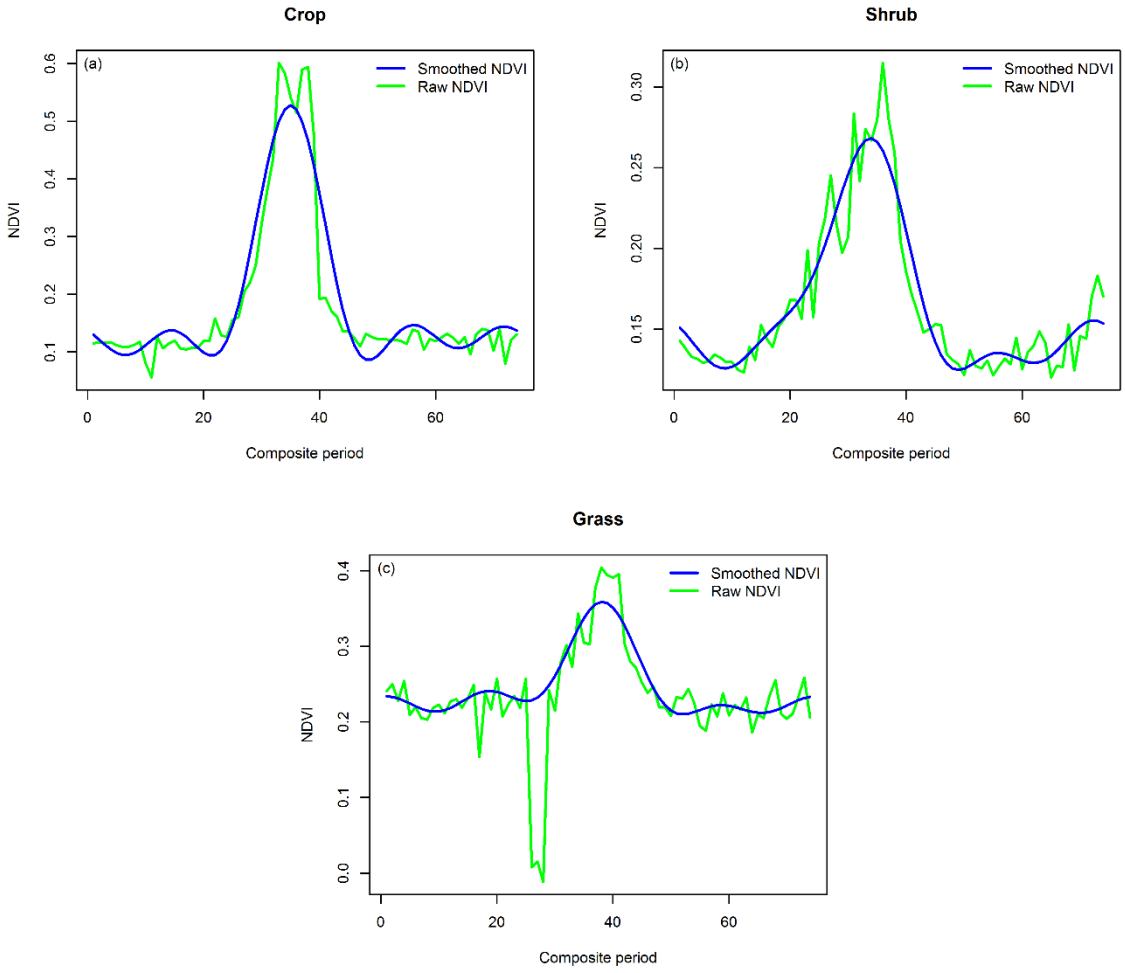

Figure 2-2 Effect of smoothing on NDVI time series data for (a) crop, (b) shrub and (c) grass.

2.4 Crop production in Iraq and role of remote sensing

Generally, Iraq can be divided into two agro-zones in terms of crop area; the north is mostly rain-fed and the central and southern parts are mainly irrigated (FAO, 2003). Iraq has a total surface area of 438 320 km^2 of which around 77.7% is not viable for agriculture in its current condition (UNEP 2007). Of the remaining 22%, around half is used for marginal agriculture and seasonal grazing. The area under cultivated crops, including cereals, vegetables, and pulses, is estimated to be around 3.5–4 million ha, of which wheat and barley account for 70%–85% of the cropland in any given year (Gibson et al. 2012; Schnepf 2004).

2.4.1 Wheat

Winter wheat is planted generally between September and November across the country, whereas the harvest time is varied, mainly between May and Jun in rain-fed area and February and March in irrigated area. Figure 2.2 presents harvested area of wheat in Iraq from 1960 to 2012. It is apparent that the three used data set has similar trend. Figure 2.3 shows production of wheat in Iraq for the same period. From 1990 the harvested area and production of wheat sharply increased mainly due to the national policy to raise crop production to combat the international economic sanctions. A clear decrease in harvested area can be seen from 1980 to 1988 because of the international war between Iraq and Iran which were taken place in wide areas of Mesopotamian plain. The drop of harvested area and wheat production in 2008 and 2009 was due to the impact of severe drought over the region. Although, figure 2.3 shows an increase of wheat production over the period, high inter-annual variation can be seen in the data. This is mainly due to the variabilty of the climatic variable such as rainfall and temperature, particularly in rain-fed area.

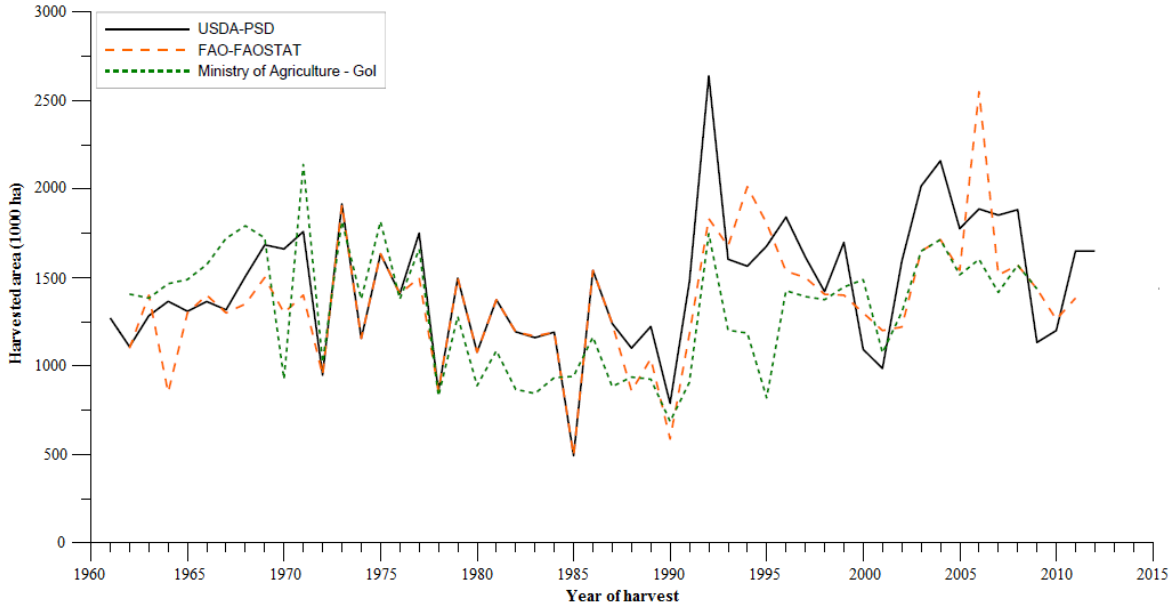

Figure 2-3 Rain-fed and irrigated harvested area for wheat in Iraq extracted from different sources (USDA-PSD, FAO-FAOSTAT and MOI-GoI) (Scoppe and Saleh 2012).

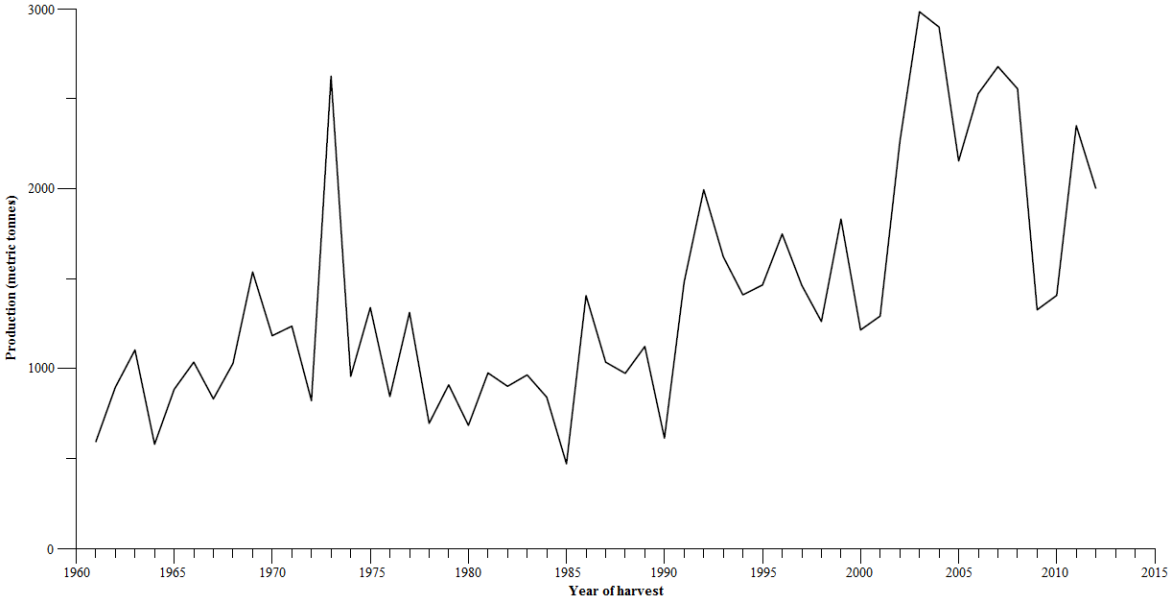

Figure 2-4 Production of wheat (rain-fed and irrigated) in Iraq (Scoppe and Saleh 2012).

2.4.2 Barley

The growing season for barley falls within the same time as wheat in Iraq. Figure 2.4 shows the total harvested area of barley over 50 years in Iraq. The impact of Iran and Iraq conflict cannot be clearly seen as declining harvested area of barley as harvested area of wheat. This is likely due to the fact that barley is a fodder crop, thus its cultivation and harvest time might not have an impact as a crop grown for cereal production or human consumption (Scoppe and Saleh 2012). Over last 50 years, barley harvested area fluctuated mostly between 400,000 ha and 2,200,000 ha, whereas wheat harvested area fluctuated between 1,000,000 ha and 2,000,000 ha. Production of barley over past 50 year presents in figure 2.5. Larger fluctuation in barley production can be seen in the figure over the period due to mainly the availability of water.

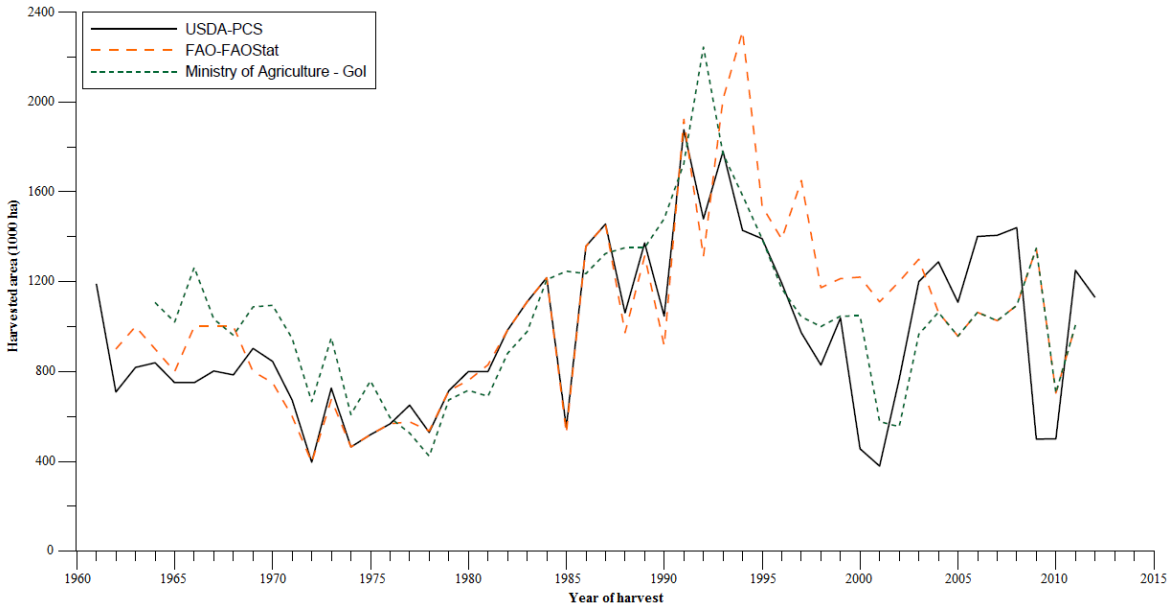

Figure 2-5 Rain-fed and irrigated harvested area for barley in Iraq extracted from different sources (USDA-PSD, FAO-FAOSTAT and MOI-GoI) (Scoppe and Saleh 2012).

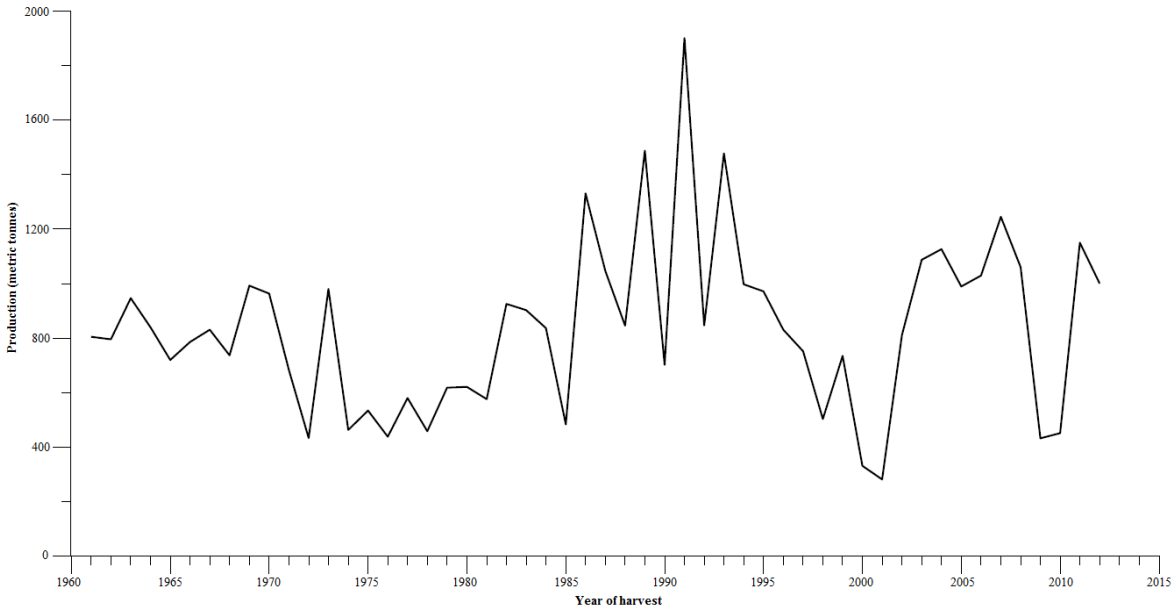

Figure 2-6 Production of barley (rain-fed and irrigated) in Iraq (Scoppe and Saleh 2012).

In Iraq, no previous study has investigated the possibility of using remote sensing-based approach to surrogate crop yield over the country. The expected fluctuation in crop production due to natural and anthropogenic stresses make it more interesting to evaluate decadal crop yield estimation with the incorporation of remotely sensed data. In general, to date there have been limited studies of crop yield estimation remotely sensed-based approach in arid and semi-arid environment in the subtropical region. The crop production in these regions is driven mostly by water availability. Therefore, there is a growing interest to characterise the agricultural production in these regions and identify the key controlling factors. The non-existence of proper ground agricultural observation and restricted access to the country due to security problems mean that remote sensing is the only viable method to estimate and map crop's area and yield.

Lack of the satellite based surveys across Iraq has obliged the federal government organization and Kurdistan Region government to rely totally on the ground information data. However, a report from USDA FAS (2008) proved that the official Iraqi government statistics is unreliable. In addition, international statistics data for the country for cultivated area and production are mostly "unofficial" or shown as an estimated figure, and alternative sources have been used to fill out missing data or uncovered areas (FAO 2012). Thus, the chance of

margining error in crop yield estimation based on the ground data is considerably high. In addition, to manage the agricultural activities across the country, Iraq's Ministry of Agriculture has assistance director at the governorate level. The entire official agricultural related statistical and report announcement such as land use, area and production are based on the governorate level. It is apparent from those data that to compute the governorate level of crop yield which cover large diverse area, only one average of crop yield was multiplied to the total crop area to obtain the governorate crop yield level. This approach is ignoring the variation in the yield of the different counties under this governorate level. Moreover, the reliability of calculating the total and harvested crop area is also under the question. Besides, a comprehensive and regular visiting to collect and update the data is often missing across the country, might be due to consistent regional instability. Therefore, up to date regional crop map and monitoring or forecasting crop yield could be helpful to improve the regional food security.

Chapter 3: **Spatiotemporal variation in the terrestrial vegetation phenology of Iraq and its relation to elevation**

3.1 Introduction

Vegetation phenology, the study of the life cycle events of plants, has become a key source of information for mapping, managing and monitoring the terrestrial ecosystem at local-to-global scales. Several studies have revealed that the phenology of plants and animals can be affected by climatic change (Sparks and Carey, 1995). For instance, the study of long-term datasets (1953-2005) of vegetation phenology events revealed an advance in the spring phenology and delay in autumn phenology in Japan and South Korea, with rapid changes in the timing of autumn phenology events compared to spring phenology events, due to global warming (Ibanez et al. 2010). This research also found that there were dissimilarities in temporal trends and vegetation phenological responses to temperature between East Asia and comparable sites in Europe, where spring events are varying more rapidly than autumn events. Jones et al. (2009) showed that increasing the global mean temperature above 2°C increased the possibility to lose forest cover in Amazonia. Thus, annual vegetation phenological variation has been used as a sensitive indicator of climatic change (Chung-Te et al. 2011). Moreover, variation in vegetation phenology may affect energy fluxes, the carbon cycle and the water cycle, mainly through the processes of both evapotranspiration and photosynthesis, which may affect the climate, and have consequences for food security and water availability (Xiao et al. 2009). Therefore, obtaining knowledge of current vegetation phenological responses can lead to greater understanding of the long-term rhythms of plant communities under various possible climatic regimes.

---

[1]QADER, S. H., ATKINSON, P. M. & DASH, J. 2015. Spatiotemporal variation in the terrestrial vegetation phenology of Iraq and its relation with elevation. International Journal of Applied Earth Observation and Geoinformation, 41, 107-117.

Vegetation phenology can be monitored either directly through ground observation or indirectly through space observation. Although the former approach is accurate for monitoring at point locations, it is time consuming and has poor spatial coverage, both in terms of extent and intensity. Moreover, data from ground observations may not be suitable for many global biogeochemical models which require information across large areas (White et al. 1997). In contrast, there has been increased interest in utilizing space observation due to the ability to provide vegetation phenological information with greater spatial coverage, potentially at the global scale.

Most space-based LSP studies rely on time-series of a vegetation index from moderate to coarse spatial resolution satellite sensors (e.g. Medium Resolution Imaging Spectrometer (MERIS), Moderate Resolution Imaging Spectroradiometer (MODIS), Advanced Very High Resolution Radiometer (AVHRR), Satellite Pour l'Observation de la Terre Vegetation (SPOT VGT)) due to their high temporal frequency (Boyd et al. 2011; Bobee et al. 2012; Chen et al. 2013; Fan et al. 2013). A considerable amount of literature has been published in which the AVHRR normalised difference vegetation index (NDVI) is used to estimate LSP due to its daily revisit frequency and extensive spatial coverage, leading to long time-series with which to map vegetation LSP parameters either at the regional scale (You et al. 2013; Wessels et al. 2011; Running et al. 1994; Loveland et al. 1997; Bradley and Mustard, 2008) or global scale (Brown et al. 2012; Nemani and Running, 1996; Eastman et al. 2013; Fensholt et al. 2012: Hansen and DeFries, 2004). For instance, at a regional scale, the SOS estimated from AVHRR NDVI data for winter wheat was in close agreement with in situ vegetation phenological observations (Huang and Lu, 2009), and at a continental scale there was also positive agreement particularly for homogeneous vegetation (Maignan et al. 2008).

Some studies have been conducted to assess the general compatibility of the AVHRR data with other sensors such as MODIS and SPOT VGT. For instance, Fontana et al. (2008) and Fensholt et al. (2006) compared the AVHRR-NDVI to the NDVI from other sensors such as MODIS and SPOT. Although the disagreement was small, the latter sensors' VIs were more accurate than the AVHRR-NDVI. The reasons for this could be that initially the AVHRR sensor was not designed for monitoring vegetation (Teillet et al. 1997) and the NDVI from AVHRR is more affected by water vapour due to the sensitivity of this sensor's spectral bands to water vapour in the atmosphere (Cihlar et al. 2001). Therefore, recent research

has been directed to using alternative satellite sensor data such as MODIS, MERIS and SPOT products to estimate LSP parameters.

Since 2000, satellite sensors such as MODIS have been available which offer significant increases in terms of spectral and spatial resolution, and the quality of cloud screening, geolocation, sensor calibration and atmospheric correction (Soudani et al. 2008). These properties have made MODIS a common choice for monitoring terrestrial vegetation and LSP in different geographic areas and ecosystems (Xia et al. 2012; Hmimina et al. 2013). In addition, a close agreement between MODIS LSP parameters and ground reference data has been demonstrated (Kang et al. 2003; Sakamoto et al. 2005; Shuai et al. 2013). Besides demonstrating accurate estimation of LSP parameters by MODIS Terra and Aqua compared to field observation, Colombo et al. (2011) used MODIS data to show that the start of the growing season may advance or delay by as much as 10 days, if the spring temperature changes by ±1 C°. Therefore, time-series MODIS data are a suitable choice for monitoring seasonal and inter-annual vegetation phenological changes which may be affected by changes in local climate.

LSP extracted from remotely sensed data have been used as a sensitive indicator of different drivers such as climate change (Chung-Te et al. 2011), and natural and anthropogenic factors exerted through land use/land cover type (de Beurs and Henebry, 2004) as well as affecting ecosystem carbon exchange (Churkina et al. 2005). Moreover, LSP information can help to improve agricultural management such as fertilization and irrigation through aiming to establish a suitable relationship between the timing of plant growth phases and carbohydrate consumption (Garcia-Tejero et al. 2010; Menke and Trlica 1981; Mooney and Billings, 1960). Amongst all natural factors, changes in ground elevation have a significant influence on the timing of LSP parameters. Some studies have been carried out to show the relationship between individual LSP parameters and elevation (Gimenez-Benavides et al. 2007 and Arroyo, 1990). For instance, Pellerin et al. (2012) stated that elevation was the main driving factor leading to delayed budburst and leaf unfolding dates of about 2.4 to 3.4 days per 100 m in the Western Alps. Delayed SOS and EOS were observed during 2001-2010 in a subtropical mountainous region in China due to the colder temperature at higher elevation (Qiu et al. 2013).

There have been limited studies of land surface phenology in arid/semi-arid environments in the subtropical region. The vegetation phenology in these regions is driven mostly by the availability of rainfall, contrary to the phenology

of much northern high latitude vegetation which is driven mostly by temperature. Therefore, there is a growing interest to characterise the vegetation phenology in these regions and identify the key controlling factors. Iraq, being situated in the subtropical region with its highly seasonal precipitation patterns presents an interesting area within which to study changes in vegetation phenology. In addition, the changes in LSP parameters across Iraq have potentially been driven by different environmental factors, both natural and anthropogenic, during the last decade. The non-existence of ground vegetation phenology data and difficulties with access to the country due to security problems mean that remote sensing is the only viable method to estimate and map LSP across the country.

It is also possible that in Iraq elevation is one of the main predictor variables influencing the country's LSP parameters. The northern part of Iraq is comprised mostly of mountainous areas relying on rainfall while the Great Mesopotamian alluvial plains of the Euphrates and Tigris rivers are located in the middle and south parts of the country (FAO Aquastat, 2008). Therefore, the altitudinal-phenology relationship may vary across the country based on local temperature and rainfall conditions.

Therefore, the aim of this research was to assess and map the spatial variation in key land surface phenology (LSP) parameters across Iraq over the last decade and explore their relation with elevation (as a surrogate of temperature and precipitation).

3.2 Material and Method

3.2.1 Study Area

Iraq is situated in the Middle East between the longitudes 38° to 48°E and latitudes 29° to 37°, with an area of 437,072 km^2, surrounded by Iran to the east, Turkey to the north, Syria, Jordan and the Kingdom of Saudi Arabia to the west and the Arabian gulf to the south (Figure 3.1). Climatologically, Iraq is described as having a subtropical continental climate (except for some parts in the north) with an extreme, hot summer (average maximum temp. in Aug. and Jul. around 43 °C) with no rainfall, and a short cool winter (FAO, 2011). Precipitation is highly seasonal and more than 90% of the precipitation occurs between November and April. The rainfall ranges from 1200 mm in the north and northeast to less than

100 mm over the majority of the south, with an average annual rainfall of around 216 mm over the whole country (FAO Aquastat, 2008). Rainfall varies considerably spatially based on altitudinal variation across the country.

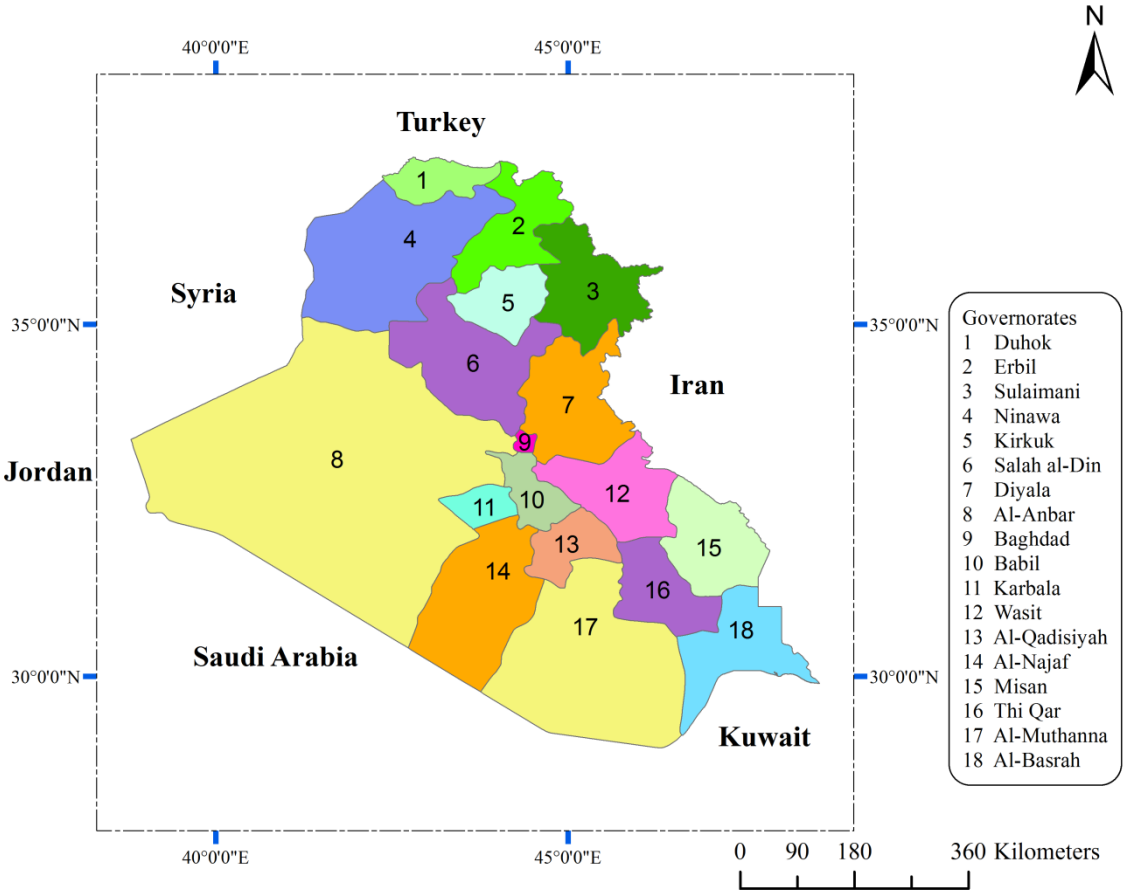

Figure 3-1 Map of Iraq showing the boundaries of 18 administrative governorates.

Generally, Iraq can be divided into two agro-zones in terms of crop area; the north is mostly rain-fed and the central and southern parts are mainly irrigated (FAO, 2003). Natural vegetation varies seasonally with rainfall. Grassland is mostly located in the high elevation area in the north, but open shrubland is distributed from the lowlands in the north to the south of the country (Figure 3.3a). In terms of the crop calendar, wheat and barley are the major winter crops; where irrigation is available sorghum, corn, millet and rice are grown in the summer. Winter crops are planted between September and November and harvested between May and June; irrigated summer crops are planted between April and May and harvested between August and September (Schnepf, 2004).

3.2.2 MODIS Land Surface Reflectance Data

This study utilised the 8-day composite data of the MODIS land surface reflectance level-3 data product, with a spatial resolution of 250 m (MOD09Q1 V5) from 2001 to 2012. The data were downloaded from NASA's Land Processes Distributed Active Archive Centre (LP DAAC) (https://lpdaac.usgs.gov/data_access). The Quality Assurance (QA) layer is a 16-bit image that is composed of values ranging from 0-65535 representing different permutations and combinations of MODIS land surface reflectance quality parameters. The QA layer was used to remove contaminated pixels due to sensor effects such as different orbits, adjacency, band quality, and MODLAND QA and non-sensor effects such as cloud state and atmospheric noise. A number of permutations and combinations were then conducted using the above criteria to finalize which values in the QA flag image were retained to represent good quality data. This ensures that only the best quality pixels were used in the analysis. For detail of this QA assessment procedure please refer to MODIS land products quality assurance tutorial on the LP DAAC website (https://lpdaac.usgs.gov/sites/default/files/public/mois/docs/MODIS_P_QA_Tutorial-1b.pdf).

For each time step (composting period) the NDVI was calculated as in equation (1):

$$NDVI = ((NIR-RED))/((NIR+RED)) \quad (1)$$

where, NIR and RED are the spectral reflectances in the near infrared and the red wavebands in the MOD09Q1 product.

Generally, the vegetation growing season in Iraq starts in September and continues until December in the next year (FAO aquastat, 2008; Schnepf, 2004). Since, many LSP parameters cross the calendar year, to extract land surface phenological variables for a specific year data from the previous year and following year were considered in the "layer stack". For example, the dataset for 2008 contained 8 day NDVI composites from July 2007 to January 2009 resulting in 72 data layers (bands).

3.2.3 Extraction of LSP parameters

The methodology for extracting LSP parameters can be divided into four main steps: moving window averaging to remove dropouts, linear interpolation for gap filling, data smoothing, and LSP parameter estimation. NDVI values in the study period were affected by noise or errors (dropouts) in the data, particularly in the Kurdistan Region, resulting from cloud cover, snow and local climate fluctuations which, in turn, led to erroneous NDVI values. Thus, a temporal three point moving window average was applied to each pixel as a first step to remove these dropouts and the missing values were then interpolated linearly in time.

To estimate the LSP parameters, different smoothing techniques have been applied to time-series vegetation index data to capture the annual growth cycles (Hmimina et al. 2013; Clerici et al. 2012; White et al 2005; Viovy et al. 1992; Zhang et al. 2003). Recently, several models were compared including Fourier analysis, and the asymmetric Gaussian, double logistic and Whittaker filter models in terms of their ability to fit a smooth time-series of a vegetation index such as to capture SOS (Atkinson et al. 2012). Several tests were applied including the root mean square error, Akaike information criterion and Bayesian information criterion, mostly indicating the advantage of Fourier analysis.

The current study used Fourier-based smoothing due to minimal user interaction and because it has been used widely in different regional-to-global AVHRR studies (Cihlar et al. 1997). The Discrete Fourier Transform (DFT) was used to decompose the information into a series of sinusoids of various frequencies (Jakubauskas et al. 2001). Then, inverse a Fourier transform on the first few harmonics was used to provide an appropriate reconstruction of the main vegetation phenological signal. Jakubauskas et al. (2001) stated that for 50-90% of the variability in a dataset, the inverse Fourier transform utilizing the first two harmonics is required. Nevertheless, this can only represent annual and semi-annual vegetation cycles. Natural vegetation phenological cycles require three to five harmonics for adequate representation (Geerken, 2009). This means that the number of harmonics might be changed due to the land cover type. For example, to reveal the agricultural land phenological signal where double or triple cropping is practiced, the first six Fourier components are required (Dash et al. 2010).

After smoothing the data, the LSP parameters can be estimated by one of several methods. These methods can be categorized into three broad groups: trend derivative methods, threshold-based methods and inflection point methods (Reed

et al., 2003). As the threshold value may vary by land cover type, there is some difficulty in implementing threshold-based methods over large areas (Reed et al. 1994). Regarding the trend derivative method, choosing a suitable moving average time interval may be challenging as a large time interval results in less sensitive trend detection and a small time interval may detect irrelevant trend changes (Reed et al. 2003). In the current research the inflection point method was applied due to easy implementation and the ability to discriminate multiple growing seasons for different land cover types such as crops (Reed et al. 1994). This technique captures LSP parameters while maximum curvatures occur in plotted time-series data (Zhang et al. 2001). The algorithm searching for the valley points in time checks the derivative information; the derivative at the beginning of green up is positive, while it changes to negative at the senescence stage. Thus, a time-series dataset can be searched for a continuous trend of four consecutive rising NDVI values and four consecutive declining NDVI values to define the key LSP parameters, SOS and EOS (Figure 3.2). However, due to local fluctuations, some valley points may appear at larger values of NDVI which may lead to unreliable detection of these parameters. Therefore, a condition that the difference between the maximum NDVI and valley point must be greater than one fifth of the maximum was applied to avoid this issue. The whole process was fully automated using Matlab code. Through this process, the SOS and EOS were mapped for each year, and then the Median was calculated and mapped for the whole period.

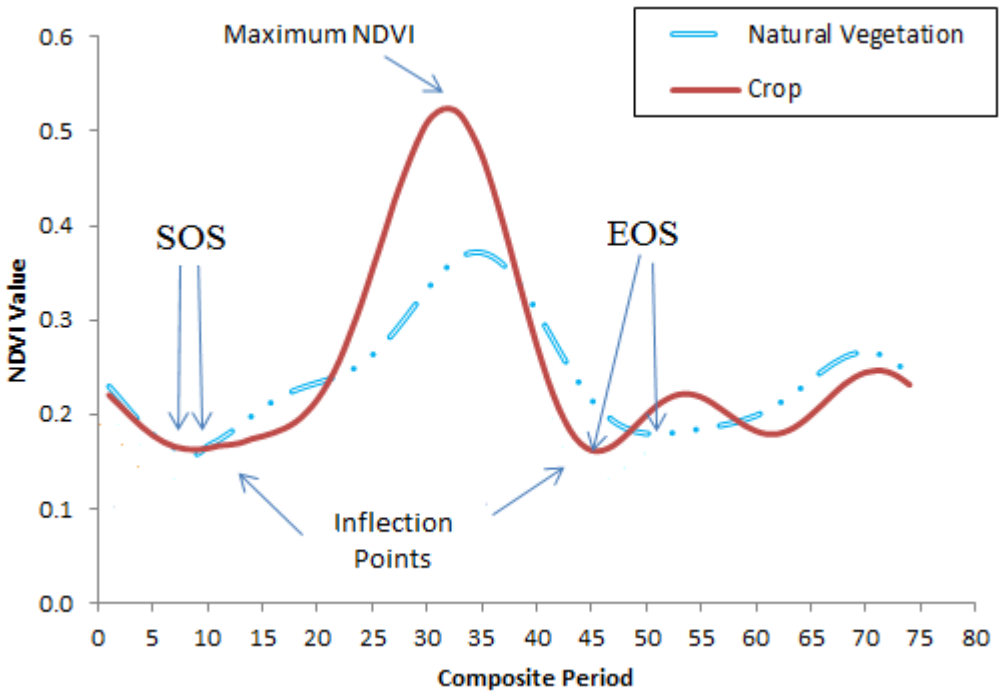

Figure 3-2 Estimating the key LSP parameters in the current study by applying the inflection point technique to define the SOS and EOS from smoothed time-series data for major vegetation types.

3.2.4 MODIS Land Cover Type

To identify the most predominant land cover types over the country and, in turn, their LSP parameters, the MODIS land cover types (MCD12Q1) from 2001 to 2012 were downloaded from NASA's LP DAAC (https://lpdaac.usgs.gov/data_access). The reason for using 12 years of MODIS land cover type is that the country's land cover type is highly dynamic and has changed from one year to another due to several natural and human factors.

The MODIS land cover product has a 500 m spatial resolution which provides broad information on Iraq's land cover types. Supervised classification (Schowengerdt, 1997) was used to create the MODIS land cover classification involving high quality land cover training sites. This approach was developed by utilizing the combination of ground reference data and fine spatial resolution imagery to increase the accuracy of the product (Muchoney et al. 1999). The International Geosphere and Biosphere Programme (IGBP), which is a primary land cover scheme, was used to identify the MODIS land cover classes: 17 classes, of which 11 are natural vegetation, 3 are developed classes and the rest are non-vegetation classes. To see the distribution of classes, the 2007 MODIS land cover type is shown as an example in Figure 3.3a.

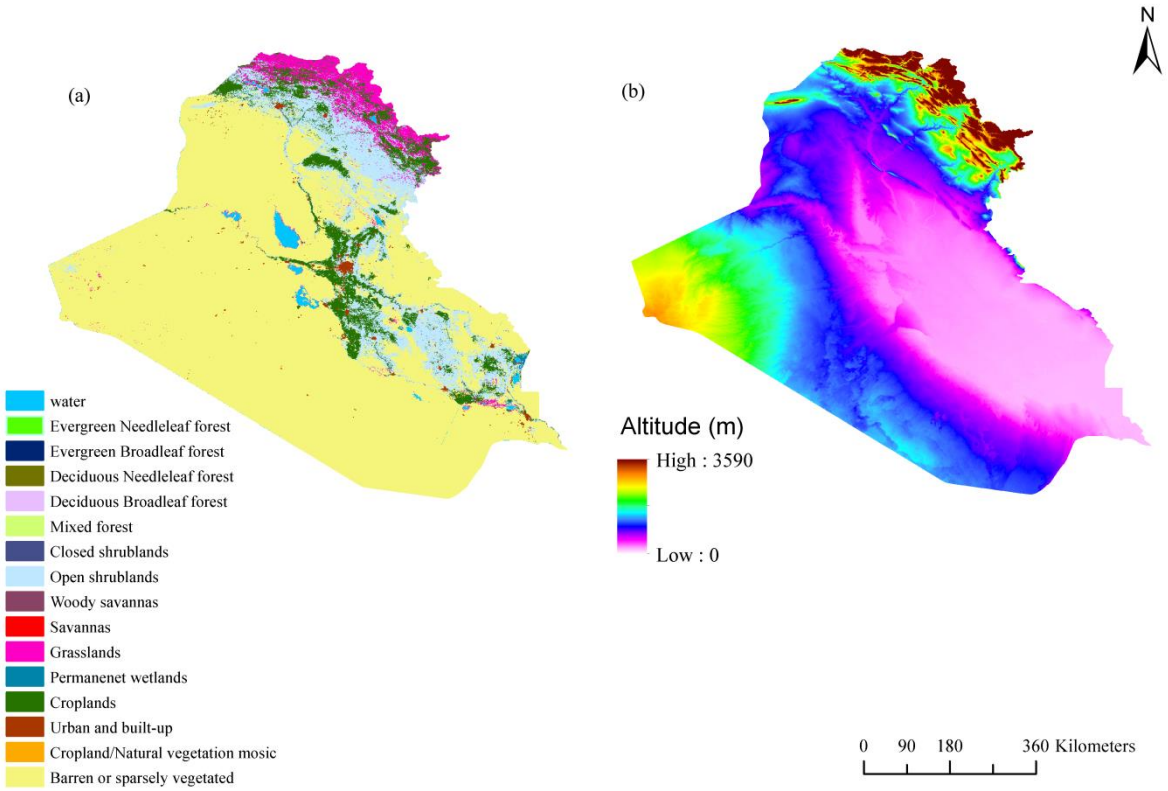

Figure 3-3 Maps of (a) MODIS land cover type with a spatial resolution of 500 m for 2007 (https://lpdaac.usgs.gov/data_access) and (b) elevation, extracted from SRTM data (Jarvis et al. 2008) for Iraq with a spatial resolution of 250 m.

3.2.5 Calculating the standard deviation (STD) and correlation between LSP parameters and elevation

After extracting Iraq's land cover from the MODIS product, it was apparent that the most dominant vegetation types are croplands, open shrublands and grasslands (Figure 3.3a). To present the temporal variation in the LSP parameters among these classes over the last decade the standard deviation (STD) was estimated for each pixel. The STD describes the variability in the LSP parameters in each pixel and can highlight the most unstable areas in terms of LSP through the time period of the study.

For the linear regression analysis described below, only those pixels which were consistently allocated to the same class through time were used. Then homogeneous areas were extracted for each permanent land cover type to reduce the number of miss-classified areas. Elevation for Iraq was estimated from the

Shuttle Radar Topography Mission dataset (SRTM) (Jarvis et al. 2008) (Figure 3.3b). To be compatible, the estimated LSP parameters (250 m) and elevation data (250 m) were resampled to the spatial resolution of the MODIS land cover types (500 m). Then linear regression was applied to estimate, for each permanent homogeneous land cover class, the coefficient of determination between the LSP parameters (Median LSP) and elevation. The composite date was converted to Julian days for the regression analysis. For example, the SOS may start at the end of September of the previous year (around 280 days) and finish in August (around 650 days) in the following year in homogeneous areas (Median LSP). A schematic diagram of the methodology can be seen in Figure 3.4.

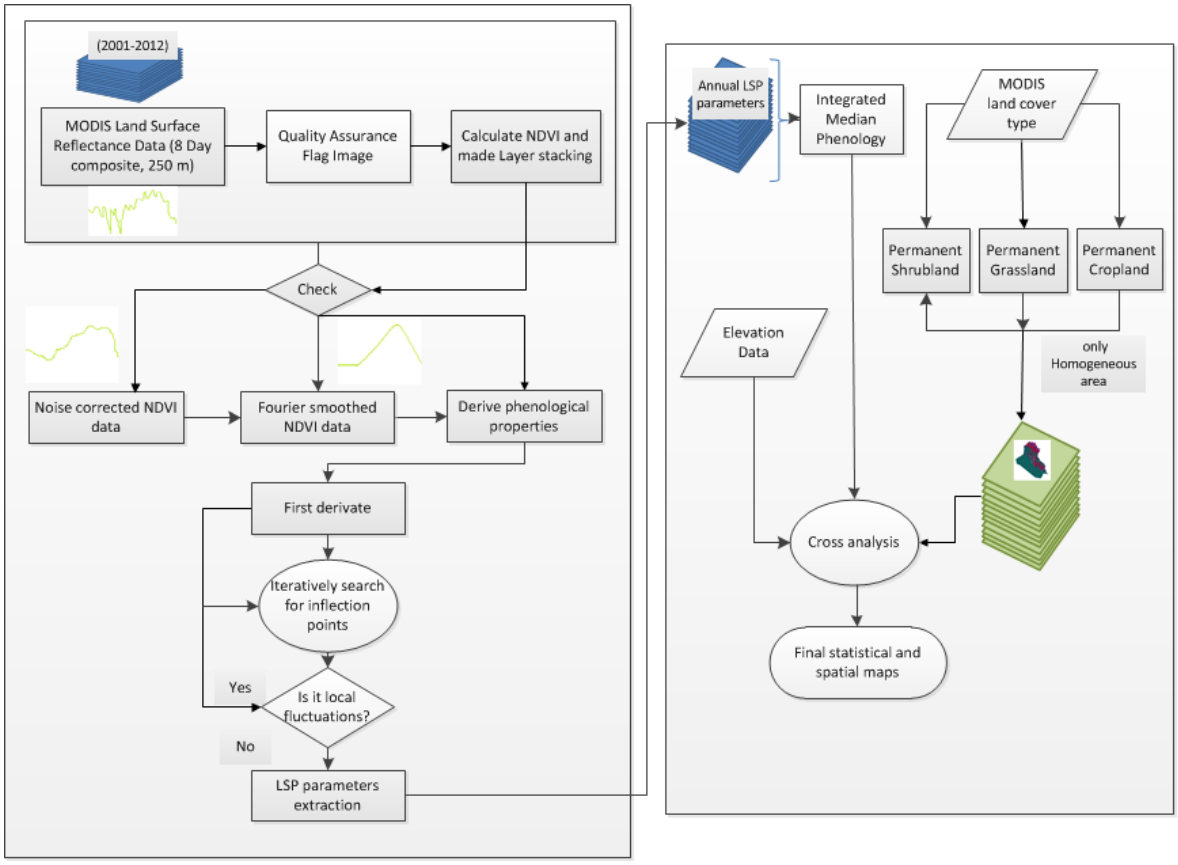

Figure 3-4 Schematic diagram showing the research methodology adopted in this study.

3.3 Results

3.3.1 Phenological parameters for specific vegetation types

The spatial distributions of the SOS (Figure 3.5a), EOS (Figure 3.5b) and LOS (Figure 3.5c) based on the multi-year median of each vegetation phenology parameter across dominant vegetation types in Iraq are shown in Figure 3.5. Generally, rainfall and elevation can be expected to influence the distribution of the LSP parameters across Iraq. Based on these factors and for ease of explanation, we divide the study area into two main parts; the north including the Kurdistan Region, Kirkuk and the northern part of Ninawa and Dyala, which are mainly rain-fed, and the central and southern parts, which are mostly irrigated (FAO aquastat, 2008; Schnepf, 2004).

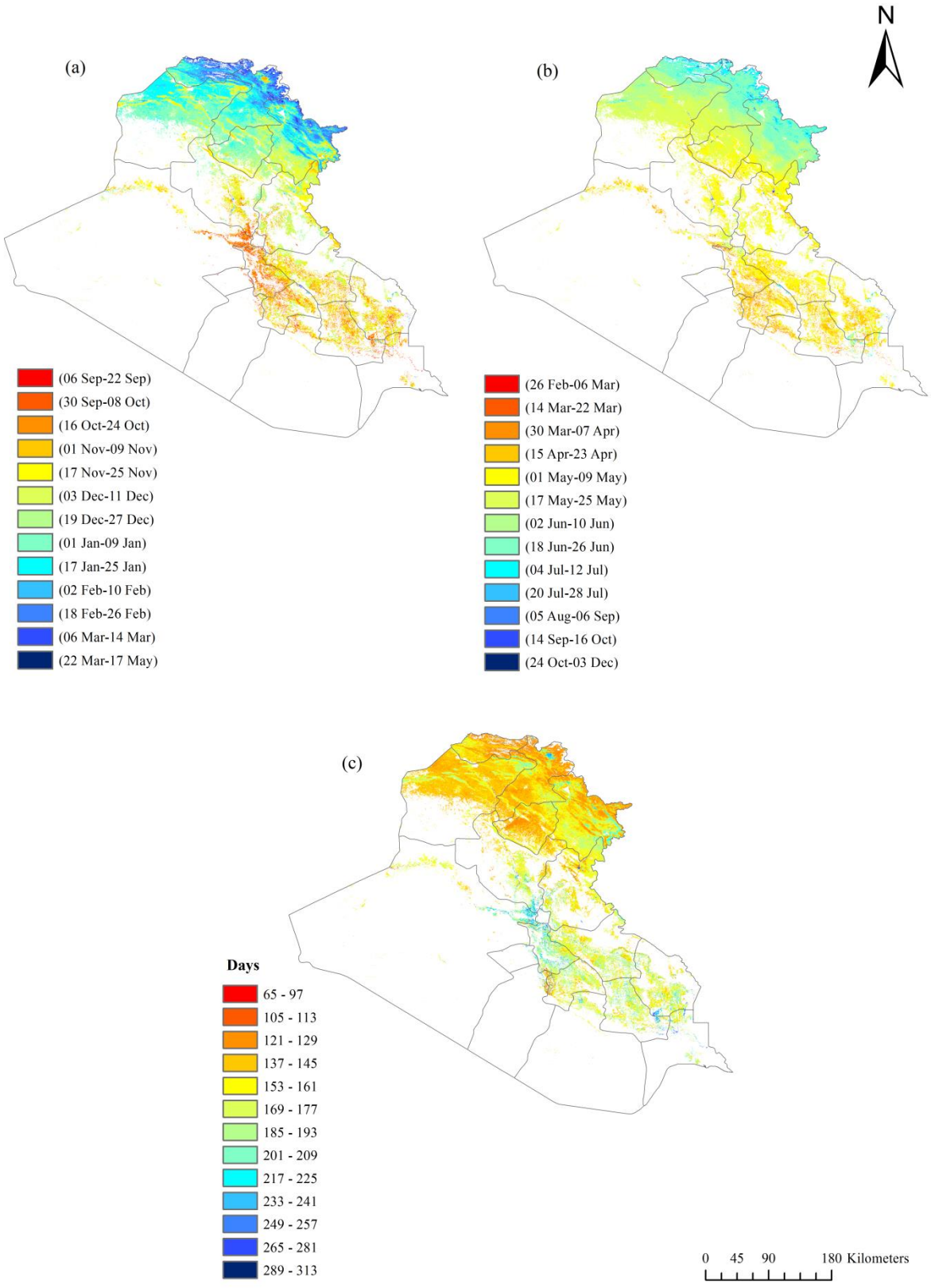

Figure 3-5 Median spatial distribution of different vegetation types for (a) SOS, (b) EOS, and (c) LOS during 2001-2012 in Iraq. The median SOS and EOS were presented in Julian days rather than composite period: the growing season starts around September of the previous year and continues to December of the

following year, for all vegetation types, to make the maps easier to read. LOS is shown in number of days representing the duration of the median growing season for all vegetation types.

A large amount of variation in the SOS across the country was observed. The earliest SOS was detected in the central and southern parts of the country, dominated by cropland, between the end of September and end of October due to the availability of water. However, for the rest of the croplands in the central and southern parts of the country, the SOS was detected from mid-to-late December. This difference might be the result of different crop types grown in these areas. For some areas in the central and southern parts of the country, the SOS was delayed to the end of March to mid-May. This is an indication of the growing of summer crops in these regions. However, the SOS of the shrubland cover type in the central and southern parts seems to range between mid-to-end of November (Figure 3.5a).

The EOS in the central and southern parts of the country is less variable, with the majority of this area exhibiting an EOS between mid-April to mid-May (Figure 3.5b). The reason could be a lack of moisture and the approach of a hot summer in the area. However, a relative delay in the EOS was detected for a few areas which might be the result of the practicing of summer cropping (beginning-to-end of June). From Figure 3.5c, it is apparent that the longest growing season was also detected for agricultural land that is connected to water in the central and southern parts of the country (217 to 257 days) due to their earlier start. For the remainder of the area, mainly occupied by shrubs, the LOS was between 137 to 161 days and 169 to 269 days for a mixture of shrub and crop land cover types.

The predicted key LSP parameters in the northern part of the country were much more heterogeneous than in the middle and southern parts (Figure 3.5a). The SOS was detected around mid-to-end of November for various places in the north dominated by open shrubs and a few areas of crops with a long growing season of 217 to 241 days (Figure 3.5c). However, these areas exhibited an EOS from beginning-to-end of May, the same as for most of the shrubland land cover type (Figure 3.5b). The SOS of cropland areas was detected for the majority of places from mid-to-end of January. The corresponding EOS of crops in this area was towards the beginning-to-mid June. However, towards Kirkuk, the southern part of Erbil and the middle of Ninawa governorates it became more difficult to discriminate between open shrublands and croplands in the period start-to-mid-January because of the similar timing of the LSP parameters. Finally, the grassland

cover type is another dominant class in this area and its SOS fell into three different periods due to elevation. A very late SOS was detected for very high elevations between the end of March to end of May, mostly located at the border of this region; the beginning to middle of March was recorded for an average elevation and mid-to-end of February for relatively low elevation compared to the previous two classes. As for SOS, the grassland cover's EOS can be divided into three classes. A very late EOS between the middle of September to December was detected for the first class; the beginning-to-mid July was detected for the second class and mid-to-end of June was recorded for the majority of the grassland cover type. Although grassland had a very late EOS compared to the other classes, the LOS for the majority of its area was very short; between 105 to 129 days due to a delay in the SOS.

From Figure 3.5, most parts of the country have no LSP parameters as there was no or very sparse vegetation cover. This result may be explained by the fact that more than 40% of the western part of the country is desert (FAO Aquastat, 2008) and in other places, LSP parameters are hard to detect because of variable or unclear vegetation phenology patterns.

3.3.2 Analysis of decadal changes in LSP parameters

To present the inter-annual variability of the LSP parameters such as SOS EOS and LOS, the STD was calculated for the entire study area for the period from 2001 to 2012 (Figure 3.6). As shown in Figure 3.6, the SOS is much more variable than the EOS. The STD of the SOS for most of the country ranges between 0 and 72 days (Figure 3.6a). However, this value increases dramatically towards the lowlands in the north to about 80 to 120 days. Some areas, which are connected directly to water, exhibited the largest STD. Generally, these areas of highly variable SOS are mostly occupied by the cropland and shrubland cover types.

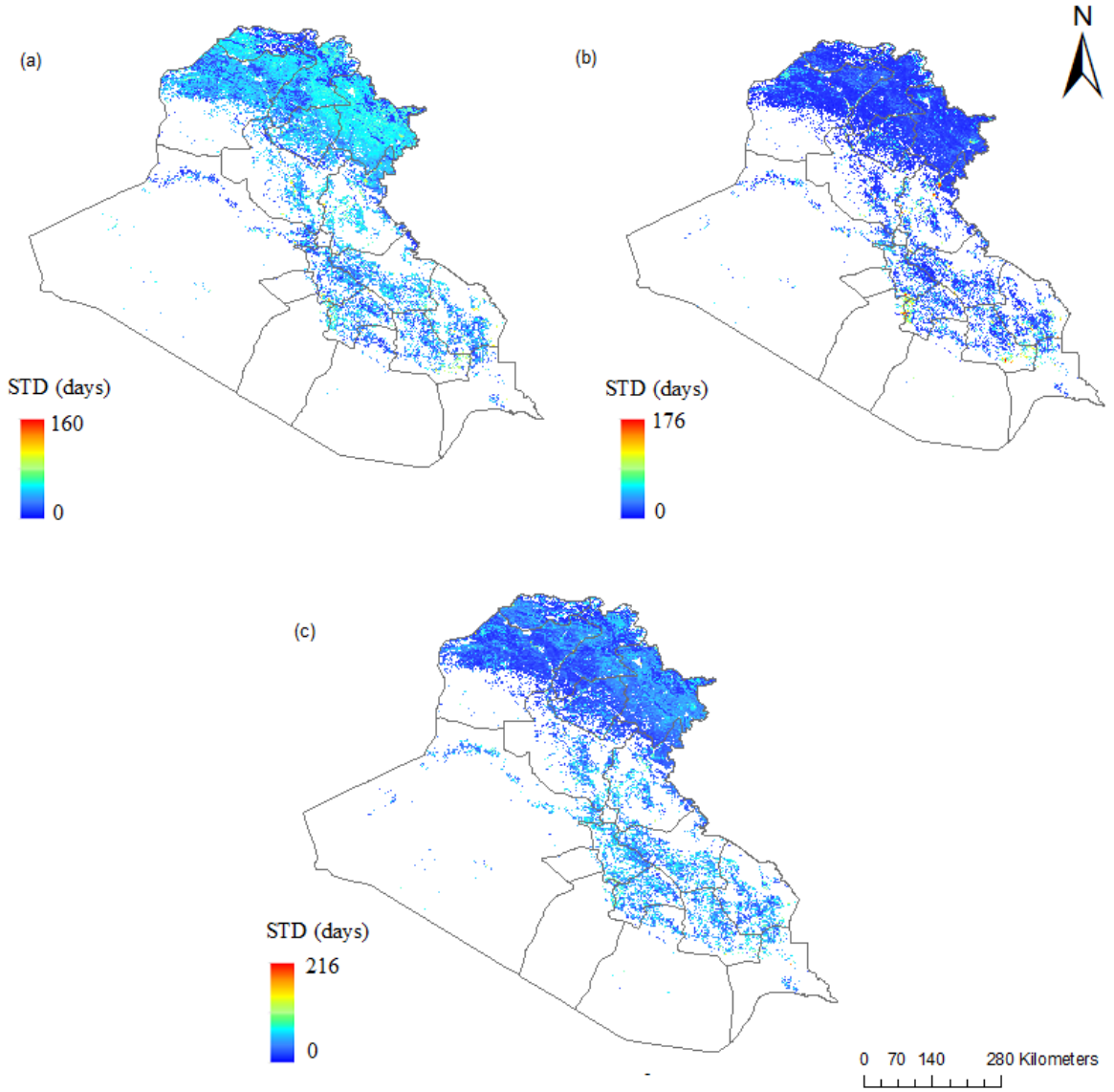

Figure 3-6 Standard deviation of LSP parameters (a) SOS (b) EOS and (c) (LOS) from 2001 to 2012.

In contrast, a relatively small STD can be observed in EOS across the country (Figure 3.6b). The STD of EOS for the majority of the country ranged between 0 to 32 days. However, the value seemed to increase to 40 to 80 days in some areas close to the source of water, particularly in the central and southern parts of Iraq. This result might be because of practicing different crop types in these areas between years. As for SOS, some areas connected directly to available water exhibited the largest STD of EOS.

As expected, it is apparent from Figure 3.6c that the STDs of LOS for natural vegetation cover types such as shrubland and grassland are relatively small,

especially in the northern part of the country which is mostly rain-fed (0 to 32 days). In contrast, a relatively large STD of LOS was detected for croplands (around 56 days and more), particularly in the middle and southern parts of the country, which are mostly irrigated areas.

3.3.3 The relation of LSP parameters of dominant vegetation types to elevation

Over the whole of Iraq, the most dominant land cover types such as cropland, shrubland and grassland were analysed to assess the effect of elevation on the LSP parameters (Figure 3.7). Because the country's rainfall and temperature vary considerably based on elevation, amongst other factors, elevation can be considered as one of the main factors potentially driving spatial variation in the LSP parameters. Generally, as expected, considerable variation in the SOS and EOS was found with elevation for all land cover types across the country (Table 3.1).

Table 3.1 Linear regression parameters defining the coefficient of determination between the median LSP parameters (SOS, EOS, LOS) and elevation.

Type	No. of samples	Y-intercept			Slope			R^2		
		SOS	EOS	LOS	SOS	EOS	LOS	SOS	EOS	LOS
Crop	99313	346.80	510.43	175.07	0.06	0.045	-0.027	0.539	0.638	0.155
Grass	41207	354.07	530.15	176.14	0.047	0.024	-0.021	0.528	0.588	0.161
Shrub	75256	325.501	502.19	160.20	0.064	0.048	0.001	0.481	0.685	0.07

The largest positive coefficient of determination between the SOS and elevation was found for croplands (R^2=0.539, $p<0.05$) (Figure 3.7a). It seems possible that this result is due to the existence of irrigation water at the beginning of the season in the south (lowlands) to irrigate croplands, which led to an earlier green up, and weather conditions varying with respect to elevation in the north (highlands), which delayed green up. In other words, the SOS was delayed with respect to elevation from the south to the north of the country which resulted in a relatively large positive coefficient of determination compared to the other classes. Similarly, grassland produced a positive coefficient of determination

between SOS and elevation (R^2 =0.528, p<0.05) (Figure 3.7d). This might be due to the location of this land cover type in mountainous areas with high relief. The temperature in this region is relatively cold, especially in winter, which delays the start of the season compared to the rest of the country. In comparison to the other classes, shrubland produced a small positive coefficient of determination (R^2 =0.481, p<0.05) due to the fact that this class is divided almost equally into lowlands and (relatively) highlands (Figure 3.7g). Thus, excluding the very high mountainous area for this land cover type may lead to a relatively small coefficient of determination compared to the other classes for SOS. However, the coefficient of determination between EOS and elevation was the largest compared to the other parameters, particularly for shrublands and croplands (R^2 =0.685 and R^2 =0.635, p<0.05, respectively) (Figure 3.7b and 3.7h). The reason could be that half of these classes are located in the lowlands and this area is expected to have an earlier EOS compared to the rest of the country. In contrast, this coefficient of determination was smaller for grasslands (R^2= 0.588, p<0.05) (Figure 3.7e).

Very small positive coefficient of determination were observed between the LOS and elevation for cropland, grassland and shrubland vegetation types (R^2=0.155, R^2=0.161 and R^2=0.07, respectively, p<0.05) (Figure 3.7c, 3.7f and 3.7i). Low elevation is effectively being used as a proxy for irrigation, which cancels out the normal effect of elevation on LOS. Although EOS in the lowlands occurred early, the source of water at the beginning of the season made the LOS in this area longer than for the rest of the country. On the other hand, a very late EOS at high elevation did not mean that the vegetation types of this area had a long LOS because the plants need to complete their growing season, which started later.

Because the MODIS land cover type is a global land cover classification, at regional level the product might not be able to adequately classify the required local land cover types. Therefore, the possibility of misclassification in some areas should be taken into account in the present study. For instance, in very high elevation areas, a large delay in EOS was recorded for some areas of shrubland which, in reality, might be caused by a mix of grassland and other cover types (Figure 3.7h). Finally, increasing the elevation by 500 m will delay the SOS in cropland and shrubland by around 30 days, and grassland about 25 days as well as delay EOS by around 22 days in cropland and shrubland, and grassland by around 12 days.

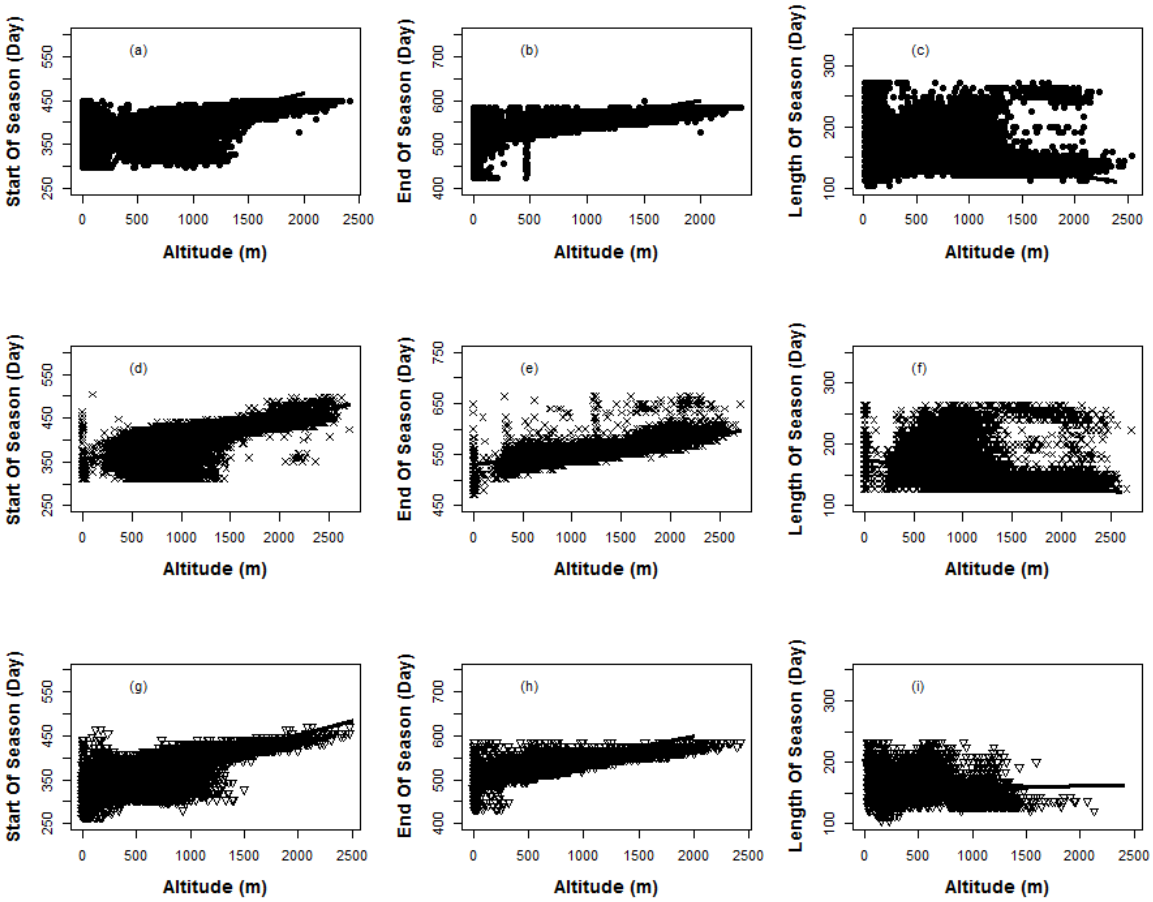

Figure 3-7 Changes in SOS, EOS and LOS for three major vegetation types with elevation variation in Iraq {(a, b and c for cropland), (d, e and f for grassland) and (g, h and i for shrubland)}. For SOS and EOS, values on the y axis up to 365 days belong to the previous year and above belong to the following year, due to the timing of the growing season in Iraq.

3.4 Discussion

In arid and semi-arid regions, LSP parameters can vary considerably spatially depending on variation in water availability, climate, soil type, and vegetation composition. Remote sensing is the only viable means of characterising and monitoring vegetation phenology at the country-scale (Ganguly et al. 2010; Dunn and De Beurs, 2011; Chuanfu et al. 2012), and this is particularly true of Iraq where access is restricted due to security issues. However, validation of the LSP parameters estimated from remotely sensed data is often absent. Both direct evaluation and indirect evaluation, through comparison of LSP estimated from remotely sensed data and in situ observations upscaled through fine spatial

resolution remote sensing data, have been applied in many cases (Zhang et al. 2006; Fontana et al. 2008; Hmimina et al. 2013; Fisher and Mustard, 2007). However, validation of the results presented here is challenging because (i) this research attempted to establish for the first time a comprehensive characterisation of the vegetation phenological characteristics of the major vegetation types over Iraq; (ii) a very limited number of earlier studies of the vegetation phenology across Iraq were attempted or available at the local scale and (iii) no ground vegetation phenological stations exist across Iraq.

Due to its climatic and topographic variation, Iraq is a land of different vegetation types. For example, in only four governorates in the Kurdistan region 67 species were detected distributed in 32 genera, 16 families and 9 orders (Aziz, 2011). Thus, spatial mixing of vegetation types at finer classification levels (e.g., species, genera) in Iraq is common. In addition, the small agricultural field size in Iraq compared to the coarse spatial resolution of the data used in this study may to lead to mixed vegetation types in the area (e.g., where adjacent fields are covered by different vegetation types). A second issue is that the land cover classification used for the current research was a global land cover classification. Thus, it might be possible that the product was not able to provide accurate mapping at a regional level for some land cover types. Pflugmacher et al. (2011) and Acharya and Punia (2013) reported some disagreement with MODIS land cover types for some vegetation covers at a local level over Northern Eurasia and India. They pointed out that the uncertainties could be related to the classification process using the training dataset. Moreover, the sample size of each class and its adjustment process led to high uncertainty resulting in overestimation or underestimation. However, the overall pattern of LSP parameters observed has a strong similarity with the expected phenological pattern for the dominant vegetation types. For example, in the cropland and shrubland areas, an earlier SOS for the central and southern parts and delayed SOS for the north were detected. This result may be explained by the fact that generally the area is divided into two agro-zones; the central and southern parts are mostly irrigated and the majority of the north is rain-fed (FAO, 2008; Schnepf, 2004). This makes the possibility for advancing SOS in the central and southern parts due the availability of the water at the beginning of the season and delaying SOS in the north (rain-fed) due to rainfall and temperature constraints which depend on elevation. Moreover, the late SOS and EOS with a short LOS were detected for grasslands located in the high elevation area. A possible explanation for this might be that a very short growing season and reduced photosynthetic activity

can be attributed to high elevation areas due to weather conditions such as snow and limited rainfall (Inouye and Wielgolaski, 2003). The current research also found that the EOS in the central and southern parts was earlier than in the north. This could be the result of moisture scarcity and temperature increasing from the north to the south of the area due to changes in elevation. In terms of vegetation phenological patterns, the current findings are consistent with those of other studies where the vegetation phenology pattern of some spatially restricted parts of Iraq (including rain-fed and irrigated areas) were shown (Griffin and Kunz 2009; Gibson et al. 2012).

The STD was used to indicate the most variable locations through the last decade in terms of specific LSP parameters. It was apparent that variation in the SOS was more obvious compared to EOS, particularly in the north. There are several possible explanations for this result. The most likely explanation is that the area is mostly reliant on rainfall for starting the growing season either directly in rain-fed areas or indirectly to recharge the two main rivers in irrigated areas (Schnepf, 2004). Another possible explanation is that these areas are under the control of human activity. Further, practising crop rotation and the traditional biennial system to recharge the depleted soil are other reasons for the observed variation (Schnepf, 2004). However, a relative homogeneity in STD for EOS may be the result of sharing a common hot season around the time of the EOS. The heterogeneity indicated by the STD for LOS for cropland area is also due to mainly human interactions such as application of different crop growing systems among years and different policies for planting and harvesting which may affect the LOS. In contrast, this variation is relatively small in natural vegetation types such as shrubland and grassland, particularly in the north of the country. Because this area is mainly reliant on rainfall, changing the timing of the start of rain might not affect much the LOS, as plants need to complete their growing season, whether SOS might be advanced or delayed. Besides, for natural vegetation less variation in LOS is expected due to lack of human interaction compared to croplands.

Relationships exist between the LSP parameters and elevation (Murray et al. 1989; Gimenez-Benavides et al. 2007; Li et al. 2010). The findings of the current study are consistent with those of Ding et al. (2013) who found that an increase in elevation delayed the SOS, delayed EOS and shortened the LOS of grassland in the Qinghai-Tibetan Plateau from 1999 to 2009. These findings further support the observed regularity of the variation in LSP parameters along with elevation in

areas of very high elevation compared to low elevation, which may reflect the influence of human activity in the lowlands (Li et al. 2010; Ding et al. 2013). More interesting is the large coefficient of determination between EOS and elevation for all land cover types, in contrast to many studies which point to a general trend of delayed EOS at lower elevation (Qiu et al. 2013; Jeganathan et al. 2010; Zhang et al. 2004). The reason could be as a result of rapid declines in moisture and rapidly rising temperatures in the hot season at the end of the vegetation growing season, moving from south to north, as a function of variation in elevation in Iraq.

Several factors affected the coefficient of determination between the LSP parameters and elevation. The main influence is likely to be the use of a global land cover product with an overall accuracy of 75% to provide the country's land cover types especially given that the product was not able to provide accurate mapping at the regional level for some land cover types. In addition, there are no studies that assess the accuracy of MODIS land cover across Iraq. The error in land cover classification might have some impact on the LSP characterisation of individual land cover types presented in this study. Moreover, the 250 m spatial resolution of MODIS land surface reflectance may also prevent capture of a pure vegetation type's phenology information in some areas since the size of agricultural land parcels in Iraq is relatively small. The middle and southern parts of the country are mainly flat, irrigated areas which are more managed in terms of planting and harvesting, which may reduce the effect of elevation on vegetation phenological variation.

3.5 Conclusion

For the first time LSP parameters of terrestrial vegetation were mapped across Iraq at a spatial resolution of 250 m. The aim was to identify and map the spatiotemporal variation in LSP parameters such as SOS, LOS and EOS across the country between 2001 and 2012, and to explore their relation with elevation. The median vegetation phenology (SOS, EOS and LOS) was mapped for different vegetation types during 2001-2012.

This study quantified the spatial variation in LSP across the whole of Iraq for all vegetation types, thus, providing an important example of mapping vegetation phenology in a semi-arid environment, for which previous research has been relatively lacking. Linear regression analysis revealed that elevation was positively

correlated with all LSP parameters particularly EOS (R^2=0.685, R^2=0.638 and R^2=0.588, p<0.05 in shrubland, cropland and grassland, respectively). In contrast, in most case studies in Europe the correlation coefficient between EOS and elevation was negative due to the effect of low temperature at high elevations as a driving factor in bringing the season to an early end. In Iraq, raising the elevation by 500 m leads to a delay in EOS by around 22 or more days in all vegetation types because conversely high temperature is the limiting factor bringing the season to an end. The results of this investigation also indicate that the relative lowland in the north of the country (mostly croplands and shrublands) exhibited the greatest variability in terms of SOS during the last decade with a STD of around 80 to 120 days, due mainly to the practice of crop rotation and the traditional biennial cropping system. However, importantly, the variation in EOS was very small, indicating an extremely consistent EOS across Iraq, implicating the effect of high temperature, overwhelming other factors. So, while elevation delays the EOS by postponing the approach of high, limiting temperatures, this effect is applied in a highly consistent manner across years.

The research has several practical applications. Firstly, knowledge of the spatial distribution of the timing of vegetation phenology events, in particular in the agricultural regions of Iraq, can be useful for agricultural management practices. For example, the timing of fertiliser application can be targeted for a few weeks after the start of the season. Secondly, the variation in vegetation phenology information from the current study can be used as a surrogate for identifying areas of changing land cover or agricultural practices during the last decade. As different land cover types have distinct phenological characteristics, changes in land cover result in a large amount of variability (large standard deviation) in the mapped phenological variables during the period.

It is recommended that future research should focus on the use of vegetation phenology to classify land cover directly, and exploring the relations between inter-annual phenological changes and climate changes in Iraq.

Chapter 4: **Decadal vegetation land cover monitoring in Iraq based on satellite derived phenological parameters**

4.1 Introduction

Monitoring crop area and crop condition, and the resulting yield, provides crucial information for ensuring food security (FAO 2012; Tilman 2001). Rapid population growth has resulted in increased global and regional demand for food production. At the same time, the effects of climate change, pests, and disease have added further pressures on the food production system to meet this rising demand. Although increases in food production have been achieved by increasing the area of land under agriculture over the last few decades, this has resulted in negative impacts on the environment and ecosystems. For example, Tilman et al. 2011 found an increase in the demand for crops commensurate to increases in the real income per capita since 1960 and this relationship forecasts a 100-110% increase in global crop demand from 2005 to 2050. The research also indicated that if current trends of greater agricultural intensification and extensification continue, ~1 billion ha of land might be cleared globally by 2050, with CO_2-C equivalent greenhouse gas emissions reaching ~3Gt y^{-1} and N use ~250 Mt y^{-1}. Many studies also highlighted the danger of land use/land cover (LULC) change driven by cropland expansion at the expense of other land cover types (such as loss of biodiversity and modification to the biogeochemical cycle), (Sitch et al. 2005; Brink and Eva 2009; Pongratz et al. 2009; Akinyemi 2013; Matinfar et al. 2013). Therefore, accurate information on LULC and its change over time is an essential requirement for national and international agencies for policy formulation. This information is even more important in areas affected by climate, environmental or socio-political changes.

---

[2]QADER, S. H., DASH, J. & ATKINSON, P. M. (2016). Classification of vegetation type in Iraq using satellite-based phenological parameters. IEEE Journal of Selected Topics in Applied Earth Observation and Remote Sensing, 9(1), 414-424.

Primary information of importance in various application areas such as food insecurity, climate change impacts and agricultural management can be obtained directly/indirectly from land cover maps (Running et al. 1994; Wardlow and Egbert 2008; Ran et al. 2012; Potgieter et al. 2013). The environmental modelling community could benefit from accurate maps of the spatial distribution of croplands and natural vegetation to better parameterize biogeochemical (Burke et al. 1991; Low et al. 2013), crop yield and water demand models Kastens et al. 2005). Furthermore, updated annual land cover maps can be utilized by policy makers and scientists to improve regional scale agricultural management practices under a variety of environmental problems.

This chapter focuses on the use of time-series remotely sensed information for the classification of cropland area in arid and semi-arid regions, using Iraq as an example. In Iraq, there is no reliable system for predicting cropland distribution and area, and forecasting yield, and the official Iraqi government statistics may be unreliable (USDA FAS 2008). Therefore, farmers and policy makers alike require accurate classified land cover maps, particularly for croplands. In future, quantifying cropland area could be essential to forecasting regional crop yield. Iraq has been subjected to major natural and anthropogenic disturbances such as drought and war during the last two decades. These factors together with an unsustainable agricultural policy have led to exploitation of Iraq's agricultural lands with frequent changes in crop area and cropping types. For instance, the impact of three decades of nearly continuous war and instability on the central cultivated area was assessed using Landsat data and the results revealed a 20% reduction in area during the Post-Gulf War period compared to the sanction period (Gibson et al. 2012). Other estimates revealed an annual degradation of around 40000 ha in arable land due to salinization, desertification, improper management and implementation of traditional irrigation systems (National development plan 2010). However, currently there is no reliable map of cropland area across the country and it has been demonstrated that the official Iraqi government statistics are likely to be unreliable (USDA FAS 2008). Therefore, a rapid agriculture monitoring system is required to provide accurate and up-to-date information to national policy makers.

Over the past decade, research on land cover classification has included the use of vegetation phenological information to differentiate between land cover types. In particular, land surface phenology (LSP) as observed by satellite sensors provides the potential opportunity to map vegetated land cover at regional-to-

global scales by identifying their distinct phenological characteristics (Lupo et al. 2007; Newstrom et al. 1994; Gu et al. 2010; Clerici et al. 2012). For example, to exploit information related to the phenological variability of different land cover types, the global MODIS land cover map employed around 135 features including annual metrics (minimum, maximum and mean values) of the enhanced vegetation index (EVI), land surface temperature (LST) and nadir BRDF-adjusted reflectance (NBAR) as inputs to classify global land cover (Freidl et al. 2010). It is also claimed that phenology-based classifications, which are based on analysis of time-series data, can produce more accurate classifications compared to traditional methods. First, at different phenological stages, time-series data can provide more discriminatory information, compared to single date image (Key et al. 2001; Singh and Glenn 2009). Second, multi-temporal data may increase the quality of data as the Sun angle changes with the seasons, which affects surface reflectance Song and Woodcock 2003). Lastly, time-series data have the potential to provide a larger number of predictor variables which can be exploited by machine learning approaches with the potential to provide more accurate and more robust classification (Pal and Mather 2005; Ham et al. 2005). For instance, a phenology-based approach to identify crop types, using phenological parameters from MODIS-NDVI, was compared to the traditional maximum-likelihood classification, revealing the advantages of the former approach (Zhong et al. 2011). Furthermore, the time-series MODIS-NDVI data were employed to estimate key phenological parameters to discriminate crop types and their areas over northern China (Zhang et al. 2008). A large coefficient of determination was found between areas estimated by MODIS and statistics at the county level. Besides the difficulties in discriminating cultivated and non-cultivated areas in the arid and semi-arid regions of northern Asia due to their similar seasonal changes, Enkhzaya and Tateishi (2011) claimed that several phenological parameters estimated from MODIS-NDVI could be used to differentiate cultivated area in these regions efficiently.

The complexity of land covers often means that LULC classification remains a challenging task. Numerous classification algorithms have been applied to solve complex classification problems for LULC monitoring (Wilkinson 2005; Lu and Weng 2007). These techniques range from unsupervised algorithms (e.g., Vogelmann et al. 1998) to supervised algorithms such as maximum likelihood (e.g., Dean and Smith 2003) and machine learning, non-parametric algorithms. Unlike parametric algorithms, non-parametric algorithms do not require the data to have a specific statistical distribution. In addition, the advantages of machine

learning classification algorithms over traditional classification algorithms have been demonstrated in many studies, particularly when the ground cover is complex and different statistical distributions exist (Paola and Schowengerdt 1995; Mas and Flores 2008; Mountrakis et al. 2011; Batistella et al. 2012; Wang et al. 2014). Furthermore, the incorporation of machine learning methods in remote sensing-based classification has increased for various reasons including: their ability to learn complex patterns, mostly non-linear; their ability to handle incomplete or noisy data due to their high generalisation capacity; and their independence with respect to the data statistical distribution, which makes it easy to deal with data from various sources (Mas and Flores 2008; Rogan et al. 2008; Mountrakis et al. 2011; Shao and Lunetta 2012).

The support vector machine (SVM) classifier, which has been utilized in many studies for the classification of remotely sensed data (Rodriguez-Galiano and M. Chica-Rivas 2012; Jia et al. 2012; Duro et al. 2012), was employed in this study. Initially, the SVM was developed by Cortes and Vapnik (Cortes and Vapnik 1995), and a detailed description of the SVM method is given by Burges (1998). Comparative studies have been conducted previously to examine the relative performance of different classification algorithms including the SVM. For instance, thematic mapping accuracies were compared using four classification algorithms: decision trees, (three-layer backpropagation) neural networks, maximum-likelihood and SVM classifiers (Huang et al. 2002). In general, the accuracy of the SVM was greater than the other three classifiers. Recently Shao and Lunetta (2012) examined the ability of the SVM classifier in terms of training sample size, landscape homogeneity (purity) and sample variability using MODIS time-series data. In this research, the SVM was compared to nonparametric classification algorithms: the multi-layer perceptron neural network and classification and regression trees (CART).

There have been limited studies of phenology-based classification in arid and semi-arid environments in the subtropical regions. Vegetation phenology in these regions is driven mainly by the availability of rainfall, whereas in northern high latitudes vegetation phenology is driven mainly by temperature. Due to their similar spectral and phenological characteristics, accurate discrimination between croplands and natural vegetation is challenging in these environments. In addition, regular changes in agricultural area, particularly croplands, increase the complexity of the task. Therefore, the current research aimed to develop and apply a phenology-based classification approach for the assessment of dominant

vegetation land cover types (VLC) in Iraq, particularly croplands from 2002 to 2012.

4.2 Methods

4.2.1 Study area

Iraq has a total surface area of 438,320 km^2 of which around 77.7% is not viable for agriculture in its current condition (UNEP 2007) ((Figure 4.1). Of the remaining 22%, around half is used for marginal agriculture and seasonal grazing. Recent political instability, soil degradation, and the practice of leaving land fallow has led to further reductions in the area of land suitable for agriculture (FAO 2012). Climatologically, Iraq is described as having a subtropical continental climate with an extreme, hot summer with no rainfall, and a short, cool winter (FAO 2011). Precipitation is highly seasonal and more than 90% occurs between November and April. The north and northeast parts have the largest range of rainfall (1200 mm) with less than 100 mm over the majority of the south, and an average of about 2016 mm over the entire region (FAO 2008). Altitudinal variation drives the rainfall considerably from north to south.

Generally, Iraq can be divided into two agro-ecological-zones in terms of crop area; the north is mostly rain-fed and the central and southern parts are mainly irrigated (FAO 2003). The area under cultivated crops, including cereals, vegetables and pulses, is estimated to be around 3.5 to 4 million ha, of which wheat and barley account for 70% to 85% of the cropland in any given year (Schnepf 2004; Gibson et al. 2012). Due to a recent proliferation of plant disease and pests, mono-cropping is practiced more commonly over the country. In terms of the crop calendar, winter wheat and barley are planted in autumn (mainly October-November) and harvested in the late spring (April-June) in accordance with the rainfall pattern, whereas irrigated summer crops such as sorghum, corn, millet and rice are planted in April-May and harvested in September-October, depending on the crop type (Schnepf 2004; FAO 2011).

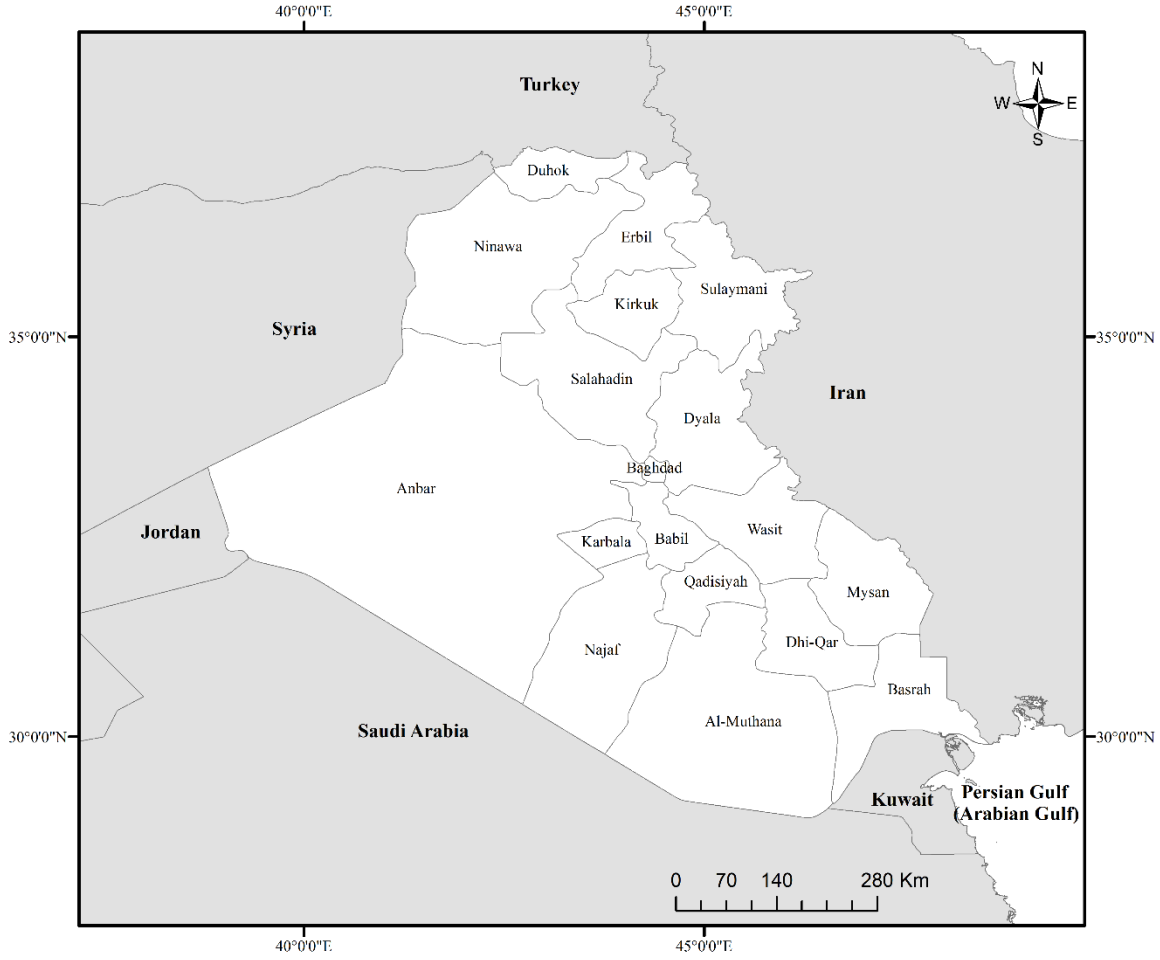

Figure 4-1 Map of the study area. The country is composed of 18 governorates.

4.2.2 Data pre-processing

A time-series of 8-day composites of the MODIS land surface reflectance level-3 data product, with a spatial resolution of 250 m (MOD09Q1 V5) from 2002 to 2013, was used to analyse seasonal phenological features. The data were downloaded from NASA's Land Processes Distributed Active Archive Centre (LP DAAC) (NASA LP DAAC 2013). The information in the QA layer in the MOD09Q1 product was used to remove contaminated pixels due to sensor effects such as different orbits, adjacency, band quality, and MODLAND QA, and non-sensor effects such as cloud state and atmospheric noise. Then, for each time step (compositing period) the NDVI was calculated from the near infrared (NIR) and red surface reflectance. Although, MODIS has a NDVI product, the VLC classification used NDVI calculated from the MODIS land surface reflectance as it has a finer temporal resolution (8-day).

Global MODIS land cover maps (MCD12Q1) at a spatial resolution of 500 m from 2002 to 2012 were acquired from NASA's LP DAAC (NASA LP DAAC 2013) for comparison with the annual VLC classification. Currently, the global MODIS land cover map is the only annual-based land cover map for the country with a hierarchical thematic class legend consisting of 17 classes, of which 11 belong to natural vegetation, three are developed classes and the rest are non-vegetation classes. After extracting the country's land cover types, it was apparent that cropland, shrubland and grassland are the dominant land cover types over the country.

Elevation was considered as an input to the VLC classification. The elevation data for Iraq were extracted from the Shuttle Radar Topography Mission (SRTM) (Jarvis et al. 2008), and to be compatible, the nearest neighbour method was used to resample the elevation data to the spatial resolution of MODIS land surface reflectance (250 m). Historical agricultural activities, including a yearly agricultural statistical record, have been managed through agricultural directors at the governorate level (Abi-Ghanem 2009). Therefore, official government statistics on land use, area and other agricultural activities are aggregated to the governorate level [58]. For the purpose of comparison, the current study employed the area of wheat and barley, as they are the major crops for the first season over the country, from 2002 to 2012 at the governorate level (COSIT 2011).

4.2.3 Estimation of Phenological Parameters and Elevation

The methodology for estimating LSP parameters can be divided into four main steps: (i) moving average window to remove drop outs, (ii) linear interpolation for gap filling, (iii) data smoothing and (iv) LSP parameter estimation. For the purpose of data smoothing, the current study used Fourier-based smoothing due to its minimal requirement for user interaction and because it has been used widely in different regional-to-global studies (Cihlar et al. 1997; Atkinson et al. 2012). The inflection point method was also employed for LSP parameter estimation, due to its easy implementation and the ability to discriminate multiple growing seasons for different land cover types such as crops (Reed et al. 1994). In this process, the start of season (SOS), end of season (EOS) and length of season (LOS) were

estimated per pixel, on an annual basis (the detailed methodology was given in Qader et al. 2015).

Based on these basic parameters, several secondary parameters were estimated from the vegetation phenological pattern to provide additional information for discriminating the vegetation types over the country. In this regard, parameters such as maximum NDVI (max-NDVI), time maximum NDVI (Tmax-NDVI), 75% maximum NDVI (75% max-NDVI), time 75% pre-maximum NDVI (TPRmax-NDVI), time 75% post-maximum NDVI (TPOmax-NDVI), cumulative NDVI, average NDVI (cumulative NDVI/TD3), time difference between max-NDVI, time difference between TPOmax-NDVI and SOS (TD1 and TD2), time difference between TPOmax-NDVI and TPRmax-NDVI (TD3) and time difference between EOS and SOS (LOS) were also estimated from the NDVI time-series profile for each pixel, per season (only season one) ((Figure 4.2).

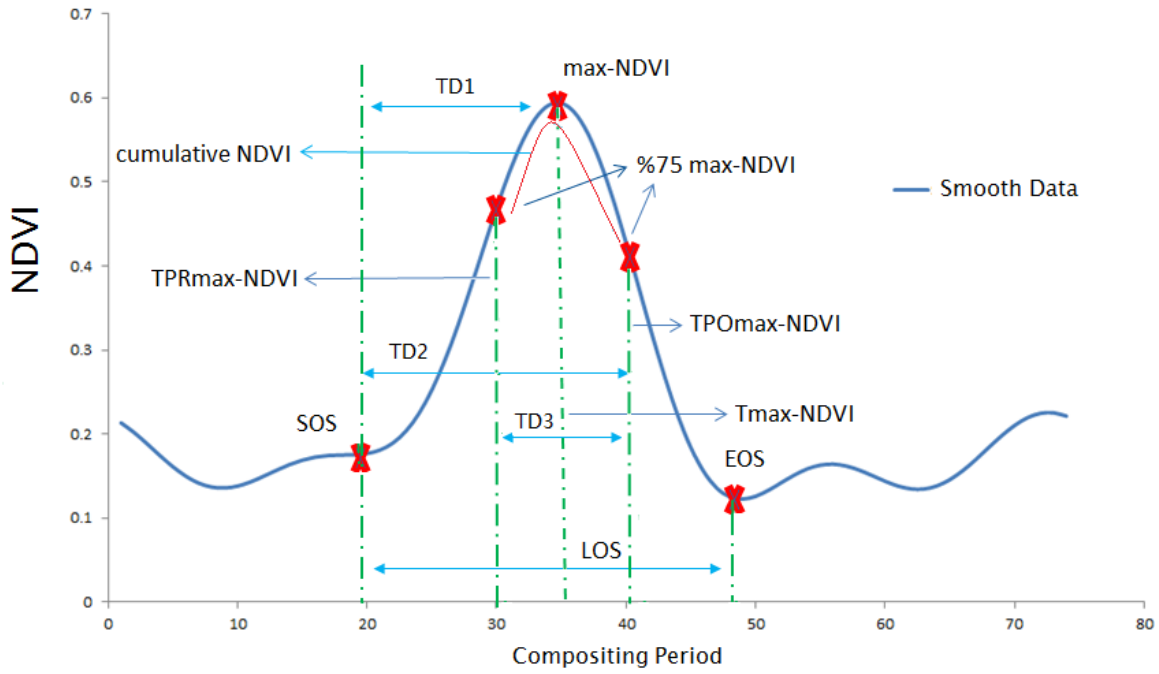

Figure 4-2 Schematic representation of the various phenological parameters estimated in this research. The acronyms are: max-NDVI (maximum NDVI), 75% max-NDVI (75% of maximum NDVI), Tmax-NDVI (time of maximum NNDI), TPRmax-NDVI (time of 75% premaximum NDVI), TPOmax-NDVI (time of 75% postmaximum NDVI), SOS (start of the season), EOS (end of the season), LOS (length of the season), TD1 (time difference between Tmax- NDVI and SOS), TD2 (time difference between TPOmax-NDVI and SOS), and TD3 (time difference between TPOmax-NDVI and TPRmax-NDVI).

The parameters can be categorised as belonging to either the NDVI temporal profile or the timing of the phenological events. Maximum NDVI, which provides an index of the greenness of the vegetation at the time of optimum greenness, can be used as a differentiating variable among vegetation types, as mostly crops have the largest value, followed by grasses and shrubs, respectively. The 75% max-NDVI is located around peak growth, and can be used as a means of classifying vegetation types as crop phenology has a steep slope when approaching the maximum compared to natural vegetation. Average NDVI, indicates the overall greenness while cumulative NDVI indicates the total greenness: both are employed because they are larger in crops compared to grasses and shrubs. Relative parameters such as TD1, TD2, TD3 and LOS were also incorporated. These parameters could be beneficial as different vegetation type's exhibit differences in completing their growing seasons. Apart from the vegetation phenological parameters, elevation was incorporated as an input variable because the region has high altitudinal variation from north to south, which is likely to be a strong influence on the country's land cover distribution (e.g., as a surrogate for the direct influences of temperature and precipitation) (Qader et al. 2015).

4.2.4 Ground reference data collection

Two independent reference datasets were obtained. The first dataset was derived using the fine spatial resolution image layer in Google Earth, including on-screen identification of broad vegetation phenological stages of various vegetation types. To obtain this dataset, a grid with spacing equivalent to a pixel of MOD9AQ1 was overlaid and grid locations with a nearly 100% coverage for the dominant classes (i.e. cropland, shrubland, grassland) were selected as training sites. In total, around 500 samples per year (2003 and 2006) were acquired randomly, in which 250 samples were cropland, 150 samples were shrubland and 100 samples were grassland.

The second dataset was obtained via fieldwork conducted in spring 2013, mainly in the Kurdistan region (Sulaimani, Erbil and Duhok), and excluding the remainder of Iraq due to security restrictions. In total, 104 samples were obtained during the fieldwork, of which 59 samples were cropland and 45 samples were natural vegetation (Figure 4.3a). The samples were taken in homogeneous areas of vegetation classes and these patches were larger than the spatial resolution of the dataset (250 m). Information on the area and height of vegetation types,

along with a field photo per sample, was obtained at each location (Figure 4.3b). In addition, coordinates were also recorded for each sample with a global positioning system (GPS) handheld receiver unit (e-Trex German International Inc) with greater than 12 m accuracy.

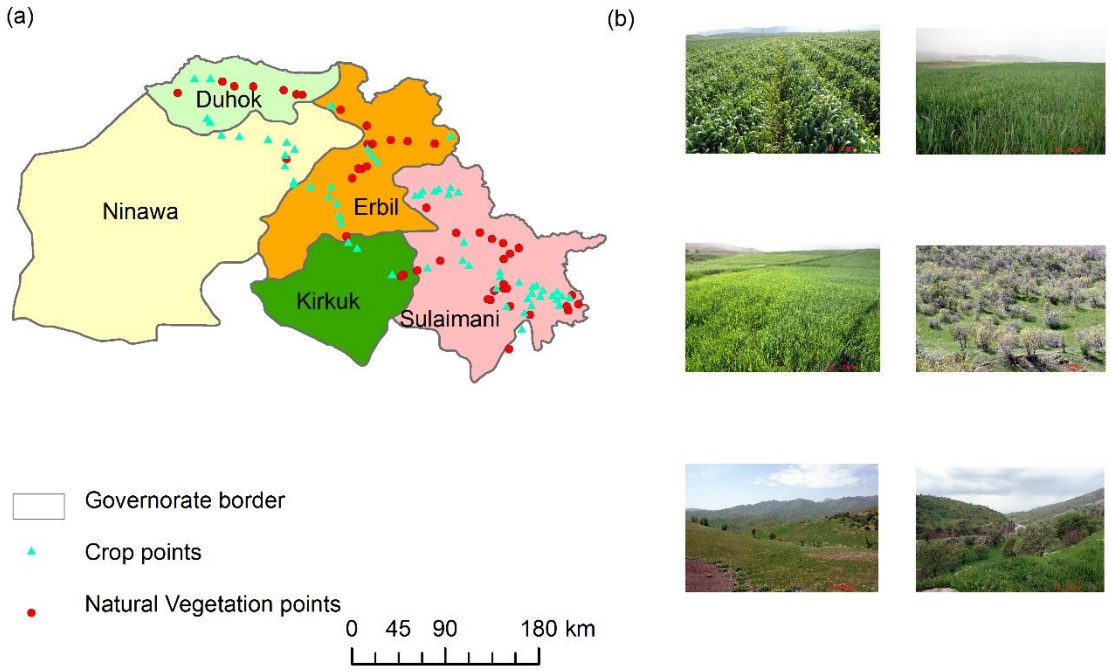

Figure 4-3 Distribution of fieldwork samples over the northern Iraq region, of which 59 sample sites were cropland and 45 sample sites were natural vegetation. (b) Example photographs of crops and natural vegetation in April 2013.

4.2.5 Classification

The SVM classifier has the ability to find the optimal non-linear separating boundary (hyperplane) between classes. The samples located on or close to the hyperplane are known as support vectors where the separability is very low. It may be apparent that there is no ideal solution if the data cannot be separated without error. Therefore, a penalty value C for misclassification errors is introduced (Huang et al. 2002). The adjustment between the complexity of SVMs and the number of separable examples is controlled by C. If the linear approach is not sufficient, non-linear transformation (via kernels) of the feature space into a higher dimensional space (called a Hilbert space) is undertaken, where the data are linearly separable (Muller et al. 2001).

This research employed the radial basis function (RBF) type of SVM where several parameters need to be optimized. The optimization of these parameters has to be sufficient to obtain generalizable models; therefore, care needs to be exercised to not over-fit or under-fit the data. For constructing the SVM model, the cost parameter (C) was explored between 0.1 and 100, at 0.1 intervals, and the gamma parameter between 0.05 and 1, at 0.05 intervals.

For the fine spatial resolution data from Google Earth (500 samples per year; 2003 and 2006), around 375 samples were assigned randomly for training the classification model and the rest were used for validation (see section 2.6). Then, a trained SVM classifier in 2003 was applied to predict the dominant VLC types in 2002, 2003 and 2004, and the trained SVM classifier in 2006 was applied to predict for the remaining years. The 2013 predicted dominant VLC types are not shown as the corresponding ground reference statistical data were not available during this research.

4.2.6 Accuracy assessment

Accuracy assessment of the VLC classification maps was conducted based on independent datasets obtained from (i) fine spatial resolution imagery from Google Earth and (ii) fieldwork data. A confusion matrix was constructed for both datasets to assess the overall accuracy of the predicted VLC classes and the Kappa coefficient per class. For the purpose of accuracy assessment using the fieldwork data, all natural vegetation classes were combined into one class, as the reference samples separated only cropland and natural vegetation, and the assessment was conducted for the northern region of Iraq (Kurdistan region). In addition, to further evaluate the accuracy, the cropland area predicted from the VLC classification at governorate level for each year was compared with estimates obtained from (i) official statistics on cropland area (COSIT 2011) and (ii) global MODIS land cover types. In this regard, linear regression was applied to show the agreement between the crop area estimated from the VLC classification and the official statistics and the global MODIS land cover types at the governorate level (18 governorates) from 2002 to 2012. A flowchart illustrating the research methodology is given in Figure 4.4.

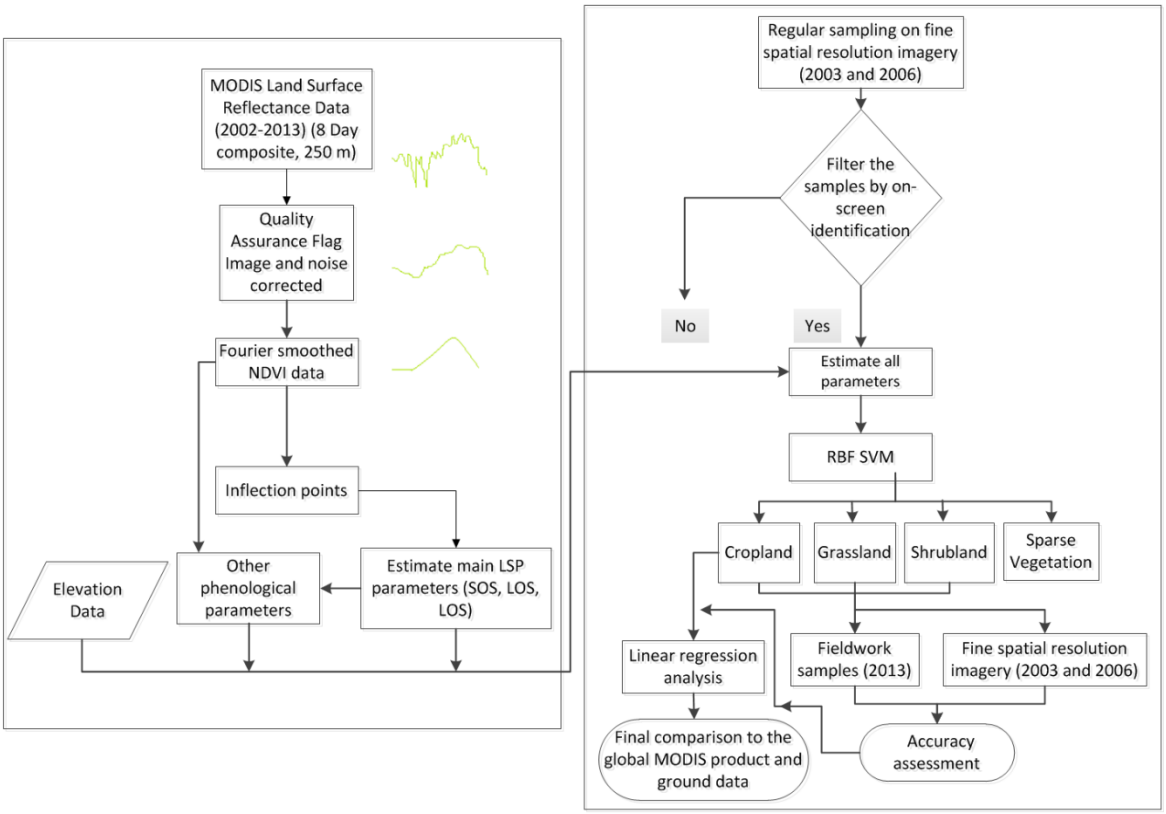

Figure 4-4 Schematic diagram representing the processing steps undertaken in this research.

4.3 Results

4.3.1 Vegetation phenological patterns

Figure 4.5 (a, b and c) gives typical phenological patterns, as depicted by NDVI time-series, for three dominant vegetation land cover types (cropland, grassland and shrubland) in Iraq. In general, the NDVI values for the cropland vegetation type are higher compared to grassland and shrubland. For cropland, there is a sharp increase in NDVI value in January (SOS), a peak at the beginning of April followed by a decrease in NDVI, which reaches a minimum by the beginning of July (EOS) (Figure 4.5a). Grassland is generally found in the rain-fed area and its phenology is controlled by the availability of rainfall. The grassland vegetation type, shown in Figure 4.5b, also has a relatively well defined phenological pattern, particularly in the area where it mixed with sparsely distributed oak trees. Generally, grassland has a late start of the growing season compared to other vegetation types, a less sharp increase in NDVI values from February (SOS),

a peak during May, and a subsequent decrease which reaches a minimum by the end of August (EOS). Shrubland vegetation exhibits an early SOS around November, a peak during the end of February and a decrease which reaches a minimum by the end of May.

It is apparent from Figure 4.5 that there are marked differences in these selected parameters between the vegetation types. Figure 4.5 (d) illustrates the differences amongst the vegetation types in terms of the 75% of maximum NDVI, where it is apparent that cropland has the largest range compared to grassland and shrubland. In general, cropland has the largest value of maximum NDVI which can be used as one of the parameters to separate vegetation types over the region (Figure 4.5e). In addition, the average NDVI parameter across the growing season also provides a good separability between the three classes of interest with the largest value belongs to cropland then grassland and shrubland (Figure 4.5f). Furthermore, these differences in parameters for three land cover types were statistically significance ($p<0.05$).

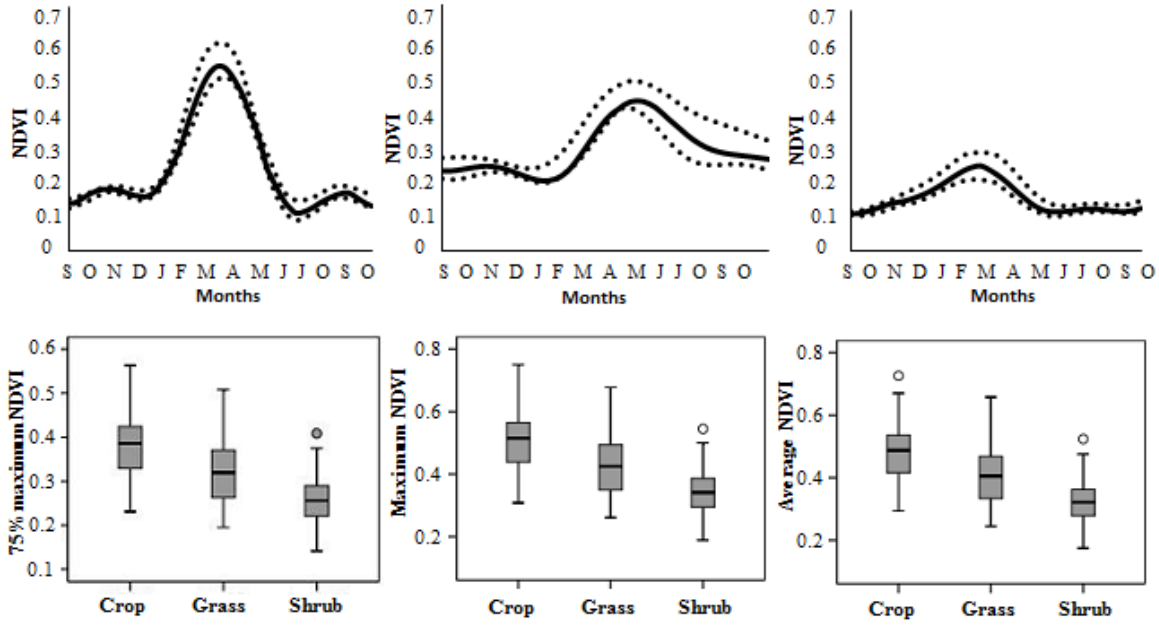

Figure 4-5 Examples of representative MODIS NDVI time-series for the dominant VLC types that have been classified for the study area: (a) cropland; (b) grassland; and (c) shrubland. Ten pure pixels were selected for each land cover type. The bold line represents the Median and the dotted envelopes represent the interquartile range (first and third quartiles). Differences among cropland, grassland, and shrubland classes for selected three parameters used in classification: (d) 75% of maximum NDVI; (e) maximum NDVI; and (f) average NDVI. Each box embodies the first and third quartile. The bold horizontal line

represents the median, whiskers are situated at the maximum and minimum of each group, and white points denote outliers.

4.3.2 Spatial distribution of VLC type in Iraq during 2002-2012

The annual maps of the dominant VLC classes for Iraq from 2002 to 2012 are presented in Figure 4.6. Three distinct types of vegetated area were predicted based on phenological information as well as another class which represents mainly non-vegetated area (or lacked a clear phenological pattern). It is clear from Figure 4.6 that the dominant VLC classes are cropland, shrubland and grassland. Grassland occupies mainly the higher altitudes, particularly in the north and the north-east border. Regular precipitation in the areas occupied by grasslands made this class appear more consistently, inter-annually compared to other VLC classes during the period. Shrubland can be seen commonly amongst the cropland (at low elevation) and may exist also in some areas of unplanted cropland where the traditional biennial cropping system is practiced. Rain-fed croplands are limited in distribution by climate variability and slope. However, accessibility to water from the main rivers (Tigris and Euphrates) together with other conditions such as salinization act as the main drivers of the extension of croplands in the middle and southern parts of Iraq. However, the existence of many phenological similarities makes it difficult to divide croplands into rain-fed and irrigated areas at this spatial resolution, and this is not attempted here.

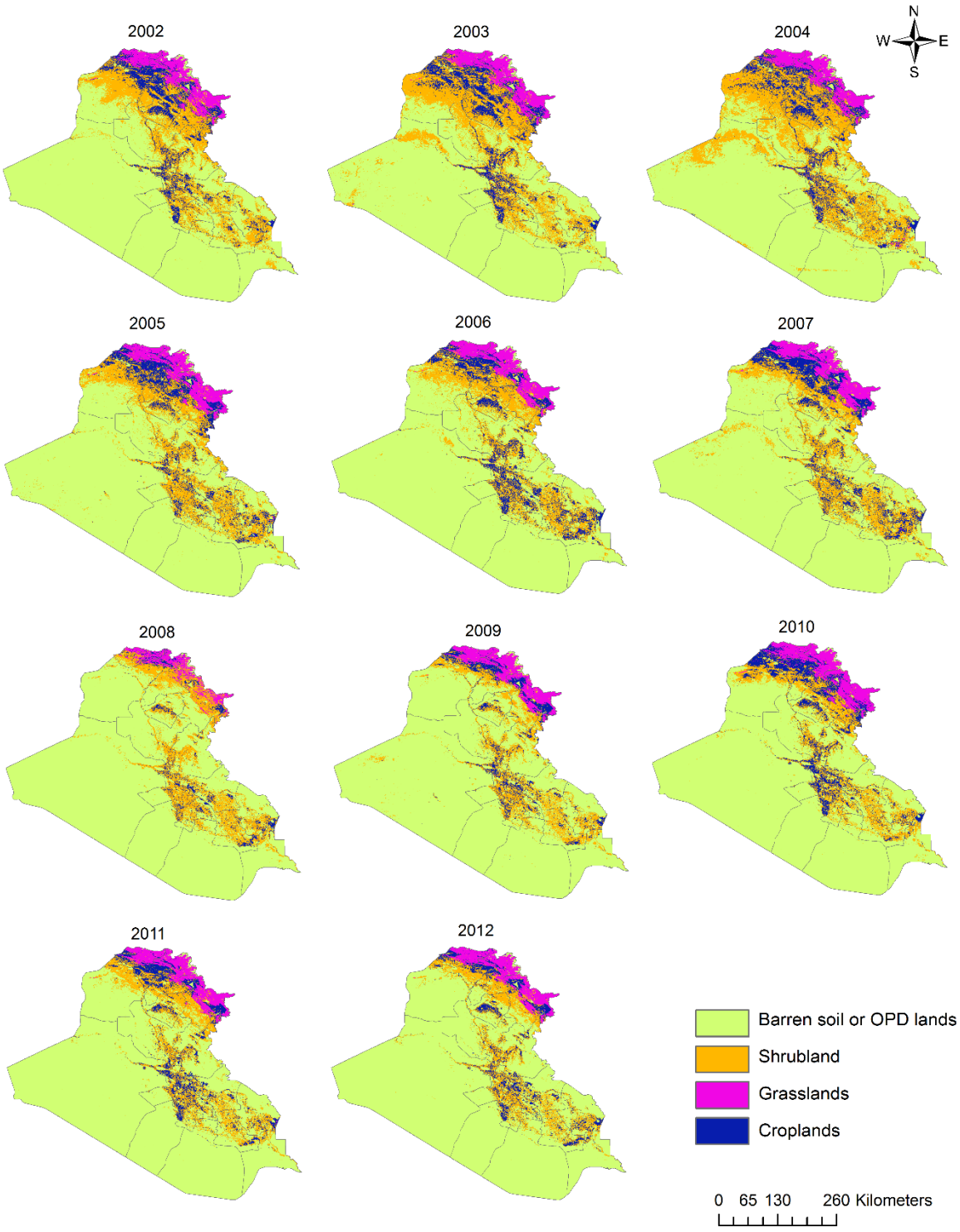

Figure 4-6 Annual maps of the dominant VLC classes for Iraq from 2002 to 2012. (OPD=out of phenological detection).

Winter croplands in Iraq are estimated to cover around 2.5 to 3.5 Mha annually in normal years (UNEP 2007), and the current VLC classification also predicted within that range (Figure 4.7). An average year constitutes 2.8 Mha of cropland, 7.16 Mha of shrubland and 2.01 Mha of grassland in Iraq. A significant decrease in all vegetation types (except shrubland) was observed in 2008 and this is

associated with a severe drought affecting most part of the country (USDA FAS 2008; Abi-Ghanem et al. 2009). The overall spatial pattern in the VLC classes accords with expectations, showing that dense grassland occurs in the high altitude, high relief northern part of Iraq, whereas areas with generally lower relief and the alluvial plains alongside rivers are occupied mostly by cropland and shrubland.

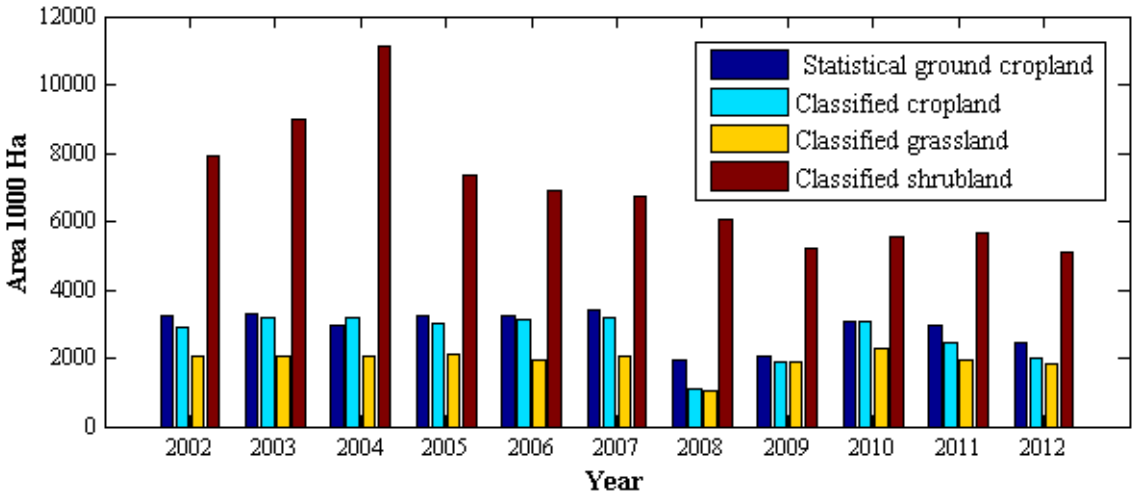

Figure 4-7 Dominant VLC types predicted by SVM classification shown against official statistics on harvested cropland of Iraq from 2002 to 2012.

4.3.3 Accuracy assessment using fine spatial resolution

The overall accuracies estimated using Google Earth fine spatial resolution imagery for 2003 and 2006 were 93.55% and 91.06%, with Kappa coefficients of 0.901 and 0.864, respectively (Table 4.1). Producer's and user's accuracies of the individual categories were consistently high with relatively higher Kappa coefficients per class (Table 4.1). The cropland class had larger errors of omission (0.096) than the shrubland and grassland classes, which suggests some difficulties in differentiating this class from natural vegetation. Most misclassified croplands were mixed pixels located in the borders of agricultural areas in the lowlands. These areas are more challenging to classify accurately due to similar phenological response or an integrated spectral response from multiple VLC types. Consequently, this could be the reason for the relatively high commission error (0.120) of grassland compared to cropland and shrubland.

Table 4.1 Confusion matrix obtained using fine spatial resolution Google Earth imagery for cropland, grassland and shrubland in 2003 and 2006.

Confusion Matrix 2003

Overall Accuracy	93.55%
Kappa Coefficient	0.9015

Class	Producer Accuracy (%)	User Accuracy (%)	Omission error	Commission error	Kappa Coefficient
Croplands	90.38	95.52	0.096	0.040	0.84
Grasslands	96.67	87.88	0.033	0.120	0.95
Shrubland	95.24	95.24	0.047	0.047	0.93

Confusion Matrix 2006

Overall Accuracy	91.06 %
Kappa Coefficient	0.864

Class	Producer Accuracy (%)	User Accuracy (%)	Omission error	Commission error	Kappa Coefficient
Croplands	86	93.48	0.140	0.065	0.78
Grasslands	90.63	93.55	0.093	0.064	0.87
Shrubland	97.56	86.96	0.024	0.130	0.96

4.3.4 Accuracy assessment using field data

Accuracy assessment using field reference data for cropland and natural vegetation in the northern part of the country is shown in Table 4.2 for 2013. The overall accuracy for the northern region map for 2013 was 88.46%, with a Kappa coefficient of 0.80 (Table 4.2). User's and Producer's accuracies were generally greater than 85%, with a Kappa coefficient of 0.86 for cropland and 0.70 for natural vegetation. The source of high omission error (0.200) in the natural vegetation class might arise from confusion when discriminating this VLC type from cropland due to their relatively similar phenological patterns. The classified map and distribution of the fieldwork data are shown in Figure 4.8.

Table 4.2 Confusion matrix obtained using fieldwork data in 2013 for the northern region of Iraq (Kurdistan).

Confusion Matrix 2013					
Overall Accuracy	88.46 %				
Kappa Coefficient	0.80				
Class	**Producer Accuracy (%)**	**User Accuracy (%)**	**Omission error**	**Commission error**	**Kappa Coefficient**
Croplands	94.92	86.15	0.050	0.138	0.86
Natural vegetation	80	92.31	0.200	0.076	0.70

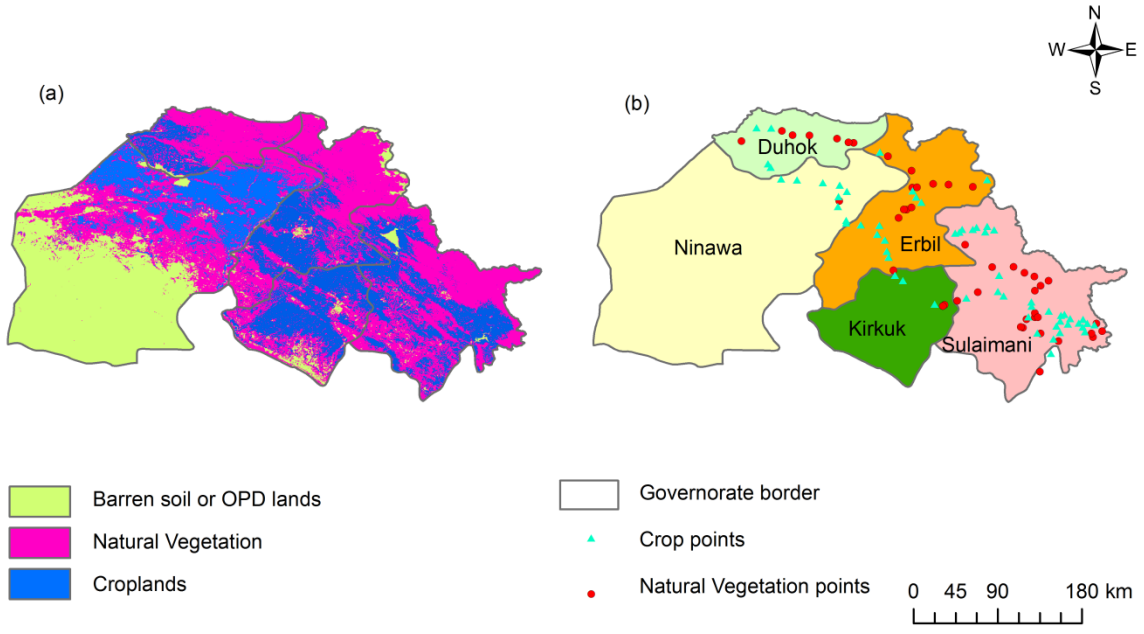

Figure 4-8 (a) Classified land covers types in 2013 for the northern region of Iraq (Kurdistan), (b) the distribution of fieldwork points over the northern region of Iraq (Kurdistan) in 2013.

4.3.5 Comparison between predicted VLC cropland, the global MODIS land cover cropland, and official government statistical data.

The VLC cropland and the global MODIS cropland predictions were compared to the governorate crop reference data to evaluate their agreement over last 12 years at the governorate level (18 governorates) (Fig. 8). Overall, the predicted VLC cropland area at the governorate level produced a larger coefficient of determination with government statistics than the MODIS cropland map. At governorate level, the average coefficient of determination between the VLC cropland area and the government statistics over the last 12 years was 0.7 ($p<0.05$), whereas it was 0.35 ($p<0.05$) for the MODIS cropland. The largest positive coefficient of determination for the VLC cropland area prediction was for 2010 (R^2=0.825, $p<0.05$). In contrast, the same coefficient of determination in 2010 for the MODIS cropland area was the smallest (R^2=0.074, $p<0.05$). Figure 4.9 also shows that the coefficient of determination values for the VLC prediction were more stable compared to the MODIS cropland area, which fluctuated during the period. The smaller coefficient of determination for the MODIS cropland area is entirely expected as it is a global product. Indeed, it is this very fact that motivated this study. Further, on a regional basis, with Iraq as an example, the global MODIS land cover dataset often overestimates cropland area. In summary, the coefficient of determination of the predicted VLC cropland area with official data supports the methodology developed here based on LSP parameters and SVM classification.

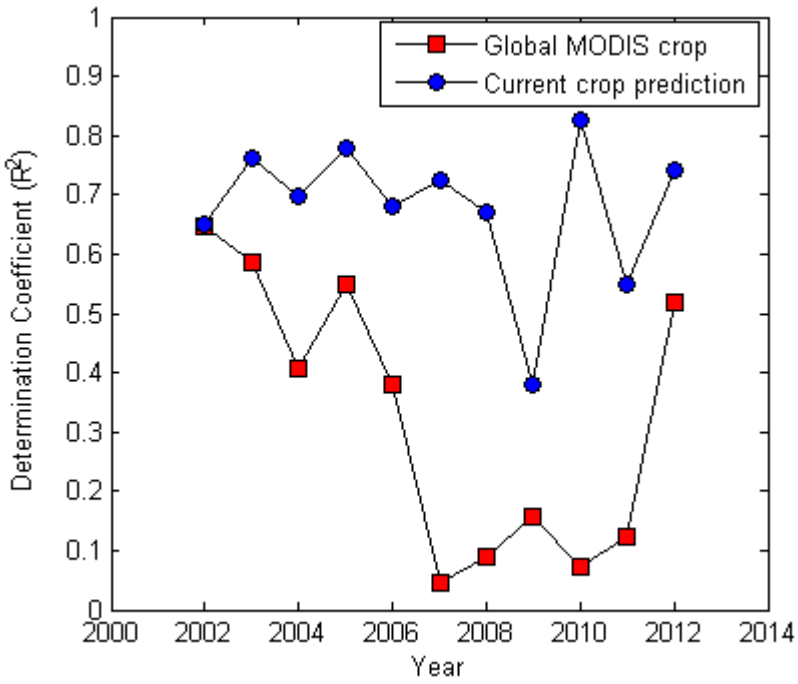

Figure 4-9 Coefficient of determination between official statistics obtained at the governorate level (18 governorates) and 1) the VLC cropland area and 2) the MODIS cropland area predictions per year from 2002 to 2012.

4.4 Discussion

4.4.1 Interannual stability of phenological parameters

Traditionally, ground data collected for a given year are used to support classification from remote sensing data for the same year. However, it may be challenging to collect yearly training data for a study area, especially when working on a historical dataset covering last 15 years. Therefore, it could be useful if training samples from a given year could be applied to estimate the land cover types of other years within a restricted time period (e.g., 4 to 5 years). It can also be argued that, since plant developments are broadly correlated with environmental conditions, years with similar climatic condition may have similar vegetation phenological response. On this basis, the current research trained the classifier for a given year using several phenological parameters and applied this to other periods. These phenological parameters for a given class may vary inter-annually based on (both natural and anthropogenic) environmental conditions.

However, within-class variation in these phenological variables is likely to be much smaller than the overall variation between classes.

The relatively high accuracy of the land cover maps produced for most years is an indicator of limited inter-annual variation in the phenological parameters for the major vegetation types within the study period. However, lower than normal rainfall in 2008 and 2009 led to a deviation in the phenological parameters compared to the training data and resulted in a lower accuracy. As very few acquisition dates were available for the fine spatial resolution Google Earth imagery for those drought years, we were unable to train the classifier to take into account these conditions. Beside of the phenological parameters, the elevation data was incorporated in the current research. This could be explained by the fact that elevation can reduce the miss-classification, particularly in northern part between cropland and grassland, since the grassland occupies the highest altitude area.

4.4.2 The VLC cropland mapping outperformed the MODIS land cover mapping

The accuracy assessment pointed to the need for a more accurate characterisation of croplands in Iraq and demonstrated clearly the need to map Iraq's dominant land covers while global land cover classifications for the country already exist. Compared to the global MODIS land cover classification, the current VLC classification led to greater potential separability and greater classification accuracies for the dominant VLC types, particularly croplands. One interesting finding is that the current VLC cropland classification produced a coefficient of determination with the official statistical crop data at the governorate level that was double that of the global MODIS land cover classification. There are several possible explanations for this result. The reason may be mainly because MODIS land surface reflectance (MOD09Q1 V5) has a finer spatial resolution (250 m) than the MODIS land cover dataset (500 m). This may help to capture more detailed phenological characteristics of the VLC types, which, in turn, helps to classify the regional dominant VLC types more accurately than the MODIS dataset. The coarse spatial resolution of the global MODIS land cover classification may make it challenging to estimate Iraq's land cover types, especially for croplands where the average field size is small compared to a 500 m pixel. In addition, in relation to

the spatial distribution of the training data used in the MODIS dataset, Iraq might be the only country that was actually excluded (Friedl et al. 2010). Most importantly, the MODIS land cover dataset is a global product with an overall accuracy of 75% (Friedl et al. 2010) with the expectation that the product may not be able to provide very accurate agreement at the regional level for some land cover types. The findings of the current research support those of Pflugmacher et al. (2011) and Acharya and Punia (2013) who reported some disagreements with the global MODIS product for some specific land cover types at the local level over India and Northern Eurasia.

4.4.3 Why use phenological parameters and two years of training data?

Initially, we attempted to classify the VLC types using a classifier trained with only a single reference dataset over the entire period, but the accuracies were low. This result may be explained by the fact that the region has been subjected to many disturbances during the last decade (due to both natural and anthropogenic factors) which may affect the phenological response of a pixel. In addition, due to its geographical location the region is affected by irregularities in precipitation resulting in the frequent occurrence of drought (the most recent one in 2008) (Griffin and Kunz 2009; Al-Timimi and Al-Jiboori 2013). The combination of these factors makes it challenging to classify the last 11 years of land cover based on one trained classifier for the entire period. Therefore, to produce VLC classifications for the 11 years of interest, the SVM classifier was trained for two years (2003 and 2006) and these models were then applied to classify the dominant VLC types for the rest of the period. These two specific years were selected for particular reasons that are worth reporting. The primary reason is that the majority of the fine spatial resolution imagery in Google Earth across the country was available for these two years, which assures that the selected samples are assigned to the correct classes (note: in most years, the image acquisition dates were not available). In terms of the climatic condition, each year has a similar climatic condition with one of the two training years. This implementation agrees with the ideas of other studies, in which the classification models were trained in a certain year and these used to predict the LULC types of a relevant period (Friedl et al. 2010; Hansen et al. 2014).

Due to its potential to provide high classification accuracy, phenological-based classification has been employed in many recent studies (e.g., (Zhong et al. 2011;

Zhong at al. 2012; Son et al. 2014; Jianhong et al. 2014; Yan et al. 2015). Incorporation of multi-temporal and phenological-based data led to comparable or increased accuracies relative to traditional approaches based on spectral information alone (Knight et al. 2008; Singh et al. 2009). The phenological-based VLC classification approach developed here for the assessment of the dominant vegetation land cover types of Iraq, particularly cropland, is commensurate with, and adds knowledge to, these studies.

The distribution of land cover types was consistent with expectations. In addition, the annual predictions of cropland area matched well with the official ground statistical data. Therefore, it can be said that the VLC classification methodology developed here based on SVM classification of phenological parameters can be generalizable to other regions with similar environments.

4.4.4 Change in the spatial distribution of VLC classes over the period

As presented in Figure 4.6, the land cover class distribution differed considerably across the country with areas dominated by cropland, grassland and shrubland. The most stable land cover during the period was grassland. This class is confined entirely to the high altitude region of the country which makes it less easily influenced by human activities. This region has a high rainfall rate and a more conducive temperature in summer than the remainder of the country, which makes this land cover type more resilient to drought and other factors. In addition, the sparse distribution of oak trees in grasslands provides some stability in the face of unfavourable climatic conditions by controlling the local micro climate. In contrast, the intervening valleys are mostly occupied either by cropland or shrubland. Surprisingly, the distribution of cropland was found to be spatially varied and decreased overall in area during the period. There are several possible explanations for this result. Due to excessive salinity, around 2.5 million ha of Iraq's irrigated cropland had become degraded by 1973, and in every subsequent year another 6,000 to 12,000 ha were lost to salinization (Schnepf 2004). Traditionally, a biennial fallow system was practiced over Iraq to recharge the depleted soil and reduce the effect of pests and diseases (Schnepf 2004; FAO 2011). This means that a winter crop of wheat and barley was planted only once in every two years. In addition, a lack of inputs of fertilizers and pesticides with

poor crop management policy limited cropland planting to every other year. Furthermore, natural and anthropogenic factors have also accelerated the magnitude of temporal variation in croplands. For example, due to political instability and insecurity during the last decade, many farmers were unable to grow crops. In addition, the region is regularly subjected to drought and its consequences. Therefore, Iraq might have a relatively consistent total annual cropland area, but this might vary spatially which can be detected efficiently through phenological-based classification.

Several important limitations need to be considered. The small agricultural field size in Iraq compared to the coarse spatial resolution of the data used in this study may lead to mixed vegetation types in the area (e.g., where adjacent fields are covered by different vegetation types). Thus, some areas may be challenging to classify accurately because of a similar phenological response or an integrated spectral response from multiple cover types. It is worth noting that regional instability and insecurity limited our fieldwork extent to the north of Iraq. Lastly, the unreliability of official statistical data also limited the ability to assess the accuracy of the classified maps in the current study, although as a function of this, the accuracies obtained can be seen as conservative (USDA 2008).

4.5 Conclusion

Land cover mapping in arid and semi-arid regions is required for a wide range of applications, including grand challenges such as agricultural intensification and food insecurity. However, land cover maps in arid and semi-arid regions are scarce, with a major obstacle to production being the lack of spectral separability between classes when observed at a single point in time. A limited number of studies have demonstrated the potential of vegetation phenology information for land cover classification generally, but until now this has not been applied to arid and semi-arid regions. This research demonstrated that vegetation phenology estimated from MODIS NDVI time-series at 250 m spatial resolution can provide consistent, high accuracy, regional-scale land cover mapping in arid and semi-arid countries such as Iraq. The application of Fourier-based smoothing provided useful phenological information for each year studied. Despite significant limitations on ground data availability due to political instability in the country, the results presented here are convincing. The SVM classifier approach produced

satisfactory classification accuracies (generally > 85%) among the dominant VLC types of Iraq. In terms of regional accuracy assessment and areal agreement with ground crop area data, the VLC classification outperformed the global MODIS land cover dataset. Correlation of VLC cropland area during the last decade with ground statistical data revealed an average coefficient of determination of 0.7 ($p<0.05$), whereas the average agreement for the MODIS product cropland class was 0.35 ($p<0.05$). This research also showed that the 2008 drought, the most extreme event during the last decade in Iraq, led to a considerable decline in all dominant VLC types. VLC instability, particularly for croplands, was evident, most likely due to more than a decade of regional instability and natural disasters across the country coupled with variable quality agricultural management practices.

Chapter 5: **Forecasting wheat and barley crop production in arid and semi-arid regions using remotely sensed primary productivity and crop phenology: a case study in Iraq**

5.1 Introduction

At present, 15% of Earth's population (841 million people) is living in arid and semi-arid regions, of which about 524 million live in semi-arid regions (Barakat, 2009). Rapid population growth (Barakat, 2009) together with rising living standards in arid and semi-arid regions imply that more food will be required to meet the demands of these populations. This is a major driver of land conversion to agricultural and grazing land within these regions (Millennium Ecosystem Assessment, 2005). Therefore, crop production forecasting is potentially a crucial tool for tackling food insecurity in arid and semi-arid regions. However, this is considered one of the most challenging tasks in crop research because of the highly variable climate in arid and semi-arid regions.

In many part of the world, wheat and barley are major grain crops and their production influences local food security in the majority of developing countries (Macdonald and Hall 1980; FAO 2003a). Vast swathes of agricultural land across the world are occupied by wheat and barley. For instance, at the global scale, more than 219 Mil and 49 Mil ha (harvested area) were dedicated to growing wheat and barley, respectively, of which over 715Mil and 143Mil tonnes of cereal were produced in 2013 (FAOSTAT, 2013). Furthermore, wheat and barley play an essential role in international trade, and it has been reported that food shortages are commonly attributable to a lack of wheat and barley (Mellor, 1972). In both developing and developed country contexts, timely and accurate estimation of wheat and barley yield and production before harvesting are, therefore, vital at different governance levels including regional, national and international levels. Such forecasts could increase regional food security, through improved policy

[3]QADER, S. H., QADER, S. H., DASH, J. & ATKINSON, P. M. (submitted). Forecasting wheat and barley crop production in arid and semi-arid regions using remotely sensed primary productivity and crop phenology: a case study in Iraq. *ISPRS Journal of Photogrammetry and Remote Sensing*.

setting and local decision-making, as well as playing a crucial role in informing international markets (Justic and Becker-Reshef, 2007).

In part due to the likelihood of unfavourable climatic events across many arid and semi-arid regions around the world, local communities are often food insecure and at risk of famine. Weather extremes such as droughts, floods and sudden climatic changes can have a direct impact on food production and can negatively affect the storage and distribution of food (Haile 2005; Wheeler and von Braun 2013). For example, the drought in 2008-2009 caused sizeable declines in crop yields, which cost $1-2 billion (USDA FAS, 2008a). In Turkey, 435,000 farmers were affected while in Iraq total wheat production was reduced by 45% compared to the previous year (USDA FAS, 2008a). It was also found that increasing aridity and more frequent and intense meteorological droughts are projected for many arid to semi-arid regions (Seager et al. 2007). Thus, timely crop monitoring and forecasting is crucial to evaluate and quantify the magnitude of any shortfall in production and warn policy-makers and local decision-makers about the possible consequences.

Another factor which makes many of the regions in the world food insecure, and in particular regions in the Middle East such as Iraq, is political instability and its consequences. War and conflict can damage the economy and incomes, disease, forced immigration, refugee populations, a collapse of social trust, and severe food insecurity (WFP, 2011). Conflict was the main cause of undernourishment in more than half of the Middle East countries in the 1990s (FAO, 2003b). There are many reasons for this, including economic crises, high food prices, regions of political instability and climate change. The main drivers of more than 35% of food emergencies from 1992 to 2003 were economic issues and conflict; in contrast, this value was 15% in the period between 1986 and 1991 (FAO, 2003a). Therefore, timely monitoring and forecasting of crop production is especially required in regions where the potential for drought occurs in the context of conflict.

Over the last decade crop production in Iraq has been negatively affected by both natural and anthropogenic events. For instance, Iraq was involved in a war 'Post-Gulf' mainly to oppose the previous regime. Due to political instability during the war, many farmers either abandoned their land or were unable to grow their crops effectively, and this affected overall crop production in the country. In addition, due to its geographical location, Iraq is affected by irregularity in precipitation resulting in the frequent occurrence of droughts. Both factors have

made the region vulnerable to irregularities in food production. However, the impacts of disaster such as drought and war could have been mitigated if decision-makers were warned in advance. For example, the NDVI as a surrogate of vegetation greenness is used in the Famine Early Warning System Network (FEWSNET) as a part of an integrated early warning system for food security (Ross et al. 2009). Such early warning systems would be useful to provide early monitoring data and forecasts of crop production and yield to local authorities to avert regional food shortages.

A wide range of the techniques to estimate and forecast crop yield have been employed during the past decades with different degrees of utility and accuracy. Crop yield estimation in many countries still relies on traditional approaches based on data collection on the ground and reporting (crop cutting experiments). Such data are frequently time consuming, costly and prone to large errors because of incomplete ground observations, leading to uncertain crop area estimation and crop yield assessment (Reynolds et al. 2000). Delayed availability of the data from such traditional approaches delays the ability to make early interventions to avoid food shortages, resulting in regional food insecurity. Crop yield can also be forecasted through either statistical or agronomic models based on historical weather, crop management and crop production data. In some countries, weather data have been employed to monitor and forecast crop production (Andarzian et al. 2008; Liu and Kogan 2002; Paul et al. 2013; de Wit and Boogaard 2001). Missing data, a lack of continuity in weather data and the sparse spatial distribution of ground weather stations for a large diverse crop area limit the utility of these approaches (Liu and Kogan 2002; Dadhwall and Ray 2000; de Wit and Boogaard 2001).

With the development of satellite sensors, there has been increased interest in utilizing satellite remote sensing data for crop monitoring and crop production forecasting due its ability to provide data synoptically, with greater spatial coverage, potentially at the global scale. In addition, remote sensing can provide timely (and potentially real-time) and objective data on crop growth at relatively low cost. In this regard, the NDVI has a long history of use for monitoring crop condition and estimating crop yield (Doraiswamy et al. 2004; Groten, 1993; Kastens et al. 2005). Either remote sensing data can be used as an input to crop simulation models or remotely sensed biophysical variables measured within-season can be used as a surrogate of crop production for use in monitoring and forecasting. One such approach involves biophysical crop simulation models,

which are calibrated and driven through remotely sensed information on crop characteristics within-season. Examples of crop simulation models includes World Food Studies (WOFOST) (Vandiepen et al. 1989), Simulateur mulTIdisciplinaire pour les Cultures Standard (STICS) (Brisson et al. 1998) and Crop Systems Simulation (CROPSYST) (Van Evert and Campbell, 1994). These models assimilate several factors that affect crop growth and development such as temperature, wind, water availability and type of management practice which lead them to be capable of capturing soil-environment-plant interactions (Moriondo et al. 2007). However, the high computational and data demands of these models makes them generally difficult to use in some regions for which data are sparse. In addition, their complexity, method of analysis and large number of tuning parameters have led them to be impractical, particularly capturing field level information in an heterogeneous landscape.

The most widely used approach to estimate crop yield at the regional scale is based on simple regression between a satellite-derived vegetation index within-season and actual crop yield (Wall et al. 2008). A linear regression model was established by Harmmar et al (1996) to estimate wheat and corn yield at the county level based on vegetation indices derived from Landsat multispectral scanner system (MSS) data in Hungary. Similarly, a relatively large coefficient of determination between wheat yield and NDVI integrated over the entire growing season, and with late season NDVI, was observed at the regional and farm scales in Montana for the years 1989-1997 (Labus et al. 2002). Ren et al. (2008) found the largest coefficient of determination between county level winter wheat production and the spatial accumulation of MODIS-NDVI, 40 days ahead of harvest time, and the accuracy was within 10% of official statistics in Shandong Province, China. NDVI, normalized difference water index (NDWI) and a two-band variant of the enhanced vegetation index (EVI2) were employed to predict the US crop yield, and showed that including crop phenology-related information increased the regression model accuracy (Bolton and Friedl 2013). The study indicated that the best dates to predict crop yield were 65-75 days and 80 days after the MODIS derived green up for maize and soybean, respectively for the US.

Because statistical regression-based approaches model the empirical relation between a satellite-derived vegetation index and historical yield data, the model is typically localized and cannot be generalised to other areas readily (Moriondo et al. 2007; Doraiswamy et al. 2003). In addition, if photosynthetic capacity at the time of measurement is not the main driver of the eventual crop yield, forecasting

may be inaccurate (Becker-Reshef et al. 2010). However, the low demand for data and simplicity of implementation has led to regression being the most widely used approach for estimating crop yield.

There have been limited attempts to monitor and forecast crops in arid and semi-arid regions based on remote sensing data. Forecasts of crop production and yield are needed by policy-makers, the academic community and crop insurance companies. In particular, due to population increases, regional instability and natural disasters, there is a growing need for micro-level forecasting of crop production and yield over Iraq. This forecasting should warn local authorities about potential changes in crop production and yield, leading to appropriate import and export decisions. Therefore, the current research aims to evaluate the potential of MODIS-derived measures of greenness and productivity, and information related to the phenology of crops to estimate crop production and yield in the arid and semi-arid regions like Iraq.

5.2 Methods

5.2.1 Study area

Iraq is predominantly an agricultural country, and has long been recognised as one of the oldest agricultural countries in the world (Figure 5.1a). For instance, according to the Meyers (1997), the village called Jarmo, situated in the Iraqi Kurdistan Region, is the oldest known agricultural and pastoral community in the world, dated to the seventh millennium (BC), and agriculture was the primary economic activity of the people of old Mesopotamia. For example, agriculture played a crucial role in the country's economic activity in the 1920s, but its contribution to the gross domestic product (GDP) fell from 42% in 1981 to 18% in 1990 (Jaradat, 2002). Although the agricultural sector is no longer the most significant contributor to the country's economy, it is a vital component in the country's GDP (Schnepf 2004). The contribution of agriculture in GDP declined considerably again during the last few decades due to some unfavourable natural and anthropogenic impacts. For example, the contribution of agriculture in GDP decreased from around 9% in 2002 to 4% in 2008 (FAO, 2009) mainly due to drought. However, this has increased to nearly 12% in 2010 because of some improvements in the sector (USAID, 2010).

Of 3.5 to 4 million ha cultivated crops, 70% to 85% is dedicated to plant wheat and barley in any given year (Schnepf 2004; Gibson et al. 2012). By international standards, Iraq has low crop yields. One third of the country's cereals are produced under rain-fed conditions and the remaining cereal production occurs within irrigated areas between, and along, the Tigris and Euphrates rivers (FAO 2008). The climate varies dramatically through the year from very cold winters to extremely hot and dry summers. The region has large spatial variability in expected rainfall from less than 100 mm year-1 to 1000 mm year-1 (FAO 2008). Estimating and forecasting crop production and yield is a key challenge as the region is still vulnerable to natural factors that impact the yield and production level of major crops. As a result, large inter-annual fluctuations in yield and production can be seen. For example, the production of wheat in 2011 was around 5.1 MT, whereas less than 2 MT and around 3 MT were recorded in 2008 and 2009, respectively (COSIT 2011). This fluctuation can be seen largely among the governorates with respect to climate, soil, water availability and workforce capability.

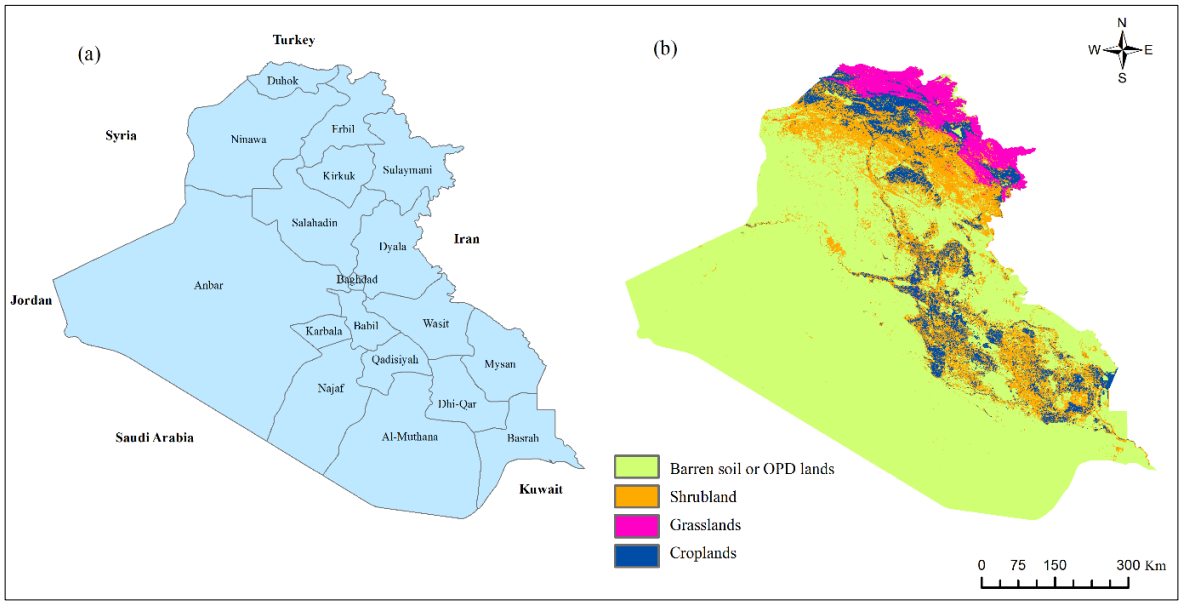

Figure 5-1 Maps (a) study area and (b) an example of phenology-based classification map with spatial resolution of 250 m for 2006 (Qader et al. 2016).

5.2.2 Data and pre-processing

A time-series of 8-day composites of the MODIS land surface reflectance product (MOD09Q1) at 250 m and MOD09A1 at 500 m spatial resolution from 2002 to 2012 were used to estimate NDVI, EVI, and the seasonal phenological parameters. The data were downloaded from NASA's Land Processes Distributed Active Archive Centre (LP DAAC) (https://lpdaac.usgs.gov/data_access). The NDVI has been used widely for crop monitoring and the production of agricultural statistics (Hatfield and Prueger, 2010; Becker-Reshef et al. 2010; Benedetti and Rossini, 1993). NDVI tends to saturate at large biomass, whereas EVI has increased sensitivity in this region (Huete, 1997). In addition, by incorporating the reflectance in the blue band of the electromagnetic spectrum, EVI reduces the impact of the soil background and atmosphere (Rocha and Shaver, 2009; Jiang et al. 2008; Huete et al. 1997). For crop yield forecasting, both indices have been applied widely (Kouadio and Newlands, 2014; Kogan et al. 2012; Moriondo et al. 2007; Doraiswamy et al. 2005).

The information in the quality assurance (QA) layer in the MOD09Q1 and MOD09A1 products was used to remove contaminated pixels due to sensor effects such as different orbits, adjacency, band quality, and MODLAND QA, and non-sensor effects such as cloud state and atmospheric noise (atmospherically corrected and clear cloud state). Then, for each time step (compositing period) the NDVI and EVI were calculated from the surface reflectance data. A temporal moving average window function was applied to correct errors in specific weeks, a linear interpolation approach was applied for gap filling, and Fourier transformation was used to smooth the data (Dash et al. 2010; Qader et al. 2015).

In addition to the vegetation indices, the MODIS Net Primary Productivity (NPP) product was also employed as a predictor of crop production and yield. The term primary productivity refers to the rate at which light energy is converted to plant biomass. The overall converted energy is known as gross primary productivity (GPP). The difference between GPP and energy lost during plant respiration is called NPP. NPP plays a crucial role in studies of global vegetation changes, particularly for global biomass mapping and crop yield estimation (Jianqiang et al. 2007). Satellite-derived NPP has been demonstrated to have a large coefficient of determination with regional crop production. For example, less than 4% error was recorded between forecasted yield and actual yield using NPP extracted from TM

images in the Yaqui Valley, Mexico (Lobell et al. 2003). The NPP model was fitted to the relation between winter wheat yield and a function of MODIS NPP, and the absolute error of estimated yield was 232.7 kg.ha-1 with a relative error of 4.28% (Jianqiang et al. 2007).

NPP (MOD17A3) is an annual product provided from 2002 to 2010 with a spatial resolution of 1000 m (https://lpdaac.usgs.gov/data_access). To retain the best quality pixels, the information in the QA flag layer was also applied for this product (only include pixels falling into the following categories, perennial salt or inland fresh water body cover type, perennial snow or ice cover type, permanent wetlands/inundated marshland, urban/built up and unclassified pixel) (https://lpdaac.usgs.gov/data_access). The product is affected mainly by cloud contamination. Valid annual QA values range from 0 to 100; the higher the number the more the cloud contamination.

5.2.3 Crop statistics data

For winter wheat and barley, data on the total area planted, total area harvested, production and yield from 2002-2012 were obtained from Statistics Iraq (COSIT 2011). In Iraq, agricultural activities are managed through agricultural directors at the governorate level (Abi-Ghanem et al. 2009). Thus, official governorate statistics on agricultural activities such as crop yield, production and area are aggregated to the governorate level. Iraq consists of 18 governorates (Figure 5.1a). The crop data were utilized to fit regression models between winter wheat and barley production and yield and the predictor variables, including various spectral indices derived from MODIS such as NDVI, EVI and NPP at the governorate level.

5.2.4 Crop map

To allow utilization of MODIS VIs and NPP in crop production and yield forecasting, it is necessary to identify the areas under cropping. The crop map for the current research is based on previous work (Qader et al. 2016) in which a phenology-based classification approach was developed to map annually the dominant vegetation land cover types over Iraq such as cropland, grassland and shrubland (Figure 5.1b). The approach employed several phenological parameters together with elevation data to discriminate the dominant vegetation land cover

types using a support vector machine (SVM) classifier. The classification approach was assessed using reference data taken from fine spatial resolution Google Earth imagery and independent testing data obtained through fieldwork. Overall the accuracies were generally >85% with relatively high Kappa coefficients (>86) over all the classified land cover types. To be compatible, the nearest neighbour method was employed to resample the crop map data (250 m) to the spatial resolution of the MODIS EVI (500 m) and MODIS NPP (1000 m). To depict the impact of the spatial resolution on spatial correlation between biophysical variables and crop production at the governorate level, the NDVI (250m) data was up scaled to 500m and 1000m using the nearest neighbour approach to be comparable with EVI (500m) and NPP (1000m) data.

5.2.5 The threshold of indices value utilized to forecast crop yield/production

Several studies indicated that the correlation between final crop production (and yield) and VIs changes through the crop growing season (Doraiswamy et al. 2005; Ren at al. 2008; Huang et al. 2013). Therefore, using crop phenology can have a significant benefit for remote sensing-based crop yield models as crop yields change as a function of time throughout the growing season (Mkhabela et al. 2011; Sakamoto et al. 2013; Bolton and Friedl 2013; Meng et al. 2014). Crop phenology varies spatially and inter-annually and, therefore, forecasting of crop yield based on a VI at a fixed calendar date is not optimal (Bolton and Friedl 2013). In the current research, three different approaches were applied to find the phenological parameters, which have the optimal correlation with crop production and yield at the governorate level in Iraq (Figure 5.2).

The maximum NDVI and EVI were estimated from the smoothed time-series data, which is equal to the peak value for each growing season, and from these maxima, seven (8-day) composite values before and after each maximum were defined. Using this information, time-series values of NDVI and EVI with an 8-day interval, which starts at the seventh 8-day composite before maximum (Maxb7) and ends at the seventh 8-day composite after maximum (Maxa7) over the growing season were extracted (Figure 5.2).

Generally, three different types of VIs variables were suggested in the literature to correlate with final yield such as the original value (Rojas 2007; Esquerdo et al.

2011), integrated value over the growing season (Mkhabela et al. 2005; Wall et al. 2008; Balaghi et al. 2008) and average value (Boken, Shaykewich 2002; Mkhabela et al. 2005). Some studies (e.g. Ren et al. 2008; Becker-Reshef et al. 2010) regressed crop production statistics at the county level on spatially-accumulated NDVI. Other studies (e.g. Tucker et al. 1980; Rojas, 2007) showed that seasonally integrated VIs, could forecast production more accurately than single measures. It has also been demonstrated that VIs around the time of maximum have a large coefficient of determination with final yield (Tucker et al. 1980; Benedetti and Rossini 1993). Therefore, three different approaches were employed in the current research:

1. Approach 1: spatial sum of the single parameter (original value) from Maxb7 to Maxa7 at the governorate level (Figure 5.2 and Table 5.1).
2. Approach 2: cumulative, integrated spatial sum of the parameters from Maxb7 to Maxa7 over the growing season (Figure 5.2 and Table 5.1).
3. Approach 3: integrated spatial sum of the vegetation indices for four composite periods before and four composite periods after the maximum value (Figure 5.2 and Table 5.1).

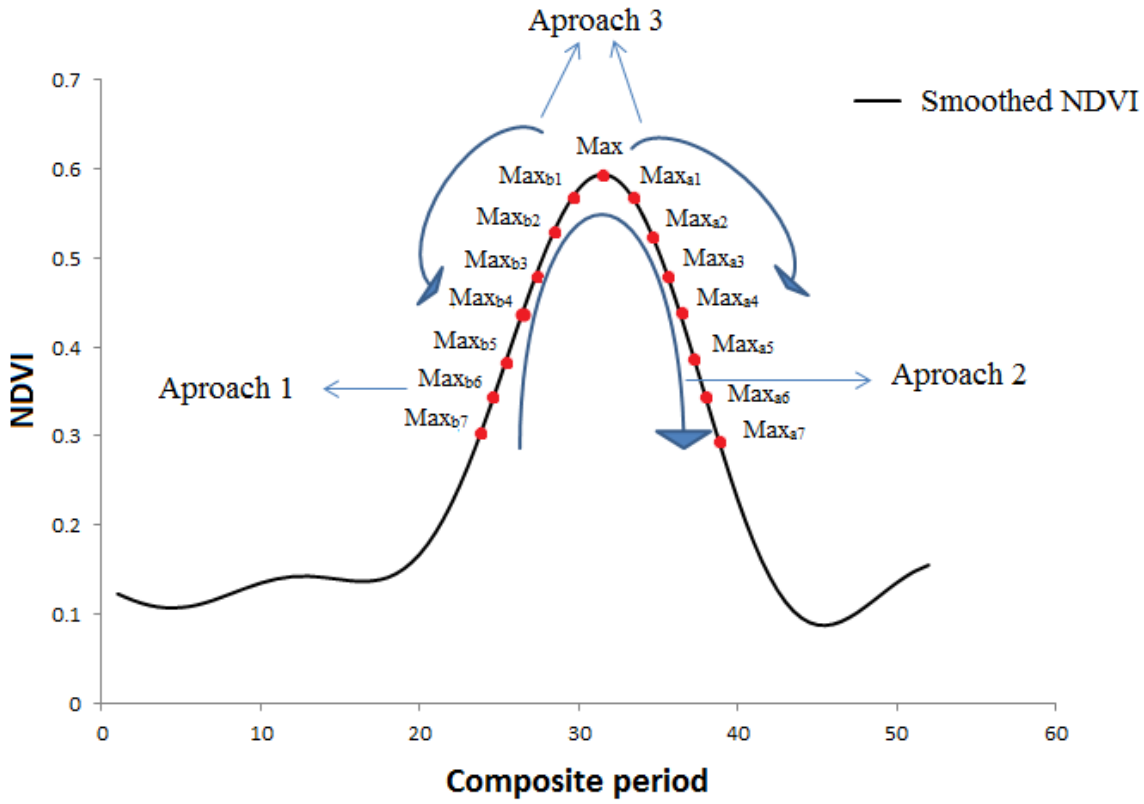

Figure 5-2 The proposed three approaches to determine the phenological parameters which have the largest coefficient of determination with crop production or yield at the governorate level.

The three algorithms search during the growing season to find the time of the phenological event that has the largest coefficient of determination with crop production or yield at the governorate level. The description of VIs, NDVI as an example, and their calculation are presented in Table 5.1. However, as NPP is an annual product, only one spatial sum NPP value can be correlated with crop production or yield at the governorate level. The main purpose of applying three different approaches is to determine which indices and phenological parameters can estimate crop production or yield most accurately in advance.

Table 5.1 Description of the employed variables, equations, and NDVI as an example.

NDVI variables	Description of equations				
	Approach one	Approach two		Approach three	
$NDVI_{maxb7}$	The seventh 8-day composite before $NDVI_{max}$	$NDVI_{maxb7}$	$NDVI_{maxb7}$		
$NDVI_{maxb6}$	The sixth 8-day composite before $NDVI_{max}$	$NDVI_{maxb7\text{-}b6}$	($NDVI_{maxb7}$+ $NDVI_{maxb6}$)		
$NDVI_{maxb5}$	The fifth 8-day composite before $NDVI_{max}$	$NDVI_{maxb7\text{-}b5}$	($NDVI_{maxb7}$+ $NDVI_{maxb6}$+ $NDVI_{maxb5}$)		
$NDVI_{maxb4}$	The fourth 8-day composite before $NDVI_{max}$	$NDVI_{maxb7\text{-}b4}$	($NDVI_{maxb7}$+ $NDVI_{maxb6}$+ $NDVI_{maxb5}$+ $NDVI_{maxb4}$)	$NDVI_{max\text{-}b4}$	($NDVI_{max}$+ $NDVI_{maxb1}$+ $NDVI_{maxb2}$+ $NDVI_{maxb3}$+ $NDVI_{maxb4}$)
$NDVI_{maxb3}$	The third 8-day composite before $NDVI_{max}$	$NDVI_{maxb7\text{-}b3}$	($NDVI_{maxb7}$+ $NDVI_{maxb6}$+ $NDVI_{maxb5}$+ $NDVI_{maxb5}$+ $NDVI_{maxb3}$)	$NDVI_{max\text{-}b3}$	($NDVI_{max}$+ $NDVI_{maxb1}$+ $NDVI_{maxb2}$+ $NDVI_{maxb3}$)
$NDVI_{maxb2}$	The second 8-day composite before $NDVI_{maxc}$	$NDVI_{maxb7\text{-}b2}$	($NDVI_{maxb7}$+ $NDVI_{maxb6}$+ $NDVI_{maxb5}$+ $NDVI_{maxb4}$+ $NDVI_{maxb3}$+ $NDVI_{maxb2}$)	$NDVI_{max\text{-}b2}$	($NDVI_{max}$+ $NDVI_{maxb1}$+ $NDVI_{maxb2}$)
$NDVI_{maxb1}$	The first 8-day composite before $NDVI_{max}$	$NDVI_{maxb7\text{-}b1}$	($NDVI_{maxb7}$+ $NDVI_{maxb6}$+ $NDVI_{maxb5}$+ $NDVI_{maxb4}$+ $NDVI_{maxb3}$+ $NDVI_{maxb2}$+ $NDVI_{maxb1}$)	$NDVI_{max\text{-}b1}$	($NDVI_{max}$+ $NDVI_{maxb1}$)
$NDVI_{max}$	Maximum NDVI	$NDVI_{maxb7\text{-}max}$	($NDVI_{maxb7}$+ $NDVI_{maxb6}$+ $NDVI_{maxb5}$+ $NDVI_{maxb4}$+ $NDVI_{maxb3}$+ $NDVI_{maxb2}$+ $NDVI_{maxb1}$+ $NDVI_{max}$)	$NDVI_{max}$	$NDVI_{max}$
$NDVI_{maxa1}$	The first 8-day composite after $NDVI_{max}$	$NDVI_{maxb7\text{-}a1}$	($NDVI_{maxb7}$+ $NDVI_{maxb6}$+ $NDVI_{maxb5}$+ $NDVI_{maxb4}$+ $NDVI_{maxb3}$+ $NDVI_{maxb2}$+ $NDVI_{maxb1}$+ $NDVI_{max}$+ $NDVI_{maxa1}$)	$NDVI_{max\text{-}a1}$	($NDVI_{max}$+ $NDVI_{maxa1}$)
$NDVI_{maxa2}$	The second 8-day composite after $NDVI_{maxc}$	$NDVI_{maxb7\text{-}a2}$	($NDVI_{maxb7}$+ $NDVI_{maxb6}$+ $NDVI_{maxb5}$+ $NDVI_{maxb4}$+ $NDVI_{maxb3}$+ $NDVI_{maxb2}$+ $NDVI_{maxb1}$+ $NDVI_{max}$+ $NDVI_{maxa1}$+ $NDVI_{maxa2}$)	$NDVI_{max\text{-}a2}$	($NDVI_{max}$+ $NDVI_{maxa1}$+ $NDVI_{maxa2}$)
$NDVI_{maxa3}$	The third 8-day composite after $NDVI_{max}$	$NDVI_{maxb7\text{-}a3}$	($NDVI_{maxb7}$+ $NDVI_{maxb6}$+ $NDVI_{maxb5}$+ $NDVI_{maxb4}$+ $NDVI_{maxb3}$+ $NDVI_{maxb2}$+ $NDVI_{maxb1}$+ $NDVI_{max}$+ $NDVI_{maxa1}$+ $NDVI_{maxa2}$+ $NDVI_{maxa3}$)	$NDVI_{max\text{-}a3}$	($NDVI_{max}$+ $NDVI_{maxa1}$+ $NDVI_{maxa2}$+ $NDVI_{maxa3}$)
$NDVI_{maxa4}$	The fourth 8-day composite after $NDVI_{max}$	$NDVI_{maxb7\text{-}a4}$	($NDVI_{maxb7}$+ $NDVI_{maxb6}$+ $NDVI_{maxb5}$+ $NDVI_{maxb4}$+ $NDVI_{maxb3}$+ $NDVI_{maxb2}$+ $NDVI_{maxb1}$+ $NDVI_{max}$+ $NDVI_{maxa1}$+ $NDVI_{maxa2}$+ $NDVI_{maxa3}$+ $NDVI_{maxa4}$)	$NDVI_{max\text{-}a4}$	($NDVI_{max}$+ $NDVI_{maxa1}$+ $NDVI_{maxa2}$+ $NDVI_{maxa3}$+ $NDVI_{maxa4}$)
$NDVI_{maxa5}$	The fifth 8-day composite after $NDVI_{max}$	$NDVI_{maxb7\text{-}a5}$	($NDVI_{maxb7}$+ $NDVI_{maxb6}$+ $NDVI_{maxb5}$+ $NDVI_{maxb4}$+ $NDVI_{maxb3}$+ $NDVI_{maxb2}$+ $NDVI_{maxb1}$+ $NDVI_{max}$+ $NDVI_{maxa1}$+ $NDVI_{maxa2}$+ $NDVI_{maxa3}$+ $NDVI_{maxa4}$+ $NDVI_{maxa5}$)		
$NDVI_{maxa6}$	The sixth 8-day composite after $NDVI_{max}$	$NDVI_{maxb7\text{-}a6}$	($NDVI_{maxb7}$+ $NDVI_{maxb6}$+ $NDVI_{maxb5}$+ $NDVI_{maxb4}$+ $NDVI_{maxb3}$+ $NDVI_{maxb2}$+ $NDVI_{maxb1}$+ $NDVI_{max}$+ $NDVI_{maxa1}$+ $NDVI_{maxa2}$+ $NDVI_{maxa3}$+ $NDVI_{maxa4}$+ $NDVI_{maxa5}$+$NDVI_{maxa6}$)		
$NDVI_{maxa7}$	The seventh 8-day composite after $NDVI_{max}$	$NDVI_{maxb7\text{-}a7}$	($NDVI_{maxb7}$+ $NDVI_{maxb6}$+ $NDVI_{maxb5}$+ $NDVI_{maxb4}$+ $NDVI_{maxb3}$+ $NDVI_{maxb2}$+ $NDVI_{maxb1}$+ $NDVI_{max}$+ $NDVI_{maxa1}$+ $NDVI_{maxa2}$+ $NDVI_{maxa3}$+ $NDVI_{maxa4}$+ $NDVI_{maxa5}$+$NDVI_{maxa6}$+ $NDVI_{maxa7}$)		

5.2.6 Model development

The first stage in fitting a model to forecast crop production or yield is to decide how to relate the vegetation indices (VIs) to the final production or yield. Several approaches were considered in the current research to select the data in the remote sensing-based crop production or yield model:

(i) the three approaches already mentioned (Figure 5.2) and annual NPP

(ii) average VIs for the previous three approaches (Figure 5.2) and average NPP at the governorate level.

(iv) applying the log transformation to the previous three approaches and NPP at the governorate level, and

(v) the regression model was developed according to the procedure used by Kogan et al. (2012).

These approaches were tested in two ways; (i) the coefficient of determination was estimated between official statistics on production or yield and transforms of the VIs among all governorates within one year, and (ii) the same based on each governorate during the period.

5.2.7 Model validation

Validating the performance of the model is an essential part of the remote sensing-based crop production or yield modelling. In this regard, several approaches to validate the model have been suggested primarily based on removal of a year or a period and then its re-estimation (Mkhabela et al. 2011; Bolton and Friedl 2013; Kouadio et al. 2014). The current regression-based models were validated in three different ways:

(i) leave-one-year-out

(ii) leave-two-years-out

(iii) leave-half-period-out

Based on the following model, using the maximum NDVI, EVI and annual NPP, crop production and yield were estimated for each governorate during the period:

$$Y = a + \Sigma b_i X_i + \varepsilon \quad (1)$$

where Y is the estimated production or yield of winter wheat and barley at the governorate level, the Xi are the spatially accumulated indices (maximum NDVI, maximum EVI and NPP) of winter wheat and barley at the governorate level, and a and b are coefficients.

5.2.8 Regression modelling

Regression models were applied separately for each year at the governorate level. The country consists of eighteen governorates. Regression was applied using decadal composite VIs and annual NPP values (independent variables) to estimate crop production or yield (dependent variable).

For each year of the study period, the fitted regression models used all the historical data excluding one year to estimate the crop production or yield for that missing year. For estimating crop production or yield and to be comparable using the leave-one-year-out approach, only the data from 2002 to 2010 were used as the NPP product is only available until 2010.

Model accuracy assessment is crucial in scientific research. Here, the performance of the models was assessed by comparing the estimated against the actual crop production or yield. The coefficient of determination and relative error were calculated between the estimated and actual crop production or yield for the held-out-year as follows:

$$Relative\ Error\% = \frac{(PPi - APi)}{APi} \times 100 \quad (1)$$

where *PPi* is the forecasted production and *APi* is the actual crop production.

5.3 Results

5.3.1 Estimating phenological parameters for forecasting crop production

Crop production was affected by the growing condition throughout each crop stage and over different years. Regression models were fitted between crop production and the spatial accumulated 8-day NDVI, EVI and annual-based NPP at the governorate level. A large coefficient of determination was found between crop production and the remotely sensed indices (Figures 5.3 and 5.4). Figure 5.3a, b and c show the multi-year average coefficients of determination obtained from linear regression utilizing the NDVI and EVI to forecast crop production at 8-day intervals over the growing season for three different approaches from 2002 to 2012. Figure 5.3a presents the multi-year average coefficients of determination for the spatial sum of a single variable (original VIs value) from Maxb7 to Maxa7 at the governorate level (approach 1). From figure 5.3a, it is apparent that the largest coefficient of determination between crop production and the remotely sensed VIs occurred at the maximum, with NDVI producing a slightly larger coefficient of determination than EVI. Figure 5.3b presents the multi-year average coefficients of determination for the integrated spatial sum of the VIs from Maxb7 to Maxa7 over the growing season (Approach 2). The largest coefficient of determination was recorded for the period around the maximum over the growing season, with NDVI producing a slightly larger coefficient of determination than EVI. Figure 5.3c presents the multi-year average coefficients of determination for the integrated spatial sum of the VIs from the maximum (approach 3). There is a clear trend of increasing coefficients of determination from the beginning of the growing season until the peak of the growing season, then decreases from the maximum towards the end of the growing season.

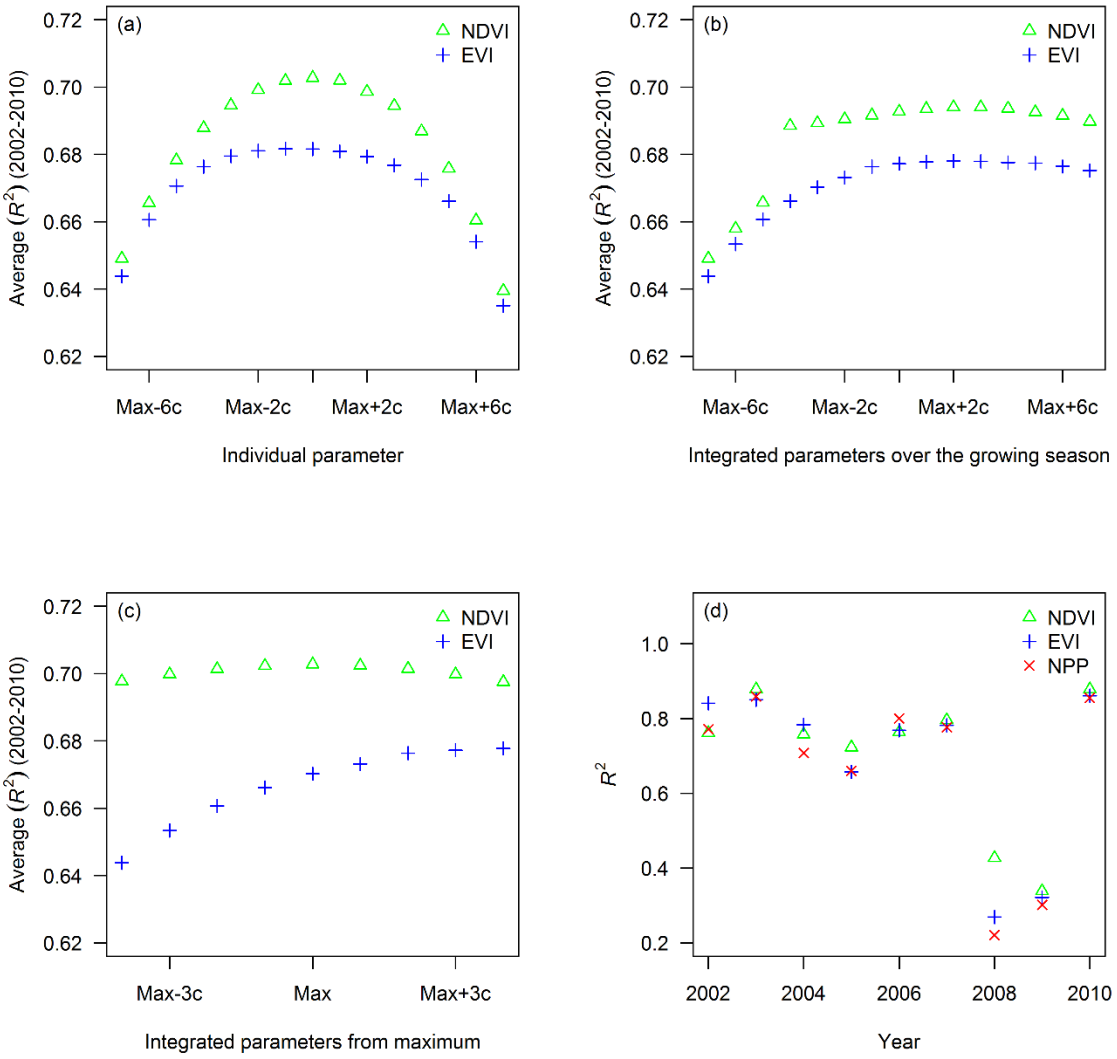

Figure 5-3 Plots showing the multi-year average coefficient of determination (y-axis) between crop production and VIs for different dates (x-axis) at the governorate level from 2002 to 2010, for three different approaches (a, b, c), and (d) maximum NDVI, maximum EVI and NPP

However, as the NPP product is annual-based, it cannot be compared at this stage with VIs (the coefficients of determination for VIs are an average of 8 years for each variable). Therefore, maximum VIs as the best predictor should be compared to the annual NPP value. Figure (5.3d) depicts the comparison of the coefficients of determination among the maximum VIs (as the best predictor to estimate crop production over the growing season) and annual based NPP over the period. It can be seen from the figure that generally all indices produce relatively large coefficient of determinations, with NDVI producing a larger coefficient of determination (Avg. R^2=0.70) than EVI (Avg. R^2=0.68) and NPP (Avg. R^2=0.66). In

general, fluctuation through the years can be seen in the figure with the smallest correlations in 2008 and 2009.

The aim here is not to compare amongst indices: such a comparison would not be fair because of differences in spatial resolution. The current research tended to use the finest spatial resolution for each product to estimate crop production as the region has a small agricultural field size.

Figure 4-5 represents the coefficients of determination between maximum (a) 500m spatial resolustion of NDVI and EVI and (b) 1000m spatial resolustion of NDVI and NPP with crop production, at the governorate level from 2002 to 2010. It can be seen from the figure that after upscaling the NDVI (250) to 500m and 1000m, still sum of maximum NDVI data has better coefficient of determination with crop prodution compare to EVI and NPP. However, with the decrease of spatial resolution from 250m to 500m and 1000m, the average coefficients of determination bewteen maximum NDVI and crop production at the governorate level was decreased from 0.70 to 0.69.

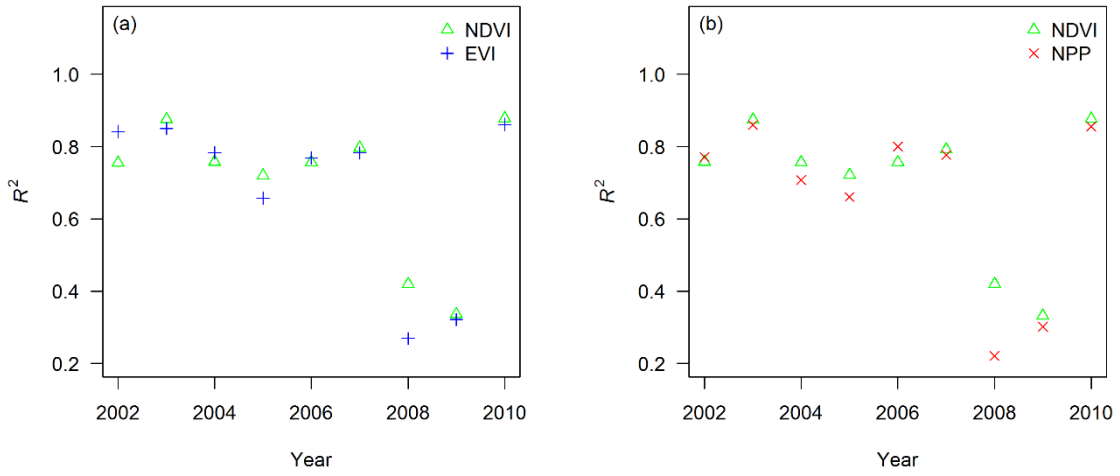

Figure 5-4 The coefficients of determination between maximum (a) 500m spatial resolustion of NDVI and EVI and (b) 1000m spatial resolustion of NDVI and NPP with crop production, at the governorate level from 2002 to 2010.

As the climatic conditions are varied from the north to the south of the region, phenological events across the country are heterogeneous spatially. In the north of the region, the maximum occurred from 7th to 23rd April, while in the central region it occurred around 22nd to 30th March and in the south of the region it occurred around 26th February to 14th March. Therefore, the present results imply that the VIs at the time of the maximum are among the predominant

predictors that can be used to forecast crop production at least one and a half months before harvesting.

5.3.2 Regression model results and accuracy assessment

Considering the climatic conditions and the phenology of winter wheat and barley in Iraq, the spatial accumulated VIs from the maximum over the growing season were found to be the best predictors to forecast crop production as it exhibited the largest coefficient of determination with production. Thus, maximum VIs and annual NPP were used to build the model to forecast crop production. Table 5.2 provides some summary statistics for the fitted regression models using the leave-one-year-out method to estimate crop production over the region for each year from 2002 to 2010. A large coefficient of determination was found using the leave-one-year-out method for the regression model between the maximum VIs and annual NPP and crop production at the governorate level for each year (Table 5.2). These coefficients of determinations were larger with NDVI compared to EVI and NPP. The regression models for each year in Table 5.2 were used to estimate crop production at the governorate level.

Table 5.2 Linear regression models for estimating wheat and barley production between crop production and the spatially accumulated remotely sensed indices (NDVI, EVI and NPP) at the governorate level. The regression models were trained on eight years of the data to forecast crop production in the hold-out year (shown in the left column).

	NDVI		**EVI**		**NPP**	
Year	Model	R^2	Model	R^2	Model	R^2
2002	y = 20.296x	0.74	y = 38.089x	0.68	y = 568.8x	0.68
2003	y = 21.568x	0.70	y = 36.968x	0.69	y = 604.55x	0.67
2004	y = 21.96x	0.73	y = 37.749x	0.72	y = 607.58x	0.70
2005	y = 21.33x	0.73	y = 36.646x	0.73	y = 596.07x	0.71
2006	y = 21.067x	0.72	y = 35.704x	0.72	y = 582.25x	0.68
2007	y = 21.481x	0.72	y = 36.362x	0.72	y = 594.04x	0.70
2008	y = 21.074x	0.72	y = 36.415x	0.72	y = 586.07x	0.70
2009	y = 21.15x	0.74	y = 36.527x	0.74	y = 588.52x	0.72
2010	y = 20.542x	0.69	y = 34.981x	0.70	y = 569.11x	0.67

n=114

Figure 5.5 shows the linear relation between forecasted crop production using the developed regression-based models in Table 5.2 and official estimates of crop

production at the governorate level from 2002 to 2010. It can be seen from the figure that the data are linearly correlated. Table 5.3 presents the summary statistics for the forecasted and actual crop production for each year over the region. In general, it can be seen from the data in Table 5.3 that R^2 is large, but there is variation amongst years and amongst VIs. Generally, large coefficient of determinations were observed for each year for all input indices employed for the modelling; R^2 values ranged from 0.65 to 0.88. However, the smallest coefficient of determinations were recorded for 2008 and 2009 (drought years). The largest coefficient of determination was obtained for NDVI (Avg R^2=0.70) followed by EVI and NPP (Avg R^2=0.68 and Avg R^2=0.66). As table 5.3 shows, there is a clear increase in relative error for forecasting crop production with a decreasing spatial resolution of the data (NDVI 250 m, EVI 500 m and NPP 1000 m). When comparing winter wheat and barley production forecasts made using NDVI against official statistics, the relative error ranged from -20 to 20%. Meanwhile for estimated production using EVI, the relative error ranged from -45 to 28% and it ranged from -48 to 22% for estimating crop production using NPP. In general, the drought years (2008 and 2009) were found to have the largest relative error over the period.

Table 5.3 Coefficients of determination and the relative error between forecasted and actual crop production for all models.

	NDVI				EVI				NPP			
Year	Forecasted MT	Actual MT	R^2	Error %	Forecasted MT	Actual MT	R^2	Error %	Forecasted MT	Actual MT	R^2	Error %
2002	3.86	4.33	0.76	-11	5.44	4.33	0.84	26	3.74	4.33	0.77	-14
2003	4.22	3.83	0.87	10	4.03	3.83	0.85	5	4.13	3.83	0.85	8
2004	4.46	3.73	0.75	20	4.14	3.23	0.78	28	3.93	3.23	0.70	22
2005	3.72	3.79	0.72	-2	3.11	3.79	0.65	-18	3.38	3.79	0.66	-11
2006	3.97	3.92	0.76	1	2.92	3.92	0.76	-26	3.45	3.92	0.80	-12
2007	4.09	4.21	0.79	-3	3.31	4.21	0.78	-21	3.57	4.21	0.77	-15
2008	1.59	1.94	0.42	-18	1.06	1.94	0.26	-45	1.01	1.94	0.22	-48
2009	2.50	3.04	0.33	-18	2.04	3.04	0.32	-33	2.08	3.04	0.30	-32
2010	4.02	5.00	0.87	-20	3.38	5.00	0.86	-32	3.69	5.00	0.85	-26

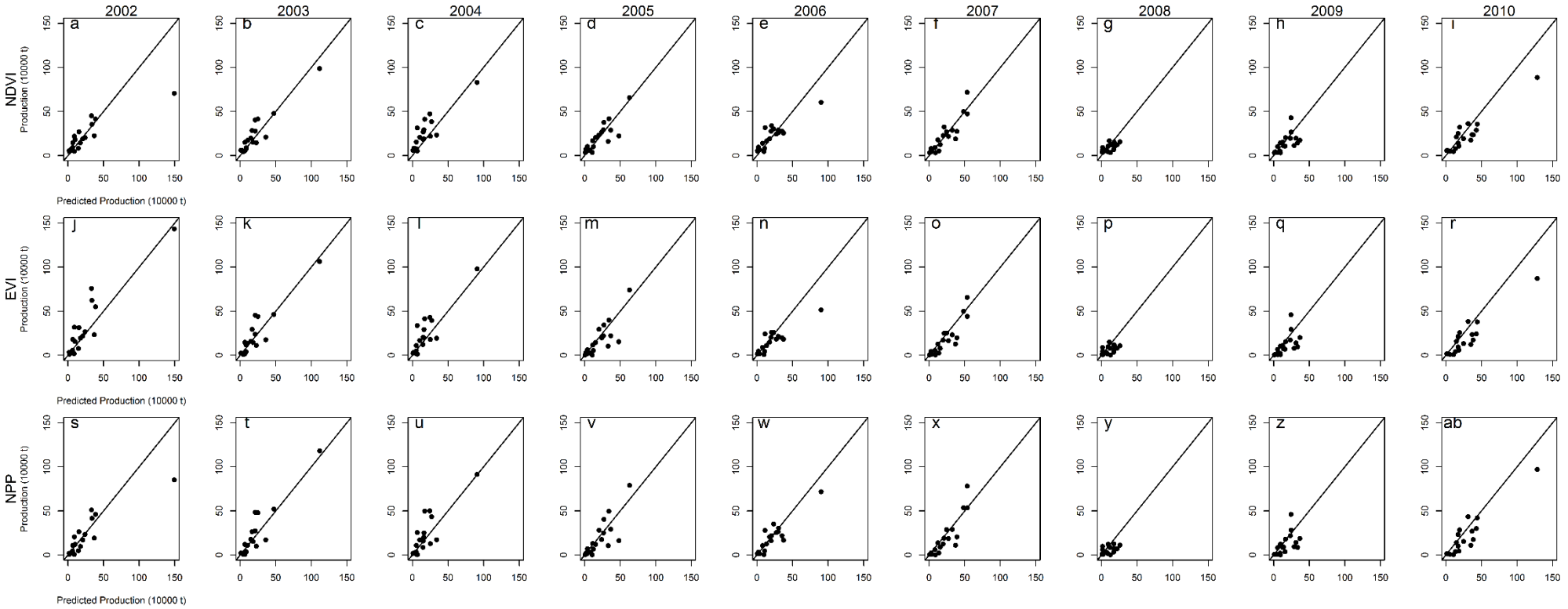

Figure 5-5 Scatterplots of official estimates of production against remotely sensed forecasts of production made using the leave-one-year-out approach, and using (a to i) NDVI from 2002 to 2010; (j to r) EVI from 2002 to 2010; (s to ab) NPP from 2002 to 2010. 1:1 line shown for comparison.

5.3.3 Crop yield estimation

The first set of analyses examined the ability of the employed remotely sensed VIs and several approaches to forecast crop yield at the governorate level in Iraq. The same methodology as presented in section 5.2.6 was used to forecast crop yield over the region. However, based on the available data, we found that crop yield could not be estimated at the governorate level in Iraq. The results of the regression analysis for two examples are shown in Figure 5.6. Figure 5.6a shows the coefficient of determination between crop yield and the average maximum NDVI for all governorates within each year. Very small coefficient of determinations were found for each year, except for 2002. In the second example, it can be seen that the coefficients of determination between crop yield and the average maximum NDVI during the period for each governorate are very small (Figure 5.6b). However, a slightly larger positive coefficient of determination was observed for the Kurdistan governorates (Sulaimani, Erbil and Duhok).

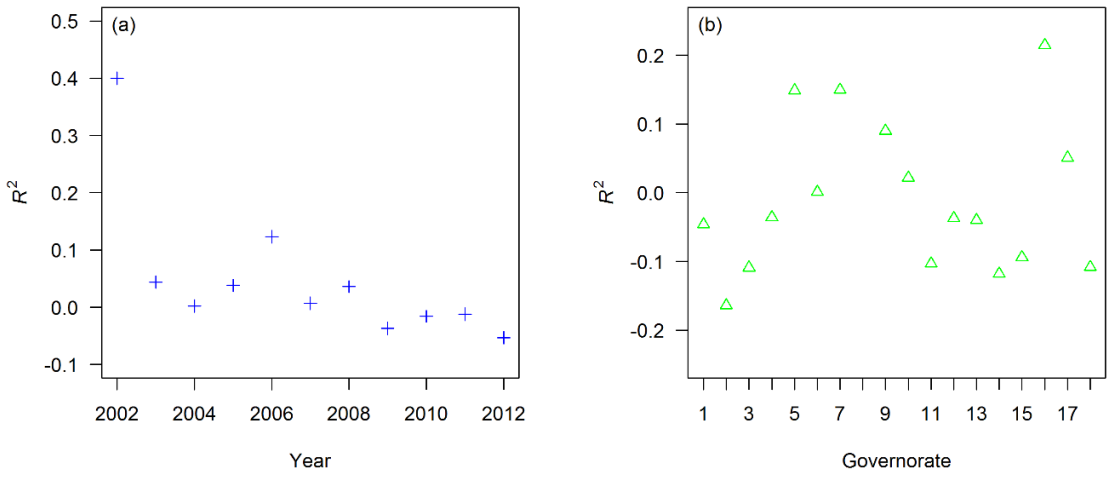

Figure 5-6 (a) the coefficients of determination between crop yield and the average maximum NDVI for all governorates within each year, (b) the coefficients of determination between crop yield and the average maximum NDVI during the period for each governorate ((1) Anbar, (2) Babil, (3) Baghdad, (4) Basrah, (5) Duhok, (6) Dyala, (7) Erbil, (8) Karbala, (9) Kirkuk, (10) Muthana, (11) Mysan, (12) Najaf, (13) Ninawa, (14) Qadsia, (15) Salahadin, (16) Sulaimani, (17) Wasit and (18) Ziqar)).

5.4 Discussion

A regression-based model was fitted between actual crop production and yield based on official crop statistics from Iraq and remotely sensed measures of winter wheat and barley productivity within-season. As yield presents the amount of production per area, many researchers have reported crop yield instead of production (Quarmby et al. 1993; Singh et al. 2002; Ferencz et al. 2004; Sakamoto et al. 2013). Meanwhile, other researchers have reported only crop production or both. For instance, the combined use of AVHRR-NDVI and drought indices at various time-scales were used to forecast wheat and barley production four months before harvest and the predictive models explained 88% and 82% of the temporal variability in wheat and barley production, respectively (Vicente-Serrano et al. 2006). The regression-based model was used to forecast winter wheat production in Kansas and then applied directly to forecast winter wheat production in the Ukraine (Becker-Reshef et al. 2010). The predicted crop production in Kansas and Ukraine closely matched the official reported production with a 7% and 15% error, respectively.

Although this research tested several methodological approaches, it was not possible to forecast crop yield at the governorate level over Iraq. There are several possible explanations for this result. It has been demonstrated that the official Iraqi government statistics are likely to be unreliable (USDA FAS, 2008b). It has also been reported that international statistics data for Iraq for production, yield and harvested area are often "unofficial" or estimated figures, or other sources have been used to estimate uncovered or missing data (FAO 2012). To support this point, this research demonstrated that the coefficient of determination between the average maximum NDVI and crop yield for 2002 was much larger compared to the rest of the period (Figure 5-6a). This result could be explained by the fact that besides more regional instability, at that time the Food Agriculture Organization (FAO) conducted a more accurate ground survey over the region. In addition, as the Kurdistan region is more stable in terms of security compared to the rest of Iraq during the last decade, slightly larger coefficient of determinations were found for Slaimani, Erbil and Duhok (Figure 5-6b). However, double counting in the agricultural statistics at the governorate level for the disputed areas between Kurdish Government and Central Government has led to the coefficient of determinations remaining very small. In addition, for many areas in Iraq access was restricted by the local authority due to security issues. Thus, for such areas the ground survey was replaced by estimation. Another

possible explanation for the lack of correlation is the coarse spatial resolution of the data used in this study compared to the small agricultural field size in Iraq. A coarse spatial resolution could prevent capture of the phenology of a pure crop in some areas since the region has small agricultural field sizes. Another source of uncertainty might be related to the crop map used for the current research, which was not able to separate wheat and barley due to their similar crop calendars and phenological responses in the region (Qader et al. 2015). Due, in part, to greater variability of their yields from one year to the next, yield forecasting is more challenging for both together. Another possible explanation for this could be the large inter-annual variation in terms of croplands at the governorate level as the traditional biennial fallow system is practiced widely in the region to recharge the depleted soil and decrease the impact of pests and disease particularly in the north (FAO 2011; Schnepf 2004).

Interestingly, winter wheat and barley production were highly and linearly correlated with the spatial accumulated NDVI and EVI obtained during maximum green canopy cover at the governorate level in Iraq, compared to the other variables. Therefore, the seasonal maximum NDVI and EVI were selected as this enabled timely forecasting of crop production around a month and half prior to harvest. These results are in line with previous studies that found similar results with either crop production or yield (Becker-Reshef et al. 2010; Doraiswamy and Cook 1995; Mahey et al. 1993; Tucker 1980). In terms of comparison amongst the employed indices, it is apparent from statistical evaluation of the results that NDVI could have an advantage relative to the EVI and NPP for forecasting crop production in the region using the leave-one-year-out approach. A possible explanation for this might be that MODIS-NDVI has a finer spatial resolution (250 m) than MODIS-EVI (500 m) and MODIS-NPP (1000 m). This might make the NDVI data more sensitive to annual variation and capture the detailed phenological characteristics of cropland cover type. In general, a large relative error was obtained for forecasting crop production for 2008 and 2009 when the region experienced a severe drought (Schnepf 2004; Griffin and Kunz 2009). This is potentially a limitation of the remotely sensed-based regression model, and this has been pointed out in several studies where it has not been possible to capture the impact of extreme events (Kouadio et al. 2014; Becker-Reshef et al. 2010).

It might be argued that production is driven mainly by crop area and using remote sensing indices might not have much impact on improving the forecast of final crop production beyond knowledge of the cropped area. Thus, we

investigated the relationship between final crop production and both (i) actual crop area and (ii) estimated crop area at the governorate level from 2002 to 2010. The average R^2 between final crop production and actual crop area was 0.58 and with estimated crop area was 0.63 at the governorate level from 2002 to 2010. However, using the remote sensing indices increased the average coefficient of determination to NDVI=0.70, EVI=0.68 and NPP=0.66. This indicates that the remote sensing indices could characterize and forecast crop production more accurately than simple cropping area, which was treated as a null model or benchmark against which to evaluate the proposed approach. In addition, multiple regression model was also fitted between crop production and (VIs + cropped area), but it did not lead to a significant increase in accuracy.

There is room for further progress in forecasting crop production and yield at the governorate level in Iraq. To increase the quality of data, an accurate and intensive ground survey with a robust experimental design is needed to obtain accurate data on crop yield. It is also important to note that low intensity agriculture and the widely practiced traditional biennial fallow system is difficult to detect at the 250 m spatial resolution of MODIS. The land cover classification map used in this study also was unable to separate wheat and barley over the region. Identification of winter wheat and barley area is a vital component to modelling and forecasting crop production and yield using remote sensing data. For example, a significant increase in the accuracy of crop yield forecasts was observed while a crop map was applied to mask NDVI values as an input to a crop yield model (Maselli et al. 2000; Genovese at al. 2001; Ren et al. 2008). In addition, the low accuracy may be related to the high sensitivity of photosynthetic activity to environmental factors. This might be improved by using VIs sensitive to chlorophyll content as they have less tendency to saturate at high biomass compared to other VIs sensitive to leaf area index (LAI) (Zhang and Liu 2014). As the region has an extreme climatic condition and crop production and yield vary considerably with the amount of rainfall, further studies, which consider climatic variables, will need to be undertaken.

5.5 Conclusion

Regression models were developed to forecast crop production in Iraq, as an example of an arid and semi-arid environment, using within-season remotely

sensed metrics of vegetation productivity. To do this, several methodological approaches using different remotely sensed indices were investigated to forecast annual crop production and yield at the governorate level. The main aim was to evaluate the potential of MODIS-derived measures of greenness and productivity, and information related to the phenology of crops to estimate crop production and yield in the arid and semi-arid regions like Iraq.

This research identified that over the winter wheat and barley growing seasons, crop production was most correlated with the maximum VIs at the governorate level compared to other MODIS derived information related to the timing of crop phenology. This research also demonstrated that the MODIS NDVI offers a more accurate basis for forecasting crop production relative to MODIS EVI and MODIS NPP. The research also found that the average R^2 between final crop production and actual crop area was 0.58 and with estimated crop area was 0.63 at the governorate level from 2002 to 2010. Meanwhile, using the remote sensing indices increased the average coefficient of determination to NDVI=0.70, EVI=0.68 and NPP=0.66. When winter wheat and barley production were forecasted using NDVI, EVI and NPP and compared to official statistics, the relative error ranged from -20 to 20%, -45 to 28% and -48 to 22%, respectively.

As Iraq is continually experiencing various natural and anthropogenic impacts on crop production, it is potentially food insecure. Therefore, quantifying its regional crop production in advance could help policy-makers, scientists and decision-makers to improve agricultural management and food security under a variety of environmental conditions. The model developed here for Iraq, as an example of an arid and semi-arid region, should be extended and tested for other similar regions.

Chapter 6: **Discussion**

This chapter aims to supply a combination discussion of the individual research papers (i.e., chapters 3, 4 and 5). The current research is based on three main research papers to address the main objectives established in the introduction. In chapter three, for the first time a comprehensive characterisation of the vegetation phenological characteristics of the dominant vegetation types was established in Iraq. Then, the major phenological parameters such as SOS, EOS and LOS for the dominant vegetation types were correlated to the altitudinal variation in the country (as a surrogate of precipitation and temperature). As in arid and semi-arid regions such as Iraq, accurate discrimination of various vegetation types is challenging due to their similar spectral signature. In addition, reliable information about croplands and natural vegetation in such a region is scares and the ground data might not be reliable. Therefore, in the fourth chapter, phenology-based classification approach using SVM was developed for the assessment of space-time distribution of the dominant VLC types in Iraq. Meanwhile, in the arid and semi-arid regions of Iraq, inter-annual variation in climatic factors (such as rainfall) and anthropogenic factors (such as civil war) pose a major risk for food security. The combination of these factors makes it challenging in this region to sustain food production. Therefore, an operational crop production estimation and forecasting system is required to help decision-makers make early estimates of the potential food availability and plan for annual imports. In fifth chapter, different MODIS spectral vegetation indices in collaboration with official crop statistics were combined to develop an empirical regression based model to estimate and forecast winter wheat and barley production in Iraq at the governorate level. These individual papers already provided the main research finding, method assessments, work limitations and discussion. Meanwhile, the aim here is to show the relevancy of the research papers, bigger scale discussion of the finding for entire thesis and locating them into context. In addition, further research are suggested based on assessment of the research finding and limitations.

6.1 Uncertainties in extracting phenological parameters

6.1.1 Uncertainties and high spatiotemporal variation of LSP parameters

In semi-arid regions, several factors such as climate, water availability, soil type, and vegetation composition can affect the spatial distribution of the LSP parameters. In order to monitor and characterise the LSP variation at the country level, remote sensing is the only viable means (Chuanfu et al. 2012; Dunn and de Beurs 2011; Ganguly et al. 2010), and this is especially efficient for Iraq as the region has been almost in a continuous war during last three decades. Although, numerous efforts have been made during last two decades to characterise of vegetation phenology through remote sensing data, still its validation with situ data is challenging. This is particularly true for Iraq because (i) limited access to the country due to restricted security issues; (ii) for the first time this research attempted to establish a comprehensive characterisation of the vegetation phenology at local scale over the country; (iii) a very limited number of earlier studies of the vegetation phenology attempted for the region and (iv) no ground vegetation phenological stations exist across the region.

Despite an overall pattern of LSP parameters observed having a strong similarity with the expected phenological pattern for the major vegetation types (Figure 3.5), some uncertainties can be found in the results such as spatial mixing among vegetation types. Some of the issues emerging from this finding relate specifically to the coarse spatial resolution of the data used in the current study compare to the small agriculture field size in Iraq. In addition, due to its climatic and topographic variation, Iraq is the land of various vegetation types. Therefore, low spatial resolution and small agriculture field size led to spatial mixing of vegetation types at finer classification scale. In order to characterise the dominant LSP parameters, global MODIS land cover type is the only available annual based land cover classification over the region (Friedl et al. 2010). It is apparent that the product is a global land cover classification which make it possible that there might be some disagreement at the local scale for some classes. The coarse resolution of the product (500 m) compare to the small agriculture field size in Iraq, make it possible that the product might not be able to discriminate some land cover types over the region. Sobrino et al. 2015 stated that the uncertainties and errors of the global MODIS product might be large as arid and semi-arid regions have large spatial and temporal variations in surface emissivity and less information is known regarding to emissivity variations with viewing angle. The

lower spatial resolution of MODIS data (i.e. 500m), for example, causes a high degree of heterogeneity, particularly in croplands because of mixing of small patches of natural vegetation.

To assess the spatial and temporal variation in term of specific LSP parameters, STD was computed and mapped to show the most variable locations during last decade (Figure 3.6). The SOS and LOS are varied noticeably throughout the country compare to EOS, especially in the north part (rain-fed) (Figure 3.6). The STD of the SOS for most of the country ranges between 0 and 72 days (Figure 3.6a). Whereas, this value rises dramatically towards the lowlands in the north to about 80 to 120 days. In contrast, a relatively small STD can be observed in EOS across the country. It is apparent from the Figure 3.6c that STDs of LOS is closely related to the type of the vegetation as less varied for natural vegetation and relatively higher for croplands. These results are likely to be related to the fact that in both rain-fed area directly and irrigated area indirectly to recharge the main two rivers, rainfall is the main driver of start of the growing season. Any disruption in the rainfall would lead to change in time of starting the growing season, particularly in the north part of the country. There are, however, other possible explanations for these variations such as human interaction, different crop growing system among years, different policies for planting and harvesting, widely practicing crop rotation and traditional biennial system to recharge the depleted soil (Schnepf 2003 and 2004). As natural vegetation is less impacted by human activity, its LOS is less varied compare to SOS. The variation in SOS is mostly driven by changing the timing of the start of rainfall which is not much compared to cropland as plants need to complete the growing season, whether SOS might be advanced or delayed. Meanwhile, a relative homogeneity in STD for EOS can be seen throughout the region compare to other LSP parameters. This result may be explained by the fact that the region is facing a common hot season around the time of the EOS.

As temperature and precipitation varied considerably across the region based on the altitudinal variation, this research explored the relationship between spatial variations in key LSP parameters and elevation (as a surrogate of temperature and precipitation) (Figure 3.7). Li et al (2010) demonstrate that inter-annual variability of SOS is greater at higher latitudes than lower latitudes at the same elevation, whereas the impact of elevation is clearer when the range of altitude achieves more than 1000m. Ding et al. (2013) also showed that the phenology of grasslands in the Qinghai-Tibetan Plateau is driven closely by elevation. For every

1000 m rise in elevation between 2500 and 5500 m, start of growth season is delayed by 9 days, end of growth season is advanced by 1 day, and length of growth season is shortened by 9 days. In the current research, a positive coefficient of determination was observed for SOS and EOS with elevation for all major land cover types with EOS producing the largest positive coefficient of determination (R^2 = 0.685, R^2 = 0.638 and R^2 = 0.588, $p < 0.05$ in shrubland, cropland and grassland, respectively). It is also found that the magnitude of delay in SOS and EOS increased in all land cover types along a rising elevation gradient where for each 500m increase, SOS was delayed by around 25 or more days and EOS delayed by around 22 or more days, except for grassland. More interesting is the large coefficient of determination between EOS and elevation for all land cover types, in contrast to many studies which point to a general trend of delayed EOS at lower elevation (Qiu et al. 2013; Jeganathan et al. 2010; Zhang et al. 2004). With low moisture availability, rise in temperature and decline in elevation from north to south of the region, EOS advancement appear gradually. According to Dry Adiabatic Rate, for each 1000 m increase in elevation will result in 9.8 c° drop in temperature will be dropt. Since the EOS of vegetation is sensitive to the temperature change in the region, there is a gradually earlier pattern from low to high altitude. Our results indicate that water deficit and temperature condition could drive the lowland LSP variation for the major vegetation types, while this variation in high-altitude environments are more stable over time.

6.1.2 Smoothing techniques

The main purposes of applying smoothing techniques on time series data are to reduce residual cloud contamination and upcoming noise because of compositing and resampling procedures (Boyd et al. 2011). Approaches of estimating phenological parameters and smoothing the time series data are a source of uncertainties and yet have not been standardized (White et al. 2009). Thus, special consideration has to be taken to select smoothing technique (Boyd et al. 2011). Several model have been developed and fitted to smooth time series vegetation index from various satellite data to estimate vegetation phenological parameters. However, comparisons among these techniques indicated that each has its own advantages and disadvantages (Viovy et al. 1992; Lu et al. 2007; Hird and McDermid 2009; Atkinson et al. 2012; Kandasamy et al. 2013; Geng et al. 2014). In addition, fine-tuning of parameters such as number of harmonic, size of

temporal neighbourhood and the noise-threshold are required for most models (Atkinson et al. 2009). Michishita et al. (2014) compared seven noise reduction techniques for NDVI temporal profile, and found that Hanning smoothing (RMMEH) and iterative Savitzky-Golay filters performed best. Jonsson and Ekundh (2002) revealed relatively better performance of a Gaussian function-fitting technique compare to a Fourier transform technique and Best Index Slope Extraction (BISE) filter (Viovy et al. (1992).

The accuracy of estimating phenological parameters might have a large influence through the type of smoothing techniques. However, assessing the impact of the type smoothing techniques on extracting phenology and annual variation are infrequent in the literature. Ten models for estimating SOS were compared and found that individual methods varies in average day of the year by ± 60 days and in STD by ± 20 days (White et al. 2009). de Beurs and Henebry (2010) tested several spatiotemporal statistical approaches to determine the SOS and EOS using a time series of remote sensing data and lack of general consequences associating model significance, nomenclature, error structure and uncertainty was revealed. The research also indicated that over a diverse landscape, it would be challenging to find a set of parameters appropriate for all the vegetation types. Therefore, the purpose of the study mainly drive a choice of the smoothing techniques (Hird and McDermid 2009).

6.2 Uncertainties and main challenges of estimating VLC types

Monitoring LULC and its change in arid and semi-arid regions is becoming a crucial issue across different fields of development and sustainable management. In Iraq, there is no reliable system for predicting cropland distribution and area, and forecasting yield, and the official Iraqi government statistics may be unreliable (USDA 2008). In addition, depending on the political, historical, social and technological contexts and environmental, the spatial extend of VLC types are highly variable between and within the years, particularly croplands.

Throughout the growing season, the area planted for harvesting of a given crop might vary. These variations could be as result of multiple events such as severe weather damage, abandonment or unexpected economic condition resulting might have an impact on final crop production estimation. For instance, area estimation can create problems particularly in regions prone to security problems

and flooding or drought issues. These events in any regions can drive false calculation of the production as inaccurate harvested area can be observed due to either inaccessibility or economic infeasibility. In addition, planting more than one crop, which may have similar timing of the growing season and spatial mixing within the same pixel add more complexity to the classification. Furthermore, landscape factor such as soil type and altitudinal variation may cause problems too. Therefore, producing high accurate classification product over the region is challenging.

Classification errors of the croplands largely occurred because of confusion with the natural vegetation classes in the arid and semi-arid regions. This is mainly due to their similar spectral and phenological characteristics. Spatial proximity can be accounted as the first reasons because many cropland areas were intermixed with natural vegetation classes. Other studies reporting the same difficulties to discriminate crops in an area with small scale farming. For example, although, hard classification of fine spatial resolution (30 m) images produced accurate results for commercial farming, it could not deal with mixed pixels because of the small agricultural field size in Ethiopia (Delrue et al. 2013). For the countries located in semi-arid zones such as Zambia, Niger and Cameroon in Africa, croplands are mostly confused with savannas and grasslands, followed by shrublands and woodlands. The results indicated that in highly heterogeneous and intermixed land uses, moderate spatial resolution data have intrinsic limitations (Hannerz and Lotsch 2006). Part of this confusion might be related to differences in crop calendars; classification might be affected as some agricultural practices might be advanced or delayed in some areas. For instance, if different crops or the same crop is planted at different times and ununiformed agriculture managements are applied to the lands resulting may add more complexity to the classification process as their growth process influences the reflectance signal. In addition, the spectral resolution of satellite sensor data also plays a vital role in controlling the level of detail at which land cover can be classified. The broad spectral, and coarse spatial, resolutions of MODIS land surface reflectance (MOD09Q1 V5) might not be adequate for mapping land cover types, particularly crop, at a finer level of detail in Iraq.

In addition to the spatial mixing of croplands with natural vegetation, discriminating crop types, in particular wheat and barley, in Iraq is a great challenge. This is mainly due to the small agriculture fields used to plant both crops. In addition, the NDVI time series of both wheat and barley presented very

similar patterns with almost similar peak over the crop growing season using the current data. This result is in line with Griffin and Kunz (2009) where the Indian Remote Sensing (IRS) AWiFS sensor was used with 56 m spatial and 4 nm spectral resolution, the spectral signature of wheat and barley was shown to be almost identical in Iraq. Currit (2005) also reported the same identical signature issue among crops such as wheat and barley using Landsat data in Chihuahua, Mexico, as both crops typically are planted and harvested at the same time. The classification was therefore not efficient for discriminating the wheat and barley over Iraq at the spatial and spectral resolution of MODIS 250 m. This might have an impact on the classification accuracy of the product and its certainties.

It is not by chance that the global MODIS croplands are not good as the MODIS (250m) croplands as the differences in their spatial resolutions poses various classification challenges. The reason may be mainly because MODIS land surface reflectance (MOD09Q1 V5) has a finer spatial resolution (250 m) than the global MODIS land cover dataset (500 m). This may help to capture more detailed phenological characteristics of the VLC types, which, in turn, helps to classify the regional dominant VLC types more accurately than the MODIS dataset. The coarse spatial resolution of the global MODIS land cover type may make it challenging to estimate Iraq's land cover types, especially for croplands where the average field size is small compared to a 500-m pixel. The overall accuracy for recent global MODIS land cover types is stated to be around 70-80% (Friedl et al. 2010). However, the accuracy level might be much lower when the product used for a particular region such as East Africa (Ge et al. 2007). This might affect the classification accuracy and produced exaggerated estimates of pixels that have truly changed (Cambell 2002). For instance, Fritz et al. 2011 found that around 360 Mha, which is equivalent to 20% of the global cropland area, are classified as cropland in GlobCover (300 m) but as non-cropland in MODIS land cover types. Another source of uncertainty may be that the official Iraq's statistical data dose not account fallows in their statistics, whereas global MODIS includes mostly the fallows (Leroux et al. 2014). Wu et al. (2014) stated that fallow areas are often not included in cropland classes because of their confusion with other vegetation types and temporal dynamics.

To monitor crops efficiently, a high temporal revisit frequency over large geographic areas is required. Meanwhile, this limits the spatial resolution of the data. A coarse spatial resolution is problematic where pixels are mixed, meaning that several signals corresponding to different land cover types occur within a

single pixel due, for example, to small agricultural field sizes. In monitoring remote sensing-extracted crop phenology, crop maps and crop growth dynamics, such data with spatial resolution of 250m (Wardlow and Egbert 2008; Zhong et al. 2011), 500 m (Zhang et al. 2008; Li et al. 2014) and coarser resolution (Atzberger and Rembold 2013) were regularly employed. In small agricultural field sizes, this variability is especially problematic as the spectral reflectance in gridded products such as the MODIS and MEdium Resolution Imagine Spectrometer (MERIS) may represent a mix of different land covers and heterogeneous cropping patterns (Tan et al. 2006; Gomez-Chova et al. 2011). Figure 6.1 depicts the spatial coverage differences between gridded Landsat-8 (30 m) and MODIS (250 m) over the fine spatial resolution Google Earth imagery for some agricultural lands in north-west of Mosul, Ninawa, Iraq. The figure shows clearly that the individual MODIS pixels cover several agricultural land covers, which may be used to plant different crops. Even if the same crop is planted in several fields covered by a MODIS pixel, within-pixel variability in crop phenology timing may exist as different agricultural management practices are applied. The mismatch in spatial resolution between remotely sensed data and the small agricultural field sizes makes it challenging to accurately derive crop phenology, identify crop types and estimate crop yield. In Iraq, agriculture field sizes are varied from the rain-fed area to the irrigated area. Although robust information regarding to the land holdings sizes is missing, in general the land holding areas may range from few donoms to around 50 donom (1dounm=2500 m^2). The largest land holding are located in rain-fed, whereas in irrigated areas, farmers have much smaller lands. The typical footprint of a 250 m gridded MODIS pixel is 25 donom (62500 m^2). Means majority of the agricultural lands cannot be detected by this resolution in Iraq. In contrast, general land cover types including agriculture can be mapped successfully in US and Brazil with MODIS 250 m. In addition, given to the region's large field sizes, Wardlow et al. (2007) demonstrated that in the Central Great Plains, U.S. fields are frequently 324,000 m^2 or larger can be mapped with MODIS 250 m, although it encompassed around five 250 m spatial resolution MODIS pixels.

(a) True colour composite of Landsat-8 in north-west Mosul, Ninawa, Iraq. (Date: 25/04/2015)

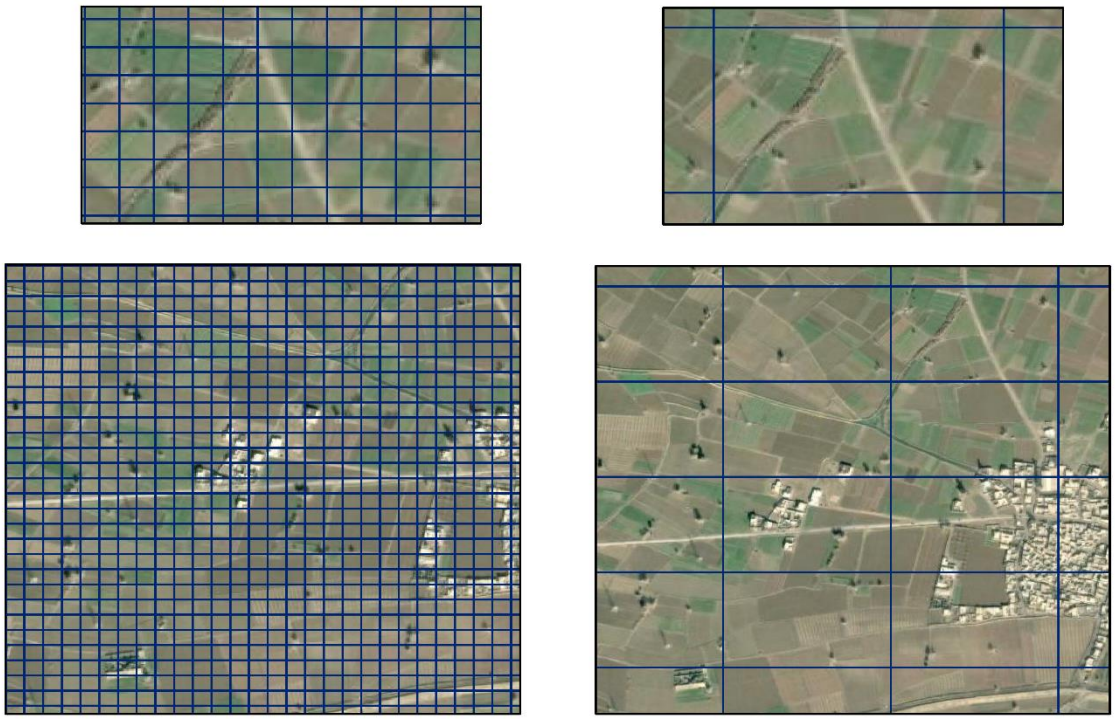

(b) Outline of Landsat-8 30 m pixels products over agriculture lands extracted from high spatial Google Earth imagery in north-west Mosul, Ninawa, Iraq.

(c) Outline of MODIS land surface reflectance 250 m pixels products over agriculture lands extracted from high spatial Google Earth imagery in north-west Mosul, Ninawa, Iraq.

Figure 6-1 (a) depicts the true colour composites of Landsat-8 for acquisition date 25th of April, 2015, (b) shows grid cell outlines from Landsat-8 (30 m) products over a small agriculture field size, and (c) represents grid cell outlines from MODIS (250 m) products over a small agriculture field size, in Iraq.

In addition to the previous factors, many other sources of uncertainty can be considered in deriving an accuracy assessment of land cover classification. First it has to be noticed that it can be challenging to generate a land cover map which is completely satisfies all the needs (Brown et al. 1999). The sampling design used to select the reference data is of the fundamental importance and must be considered when conducting accuracy assessment (Stehman and Czaplewski 1998). Another source of uncertainty is the nature of the classifier used to derive

land cover from the remotely sensed data. Part of the misclassification might be related to the quality of the ground or reference data rather than a mistake in the classification employed to produce the map. Thus, including some measure of confidence could be useful in the ground data used (Estes et al. 1999; Scepan 1999). In addition, the class labels used in both image classification and ground data should have the same meaning (Strahler et al. 2006).

To sum up, in the validation phase, the relative difference between the classification model and ground based estimates of wheat and barley area might be associated with one or more of the following factors: i) the spatial resolution (250 m) of the used MODIS data may not be efficient for all the crop fields as most of the agriculture fields size in Iraq are small and heterogeneous in nature, ii) due to various climatic conditions over the regions, the initial/transplanting stage might have a few weeks shifting in some areas, iii) the official statistical data of the crop area obtained through ground visits have been claimed to be unreliable (USDA FAS 2008), (iv) percentage of occurrence of pure or mixed pixels and (v) spectral resolution of the chosen data.

6.2.1 Uncertainties of estimating crop yield.

Generally, the product of crop production forecasts is based on two essential components: area harvested and yield per unit area (Michael and Atkinson 2013). Thus, an accurate estimating of harvested area and yield will guarantee to generate an accurate crop production estimation. In several cases, the results of predicting yield using remote sensing data are generally in a good agreement with the field data. This is mainly due to the availability of the data such as ground data, reference data and images in term of quality and quantity which make the possibility to drive a better crop yield prediction. For instance, in Canadian Prairies, regression based model using MODIS NDVI was developed to predict crop yield and the difference of the predicted from the actual crop yield was within ±10% (Mkhabela et al. 2011). In China, Independent validation between stepwise regression based models for the remotely sensed rice yield predictions and observed data found that the overall relative error is nearly 5.82%. Most assessments of remote sensing yield predictions are on the broader scale rather than individual fields by comparing counties or district predicted yield and official statistics (Doraiswamy et al. 2005; Becker-Reshef at al. 2010; Lobell et al. 2010). The accuracy of predicted yield with ground data might be varied based on the level of the prediction and the spatial resolution of the data

used. For instance, using 1km MODIS data, yield was estimated sufficiently (≤5% deviation from actual yield) at the state level in Montana and North Dakota, whereas very low accuracy was yielded at the county level (Reeves at al. 2004).

In contrast, obtaining such accurate information in arid and semi-arid regions through remote sensing is a challenge. This is mainly due to: (i) lack of reliable administrative data, (ii) high inter-annual variation in yields, (iii) limited numbers of survey data (Michael 2007), (iv) the heterogeneity of the landscape, (v) extreme weather including droughts and (vi) the coarse spectral and spatial resolutions of the available remote sensing data. This clearly implies for Iraq as the country meets own issues which are difference to other regions. The region is still influenced by natural factors on determining the yield and production level of the major crops. This leads to have a strong fluctuated yield and production according to the year. For instance, the production of wheat in 2002 was around 2.6 millions tons and the productivity of the donom (1 donom= 2500 m^2) was around 329 kg, whereas less than 1 million tons and 172 kg of production and productivity were recorded in 1997 (National Development Plan 2020). This variation can be seen largely among the governorates with respect to climate, water resources and soil as well as work force capabilities. In addition, due to its insecurity issues, the region is affected by lack of quality and quantity of the ground survey data. Thus, the international statistics data for Iraq for production, yield and harvested area are often “unofficial”, or estimated figures or other sources have been used to estimate uncovered or missing data (FAO 2012). Production might be miss-leaded when an appropriate ground survey is not conducted which can create a problem for space observation validation. This is particularly true for Iraq as severe events such as drought and political instability can take harvested area out of production. The influence of regional instability and related wheatear factors on yearly crop yield in addition to the quality of the ground data make it a real challenging to estimate and predict crop yield/production at the governorate level in Iraq and drive the main uncertainties in computing agriculture productivity.

Another source of uncertainty might emerge due to the type of vegetation index. NDVI was the most widely used VI for crop monitoring and yield forecasting (Groten 1993; Benedetti and Rossini 1993; Labus et al. 2002; Doraiswamy et al. 2003; Huang et al. 2013). The most common approach to forecast crop yield at the regional scale is based on simple regression between a satellite-derived vegetation index within-season and eventual crop yield (Prasad et al. 2007; Wall

et al. 2008). These approaches are based on the assumption that measures of the photosynthetic capacity from spectral vegetation indices are strongly correlated to the eventual crop yield. Several studies revealed that prediction accuracy can be improved by using cumulative NDVI over a growing season as grain yield is normally represented by the cumulative photosynthetic activity (Hayes and Decker 1996 and 1998; Maselli et al. 2000; Rent et al. 2008). However, the high sensitivity of photosynthetic activity to environmental factors is a serious issue in forecasting crop yield based on such VIs particularly in arid and semi-arid regions.

Some of the works mentioned earlier forecasted crop yield depended on variables related to crop growth variables such as biomass and LAI. An alternative way to increase the accuracy of yield forecasts, particularly in arid and semi-arid regions as the environment is highly variable, is to use vegetation biochemical and biophysical parameters to surrogate crop yield. Long at al. (2006) found that increase in leaf photosynthesis is closely related with similar increase in yield. However, relatively fewer studies have considered remotely sensed VIs as estimate for vegetation biochemical and biophysical parameters to surrogate crop yield at regional scale. Chlorophyll is a key biochemical parameter, which has large correlation with crop productivity (Gitelson et al. 2006). Photosynthesis is the process underpinned by chlorophyll. In addition, many studies revealed the close relationship between chlorophyll content and the GPP (Gitelson et al. 2006 and 2008, Houborg et al. 2013). Thus, compared to the leaf area index (LAI) or biomass, the content of chlorophyll might be more associated to crop yield. The chlorophyll content of vegetation, which is a function of the biochemical variables of chlorophyll concentration and the biophysical variable of LAI, can be surrogated by the MERIS Terrestrial Chlorophyll Index (MTCI) (Dash and Curran 2007). Thus, the stronger relationship between yield and MTCI would be expected. Zhang and Liu (2014) assessed the potential of a MTCI-based model for crop yield forecasting compared to NDVI in Henan Province, China from 2003 to 2011. Their results revealed several advantages for the MTCI-based model compared to an NDVI-based model such as (i) larger significant correlation coefficient and smaller error, (ii) crop yield can be forecasted 30 days earlier than using the NDVI-based model. Although, the results were not compared to other VIs, a significant correlation between MTCI and crop yield was found at regional scales for the state of South Dakota, USA (Dash and Curran 2007). Crop yield forecasting relied on remote sensed chlorophyll content might be more efficient than remote sensed LAI. Therefore, employing a VI sensitive to chlorophyll

content in the current research might have the potential to improve the accuracy of the prediction model.

6.3 Spatiotemporal variation of Vegetation land cover types in Iraq during the period

Different natural and anthropogenic factors such as war and drought in arid and semi-arid regions led to instable LCLU types during last decade. Iraq is geographically located in an arid to semi-arid region and has been struggling with different anthropogenic and natural factors resulting to have an inconsistent land cover types during the last decade. To assess the class stability, the areas consistently allocated within the same class through time were used to calculate its stability regarding to the average area of the same class during the period. The least stable land cover type was found for cropland (9.367%) during last decade (Table 6.1). It can be seen from figure 6.2 that the spatial distributions of stable crop areas are mainly situated in the areas close to available water. However, the highest stable vegetation class was detected for grassland (74.464%) as this class was mainly located in high altitude areas. Grasslands were more resilient in very high altitude area than low land. The absence of grasslands at the top border of the country may refer to presence of ice and cloud from year to year which might occurred as a result of exclusion of those pixels during flag quality assessment (Figure 6.1). Shrublands were the second category with the largest instability, with an 11.155% over the period. In general, annual variation of croplands is not much among the normal years, whereas its interannual spatial variation is considerably high. The figure 6.1 shows the spatial location of different land cover types that has been allocated within the same class during last decade over Iraq.

Table 6.1 Land covers instability in Iraq during 2002-2012.

Class	Consistent areas with the same class during the period	Average land cover areas during the period	Class stability
	1000 ha	1000 ha	%
Cropland	262.509	2802.555	9.367
Grassland	1503.623	2019.271	74.464
Shrubland	798.122	7167.978	11.135

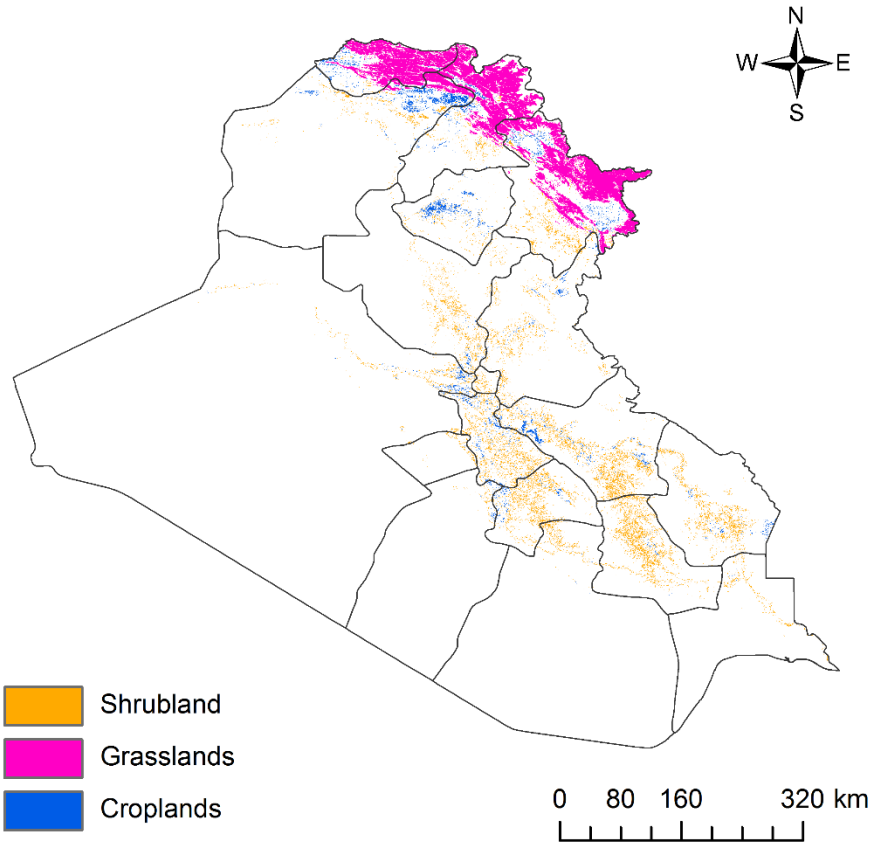

Figure 6-2 Spatiotemporal variations of (a) croplands and (b) crop production, during last decade in Iraq.

As presented in figure 4.6, land covers distribution varied considerably across the country with area dominated by cropland, grassland and shrubland. The most stable land cover during the last decade was grassland. This class is confined entirely to the high altitude region of the country which made difficult to be influenced by human interaction. This region has high rainfall rate and adequate temperature in summer than rest of the country which made this land cover type more resilience to drought and other factors. In addition, the sparse distribution of Oak trees in grassland helped this class to be more challengeable to unfavourable climatic conditions. Differently, the intervening valleys are mostly occupied either by cropland or shrubland. Surprisingly, cropland was found as the least stable land cover types over the period. These factors may explain the relatively good correlation between croplands and its instability. Due to excessive salinity, around 2.5 million hectares of Iraq's irrigated cropland had become degraded in 1973, and that every year another 6000 to 12000 hectares were vanished to salinization (Schnepf, 2004). Traditionally, a biennial fallow system was practiced in crop system over the country to recharge depleted soil and reduce the effect of pests and diseases (FAO, 2011; Schnepf, 2004). It means a winter crop of wheat and barley was planted once in every two years. In addition, lack inputs of fertilizers and pesticides with poor crop management policy limited the agricultural land to be planted every year. On the other hand, natural and anthropogenic factors have also accelerated this land cover's instabilities.

6.4 Why does Iraq have low crop yields by international standards?

By international standards, Iraq has low crop yields. For example, the average wheat yield in Iraq is 1.1 T/Ha, whereas the global average is around 2.8 T/Ha. This might be related to a long history of regional instability and natural factors which have devastated the agricultural infrastructure. For example, Iraq was involved in nearly continuous conflict during the last three decades including the Iran-Iraq war from 1980 to 1988, the Gulf War from 1990 to 1991, sanctions and economic warfare against Iraq from 1990 to 2003 and the recent Post-Gulf War from 2003 to 2011. These wars had serious negative impacts on agricultural

infrastructure by affecting: (i) human resources, (ii) the quality of agricultural land, (iii) water for irrigation. For example, during the Iraq-Iran war, many farmers were forced to join the army. The contribution of agriculture to GDP decreased to around 14% in 1985 due to the impact of war. The main issues during the Gulf war were air pollution due to oil well fires and incursion by oil into a wide area of the coastline of the Gulf because of oil spills, which led to a decline in Gulf water productivity (El-Baz, 1992). After a short invasion of Kuwait by Iraq, the United Nations Security Council decided to set Iraq under resolution 661, which imposed inclusive sanctions on the country (http://www.un.org/Depts/oip/background/index.html). Foreign companies were prohibited to invest in the country and major restrictions were placed on importing essential agricultural resources such as farm machinery, fertilizers, herbicides and pesticides (Schnepf, 2004). Continuous war and its consequences have increased the poverty rate over the region. Thus, the resolution 986 'Oil-for-Food' by the United Nations on 14 April 1995 gave permission to Iraq to sell limited quantities of oil to provide primarily basic needs to the Iraqi people. (http://www.un.org/Depts/oip/background/index.html). Although this programme reached its targets, albeit with some serious issues, it discouraged local food production. In 2003, Iraq was again involved in war (Post-Gulf War). During the period, the agricultural sector suffered greatly; e.g., reduction in the fertility of the land by mismanagement, limited access to fertilizers, farm machinery and pesticides, and the devastation of the irrigation system (Schnepf, 2003). In the recent history of the Middle East, the new Iraq conflict was the largest in terms of displacement, and this vast displacement has placed great pressure on food security and human assistance in Syria and Jordan (Doocy, 2011).

In addition to the long periods of regional instability, other environmental conditions should be considered that have affected the region's productivity. The north of Iraq is mostly rain-fed and its agriculture yields are generally poor and change considerably with the amount of rainfall. Traditionally, a biennial fallow system is practiced over the country to recharge the depleted soil and reduce the effect of pests and diseases (Schnepf, 2004). In addition to crop rotation, agricultural productivity suffers from lack of crop management practices, fertilizers and pesticides. In addition, after neglecting the infrastructure of the irrigation system for many years and overexploitation of the land to increase production, widespread salinization and saturation were observed over the region, which significantly reduced productivity (Mahdi 2000). Therefore,

although Iraq has a strong agricultural heritage, decades of war, political instability, sanctions, mismanagement, and climatic variability have reduced the region's productivity.

With the development of satellite, there has been increased interest in utilizing space observation due to the ability to provide crop monitoring information with greater spatial coverage, potentially at the global scale. Such a system could monitor water quality and land and irrigation efficiency, quantify the type and amount of agriculture crops, provide surrogates of crop yield and production. Predicting crop yield before the harvest is one of the vital concerns in agriculture since the inter-annual differences in crop yield affect international trade, market prices and food supply (Hayes and Decker 1998). Early estimation of crop production on the regional and global scales provides crucial information to policy planners. In addition, appropriate identification of crop productivity is important for sound economic policy and land use planning (Hayes and Decker 1996). Furthermore, an advance crop yield estimation is an essential base of organising food aid missions, as it supplies adequate information about when and where surpluses and shortages are expected to happen.

6.5 Main Causes of variations

6.5.1 Drought

Recently, regular and severe drought has become a major risk to agricultural activity throughout Iraq. For example, a severe drought affected the region during 2008, which resulted in a loss of production of more than 2 Mt (figure 6.4). Like many other arid and semi-arid countries, rainfall in Iraq has been sparse throughout the essential planting season with few areas receiving adequate rains in the north. Figure (6.3) depicts the total harvested area of winter wheat and barley and the total production of winter wheat and barley, along with the average rainfall, from 2000 to 2010 for a) Iraq, b) Iraq excluding the Kurdistan Region and c) the Kurdistan Region. As the Kurdistan Region is mostly rain-fed and was not involved directly in the war during the study period, it is shown separately.

Wheat and barley require a specific amount of water. In the north part of the region (rain-fed area), wheat and barley mainly depend upon the amount and frequency of rainfall as well as its temporal and spatial distribution. For instance,

annually the region may receive adequate rain, but a surplus or shortage in rainfall at any of the growing stages might have a significant impact on final crop production. In Iraq, the total harvested area and production of the cereals wheat and barley fluctuate greatly inter-annually. The average rainfall also fluctuates annually with a similar pattern and, therefore, is considered the main contributing factor for wheat and barley production. Although, the majority of the country is irrigated, rainfall is nevertheless considered the main driver of production. This is likely related to the fact that rainfall is the major source of recharging the two main rivers in the country, which are used to irrigate crops. Thus, any disruption in the rainfall pattern can cause water deficiency, resulting in lack of production. It is apparent from figure 6.3 that the smallest harvested area, production and rainfall were recorded for 2000 and 2008 when the region experienced severe droughts.

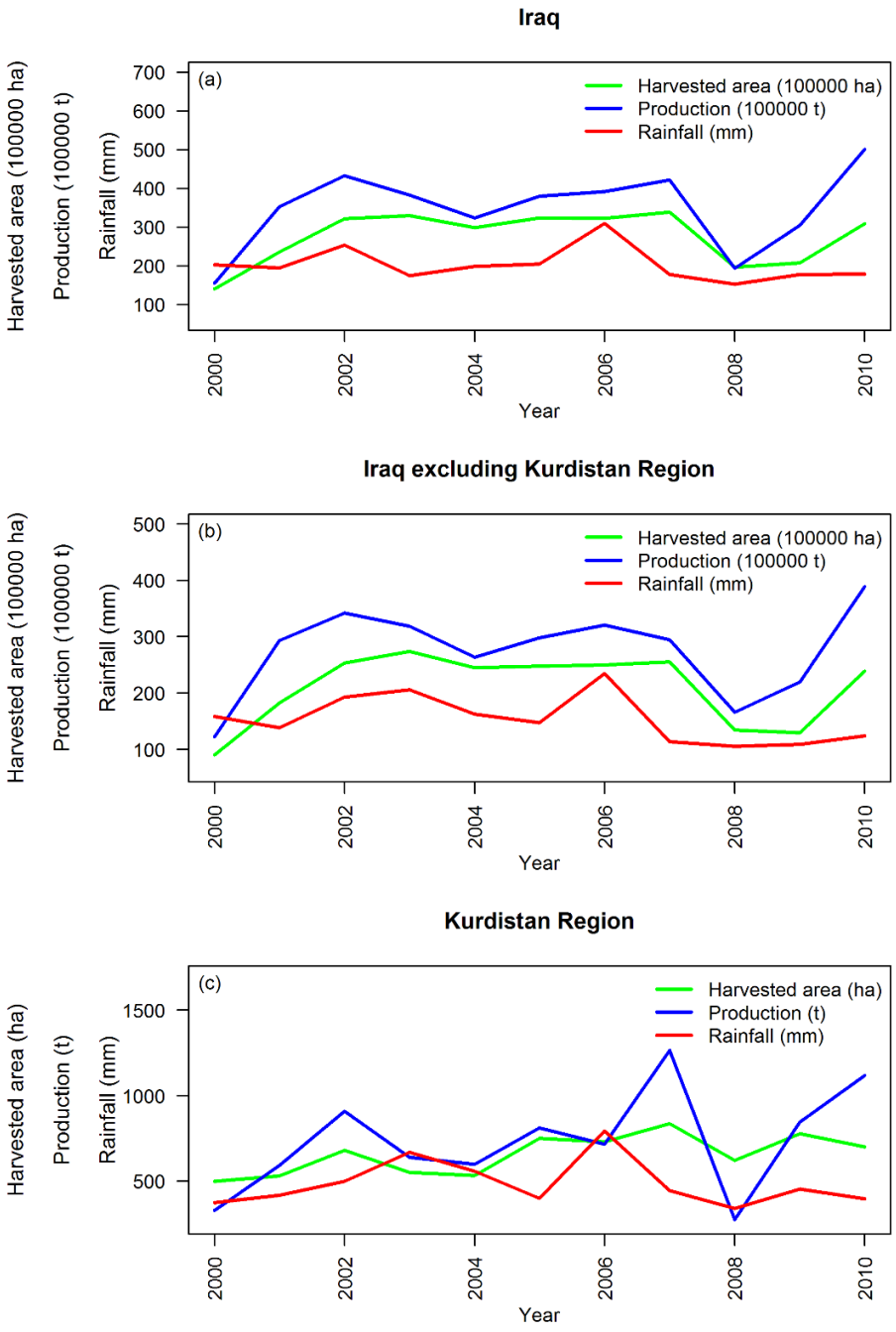

Figure 6-3 Winter wheat and barley harvested area and production, with average rainfall, from 2000 to 2010 for a) Iraq, b) Iraq excluding Kurdistan Region and c) Kurdistan Region.

Interannual rainfall variability considerably affects soil water availability in return pose major risk on crop production. It has been reported that the recent droughts in 2008 and 2009 caused sizeable declines in crop production in Iraq and the reduction was estimated to be 45% from 2007 to 2008 (USDA 2008). This result is consistent with data obtained in this study where the reduction is estimated to be about 50%. To illustrate the impact of drought on regional crop production, the estimated 2008 and 2007 crop production maps are estimated and

compared. Figure 6.4 shows the distribution of the estimated crop production (1000 tons) over Iraq for (a) 2007, (b) 2008 and (c) the relative change (percentage) between these two years. It is apparent from figure 6.4a that the winter wheat and barley production were distributed normally over the region in 2007. Mostly, the north and the areas alongside the rivers are having the highest amount of the production compare to very south, south-western and middle-western parts of the country. In 2008, the region was experienced a severe drought. In figure 6.4b there is a clear decrease of winter wheat and barley production throughout the region due to the impact of drought. During the 2007-2008 growing season, the vegetation indices and NPP were generally very poor. As figure 6.4a and 6-4b cannot show which area had been impacted more due to drought, the relative change between these years was computed. It can be seen from figure 6.4c that the crop production decreased for all governorates except Karbala and Baghdad. The north part of the region, which is considered as rain-fed, is the most affected area by drought. The largest reduction in crop production was recorded for Ninawa followed by Erbil, and Sulaimani (by -86%, -74% and -62%, respectively) as these are mainly rain-fed areas. In total, the winter wheat and barley production decreased by -50% from 2007 to 2008.

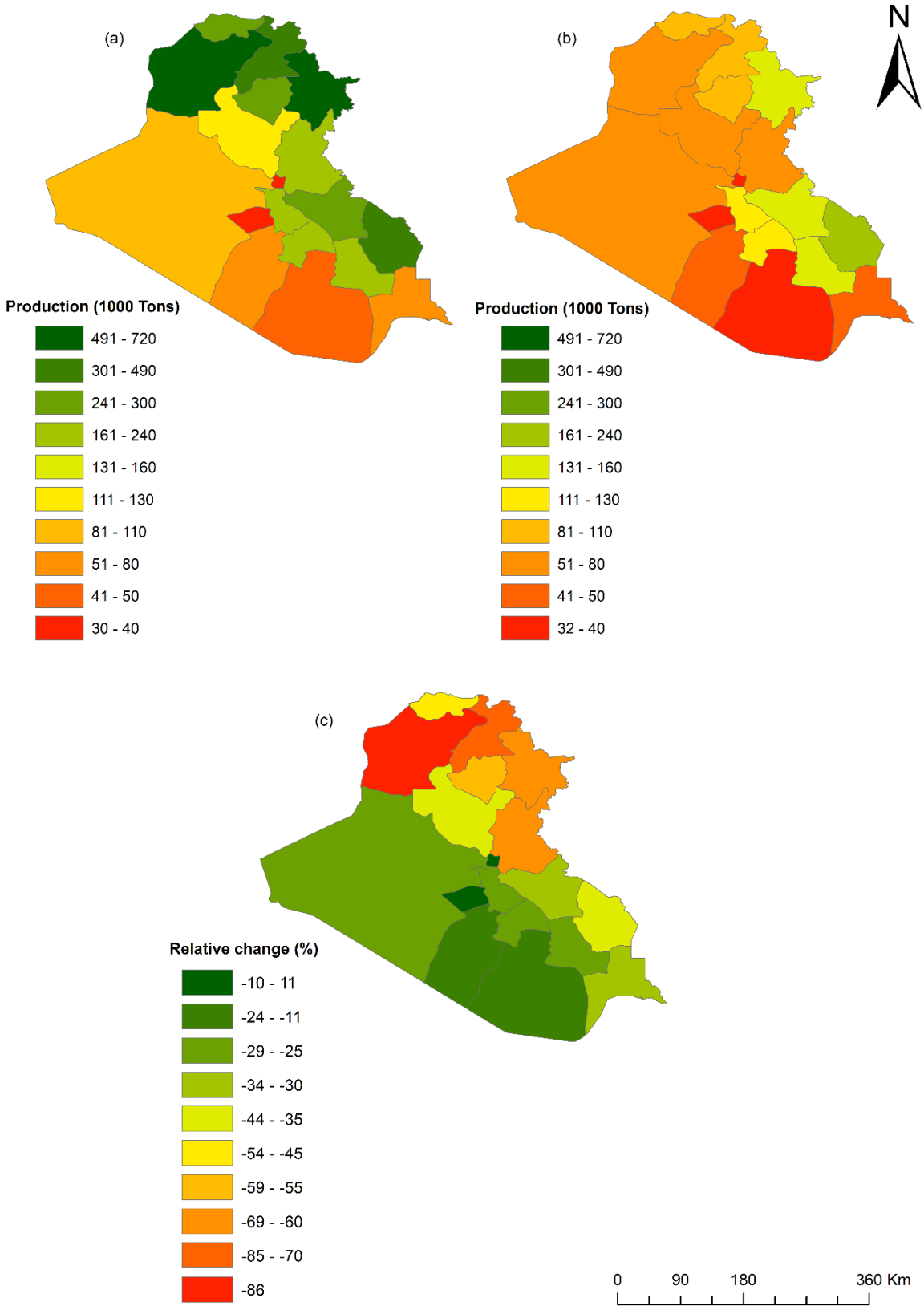

Figure 6-4 The figure shows the impact of severe drought in 2008 on winter wheat and barley production with the comparison of 2007.

6.5.2 War/Conflict

In Iraq, since the 1980s international cooperation and assistance in the environmental sector has been limited due to political instability. Although, after 2003 the country was partially opened to some organizations, they had limited powers and resources. Therefore, even today insufficient robust scientific data exist to address natural and human issues in Iraq. The country has faced several major turbulences where some of them are directly or indirectly related to recent military conflicts during last decade.

The 'Post-Gulf' war, which started in 2003, lasted for around eight years. During this time, due to political instability and insecurity, many farmers were unable to grow crops. This, in turn, affected the overall crop production of the country. The US Department of Defence estimated that around 1700 tonnes of depleted uranium was used during the 2003 war which contaminated soil, water and air with higher levels of radiation than normal (United Nations, 2013). The consequence of these major turbulences have significantly polluted the environment and this might have a negative impact on overall vegetation cover, particularly crop production. Cordesman and Burke (2007) reported that the Anbar, Baghdad and Salahadin governorates accounted for 80% of the total attacks during 2006 to 2007. Therefore, these governorates were selected to identify the extent to which regional instability has impacted on regional crop production. The number of attacks was obtained from the individual reports to Congress on measuring stability and security in Iraq (DOD, 2005-2007). The "attacks" range from an individual insurgent executing an ineffective attack to a coordinated attack with several insurgents using various weapons systems. The crop production of these governorates in 2005 to 2007 was compared to the crop production in 2002 when the region was relatively stable (Figure 6.5).

The recent conflicts in Iraq are complex and highly dependent on geographical location. Some governorates in Iraq faced more attacks than others, mainly due to different sectarian and ethnic tensions. The peak in violence was reached during 2005 to 2007 and the most conflicted affected governorates were Baghdad, Al-Anbar and Salahadin in term of the number of attacks. It is apparent from figure 6.5 that, in total, Baghdad had the largest number of attacks during the period (27711) followed by Al-Anbar and Salahadin by 18058 and 14886, respectively. Given large population displacements, and extensive disruption of markets and trade flow, it might be expected that the governorates of Baghdad, Al-Anbar and Salahadin might face elevated food insecurity levels over the period. The figure

6.5 shows the amount of winter wheat and barley production for Baghdad, Al-Anbar and Salahadin from 2005 to 2007 in comparison to 2002. Although agriculture management has been improved and farmers have received more support from the government since 2002, the winter crop production was generally low during that period. These results are likely to be related to high regional instability in those governorates over the period.

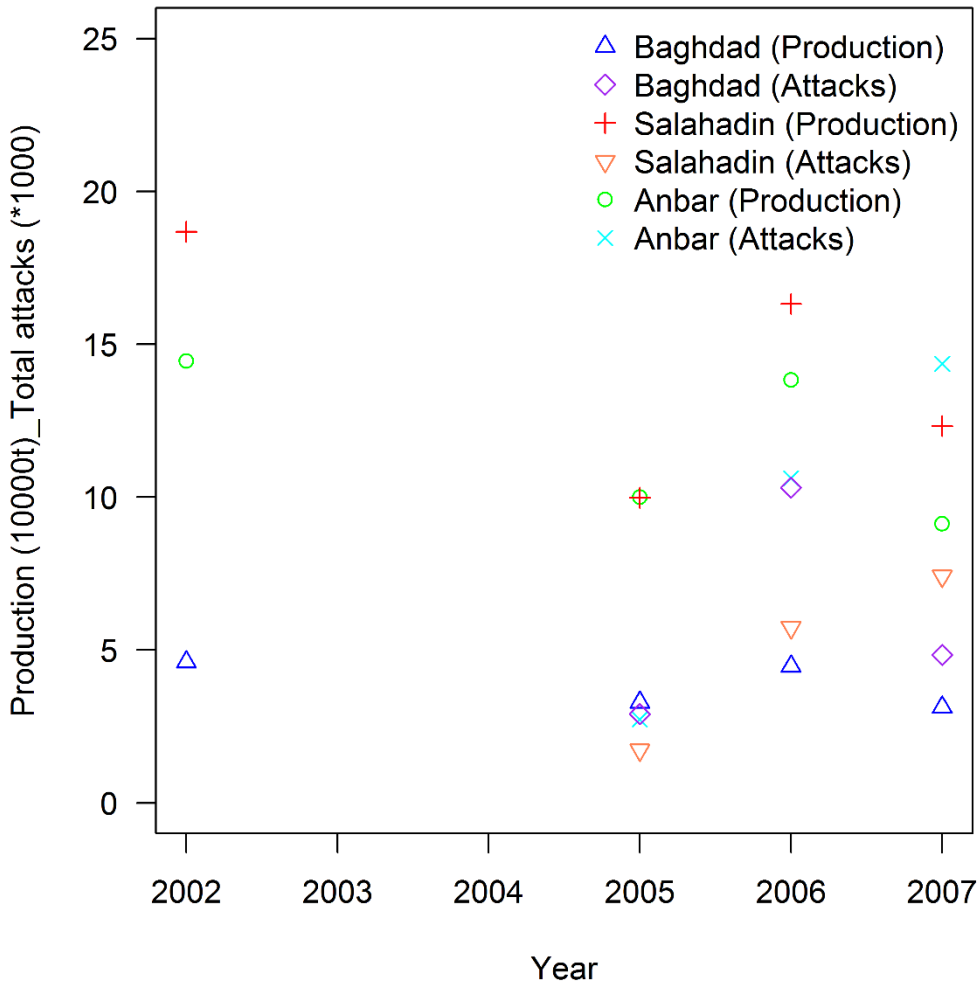

Figure 6-5 The figure illustrates the impact of regional instability of the most affected area on governorate crop production from 2005 to 2007 with the comparison of 2012.

Surprisingly, we found that, although the region experienced a severe drought in 2008, crop production in Baghdad was greater than in 2007 when Baghdad

experienced the largest number of attacks (this is also in line with statistical ground data). This suggests that regional instability might have an impact similar to extreme events such as drought. This result is likely to be related to the largest number of attacks in the area. Baghdad is the capital city of Iraq, and it holds around a quarter of Iraq's population. Since 2003, when the US forces arrived, incidents started in Baghdad. In Baghdad, several districts experienced not only ground fighting, but also revenge killings and bombings (Serdan, 2013). As a consequence of being the most affected by conflict, Baghdad had the highest rate of movement with 8% of household members leaving their dwellings (United Nations WFP, 2008), which might have impacted the workforce in the agriculture sector.

Due to their geographical locations, Anbar and Salahadin faced a large numbers of incidents during the period and, thus, their food security was consistently at risk. For example, one of the most violent governorates in the Coalitions in Iraq was Anbar. Violent attacks increased to an average of 50 per day by August 2006, up 57% from February, and this rate continued to rise (Lindsay and Roger, 2012). In particular, inside Anbar, Fallujah suddenly arose as the major battleground of the Iraqi insurgency. Besides, it was the most heavily bombarded city during the war (United Nations, 2013. ''The insurgency has created complex patterns of conflict that have become a broad struggle for sectarian and ethnic control of political and economic peace'' (Cordesman and Burke, 2007). Therefore, the deterioration of crop production in the three most attacked governorates during the period, compared to production in 2002, could be attributed to their regional instability.

4. Why drought has to be monitored?

Based on the human history, it can be seen that natural disaster such as drought has had a substantial role in agriculture growth and economic cost. Drought can have both direct impact such as water scarcity, hydropower supply and agricultural losses, and indirect impact such as industry losses, expensive payment for food imports, reduced export earnings (Benson and Clay 1994). The level of the losses realised depends on the experience of the local society and the vulnerability of the infrastructure of the country to the hazard (Below et al. 2007). In term of the number of people killed globally over 100 years, drought positioned number one among all natural hazards, and the most frequent

occurrence of droughts taken place in Asia and Africa (Below et al. 2007). The research also reported that Asia and the Middle East recorded the largest increase in deaths by 25% followed by Africa (8%) over the period. Although increased in economic losses was observed for all regions in the research, the 68% increase in Asia and Middle East was double that of any other region. In developing countries, drought was considered as the main cause of severe food deficiency and was the cause of the majority of food emergencies (FAO, 2003).

Due to its geographical location, Iraq is affected by irregularities in precipitation resulting in frequent occurrence of drought. At the 39 meteorological stations over past 30 years (1980-2010), the SPI was computed at various time scales as an indicator to determine the impact of drought severity over Iraq (Al-Timimi and Al-Jiboori 2013). They highlighted the years 1983, 1998, 1999, 2000 and 2008 as the most impacted years by drought over the investigation period, whereas 2008 was announced the worst drought during the period. Barley production fluctuation was evaluated from 1961 to 2000 in Iraq, Morocco, Syria and Turkey, and found that severe fluctuations closely related to precipitation fluctuations (De Pauw 2005). During 1999 drought, water level in Iraq's main rivers dropped by more than 50 % and rainfall was 30% below average (ESCWA 2005). This led to a 70% failure in crop germination in rain-fed agriculture areas and reduction of 37% and 83% of wheat and barley production, respectively in central and southern parts of the country.

Drought is a common event in many arid and semi-arid regions due to the prevailing climate. Many research and operational drought monitoring models have been developed regionally and globally to estimate and predict drought. In these models past, current and future condition with the frequency of drought were evaluated. For example, model simulations under a low-to-moderate scenario were used to investigate the magnitude and key drivers of drying land globally (Figure 6.6) (Zhao and Dai 2015). The results indicated that over most parts of East and West Asia, southern Africa, America, Australia and Europe, the frequency of the SM-based moderate (severe) agricultural drought is expected to increase by 50-100% (100%-200%) in a relative sense by the 2090s (Figure 6.6 c and d). It was also expected that the runoff-based hydrological drought frequency would increase by 10%-50% over the majority of lands. It can be seen from figure 6.6 that drought frequency, using the three drought measures, is expected to increase over most areas including Iraq. These results are also in line with both climatic models (Evans 2009; Evans 2010) and regional climatic simulations (Kitoh

et al. 2008; Mariotti et al. 2009; Jin et al. 2010; Seager et al. 2014) where significant drying under future climate was projected for the Eastern Mediterranean. In addition, Zakaria et al. (2013) employed the climatic model CGCM3.1 (T47)2 to demonstrate the variation in average rainfall and temperature in the countries of the Middle East and North Africa (MENA), with particular emphasis on Iraq, by comparing historical (1990-2009) to future (2020-2100) data. The study revealed that average future monthly temperature tends to be higher and average monthly rainfall lower by 36.47% relative to the historical record of rainfall for the same months (Figure 6.7 a and b). World Bank (2011) also stated that MENA countries would face higher temperature because of climate changes. Warmer climate and increased variability will lead to frequent occurrence of both droughts and floods (Wetherald and Manabe 2002). Drought is one of the most frequently issues for agriculture life and water supply in MENA regions. This particularly effective in MENA countries as most of the agricultural land is under rain-fed condition. For instance, one third of Iraq's winter wheat and barley production is produced under rain-fed condition (Schnepf 2004). Based on previous evidence, Iraq might face further droughts and its consequences in the future. Therefore, a comprehensive method to provide timely information, wide adaptation and mitigation policy is required to make the region more drought resistant.

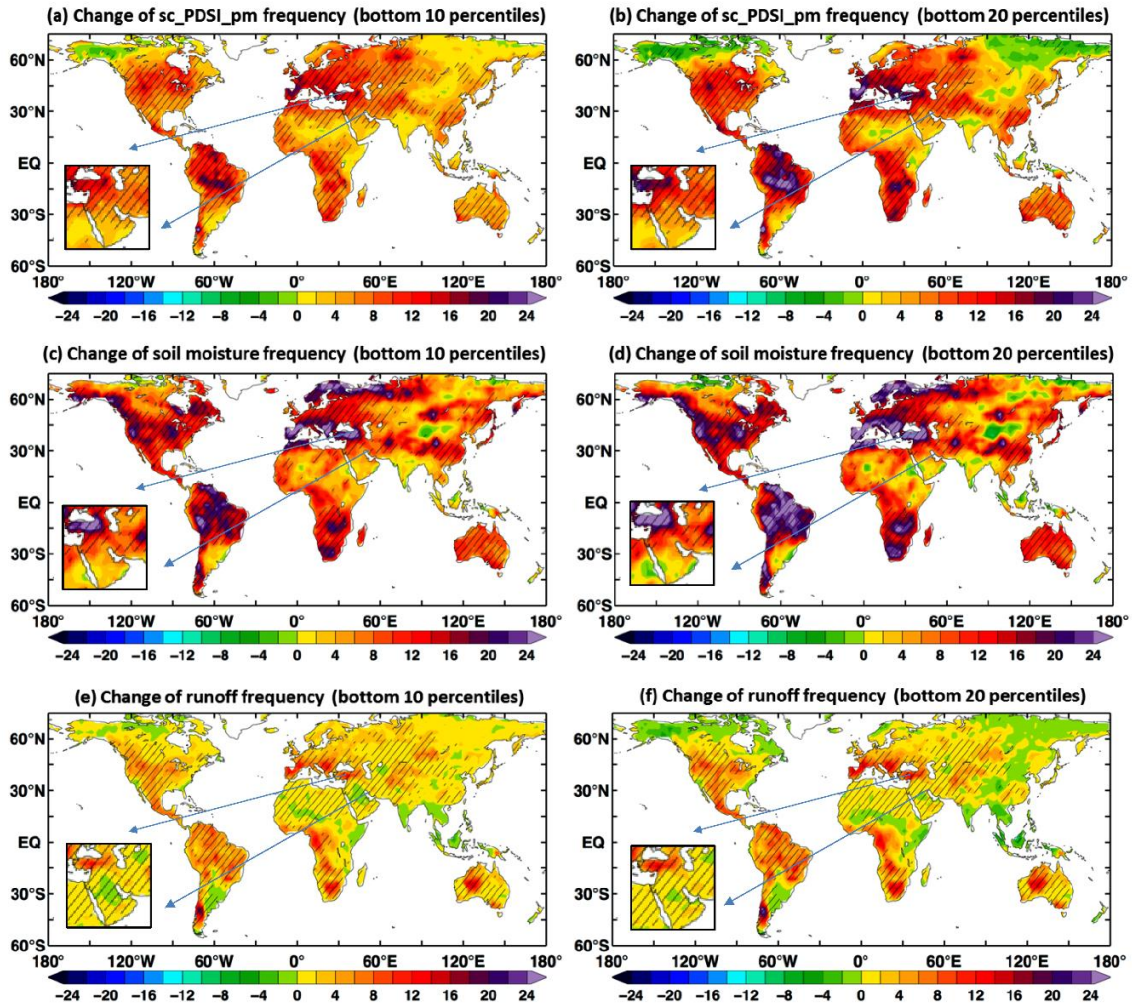

Figure 6-6 “Multimodel ensemble averaged changes of drought frequency (defined as the percentage of the time in drought conditions, not percentage changes) from 1970–99 to 2070–99 under the RCP 4.5 scenario, with drought being defined locally as months below the (a),(c),(e) 10th and (b),(d),(f) 20th percentile of the 1970–99 period based on monthly anomalies of (a),(b) sc_PDSI_pm, (c),(d) normalized SM in the top 10-cm layer, and (e),(f) normalized runoff R in individual model runs. The monthly anomalies of SM and R were normalized using the standard deviation over the 1970–99 period. The stippling indicates at least 80% of the models agreeing on the sign of change” (Zhao and Dai 2015).

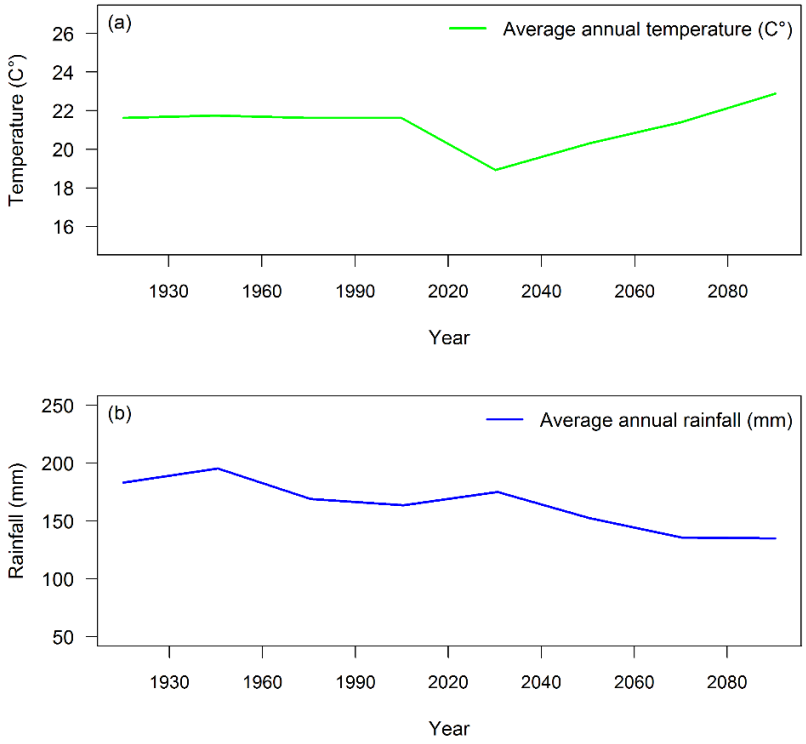

Figure 6-7 Average annual (a) temperature (c°) and (b) rainfall (mm) over the study area for historical and future periods in Iraq (Zakaria et al. 2013).

6.6 Drought mitigation plan

In term of the agriculture drought mitigation, directly or indirectly the results of the current research might have a significant contribution to improve the regional agriculture management. In addition, previous researches have demonstrated that using remote sensing data might help the region in supporting local and policy making decisions. The results of the current work could improve the agriculture practice management toward better drought mitigation plan. For example, spatiotemporal variation in key land surface phenology parameters were assessed and mapped across Iraq over last decade (Qader et al. 2015). Such information can assist to improve agricultural management such as irrigation and fertilization through aiming to establish a suitable relationship between the timing of plant growth stages and carbohydrate consumption (Garcia-Tejero et al., 2010; Menke and Trlica 1981; Mooney and Billings, 1960). The dominant vegetation land cover types were classified over the region using automated phenology-based classification approaches during the last decade (Qader et al. 2016). Updated annual land cover maps can be employed by policy-makers and scientists to

improve regional scale agricultural management practices under a variety of environmental conditions. It was also found that the date of maximum MODIS NDVI can be used to estimate crop production in Iraq using linear regression model (Qader et al. in submission). Local crop production and yield needs to be forecasted regularly using remote sensing data. This forecasting could help notify local authorities about potential decreases in crop production and yield, leading to appropriate import and export decisions (Garcia-Tejero et al., 2010; Menke and Trlica 1981; Mooney and Billings, 1960). The results of LSP, VLC types and crop production were mapped in the current research. The products consists of colour maps, depicting which parts of Iraq are suffering from various degrees of drought. The maps quantify the area and production loss over the region due to the impact of drought. This could help the local authority to take careful consideration to those areas which are more vulnerable or exposed to the impact of drought.

Any reconstruction project aiming to improve agricultural conditions, including based on developing an agricultural monitoring system, might be challenging in Iraq until security conditions improve. In addition, reliable socioeconomic and environmental information are needed to improve agricultural decision support systems. For the current condition, an agricultural monitoring system based on remotely sensed data is required to provide comprehensive information to local farmers and policy makers. This system should have the ability to quantify the type and amount of agricultural crops, monitor water quality, land quality and irrigation efficiency, and estimate and forecast crop yield and production. A drought early warning system should be at the top of regional plans and this should be capable of characterising water supply and climate trends and therefore identify the onset or likelihood of occurrence and severity of drought. This could reduce the impact of drought if the information is delivered in time to the right people, and mitigation and preparedness plans are put in place. Drought mitigation and preparedness plan can be consisted of different components; i) prediction can advantages from climatic studies, soil moisture and remote sensing data, ii) monitoring based on the ground based knowledge such as weather stations, iii) impact assessment can be obtained indirectly such land cove types and iv) response by providing better management.

As the region is struggling with water scarcity, water conservation could be another mitigation strategy to combat drought. This could be done by building dams or holding surface water in reservoirs as the region has intense rainfall in

winter resulting in the frequent occurrence of floods. The mitigation plan could also be implemented through improving water use efficiency. Up to now, many irrigated areas rely on traditional irrigation systems such as surface irrigation. In this method, a massive amount of water is needed to irrigate crops. Therefore, promotion of the irrigation system to modern systems such as drip and sprinkler irrigation is potentially beneficial. In addition, the government and farmers could consider adopting a range of plants that can tolerate dry conditions or using genetically modified varieties that are more resistant to drought. Other strategies for drought mitigation or relief should be considered such as cloud seeding, crop rotation, and using recycled water as part of improving agricultural management. Research should also be encouraged that seeks to find the optimal method to mitigate drought by incorporating more technologies that can assess and forecast potential crop production failures and provide possible solutions in the region.

6.7 Future work

The global impacts of land use land cover change might be as important or more than those related with potential climate change over the coming decades (IPCC 2000). Over last 50 years, 33% of the total anthropogenic carbon emission accounted for the contribution of LULC change (Houghton et al. 1999), from 19980s to 1990s was 20% of total emission (IPCC 2007), and was 12.5% over 2000 to 2009 (Friedingstein et al. 2010). Despite of less information regarding to the rates and types of the land use land cover change, evidence of natural and anthropogenic causes of such change are frequently missing (Turner et al. 1999). Natural and anthropogenic factor are the main causes of LULC changes. Future research on investigating rapid changes in land use/land cover are therefore recommended in Iraq. These changes can be used as a surrogate of the impact of natural factor such as drought and anthropogenic factor such as civil war over the region. For instance, Stevens et al. (2011) used Landsat satellite images to investigate the changes of forest area caused by civil war in Atlantic Coast of Nicaragua from 1978 to 1993. The result revealed that the beginning of five to seven years of the conflicts, the rate of reforestation is higher than deforestation, as compare to the later years of conflicts where deforestation land was nearly doubled to reforestation. In South Vietnam, the results obtained from GIS and remote sensing data indicated that war caused the reduction of the total mangrove area by one third because of using herbicides by US (Thu and Populus, 2007). Further research should also be undertaken to investigate which combination of remotely sensed and phenological data results in the best

classification of abundant agriculture land in Iraq due to regional instability (Alcantara et al. 2012). In addition, the smoothed MODIS time series can be used to understand the degree of extensification and intensification in croplands during last decade (Galford et al. 2008). With higher quality and more accurate maps of agricultural lands, decision makers at the regional level will be much better positioned to reliably assess land use policy.

The current regional land cover classification can serve as a start point. More research efforts should be undertaken toward finding approaches to improve regional VLC types. Although, moderate resolution such as MODIS 250m can be employed to monitor area with large field sizes, higher spatial resolution data are required with finer temporal resolution for monitoring agricultural lands with smaller field size (Justice and Becker-Reshef 2007). A new data source for monitoring land cover can be obtained from Landsat 8 which has the potential to improve the characterization of land's surface significantly. Compare to previous Landsat data, the new data set has several new features such as two spectral bands, two sensors, an improved spectral range for some bands, and refined radiometric resolution from 8-bit to 12-bit (Pahlevan and Schott 2013. However, validation of the future classification over Iraq remains a crucial issue. This will need larger involvement of experts on the ground and the obtaining a higher quality and quantity of ground data. In addition, further input data in both reference data and images might improve the performance of the classification. The reference data in different agro-ecological zones and the ground reflectance for various crop growth stages should be collected in order to achieve maximum accuracy in crop mapping. One of the main sources of misclassification could be related to the variations in planting and harvesting dates. In addition, in order to improve the classification accuracy and discriminate different crop types such as wheat and barley, using of the rich spectral data (hyperspectral data) is crucial. For instance, in Iran, a neighbouring country with a similar environment, an effort was made to discriminate wheat and barley using the hyperspectral sensor Hyperion, which has 242 spectral bands and 30 m spatial resolution (Fahimnejad et al. 2007). The results of the classification indicated that Hyperion data could be used to discriminate both crops. Therefore, fine spatial and multi-spectral remote sensing data are needed to identify and map crops in the arid and semi-arid regions.

To overcome this issue and increase the accuracy, researchers have used fusion approaches to combine the fine spatial resolution of Landsat with the high

temporal frequency of coarse resolution data such as MODIS (Gao et al. 2006; Lobel at al. 2013), which can be applied in arid and semi-arid regions. Such a product could have additional value for many applications, which need both fine spatial and temporal resolution such as land cover classification and forecasting crop yield. One approach, called the spatial and temporal adaptive reflectance fusion model (STARFM) is based upon a spatial relationship between Landsat and MODIS spectral reflectance. The MODIS spectral reflectance can be downscaled to the spatial resolution of Landsat obtained at the same dates (Gao et al. 2006). An extension of STARFM was developed to enhance the accuracy of predicting the surface reflectance of heterogeneous landscapes (ESTARFM) (Zhu et al 2010). Linear mixture models were also used to downscale MERIS to a Landsat-like spatial resolution and results indicated that vegetation dynamics, discrimination of crop types, phenology and capturing rapid land cover types can be monitored effectively (Zurita-Milla et al. 2009; Amoros-Lopez et al. 2013). In addition, new products such as the Sentinel data provided by the European Space Agency (ESA) have become accessible to the remote sensing community and increase the spatial and spectral properties for services such as complex land cover/land use, forest monitoring, and change detection. For example, Balzter et al. 2015 recently reveal that Sentinel-1 can be employed to recognise several land cover classes of the CORINE Land Cover nomenclature. The Sentinel satellite missions comprise five different satellite, one and two for agriculture interest, three for sea and land surface temperature, ocean colour and land colour and sea surface topography, and five for atmospheric monitoring. The data extracted from Sentinel imagery can be used in isolation such as Sentinel-2 and 3, or both can be combined, or both can be combined with MODIS and Landsat 8 through data fusion techniques. This may also advance the LULC classification and forecasting of crop yield in the future in arid and semi-arid regions.

Increasing global population to around 9 billion people by 2050 and impact of climate change pose a major risk on the world's agriculture, researchers are seeking to develop space based technology to help maintain the global food supply. Until now, we have focused on reflected light in the solar spectrum as the main source of information about vegetation condition. However, there is an extra source of information in the spectral range of optical and near infrared which can provide information about vegetation productivity. This source of information is associated to the emission of fluorescence of plant leaf chlorophyll where it can be yielded as re-emitted energy as fluorescence because this part cannot be utilized in carbon fixation. In addition, observational evidence in many

studies revealed that chlorophyll fluorescence provides information content independent of reflectance based spectral VIs (Guanter et al. 2007; Middleton et al. 2008). Recent advances in remotely sensed-based approaches to estimate photosynthesis relied on the flux of chlorophyll fluorescence emitted by the canopy, which has given opportunities to develop many satellite retrieval algorithms (Joiner et al. 2011; Frankenberg et al. 2011; Parazoo et al. 2014). Recently, Guan et al. (2016) for the first time provided a framework to correlate solar-induced fluorescence (SIF) retrievals and crop yield. In their work, crop productivity was estimated for 2007-2012 using spaceborne SIF retrieval from the Global Ozone Monitoring Experiment-2 satellite in United States. Besides more accurate and efficient measurement of crop productivity compared to traditional crop monitoring approaches, the SIF was able to measure the impact of environmental stresses on carbon use efficiency and autotrophic respiration, with considerable sensitivity of both to high temperatures. These outcomes revealed new opportunities to improve crop yield forecasting and increase understanding of crop yield responses to different climatic conditions in arid and semi-arid regions.

Furthermore, to forecast regional crop production and yield, as the region has high climatic flactuations and crop production/yield are significantly vary with the amount of rainfall, thus use of the crop forecasting model based on climatic data should be considered in the future work in Iraq. These models are mainly based on two components, rainfall and temperature (Barnett and Thompson 1982) as they are related to cop yield. Temperature and rainfall data can be obtained either through meteorological stations or through satellite measurements. For instance, AVHRR-NDVI data and SPI at different time scales was combined to predict wheat and barley production in Middle Ebro valley (Vicente-Serrano et al. 2006). In Spain and Kenya, The FAO Crop Specific Water Balance model (CSWB), SPOT-NDVI and meteorological data were combined to improve the crop yield forecasting (Rojas 2007). Similarly. In Iowa, USA, crop yield was assessed and predicted using the combination of NDVI, soil moisture, rainfall and surface temperature (Prasad et al. 2006). In Morocco, predictive models, that combined NDVI, air temperature and rainfall, were developed to forecast wheat yield (Balaghi et al. 2008). Improvements were reported in all studies to predict and forecast crop yield. Therefore, in the future works, the performance of the model can be improved by combining MODIS-NDVI data with meteorological data such as SPI and evapotranspiration (ET).

Chapter 7: **Conclusion**

This chapter provides a list of key findings extracted from the three research papers. These findings are all key to improve the regional crop production and monitoring vegetation land cover types. In addition, primary information of great importance to various applications such as food security, climate, agriculture management, biodiversity, natural and anthropogenic impact and carbon cycle modelling can be obtained directly or indirectly from these findings.

For the first time LSP parameters of terrestrial vegetation were mapped across Iraq at a spatial resolution of 250 m. The spatial variation in LSP across the whole of Iraq for all vegetation types was quantified, thus, providing an important example of mapping vegetation phenology in a semi-arid environment, for which previous research has been relatively lacking.

- Greater spatial variation occurred in the SOS than end of season (EOS), which may be due to the spatial distribution of rainfall and temperature as a function of elevation.
- Linear regression analysis indicated that elevation was positively correlated with all LSP parameters particularly EOS (R^2 = 0.685, R^2 = 0.638 and R^2 = 0.588, $p < 0.05$ in shrubland, cropland and grassland, respectively). In contrast, in most case studies in Europe the coefficient of determination between EOS and elevation was negative due to the effect of low temperature at high elevations as a driving factor in bringing the season to an early end.
- The magnitude of delay in SOS and EOS increased in all land cover types along a rising elevation gradient where for each 500 m increase, SOS was delayed by around 25 or more days and EOS delayed by around 22 or more days, except for grassland.
- The SOS and EOS also varied temporally during the last decade, particularly the SOS in the lowland, north of the country where the standard deviation was around 80 to 120 days, due mainly to the practice of crop rotation and the traditional biennial cropping system.

Reliable information about croplands and natural vegetation in such regions is generally scarce. Such an information can be of interest to several applications such climate, food security, biodiversity and agriculture management. Therefore, a phenological-based classification approach using SVM at the regional scale for

the first time was developed to derive dominant VLC types in arid to semi-arid regions such as Iraq, particularly croplands, from 2002 to 2012.

- The SVM classifier approach produced satisfactory classification accuracies (generally > 85%) with relatively high Kappa coefficients (> 0.86) among the dominant VLC types of Iraq.
- Correlation of VLC cropland area during the last decade with ground statistical data revealed an average coefficient of determination of 0.7 ($p < 0.05$), whereas the average agreement for the global MODIS product cropland class was 0.35 ($p < 0.05$).
- This research also showed that the 2008 drought, the most extreme event during the last decade in Iraq, led to a considerable decline in all dominant VLC types.
- VLC instability, particularly for croplands, was evident, most likely due to more than a decade of regional instability and natural disasters across the country coupled with variable quality agricultural management practices.

Using the current crop area to mask croplands, this study combines the data from NASA's MODIS in collaboration with official crop statistics to develop an empirical regression based model to forecast winter wheat and barley yield/production in Iraq. Although, several methodological approaches were tested with using various remotely sensed indices to estimate and forecast crop yield at the governorate level, the research was unable to do so. This is due to mainly lack of the reliability of the ground data and low spatial resolution data used in the current study compare to the small agriculture field size in the country. However, better estimation and forecasting of crop production were obtained at the governorate level in Iraq.

- The result of the current research imply that time of the maximum VIs are among the predominant predictors that can be used to predict crop production at least one and half month prior to the harvest.
- The result indicated that MODIS NDVI offers a better basis for estimating and forecasting crop production, with an average R^2=0.70, relative to MODIS EVI (Avg R^2=0.68) and NPP (Avg R^2=0.66) using the leave-one-year-out approach.
- This study has shown that remote sensing indices could characterize and forecast crop production more accurately than simple cropping area,

which was treated as a null model or benchmark against which to evaluate the proposed approach.

- Generally, the results from this work suggest that remote sensing related to vegetation phenology is valuable for agriculture monitoring, land cover classification and crop production forecasting. For the homogeneous pixels, the MODIS data are performed better for such application in the region. However, due to its coarse spatial resolution compare to the small agricultural field size, separating crop types and forecasting yield are challenging in Iraq.

Quantifying crop production is essential for the wide range of application such as food security, management and carbon cycle modelling. This is particularly crucial for such a region as Iraq, as its food security is always at risk due to the impact of decadal natural and anthropogenic factors. Thus, such an estimation in advance could help scientists and policy planners to improve regional agriculture management and food security under a variety of environmental condition.

List of References

Abi-Ghanem, R., Carpenter-Boggs, L., Koenig, R., Pannkuk, C., Pan, W., & Parker, R. (2009). Extension Education for Dryland Cropping Systems in Iraq. Journal of Natural Resources and Life Sciences Education, 38, 133-139.

Acharya, P., & Punia, M. (2013). Comparison of MODIS derived land use and land cover with Ministry of Agriculture reported statistics for India. Journal of Applied Remote Sensing, 7.

Akinyemi, F. O. (2013). An assessment of land-use change in the Cocoa Belt of south-west Nigeria. International Journal of Remote Sensing, 34(8), 2858-2875.

Alcantara, C., Kuemmerle, T., Prishchepov, A. V., & Radeloff, V. C. (2012). Mapping abandoned agriculture with multi-temporal MODIS satellite data. Remote Sensing of Environment, 124, 334-347.

Allen, R., Hanuschak, G., & Craig, M. (2002). Limited Use of Remotely Sensed Data for Crop Condition monitoring and Crop Yield forecasting in NASS.

Alnasrawi, A. (2004). State and agriculture in Iraq: Modern development, stagnation and the impact of oil. International Journal of Middle East Studies, 36(2), 318-320.

Al-Timimi, Y. K., & Al-Jiboori, M. H. (2013). Assessment of spatial and temporal drought in Iraq during the period 1980-2010. International Journal of Energy and Environment, 4(2), 291-302.

Al-Timimi, Y. K., & Al-Jiboori, M. H. (2013). Assessment of spatial and temporal drought in Iraq during the period 1980-2010. International Journal of Energy and Environment, 4(2), 291-302.

American Meteorological Society (2004). "Statement on Meteorological Drought." American Meteorological Society 85: 771-773.

Amoros-Lopez, J., Gomez-Chova, L., Alonso, L., Guanter, L., Zurita-Milla, R., Moreno, J., & Camps-Valls, G. (2013). Multitemporal fusion of Landsat/TM and ENVISAT/MERIS for crop monitoring. International Journal of Applied Earth Observation and Geoinformation, 23, 132-141.

Andarzian, B., Bakhshandeh, A. M., Bannayan, M., Emam, Y., Fathi, G., & Saeed, K. A. (2008). WheatPot: A simple model for spring wheat yield potential using monthly weather data. Biosystems Engineering, 99(4), 487-495.

Antônio, H., Teixeira, C. d., & Bassoi, L. H. (2009). Crop Water Productivity in Semi-arid Regions: From Field to Large Scales. Annals of Arid Zone, 48(3), 1-13.

Arroyo, J. (1990). Spatial variation of flowering phenology in the mediteranian shrublands of south Spain. Israel Journal of Botany, 39(3), 249-262.

Atkinson, P. M., Jeganathan, C., & Dash, J. (2009). Analysing the effect of different geocomputational techniques on estimating phenology in India. In B. G. Lees, & S.W. Laffan (Eds.), 10th International Conference on GeoComputation. Sydney: UNSW November-December, 2009.

Atkinson, P. M., Jeganathan, C., Dash, J., & Atzberger, C. (2012). Inter-comparison of four models for smoothing satellite sensor time-series data to estimate vegetation phenology. Remote Sensing of Environment, 123, 400-417.

Atzberger, C., & Rembold, F. (2013). Mapping the Spatial Distribution of Winter Crops at Sub-Pixel Level Using AVHRR NDVI Time Series and Neural Nets. Remote Sensing, 5(3), 1335-1354.

Aziz, F. H. (2011). Seventeen spp. new records for the Moss flora of Iraq. Phyton-International Journal of Experimental Botany, 80, 35-46.

Badhwar, G. D., Carnes, J. G., & Austin, W. W. (1982). Use of Landsat-derived temporal profiles for corn soybean feature-extraction. Remote Sensing of Environment, 12(1), 57-79.

Balaghi, R., Tychon, B., Eerens, H., & Jlibene, M. (2008). Empirical regression models using NDVI, rainfall and temperature data for the early prediction of wheat grain yields in Morocco. International Journal of Applied Earth Observation and Geoinformation, 10(4), 438-452.

Balzter, H., Cole, B., Thiel, C., & Schmullius, C. (2015). Mapping CORINE Land Cover from Sentinel-1A SAR and SRTM Digital Elevation Model Data using Random Forests. Remote Sensing, 7(11), 14876-14898.

Barakat H. N. (2009). Arid lands: challenges and hopes. Earth system: history and natural variability-Vol. III. EOLSS publishers.

Barnett, T. L., & Thompson, D. R. (1982). The use of large-area spectral data in wheat yield estimation. Remote Sensing of Environment, 12(6), 509-518.

Battisti, D. S., & Naylor, R. L. (2009). Historical Warnings of Future Food Insecurity with Unprecedented Seasonal Heat. Science, 323(5911), 240-244.

Bauer, M. E. (1985). Spectral Inputs to Crop Identification and Condition Assessment. Proceedings of the IEEE, 73(6), 1071-1085.

Becker-Reshef, I., Justice, C., Sullivan, M., Vermote, E., Tucker, C., Anyamba, A., Doorn, B. (2010). Monitoring Global Croplands with Coarse Resolution Earth Observations: The Global Agriculture Monitoring (GLAM) Project. Remote Sensing, 2(6), 1589-1609.

Becker-Reshef, I., Vermote, E., Lindeman, M., & Justice, C. (2010). A generalized regression-based model for forecasting winter wheat yields in Kansas and Ukraine using MODIS data. Remote Sensing of Environment, 114(6), 1312-1323.

Below, R., Grover-Kopec, E., & Dilley, M. (2007). Documenting Drought-Related Disasters: A Global Reassessment. The Journal of Environment & Development, 16(3), 328-344.

Benedetti, R., & Rossini, P. (1993). On the use of NDVI profiles as a tool for agricultural statistics: The case study of wheat yield estimate and forecast in Emilia Romagna. Remote Sensing of Environment, 45(3), 311-326.

Benson, C., & Clay, E. (1994). The impact of drought on sub-Saharan African economies. Ids Bulletin-Institute of Development Studies, 25(4), 24-36.

Bewket, W. (2009). Rainfall variability and crop production in Ethiopia Case study in the Amhara region. Paper presented at the Proceedings of the 16th International Conference of Ethiopian Studies, Trondheim.

Bobee, C., Ottle, C., Maignan, E., de Noblet-Ducoudre, N., Maugisa, R., Lezine, A. M., & Ndiaye, M. (2012). Analysis of vegetation seasonality in Sahelian environments using MODIS LAI, in association with land cover and rainfall. Journal of Arid Environments, 84, 38-50.

Bognar, P., Ferencz, C., Pasztor, S., Molnar, G., Timar, G., Hamar, D., Ferencz, O. E. (2011). Yield forecasting for wheat and corn in Hungary by satellite

remote sensing. International Journal of Remote Sensing, 32(17), 4759-4767.

Bolten, J. D., Crow, W. T., Zhan, X. W., Jackson, T. J., & Reynolds, C. A. (2010). Evaluating the Utility of Remotely Sensed Soil Moisture Retrievals for Operational Agricultural Drought Monitoring. IEEE Journal of Selected Topics in Applied Earth Observations and Remote Sensing, 3(1), 57-66.

Bolton, D. K., & Friedl, M. A. (2013). Forecasting crop yield using remotely sensed vegetation indices and crop phenology metrics. Agricultural and Forest Meteorology, 173, 74-84.

Boyd, D. S., Almond, S., Dash, J., Curran, P. J., & Hill, R. A. (2011). Phenology of vegetation in Southern England from Envisat MERIS terrestrial chlorophyll index (MTCI) data. International Journal of Remote Sensing, 32(23), 8421-8447.

Bradley, B. A., & Mustard, J. F. (2008). Comparison of phenology trends by land cover class: a case study in the Great Basin, USA. Global Change Biology, 14(2), 334-346.

Brink, A. B., & Eva, H. D. (2009). Monitoring 25 years of land cover change dynamics in Africa: A sample based remote sensing approach. Applied Geography, 29(4), 501-512.

Brisson, N., Mary, B., Ripoche, D., Jeuffroy, M. H., Ruget, F., Nicoullaud, B., Delecolle, R. (1998). STICS: a generic model for the simulation of crops and their water and nitrogen balances. I. Theory and parameterization applied to wheat and corn. Agronomie, 18(5-6), 311-346.

Brown, J. F., Loveland, T. R., Ohlen, D. O., & Zhu, Z. L. (1999). The global land-cover characteristics database: The users' perspective. Photogrammetric Engineering and Remote Sensing, 65(9), 1069-1074.

Brown, L., R. (2006). Rescuing planet under stress and a civilization in trouble. New York, Norton.

Brown, M. E. (2008). Famine Early Warning Systems and Remote Sensing Data. Springer Berlin-Heidelberg.

Brown, M. E., de Beurs, K. M., & Marshall, M. (2012). Global phenological response to climate change in crop areas using satellite remote sensing of

vegetation, humidity and temperature over 26 years. Remote Sensing of Environment, 126, 174-183.

Burges, C. J. C. (1998). A tutorial on Support Vector Machines for pattern recognition. Data Mining and Knowledge Discovery, 2(2), 121-167.

Burke, I. C., Kittel, T. G. F., Lauenroth, W. K., Snook, P., Yonker, C. M., & Parton, W. J. (1991). Regional-analysis of the central Great-Plains-Sensitivity to climate variability. Bioscience, 41(10), 685-692.

Centre for Research on the Epidemiology of Disasters-CRED. EM-DAT: The OFDA/CRED

Chahbi, A., Zribi, M., Lili-Chabaane, Z., Duchemin, B., Shabou, M., Mougenot, B., & Boulet, G. (2014). Estimation of the dynamics and yields of cereals in a semi-arid area using remote sensing and the SAFY growth model. International Journal of Remote Sensing, 35(3), 1004-1028.

Chang, K. W., Shen, Y., & Lo, J. C. (2005). Predicting rice yield using canopy reflectance measured at booting stage. Agronomy Journal, 97(3), 872-878.

Chen, J., Jonsson, P., Tamura, M., Gu, Z. H., Matsushita, B., & Eklundh, L. (2004). A simple method for reconstructing a high-quality NDVI time-series data set based on the Savitzky-Golay filter. Remote Sensing of Environment, 91(3-4), 332-344.

Chen, W., Foy, N., Olthof, I., Latifovic, R., Zhang, Y., Li, J. Stewart, H. M. (2013). Evaluating and reducing errors in seasonal profiles of AVHRR vegetation indices over a Canadian northern national park using a cloudiness index. International Journal of Remote Sensing, 34(12), 4320-4343.

Christou, P., & Twyman, R. M. (2004). The potential of genetically enhanced plants to address food insecurity. Nutrition Research Reviews, 17(1), 23-42.

Chuanfu, X., Jing, L., & Qinhuo, L. (2012). Monitoring vegetation phenology in China using time-series MODIS LAI data. IGARSS 2012 - 2012 IEEE International Geoscience and Remote Sensing Symposium, 48-51.

Chung-Te, C., Teng-Chiu, L., Su-Fen, W., & Vadeboncoeur, M. A. (2011). Assessing growing season beginning and end dates and their relation to climate in

Taiwan using satellite data. International Journal of Remote Sensing, 32(18), 5035-5058.

Churkina, G., Schimel, D., Braswell, B. H., & Xiao, X. M. (2005). Spatial analysis of growing season length control over net ecosystem exchange. Global Change Biology, 11(10), 1777-1787.

Cihlar, J., Ly, H., Li, Z. Q., Chen, J., Pokrant, H., & Huang, F. T. (1997). Multitemporal, multichannel AVHRR data sets for land biosphere studies - Artifacts and corrections. Remote Sensing of Environment, 60(1), 35-57.

Cihlar, J., Tcherednichenko, I., Latifovic, R., Li, Z., & Chen, J. (2001). Impact of variable atmospheric water vapor content on AVHRR data corrections over land. IEEE Transactions on Geoscience and Remote Sensing, 39(1), 173-180.

Clerici, N., Weissteiner, C. J., & Gerard, F. (2012). Exploring the Use of MODIS NDVI-Based Phenology Indicators for Classifying Forest General Habitat Categories. Remote Sensing, 4(6), 1781-1803.

Collier, P, Elliott, V L, Hegre, H, Hoeffler, A, Reynal-Querol, M and Sambanis, N 2003. Breaking the Conflict Trap: Civil War and Development Policy. World Bank and Oxford University press.

Colombo, R., Busetto, L., Fava, F., Di Mauro, B., Migliavacca, M., Cremonese, E., di Cella, U. M. (2011). Phenological monitoring of grassland and larch in the Alps from Terra and Aqua MODIS images. Italian Journal of Remote Sensing-Rivista Italiana Di Telerilevamento, 43(3), 83-96.

Comber, A. J., Fisher, P. F., & Wadsworth, R. A. (2005). Identifying land cover change using - a semantic statistical approach.

Cortes, C., & Vapnik, V. (1995). Support Vector Networks. Machine Learning, 20(3), 273-297.

COSIT. Central Organization for Statistics and Information Technology in Iraq, 2011 Area and Number of Holdings by Land Use on National Level and Governorates According to the Agricultural Censuses of the Year 2001 http://www.cosit.gov.iq/en/, (accessed on Jan. 16, 2015)

Crist, E. P., & Malila, A. (1980). A temporal spectral analysis technique for vegetation applications of Landsat. Paper presented at the In: 14th

International Symposium on Remote Sensing of Environment., San Jose, Costa Rica.

Curran, P. J., Dungan, J. L., & Gholz, H. L. (1990). Exploring the relationship between reflectance red edge and chlorophyll content in slash pine. Tree Physiology, 7(1-4), 33-48.

Currit, N. (2005). Development of a remotely sensed, historical land-cover change database for rural Chihuahua, Mexico. International Journal of Applied Earth Observation and Geoinformation, 7(3), 232-247.

Dadhwall, V. K., & Ray, S. S. (2000). Crop assessment using remote sensing -Part II: Crop condition and yield assessment. Indian Journal of Agriculture Economy, 2 (1947-4, 55-67.

Dai, A. G. (2013). Increasing drought under global warming in observations and models. Nature Climate Change, 3(1), 52-58.

Dash, J., and P. J. Curran. 2007. "Relationship between the MERIS Vegetation Indices and Crop Yield for the State of South Dakota, USA." Proceedings Envisat Symposium, Montreux, April 23–27 (ESA SP-636, July 2007).

Dash, J., Jeganathan, C., & Atkinson, P. M. (2010). The use of MERIS Terrestrial Chlorophyll Index to study spatio-temporal variation in vegetation phenology over India. Remote Sensing of Environment, 114(7), 1388-1402.

de Beurs, K. M., & Henebry, G. M. (2004). Land surface phenology, climatic variation, and institutional change: Analyzing agricultural land cover change in Kazakhstan. Remote Sensing of Environment, 89(4), 497-509.

De Pauw, E. (2005) Chapter 16: Monitoring Agricultural Drought in the Near East, In: V.K. Boken, A. P. Cracknell, and R.L. Heathcote, eds., Monitoring and Predicting Agricultural Drought, Oxford University Press: New York.

De Wit, A. J. W. and Boogaard, H. L. 2001. Monitoring of Crop Development and Crop Model Optimization Using NOAA –AVHRR: Towards an Integrated Satellite and Model-based Crop Monitoring System in the European Context, Delft: Beleids Commissies Remote Sensing (BCRS). BCRS Report 2000: USP-2, Report 2000, 00–12.

Dean, A. M., & Smith, G. M. (2003). An evaluation of per-parcel land cover mapping using maximum likelihood class probabilities. International Journal of Remote Sensing, 24(14), 2905-2920.

Deininger, K., & Castagnini, R. (2006). Incidence and impact of land conflict in Uganda. Journal of Economic Behavior & Organization, 60(3), 321-345.

Delrue, J., Bydekerke, L., Eerens, H., Gilliams, S., Piccard, I., & Swinnen, E. (2013). Crop mapping in countries with small-scale farming: a case study for West Shewa, Ethiopia. International Journal of Remote Sensing, 34(7), 2566-2582.

Ding, M., Zhang, Y., Sun, X., Liu, L., Wang, Z., & Bai, W. (2013). Spatiotemporal variation in alpine grassland phenology in the Qinghai-Tibetan Plateau from 1999 to 2009. Chinese Science Bulletin, 58(3), 396-405.

Ding, M., Zhang, Y., Sun, X., Liu, L., Wang, Z., & Bai, W. (2013). Spatiotemporal variation in alpine grassland phenology in the Qinghai-Tibetan Plateau from 1999 to 2009. Chinese Science Bulletin, 58(3), 396-405.

Doraiswamy, P. C., Hatfield, J. L., Jackson, T. J., Akhmedov, B., Prueger, J., & Stern, A. (2004). Crop condition and yield simulations using Landsat and MODIS. Remote Sensing of Environment, 92(4), 548-559.

Doraiswamy, P. C., Moulin, S., Cook, P. W., & Stern, A. (2003). Crop yield assessment from remote sensing. Photogrammetric Engineering and Remote Sensing, 69(6), 665-674.

Doraiswamy, P. C., Sinclair, T. R., Hollinger, S., Akhmedov, B., Stern, A., & Prueger, J. (2005). Application of MODIS derived parameters for regional crop yield assessment. Remote Sensing of Environment, 97(2), 192-202.

Dunn, A. H., & de Beurs, K. M. (2011). Land surface phenology of North American mountain environments using moderate resolution imaging spectroradiometer data. Remote Sensing of Environment, 115(5), 1220-1233.

Duro, D. C., Franklin, S. E., & Dube, M. G. (2012). A comparison of pixel-based and object-based image analysis with selected machine learning algorithms for the classification of agricultural landscapes using SPOT-5 HRG imagery. Remote Sensing of Environment, 118, 259-272.

Eastman, J. R., Sangermano, F., Machado, E. A., Rogan, J., & Anyamba, A. (2013). Global Trends in Seasonality of Normalized Difference Vegetation Index (NDVI), 1982-2011. Remote Sensing, 5(10), 4799-4818.

Economic and Social Commission for Western Asia (ESCWA) (2005) ESCWA Water Development Report 1: Vulnerability of the Region to Socio-Economic Drought, United Nations: New York.

El-Magd, I. A., & Tanton, T. W. (2003). Improvements in land use mapping for irrigated agriculture from satellite sensor data using a multi-stage maximum likelihood classification. International Journal of Remote Sensing, 24(21), 4197-4206.

Enkhzaya, T., & Tateishi, R. (2011). Use of phenological features to identify cultivated areas in Asia. International Journal of Environmental Studies, 68(1), 9-24.

Esquerdo, J. C. D. M., Zullo Junior, J., & Antunes, J. F. G. (2011). Use of NDVI/AVHRR time-series profiles for soybean crop monitoring in Brazil. International Journal of Remote Sensing, 32(13), 3711-3727.

Estes, J., Belward, A., Loveland, T., Scepan, J., Strahler, A., Townshend, J., & Justice, C. (1999). The way forward. Photogrammetric Engineering and Remote Sensing, 65(9), 1089-1093.

Evidence and Lessons from Latin America (ELLA) 2011. Improving small farmers' adaptive capacity in semi-arid regions. ELLA theme, adaptation in semi-regions.

Fahimnejad, H., Soofbaf, S., Alimohammadi, A., Zoej M., 2007. Crop Types Classification By Hyperion Data And Unmixing Algorithm. GIS development, Map World Forum, Hyderabad, India.

Fan, J., Huang, J., & Zhang, M. (2013). Retrieval of Cropping Index in China Using Time Series of SPOT Vegetation NDVI. Sensor Letters, 11(6-7), 1134-1140.

FAO, IFAD and WFP (2014). The State of Food Insecurity in the World 2014. Strengthening the enabling environment for food security and nutrition. Rome, FAO.

Fensholt, R., Langanke, T., Rasmussen, K., Reenberg, A., Prince, S. D., Tucker, C. Wessels, K. (2012). Greenness in semi-arid areas across the globe 1981-

2007 - an Earth Observing Satellite based analysis of trends and drivers. Remote Sensing of Environment, 121, 144-158.

Fensholt, R., Nielsen, T. T., & Stisen, S. (2006). Evaluation of AVHRR PAL and GIMMS 10-day composite NDVI time series products using SPOT-4 vegetation data for the African continent. International Journal of Remote Sensing, 27(13), 2719-2733.

Ferencz, C., Bognar, P., Lichtenberger, J., Hamar, D., Tarscai, G., Timar, G., Ferencz-Arkos, I. (2004). Crop yield estimation by satellite remote sensing. International Journal of Remote Sensing, 25(20), 4113-4149.

Fisher, J. I., & Mustard, J. F. (2007). Cross-scalar satellite phenology from ground, Landsat, and MODIS data. Remote Sensing of Environment, 109(3), 261-273.

Fontana, F., Rixen, C., Jonas, T., Aberegg, G., & Wunderle, S. (2008). Alpine grassland phenology as seen in AVHRR, VEGETATION, and MODIS NDVI time series - a comparison with in situ measurements. Sensors, 8(4), 2833-2853.

Food Agriculture Organization of the United Nations (FAO) (2000). The state of food insecurity in the world (SOFI). Rome, Italy: FAO, UN. www.fao.org/FOCUS/E/SOFI00/sofi001-e.htm.

Food Agriculture Organization of the United Nations (FAO) (2001) the state of food insecurity in the world. Rome, Food and Agricultural Organization of the United Nations, p 58.

Food Agriculture Organization of the United Nations (FAO) 2003."Special report FAO/WFP crop, food supply and nutrition assessment mission to Iraq." (Accessed Jun 25, 2013) http://www.fao.org/docrep/005/j0465e/j0465e00.HTM

Food Agriculture Organization of the United Nations (FAO) 2011."Country Pasture/Forage Resource Profiles". Rome, Italy. (Accessed October 23, 2013). http://www.fao.org/ag/agp/AGPC/doc/Counprof/Iraq/Iraq.html

Food Agriculture Organization of the United Nations Aquastat (FAO aquastst). 2008. "IRAQ, Geography, Climate and Population." (Accessed July 15, 2013). http://www.fao.org/nr/water/aquastat/main/index.stm

Food and Agriculture Organization of the United Nation (FAO, 2002). Land degradation assessment in drylands - LADA project. World Soil Resources Reports No. 97. Rome.

Food and Agriculture Organization of the United Nation (FAO, 2003a). "The State of Food and Agriculture" in 32nd Session of the FAO Conference Rome, Italy.

Food and Agriculture Organization of the United Nation (FAO, 2003b). "The State of Food Insecurity in the World. Monitoring progress towards the World Food Summit and Millennium Development Goals," Food and Agriculture Organization of the United Nations, Rome, Italy.

Food and Agriculture Organization of the United Nation (FAO, 2009a). Global agriculture towards 2050. Rome.

Food and Agriculture Organization of the United Nation (FAO, 2009b). Agriculture overview.

Food and Agriculture Organization of the United Nation (FAO, 2011). Global strategy to improve agricultural and rural statistics. Rome, Italy.

Food and Agriculture Organization of the United Nation (FAO, 2013a). World food and Agriculture. Rome, Italy.

Food and Agriculture Organization of the United Nations (FAO) (2013b). Resilient livelihoods Disaster risk reduction for food and nutrition security. Rome, Italy. http://www.fao.org/docrep/015/i2540e/i2540e00.pdf.

Food and Agriculture Organization of the United Nations (FAO) 2008. A Review of Drought Occurrence and Monitoring and Planning Activities in the Near East Region. National Drought Centre, University of Nebraska-Lincoln, Nebraska, USA.

Food and Agriculture Organization of the United Nations (FAO) 2000. The state of food insecurity in the world. Rome, Italy. http://www.fao.org/docrep/x4400e/x4400e00.htm.

Food and Agriculture Organization of the United Nations (FAO) 2014. Syrian Arab Republic: Continued conflict and drought conditions worsen 2014 crop production prospects. Rome, Italy. http://www.fao.org/giews/english/shortnews/Syria15052014.pdf.

Frankenberg, C., Fisher, J. B., Worden, J., Badgley, G., Saatchi, S. S., Lee, J.-E., Yokota, T. (2011). New global observations of the terrestrial carbon cycle from GOSAT: Patterns of plant fluorescence with gross primary productivity. Geophysical Research Letters, 38.

Friedl, M. A., Sulla-Menashe, D., Tan, B., Schneider, A., Ramankutty, N., Sibley, A., & Huang, X. M. (2010). MODIS Collection 5 global land cover: Algorithm refinements and characterization of new datasets. Remote Sensing of Environment, 114(1), 168-182.

Friedl, M. A., Sulla-Menashe, D., Tan, B., Schneider, A., Ramankutty, N., Sibley, A., & Huang, X. (2010). MODIS Collection 5 global land cover: Algorithm refinements and characterization of new datasets. Remote Sensing of Environment, 114(1), 168-182.

Friedlingstein, P., Houghton, R. A., Marland, G., Hackler, J., Boden, T. A., Conway, T. J., Le Quere, C. (2010). Update on CO2 emissions. Nature Geoscience, 3(12), 811-812.

Friedlingstein, P., Houghton, R. A., Marland, G., Hackler, J., Boden, T. A., Conway, T. J., Le Quere, C. (2010). Update on CO2 emissions. Nature Geoscience, 3(12), 811-812.

Fritz, S., & Lee, L. (2005). Comparison of land cover maps using fuzzy agreement. International Journal of Geographical Information Science, 19(7), 787-807.

Fritz, S., See, L., McCallum, I., Schill, C., Obersteiner, M., van der Velde, M., Achard, F. (2011). Highlighting continued uncertainty in global land cover maps for the user community. Environmental Research Letters, 6(4).

Funk, C., & Budde, M. E. (2009). Phenologically-tuned MODIS NDVI-based production anomaly estimates for Zimbabwe. Remote Sensing of Environment, 113(1), 115-125.

Galford, G. L., Mustard, J. F., Melillo, J., Gendrin, A., Cerri, C. C., & Cerri, C. E. P. (2008). Wavelet analysis of MODIS time series to detect expansion and intensification of row-crop agriculture in Brazil. Remote Sensing of Environment, 112(2), 576-587.

Gallego, F. J. (2006) “Review of the Main Remote Sensing Methods for Crop Area Estimates Agriculture unit”, Compilation of ISPRS WG VIII/10 Workshop

2006, Remote Sensing Support to Crop Yield Forecast and Area Estimates, Stresa, Italy, Agriculture Unit, IPSC, JRC.

Gallego, J.; Craig, M.; Michaelsen, J.; Bossyns, B.; and Fritz, S. (2008) "Workshop on Best Practices for Crop Area Estimation with Remote Sensing Data: Summary of Country Inputs", Group on Earth Observations (GEO), GEOSS Community of Practice Ag Task 0703a, EC JRC, Ispra, Italy.

Ganguly, S., Friedl, M. A., Tan, B., Zhang, X., & Verma, M. (2010). Land surface phenology from MODIS: Characterization of the Collection 5 global land cover dynamics product. Remote Sensing of Environment, 114(8), 1805-1816.

Gao, F., Masek, J., Schwaller, M., & Hall, F. (2006). On the blending of the Landsat and MODIS surface reflectance: Predicting daily Landsat surface reflectance. IEEE Transactions on Geoscience and Remote Sensing, 44(8), 2207-2218.

Garcia-Tejero, I., Romero-Vicente, R., Jimenez-Bocanegra, J. A., Martinez-Garcia, G., Duran-Zuazo, V. H., & Muriel-Fernandez, J. L. (2010). Response of citrus trees to deficit irrigation during different phenological periods in relation to yield, fruit quality, and water productivity. Agricultural Water Management, 97(5), 689-699.

Ge, J., Qi, J., Lofgren, B. M., Moore, N., Torbick, N., & Olson, J. M. (2007). Impacts of land use/cover classification accuracy on regional climate simulations. Journal of Geophysical Research-Atmospheres, 112(D5).

Geerken, R. A. (2009). An algorithm to classify and monitor seasonal variations in vegetation phenologies and their inter-annual change. Isprs Journal of Photogrammetry and Remote Sensing, 64(4), 422-431.

Geng, L. Y., Ma, M. G., Wang, X. F., Yu, W. P., Jia, S. Z., & Wang, H. B. (2014). Comparison of Eight Techniques for Reconstructing Multi-Satellite Sensor Time-Series NDVI Data Sets in the Heihe River Basin, China. Remote Sensing, 6(3), 2024-2049.

Geng, L. Y., Ma, M. G., Wang, X. F., Yu, W. P., Jia, S. Z., & Wang, H. B. (2014). Comparison of Eight Techniques for Reconstructing Multi-Satellite Sensor Time-Series NDVI Data Sets in the Heihe River Basin, China. Remote Sensing, 6(3), 2024-2049.

Genovese, G., Vignolles, C., Negre, T., & Passera, G. (2001). A methodology for a combined use of normalised difference vegetation index and CORINE land cover data for crop yield monitoring and forecasting. A case study on Spain. Agronomie, 21(1), 91-111.

Gibson, G. R., Campbell, J. B., & Wynne, R. H. (2012). Three Decades of War and Food Insecurity in Iraq. Photogrammetric Engineering and Remote Sensing, 78(8), 885-895.

Gimenez-Benavides, L., Escudero, A., & Iriondo, J. M. (2007). Reproductive limits of a late-flowering high-mountain Mediterranean plant along an elevational climate gradient. New Phytologist, 173(2), 367-382.

Gitelson, A. A., Merzlyak, M. N., & Lichtenthaler, H. K. (1996). Detection of red edge position and chlorophyll content by reflectance measurements near 700 nm. Journal of Plant Physiology, 148(3-4), 501-508.

Gitelson, A. A., Merzlyak, M. N., & Lichtenthaler, H. K. (1996). Detection of red edge position and chlorophyll content by reflectance measurements near 700 nm. Journal of Plant Physiology, 148(3-4), 501-508.

Gomez-Chova, L., Zurita-Milla, R., Alonso, L., Amoros-Lopez, J., Guanter, L., & Camps-Valls, G. (2011). Gridding Artifacts on Medium-Resolution Satellite Image Time Series: MERIS Case Study. Ieee Transactions on Geoscience and Remote Sensing, 49(7), 2601-2611.

Gongalton, R. C., & Green, K. (2009). Assesing the Accuracy of Remotely Sensed Data. New York: 2nd ed. CRC Press.

Gourdji, S. M., Sibley, A. M., & Lobell, D. B. (2013). Global crop exposure to critical high temperatures in the reproductive period: historical trends and future projections. Environmental Research Letters, 8(2).

Groten, S. M. E. (1993). NDVI – crop monitoring and early yield assessment of Burkina-Faso. International Journal of Remote Sensing, 14(8), 1495-1515.

Group on Earth Observations (GEO) (2011) GEO-GLAM (Global Agriculture Monitoring Initiative). http://www.earthobservations.org/geoglam.php. Accessed 02 December 2016.

Gu, Y., Brown, J. F., Miura, T., van Leeuwen, W. J. D., & Reed, B. C. (2010). Phenological Classification of the United States: A Geographic Framework

for Extending Multi-Sensor Time-Series Data. Remote Sensing, 2(2), 526-544.

Guan, K., Berry, J. A., Zhang, Y., Joiner, J., Guanter, L., Badgley, G., & Lobell, D. B. (2016). Improving the monitoring of crop productivity using spaceborne solar-induced fluorescence. Global Change Biology, 22(2), 716-726.

Guanter, L., Alonso, L., Gomez-Chova, L., Amoros-Lopez, J., Vila, J., & Moreno, J. (2007). Estimation of solar-induced vegetation fluorescence from space measurements. Geophysical Research Letters, 34(8), 5.

Gusso, A., Formaggio, A. R., Rizzi, R., Adami, M., & Theodor Rudorff, B. F. (2012). Soybean crop area estimation by Modis/Evi data. Pesquisa Agropecuaria Brasileira, 47(3), 425-435.

Haile, M. (2005). Weather patterns, food security and humanitarian response in sub-Saharan Africa. Philosophical Transactions of the Royal Society B-Biological Sciences, 360(1463), 2169-2182.

Ham, J., Chen, Y. C., Crawford, M. M., & Ghosh, J. (2005). Investigation of the random forest framework for classification of hyperspectral data. IEEE Transactions on Geoscience and Remote Sensing, 43(3), 492-501.

Hamar, D., Ferencz, C., Lichtenberger, J., Tarcsai, G., & FerenczArkos, I. (1996). Yield estimation for corn and wheat in the Hungarian great plain using Landsat MSS data. International Journal of Remote Sensing, 17(9), 1689-1699.

Hannerz, F.; Lotsch, A. Assessment of Land Use and Cropland Inventories for Africa; Centre for Environmental Economics and Policy in Africa, University of Pretoria: Pretoria, South Africa, 2006.

Hansen, M. C., & DeFries, R. S. (2004). Detecting long-term global forest change using continuous fields of tree-cover maps from 8-km advanced very high-resolution radiometer (AVHRR) data for the years 1982-99. Ecosystems, 7(7), 695-716.

Hansen, M. C., Egorov, A., Potapov, P. V., Stehman, S. V., Tyukavina, A., Turubanova, S. A., Bents, T. (2014). Monitoring conterminous United States (CONUS) land cover change with Web-Enabled Landsat Data (WELD). Remote Sensing of Environment, 140, 466-484.

Hansen, M. C., Egorov, A., Potapov, P. V., Stehman, S. V., Tyukavina, A., Turubanova, S. A., Bents, T. (2014). Monitoring conterminous United States (CONUS) land cover change with Web-Enabled Landsat Data (WELD). Remote Sensing of Environment, 140, 466-484.

Hatfield, J. L., & Pinter, P. J. (1993). REMOTE-SENSING FOR CROP PROTECTION. Crop Protection, 12(6), 403-413.

Hatfield, J. L., & Prueger, J. H. (2010). Value of Using Different Vegetative Indices to Quantify Agricultural Crop Characteristics at Different Growth Stages under Varying Management Practices. Remote Sensing, 2(2), 562-578.

Hayes, M. J., & Decker, W. L. (1996). Using NOAA AVHRR data to estimate maize production in the United States Corn Belt. International Journal of Remote Sensing, 17(16), 3189-3200.

Hayes, M. J., & Decker, W. L. (1998). Using satellite and real-time weather data to predict maize production. International Journal of Biometeorology, 42(1), 10-15.

Hendrix, C and Brinkman, H 2013. Food Insecurity and Conflict Dynamics: Causal Linkages and Complex Feedbacks. Stability: International Journal of Security and Development 2(2):26.

Hielkema, J. U., & Snijders, F. L. (1994). Operational use of environmental satellite remote sensing and satellite communications technology for global food security and locust control by FAO: The ARTEMIS and DIANA systems. Acta Astronautica, 32(9), 603-616.

Hird, J. N., & McDermid, G. J. (2009). Noise reduction of NDVI time series: An empirical comparison of selected techniques. Remote Sensing of Environment, 113(1), 248-258.

Hmimina, G., Dufrene, E., Pontailler, J. Y., Delpierre, N., Aubinet, M., Caquet, B., Soudani, K. (2013). Evaluation of the potential of MODIS satellite data to predict vegetation phenology in different biomes: An investigation using ground-based NDVI measurements. Remote Sensing of Environment, 132, 145-158.

Houborg, R., Cescatti, A., Migliavacca, M., & Kustas, W. P. (2013). Satellite retrievals of leaf chlorophyll and photosynthetic capacity for improved modeling of GPP. Agricultural and Forest Meteorology, 177, 10-23.

Houghton, R. A., Hackler, J. L., & Lawrence, K. T. (1999). The US carbon budget: Contributions from land-use change. Science, 285(5427), 574-578.

Houghton, R. A., House, J. I., Pongratz, J., van der Werf, G. R., DeFries, R. S., Hansen, M. C., Ramankutty, N. (2012). Carbon emissions from land use and land-cover change. Biogeosciences, 9(12), 5125-5142.

Howitt, R. E., MacEwan, D., & Medellin-Azuara, J. (2011). Drought, Jobs, and Controversy: Revisiting 2009: University of California Giannini Foundation.

Huang, C., Davis, L. S., & Townshend, J. R. G. (2002). An assessment of support vector machines for land cover classification. International Journal of Remote Sensing, 23(4), 725-749.

Huete, A. R., Liu, H. Q., Batchily, K., & vanLeeuwen, W. (1997). A comparison of vegetation indices global set of TM images for EOS-MODIS. Remote Sensing of Environment, 59(3), 440-451.

Hutchinson, C. F. (1991). Use of satellite data for famine early warning in sub-Saharan Africa. International Journal of Remote Sensing, 12(6), 1405-1421.

Ibanez, I., Primack, R. B., Miller-Rushing, A. J., Ellwood, E., Higuchi, H., Lee, S. D., Silander, J. A. (2010). Forecasting phenology under global warming. Philosophical Transactions of the Royal Society B-Biological Sciences, 365(1555), 3247-3260.

Inouye, D.W., Wielgolaski, F.E., 2003. Phenology at high altitude. In: Schwartz, M.D. (Ed.), Phenology: An Integrative Environmental Science. SPRINGER, Dordrecht, Netherlands, pp. 225–247.

Intergovernmental Panel on Climate Change IPCC (2000). Land use, land-use change, and forestry. Special report (pp. 184). Cambridge: Cambridge University Press.

International Disaster Database; Université Catholique de Louvain, Brussels, Belgium, 2011. Available online: www.emdat.be (accessed on 8 May 2015).

International Fund for Agriculture Development (IFAD) (2000) “The rangelands of arid and semiarid areas.” (14/01/2015). http://www.ifad.org/lrkm/theme/range/arid/arid_2.htm.

IPCC (2007): Climate Change 2007: The Physical Science Basis. Contribution of Working Group I to the Fourth Assessment Report of the

Intergovernmental Panel on Climate Change [Solomon, S., D. Qin, M. Manning, Z. Chen, M. Marquis, K.B. Averyt, M. Tignor and H.L. Miller (eds.)]. Cambridge University Press, Cambridge, United Kingdom and New York, NY, USA, 996 pp.

Jakubauskas, M. E., Legates, D. R., & Kastens, J. H. (2001). Harmonic analysis of time-series AVHRR NDVI data. Photogrammetric Engineering and Remote Sensing, 67(4), 461-470.

Jakubauskas, M. E., Legates, D. R., & Kastens, J. H. (2001). Harmonic analysis of time-series AVHRR NDVI data. Photogrammetric Engineering and Remote Sensing, 67(4), 461-470.

Jakubauskas, M. E., Legates, D. R., & Kastens, J. H. (2002). Crop identification using harmonic analysis of time-series AVHRR NDVI data. Computers and Electronics in Agriculture, 37(1-3), 127-139.

Jaradat, A. A. 2002. Agriculture in Iraq: Resources, Potentials, Constraints, and Research needs and priorities. NCSC research lab, ARS-USDA. Washington, D. C., USA.

Jarvis, A., H.I. Reuter, A. Nelson, and E. Guevara. 2008. "Hole-filled SRTM for the globe Version 4, available from the CGIAR-CSI SRTM 90m Database." (Accessed December 12). http://srtm.csi.cgiar.org.

Jeganathan, C., Dash, J., & Atkinson, P. M. (2010). Mapping the phenology of natural vegetation in India using a remote sensing-derived chlorophyll index. International Journal of Remote Sensing, 31(22), 5777-5796.

Jeganathan, C., Dash, J., & Atkinson, P. M. (2010a). Characterising the spatial pattern of phenology for the tropical vegetation of India using multi-temporal MERIS chlorophyll data LANDSCAPE ECOLOGY, 25(7), 1125-1141.

Jeganathan, C., Ganguly, S., Dash, J., Friedl, M., & Atkinson, P. M. (2010). Terrestrial vegetation phenology from MODIS and MERIS sensor data. Proceedings 2010 IEEE International Geoscience and Remote Sensing Symposium (IGARSS 2010), 2699-2702.

Jia, K., Li, Q. Z., Tian, Y. C., Wu, B. F., Zhang, F. F., & Meng, J. H. (2012). Crop classification using multi-configuration SAR data in the North China Plain. International Journal of Remote Sensing, 33(1), 170-183.

Jiang, Z. Y., Huete, A. R., Didan, K., & Miura, T. (2008). Development of a two-band enhanced vegetation index without a blue band. Remote Sensing of Environment, 112(10), 3833-3845.

Jianhong, L., Yaozhong, P., Xiufang, Z., & Wenquan, Z. (2014). Using phenological metrics and the multiple classifier fusion method to map land cover types. Journal of Applied Remote Sensing, 8, 083691 (083615 pp.)-083691 (083615 pp.).

Jianqiang, R., Su, L., Zhongxin, C., Qingbo, Z., & Huajun, T. (2008). Regional yield prediction for winter wheat based on crop biomass estimation using multi-source data. 2007 IEEE International Geoscience and Remote Sensing Symposium, IGARSS 2007, 805-808.

Jiao, X. F., Kovacs, J. M., Shang, J. L., McNairn, H., Walters, D., Ma, B. L., & Geng, X. Y. (2014). Object-oriented crop mapping and monitoring using multi-temporal polarimetric RADARSAT-2 data. Isprs Journal of Photogrammetry and Remote Sensing, 96, 38-46.

Joiner, J., Yoshida, Y., Vasilkov, A. P., Yoshida, Y., Corp, L. A., & Middleton, E. M. (2011). First observations of global and seasonal terrestrial chlorophyll fluorescence from space. Biogeosciences, 8(3), 637-651.

Jones, C., Lowe, J., Liddicoat, S., & Betts, R. (2009). Committed terrestrial ecosystem changes due to climate change. Nature Geoscience, 2(7), 484-487.

Jonsson, P., & Eklundh, L. (2002). Seasonality extraction by function fitting to time-series of satellite sensor data. Ieee Transactions on Geoscience and Remote Sensing, 40(8), 1824-1832.

Jonsson, P., & Eklundh, L. (2004). TIMESAT - a program for analyzing time-series of satellite sensor data. Computers & Geosciences, 30(8), 833-845.

Justice, C., & Becker-Reshef, I. (2007). Report from the Workshop on Developing a Strategy for Global Agricultural Monitoring in the framework of Group on Earth Observations (GEO). Rome, Italy: Geography Department, University of Maryland.

Justice, C.; Becker-Reshef, I. Report from the Workshop on Developing a Strategy for Global Agricultural Monitoring in the framework of Group on Earth

Observations (GEO) 16–18 July 2007, FAO, Rome; University of Maryland: College Park, MD, USA, 2007.

Kandasamy, S., Baret, F., Verger, A., Neveux, P., & Weiss, M. (2013). A comparison of methods for smoothing and gap filling time series of remote sensing observations - application to MODIS LAI products. Biogeosciences, 10(6), 4055-4071.

Kang, S. Y., Running, S. W., Lim, J. H., Zhao, M. S., Park, C. R., & Loehman, R. (2003). A regional phenology model for detecting onset of greenness in temperate mixed forests, Korea: an application of MODIS leaf area index. Remote Sensing of Environment, 86(2), 232-242.

Kastens, J. H., Kastens, T. L., Kastens, D. L. A., Price, K. P., Martinko, E. A., & Lee, R. Y. (2005). Image masking for crop yield forecasting using AVHRR NDVI time series imagery. Remote Sensing of Environment, 99(3), 341-356.

Key, T., Warner, T. A., McGraw, J. B., & Fajvan, M. A. (2001). A comparison of multispectral and multitemporal information in high spatial resolution imagery for classification of individual tree species in a temperate hardwood forest. Remote Sensing of Environment, 75(1), 100-112.

Kirby, M., Connor, J., Bark, R., Qureshi, E., & Keyworth, S. (2012). The economic impact of water reductions during the Millennium Drought in the Murray-Darling Basin. Paper presented at the Australian Agricultural and Resource Economics Society Annual Conference 2012, Freemantle, Australia.

Kitoh, A., Yatagai, A., & Alpert, P. (2008). First super-high-resolution model projection that the ancient “Fertile Crescent” will disappear in this century. Hydrological Research Letters, 2, 1-4.

Knight, J. F., Lunetta, R. S., Ediriwickrema, J., & Khorrarn, S. (2006). Regional scale land cover characterization using MODIS-NDVI 250 m multi-temporal imagery: A phenology-based approach. Giscience & Remote Sensing, 43(1), 1-23.

Kogan, F., Kussul, N., Adamenko, T., Skakun, S., Kravchenko, O., Kryvobok, O. Lavrenyuk, A. (2013). Winter wheat yield forecasting in Ukraine based on Earth observation, meteorological data and biophysical models. International Journal of Applied Earth Observation and Geoinformation, 23, 192-203.

Kogan, F., Salazar, L., & Roytman, L. (2012). Forecasting crop production using satellite-based vegetation health indices in Kansas, USA. International Journal of Remote Sensing, 33(9), 2798-2814.

Kouadio, L., Newlands, N. K., Davidson, A., Zhang, Y. S., & Chipanshi, A. (2014). Assessing the Performance of MODIS NDVI and EVI for Seasonal Crop Yield Forecasting at the Ecodistrict Scale. Remote Sensing, 6(10), 10193-10214.

Krishna, G., Sahoo, R. N., Pargal, S., Gupta, V. K., Sinha, P., Bhagat, S., Chattopadhyay, C. (2014). Assessing Wheat Yellow Rust Disease through Hyperspectral Remote Sensing. In V. K. Dadhwal, P. G. Diwakar, M. V. R. Seshasai, P. L. N. Raju & A. Hakeem (Eds.), Isprs Technical Commission Viii Symposium (Vol. 40-8, pp. 1413-1416). Gottingen: Copernicus Gesellschaft Mbh.

Krishna, T. M., Ravikumar, G., & Krishnaveni, M. (2009). Remote Sensing Based Agricultural Drought Assessment in Palar Basin of Tamil Nadu State, India. Journal of the Indian Society of Remote Sensing, 37(1), 9-20.

Labus, M. P., Nielsen, G. A., Lawrence, R. L., Engel, R., & Long, D. S. (2002). Wheat yield estimates using multi-temporal NDVI satellite imagery. International Journal of Remote Sensing, 23(20), 4169-4180.

Leite, P. B. C., Feitosa, R. Q., Formaggio, A. R., da Costa, G., Pakzad, K., & Sanches, I. D. (2011). Hidden Markov Models for crop recognition in remote sensing image sequences. Pattern Recognition Letters, 32(1), 19-26.

Leroux, L., Jolivot, A., Begue, A., Lo Seen, D., & Zoungrana, B. (2014). How Reliable is the MODIS Land Cover Product for Crop Mapping Sub-Saharan Agricultural Landscapes? Remote Sensing, 6(9), 8541-8564.

Li, J. (2002). Crop Condition Monitoring and Production Prediction System with Meteorological Satellite Data. Meteorological Science and Technology, 30(2), 108-111

Li, J., Zheng Y. & Ying, J. (2001). Application of 3S to Growth Vigour Monitoring for Late Rice of Double Harvest. Journal of Nanjing Institute of Meteorology, 24 (1), 106-112

Li, L., Friedl, M. A., Xin, Q. C., Gray, J., Pan, Y. Z., & Frolking, S. (2014). Mapping Crop Cycles in China Using MODIS-EVI Time Series. Remote Sensing, 6(3), 2473-2493.

Li, M., Qu, J. J., & Hao, X. (2010). Investigating phenological changes using MODIS vegetation indices in deciduous broadleaf forest over continental U.S. during 2000-2008. Ecological Informatics, 5(5), 410-417.

Li, X. L., Ma, Z. H., Zhao, L. L., Li, J. H., & Wang, H. G. (2013). Early diagnosis of wheat stripe rust and wheat leaf rust using near infrared spectroscopy. Spectroscopy and Spectral Analysis, 33(10), 2661-2665.

Lin, C., Gao-huan, L., Chong, H., Qing-sheng, L., & Lin, C. (2014). Phenology detection of winter wheat in the Yellow River delta using MODIS NDVI time-series data. 2014 Third International Conference on Agro-Geoinformatics, 5 pp.-5 pp.

Liu, K. & Zhang, X. (1997). Study on Monitor of Rice Growing And Rice Yield Estimation By Remote Sensing In Jianghan Plain. Journal of Central China Normal University (Nat. Sci.), 31(4), 482-487.

Liu, L. Y., Wang, J. H., Huang, W. J., Zhao, C. J., Zhang, B., & Tong, Q. X. (2004). Estimating winter wheat plant water content using red edge parameters. International Journal of Remote Sensing, 25(17), 3331-3342.

Liu, W. T., & Kogan, F. (2002). Monitoring Brazilian soybean production using NOAA/AVHRR based vegetation condition indices. International Journal of Remote Sensing, 23(6), 1161-1179.

Lobell, D. B. (2013). The use of satellite data for crop yield gap analysis. Field Crops Research, 143, 56-64.

Lobell, D. B., Asner, G. P., Ortiz-Monasterio, J. I., & Benning, T. L. (2003). Remote sensing of regional crop production in the Yaqui Valley, Mexico: estimates and uncertainties. Agriculture Ecosystems & Environment, 94(2), 205-220.

Lobell, D. B., Cassman, K. G., & Field, C. B. (2009). Crop Yield Gaps: Their Importance, Magnitudes, and Causes Annual Review of Environment and Resources (Vol. 34, pp. 179-204).

Lobell, D. B., Sibley, A., & Ivan Ortiz-Monasterio, J. (2012). Extreme heat effects on wheat senescence in India. Nature Climate Change, 2(3), 186-189.

Long, S. P., Zhu, X. G., Naidu, S. L., & Ort, D. R. (2006). Can improvement in photosynthesis increase crop yields? Plant Cell and Environment, 29(3), 315-330.

Los, S. O., Collatz, G. J., Sellers, P. J., Malmstrom, C. M., Pollack, N. H., DeFries, R. S., Dazlich, D. A. (2000). A global 9-yr biophysical land surface dataset from NOAA AVHRR data. Journal of Hydrometeorology, 1(2), 183-199.

Loveland, T. R., Merchant, J. W., Brown, J. F., Ohlen, D. O., Reed, B. C., Olson, P., & Hutchinson, J. (1995). Seasonal Land-Cover Regions of the United States. Annals of the Association of American Geographers, 85(2), 339-355.

Low, F., Michel, U., Dech, S., & Conrad, C. (2013). Impact of feature selection on the accuracy and spatial uncertainty of per-field crop classification using Support Vector Machines. Isprs Journal of Photogrammetry and Remote Sensing, 85, 102-119.

Lu, D., & Weng, Q. (2007). A survey of image classification methods and techniques for improving classification performance. International Journal of Remote Sensing, 28(5), 823-870.

Lu, D., Batistella, M., Li, G., Moran, E., Hetrick, S., Freitas, C. d. C. Siqueira Sant'Anna, S. J. (2012). Land use/cover classification in the Brazilian Amazon using satellite images. Pesquisa Agropecuaria Brasileira, 47(9), 1185-1208.

Lupo, F., Linderman, M., Vanacker, V., Bartholome, E., & Lambin, E. F. (2007). Categorization of land-cover change processes based on phenological indicators extracted from time series of vegetation index data. International Journal of Remote Sensing, 28(11), 2469-2483.

Macdonald, R. B., & Hall, F. G. (1980). Global crop forecasting. Science, 208(4445), 670-679.

Mahey, R. K., Singh, R., Sidhu, S. S., Narang, R. S., Dadhwal, V. K., Parihar, J. S., & Sharma, A. K. (1993). Preharvest state-level wheat acreage estimation using IRS-IA LISS-I data in Punjab (India). International Journal of Remote Sensing, 14(6), 1099-1106.

Maignan, F., Breon, F. M., Bacour, C., Demarty, J., & Poirson, A. (2008). Interannual vegetation phenology estimates from global AVHRR

measurements - Comparison with in situ data and applications. Remote Sensing of Environment, 112(2), 496-505.

Mariotti, A., Zeng, N., Yoon, J.-H., Artale, V., Navarra, A., Alpert, P., & Li, L. Z. X. (2008). Mediterranean water cycle changes: transition to drier 21st century conditions in observations and CMIP3 simulations. Environmental Research Letters, 3(4).

Mas, J. F., & Flores, J. J. (2008). The application of artificial neural networks to the analysis of remotely sensed data. International Journal of Remote Sensing, 29(3), 617-663.

Maselli, F., Romanelli, S., Bottai, L., & Maracchi, G. (2000). Processing of GAC NDVI data for yield forecasting in the Sahelian region. International Journal of Remote Sensing, 21(18), 3509-3523.

Masialeti, I., Egbert, S., & Wardlow, B. D. (2010). A Comparative Analysis of Phenological Curves for Major Crops in Kansas. Giscience & Remote Sensing, 47(2), 241-259.

Matinfar, H. R., Panah, S. K. A., Zand, F., & Khodaei, K. (2013). Detection of soil salinity changes and mapping land cover types based upon remotely sensed data. Arabian Journal of Geosciences, 6(3), 913-919.

Maxwell S, Smith M (1992) Household food security: a conceptual review. In: Maxwell S, Frankenberger T (eds) Household food security: concepts, indicators, measurements. IFAD and UNICEF, Rome and New York.

Maystadt, J. F., Tan, J. F. T., & Breisinger, C. (2014). Does food security matter for transition in Arab countries? Food Policy, 46, 106-115.

McCallum, I., Obersteiner, M., Nilsson, S., & Shvidenko, A. (2006). A spatial comparison of four satellite derived 1 km global land cover datasets. International Journal of Applied Earth Observation and Geoinformation, 8(4), 246-255.

McCallum, I., Obersteiner, M., Nilsson, S., & Shvidenko, A. (2006). A spatial comparison of four satellite derived 1 km global land cover datasets. International Journal of Applied Earth Observation and Geoinformation, 8(4), 246-255.

Mellor, J. W. (1972). Accelerated Growth in Agricultural Production and Intersectional Transfer of Resources: Department of Agricultural Economics Cornell University, No 34.

Meng, J.-h., & Wu, B.-f. (2008). Study on the crop condition monitoring methods with remote sensing.

Menke, J. W., & Trlica, M. J. (1981). Carbohydrate reserve, phenology, and growth cycles of 9 Colorado range species. Journal of Range Management, 34(4), 269-277.

Menzel, A., Sparks, T. H., Estrella, N., Koch, E., Aasa, A., Ahas, R., Zust, A. (2006). European phenological response to climate change matches the warming pattern. Global Change Biology, 12(10), 1969-1976.

Meyers, E. M. (Ed.). (1997). The Oxford Encyclopedia of Archaeology in the Near East. United Kingdom: Oxford University Press.

Michael E. B. (2007). Comparison of Estimating Crop Yield at the County Level. United States Department of Agriculture (USDA), National Agricultural Statistics Service. RDD-07-05. Washington DC 20250. Pp2.

Michishita, R., Jin, Z. Y., Chen, J., & Xu, B. (2014). Empirical comparison of noise reduction techniques for NDVI time-series based on a new measure. Isprs Journal of Photogrammetry and Remote Sensing, 91, 17-28.

Middleton, E. M., Corp, L. A., & Campbell, P. K. E. (2008). Comparison of measurements and FluorMOD simulations for solar-induced chlorophyll fluorescence and reflectance of a corn crop under nitrogen treatments. International Journal of Remote Sensing, 29(17-18), 5193-5213.

Millennium Ecosystem Assessment, 2005. Ecosystems and Human Well-being: Biodiversity Synthesis. World Resources Institute, Washington, DC.

Millennium Ecosystem Assessment, 2005. Ecosystems and Human Well-being: Biodiversity Synthesis. World Resources Institute, Washington, DC.

Mkhabela, M. S., Bullock, P., Raj, S., Wang, S., & Yang, Y. (2011). Crop yield forecasting on the Canadian Prairies using MODIS NDVI data. Agricultural and Forest Meteorology, 151(3), 385-393.

Modarres, R., & da Silva, V. D. R. (2007). Rainfall trends in arid and semi-arid regions of Iran. Journal of Arid Environments, 70(2), 344-355.

Mooney, H. A., & Billings, W. D. (1960). The annual carbohydrate cycle of alpine plants as related to growth. Amer Jour Bot, 47((7)), 594-598.

Moran, M. S., Alonso, L., Moreno, J. F., Mateo, M. P. C., de la Cruz, D. F., & Montoro, A. (2012). A RADARSAT-2 Quad-Polarized Time Series for Monitoring Crop and Soil Conditions in Barrax, Spain. IEEE Transactions on Geoscience and Remote Sensing, 50(4), 1057-1070.

Moriondo, M., Maselli, F., & Bindi, M. (2007). A simple model of regional wheat yield based on NDVI data. European Journal of Agronomy, 26(3), 266-274.

Morisette, J. T., Richardson, A. D., Knapp, A. K., Fisher, J. I., Graham, E. A., Abatzoglou, J., . . . Liang, L. (2009). Tracking the rhythm of the seasons in the face of global change: phenological research in the 21st century. Frontiers in Ecology and the Environment, 7(5), 253-260.

Mountrakis, G., Im, J., & Ogole, C. (2011). Support vector machines in remote sensing: A review. Isprs Journal of Photogrammetry and Remote Sensing, 66(3), 247-259.

Muchoney, D., Strahler, A., Hodges, J., & LoCastro, J. (1999). The IGBP DISCover confidence sites and the system for terrestrial ecosystem parameterization: Tools for validating global land-cover data. Photogrammetric Engineering and Remote Sensing, 65(9), 1061-1067.

Mulianga, B., Begue, A., Simoes, M., & Todoroff, P. (2013). Forecasting Regional Sugarcane Yield Based on Time Integral and Spatial Aggregation of MODIS NDVI. Remote Sensing, 5(5), 2184-2199.

Muller, K. R., Mika, S., Ratsch, G., Tsuda, K. & Scholkopf, B. (2001). An introduction to kernel-based learning algorithms. IEEE Transactions on Neural Networks, 12(2), 181-201.

Murray, M. B., Cannell, M. G. R., & Smith, R. I. (1989). Date of 15 three species Britain following climatic warming. Journal of Applied Ecology, 26(2), 693-700.

Narciso, G., Baruth, B., Klisch, A. (2008) “Crop Area Estimates with Radarsat: Feasibility Study in the Toscana Region – Italy”, Internal report, JRC, IPSC – Agriculture Unit.

NASA Land Processes Distributed Active Archive Centre (LP DAAC). MODIS land surface reflectance (MOD09Q1) and MODIS land cover type (MCD12Q1) 2014. (https://lpdaac.usgs.gov/data_access).

National development plan, "Republic of Iraq, ministry of planning," Baghdad, Iraq, 2010.

Nemani, R., & Running, S. W. (1996). Implementation of a hierarchical global vegetation classification in ecosystem function models. Journal of Vegetation Science, 7(3), 337–346.

Newstrom, L. E., Frankie, G. W., & Baker, H. G. (1994). A new classification for plant phenology based on flowering patterns in lowland tropical rain-forest trees at La-Selva, Costa-Rica. Biotropica, 26(2), 141-159.

Ozdogan, M. (2010). The spatial distribution of crop types from MODIS data: Temporal unmixing using Independent Component Analysis. Remote Sensing of Environment, 114(6), 1190-1204.

Pahlevan, N., & Schott, J. R. (2013). Leveraging EO-1 to Evaluate Capability of New Generation of Landsat Sensors for Coastal/Inland Water Studies. Ieee Journal of Selected Topics in Applied Earth Observations and Remote Sensing, 6(2), 360-374.

Pal, M., & Mather, P. M. (2005). Support vector machines for classification in remote sensing. International Journal of Remote Sensing, 26(5), 1007-1011.

Paola, J. D., & Schowengerdt, R. A. (1995). A detailed comparison of backpropagation neural-network and maximum-likelihood classifier for urban land-use classification. IEEE Transactions on Geoscience and Remote Sensing, 33(4), 981-996.

Parazoo, N. C., Bowman, K., Fisher, J. B., Frankenberg, C., Jones, D. B. A., Cescatti, A., Montagnani, L. (2014). Terrestrial gross primary production inferred from satellite fluorescence and vegetation models. Global Change Biology, 20(10), 3103-3121.

Pau, S., Wolkovich, E. M., Cook, B. I., Davies, T. J., Kraft, N. J. B., Bolmgren, K., . . . Cleland, E. E. (2011). Predicting phenology by integrating ecology, evolution and climate science. Global Change Biology, 17(12), 3633-3643.

Paul, R. K., Prajneshu, & Ghosh, H. (2013). Statistical modelling for forecasting of wheat yield based on weather variables. Indian Journal of Agricultural Sciences, 83(2), 180-183.

Pflugmacher, D., Krankina, O. N., Cohen, W. B., Friedl, M. A., Sulla-Menashe, D., Kennedy, R. E., Kharuk, V. I. (2011). Comparison and assessment of coarse resolution land cover maps for Northern Eurasia. Remote Sensing of Environment, 115(12), 3539-3553.

Polgar, C. A., & Primack, R. B. (2011). Leaf-out phenology of temperate woody plants: from trees to ecosystems. New Phytologist, 191(4), 926-941.

Pongratz, J., Reick, C. H., Raddatz, T., & Claussen, M. (2009). Effects of anthropogenic land cover change on the carbon cycle of the last millennium. Global Biogeochemical Cycles, 23.

Potgieter, A. B., Apan, A., Dunn, P., & Hammer, G. (2007). Estimating crop area using seasonal time series of Enhanced Vegetation Index from MODIS satellite imagery. Australian Journal of Agricultural Research, 58(4), 316-325.

Potgieter, A. B., Apan, A., Hammer, G., & Dunn, P. (2010). Early-season crop area estimates for winter crops in NE Australia using MODIS satellite imagery. Isprs Journal of Photogrammetry and Remote Sensing, 65(4), 380-387.

Potgieter, A. B., Everingham, Y. L., & Hammer, G. L. (2003). On measuring quality of a probabilistic commodity forecast for a system that incorporates seasonal climate forecasts. International Journal of Climatology, 23(10), 1195-1210.

Potgieter, A. B., Lawson, K., & Huete, A. R. (2013). Determining crop acreage estimates for specific winter crops using shape attributes from sequential MODIS imagery. International Journal of Applied Earth Observation and Geoinformation, 23, 254-263.

Potgieter, A., Apan, A., Hammer, G., & Dunn, P. (2011). Estimating winter crop area across seasons and regions using time-sequential MODIS imagery. International Journal of Remote Sensing, 32(15), 4281-4310.

Prasad, A. K., Chai, L., Singh, R. P., & Kafatos, M. (2006). Crop yield estimation model for Iowa using remote sensing and surface parameters.

International Journal of Applied Earth Observation and Geoinformation, 8(1), 26-33.

Qader, S. H., Atkinson, P. M., & Dash, J. (2015). Spatiotemporal variation in the terrestrial vegetation phenology of Iraq and its relation with elevation. International Journal of Applied Earth Observation and Geoinformation, 41, 107-117.

Qader, S. H., Dash, J., Atkinson, P. M., & Rodriguez-Galiano, V. (2016). Classification of Vegetation Type in Iraq Using Satellite-Based Phenological Parameters. Ieee Journal of Selected Topics in Applied Earth Observations and Remote Sensing, 9(1), 414-424.

Qiu, B., Zhong, M., Tang, Z., & Chen, C. (2013). Spatiotemporal variability of vegetation phenology with reference to altitude and climate in the subtropical mountain and hill region, China. Chinese Science Bulletin, 58(23), 2883-2892.

Quarmby, N. A., Milnes, M., Hindle, T. L., & Silleos, N. (1993). The use of multitemporal NDVI measurements from AVHRR data for crop yield estimation and prediction. International Journal of Remote Sensing, 14(2), 199-210.

Ran, Y. H., Li, X., Lu, L., & Li, Z. Y. (2012). Large-scale land cover mapping with the integration of multi-source information based on the Dempster-Shafer theory. International Journal of Geographical Information Science, 26(1), 169-191.

Rasmussen, M. S. (1997). Operational yield forecast using AVHRR NDVI data: Reduction of environmental and inter-annual variability. International Journal of Remote Sensing, 18(5), 1059-1077.

Reed, B. C., Brown, J. F., Vanderzee, D., Loveland, T. R., Merchant, J. W., & Ohlen, D. O. (1994). Measuring phenological variability from satellite imagery. Journal of Vegetation Science, 5(5), 703-714.

Reed, B. C., White, M., & Brown, J. F. (2003). Remote sensing phenology. Phenology: An Integrative Environmental Science, 39, 365-381.

Reeves, M. C., Zhao, M., & Running, S. W. (2005). Usefulness and limits of MODIS GPP for estimating wheat yield. International Journal of Remote Sensing, 26(7), 1403-1421.

Ren, J. Q., Chen, Z. X., Zhou, Q. B., & Tang, H. J. (2008). Regional yield estimation for winter wheat with MODIS-NDVI data in Shandong, China. International Journal of Applied Earth Observation and Geoinformation, 10(4), 403-413.

Reynolds, C. A., Yitayew, M., Slack, D. C., Hutchinson, C. F., Huete, A., & Petersen, M. S. (2000). Estimating crop yields and production by integrating the FAO Crop specific Water Balance model with real-time satellite data and ground-based ancillary data. International Journal of Remote Sensing, 21(18), 3487-3508.

Richardson, A. D., Keenan, T. F., Migliavacca, M., Ryu, Y., Sonnentag, O., & Toomey, M. (2013). Climate change, phenology, and phenological control of vegetation feedbacks to the climate system. Agricultural and Forest Meteorology, 169, 156-173.

Rocha, A. V., & Shaver, G. R. (2009). Advantages of a two band EVI calculated from solar and photosynthetically active radiation fluxes. Agricultural and Forest Meteorology, 149(9), 1560-1563.

Rodriguez-Galiano, V. F., & Chica-Rivas, M. (2014). Evaluation of different machine learning methods for land cover mapping of a Mediterranean area using multi-seasonal Landsat images and Digital Terrain Models. International Journal of Digital Earth, 7(6), 492-509.

Rogan, J., Franklin, J., Stow, D., Miller, J., Woodcock, C., & Roberts, D. (2008). Mapping land-cover modifications over large areas: A comparison of machine learning algorithms. Remote Sensing of Environment, 112(5), 2272-2283.

Rojas, O. (2007). Operational maize yield model development and validation based on remote sensing and agro-meteorological data in Kenya. International Journal of Remote Sensing, 28(17), 3775-3793.

Ross, K. W., Brown, M. E., Verdin, J. P., & Underwood, L. W. (2009). Review of FEWS NET biophysical monitoring requirements. Environmental Research Letters, 4(2), 10.

Royal Society of London (2009). Reaping the benefits: science and the sustainable intensification of global agriculture.

Running, S. W., Loveland, T. R., & Pierce, L. L. (1994). A vegetation classification logic-based on remote-sensing for use in global biochemical models. Ambio, 23(1), 77-81.

S. Griffin and E. Kunz, "Data fusion and integration of high and medium resolution imagery for crop analysis," in ASPRS 2009 Annual Conference, A. S. f. P. a. R. Sensing, Ed., ed. Baltimore, Maryland, 2009.

Sakamoto, T., Gitelson, A. A., & Arkebauer, T. J. (2013). MODIS-based corn grain yield estimation model incorporating crop phenology information. Remote Sensing of Environment, 131, 215-231.

Sakamoto, T., Yokozawa, M., Toritani, H., Shibayama, M., Ishitsuka, N., & Ohno, H. (2005). A crop phenology detection method using time-series MODIS data. Remote Sensing of Environment, 96(3-4), 366-374.

Scepan, J. (1999). Thematic validation of high-resolution global land-cover data sets. Photogrammetric Engineering and Remote Sensing, 65(9), 1051-1060.

Schnepf, R. (2003). Iraq's Agriculture: Background and Status, Congressional Research Service Report for Congress, The Library of Congress. Washington, D.C.

Schnepf, R. (2004). Iraq Agriculture and Food Supply: Background and Issues, Congressional Research Service. Washington, D.C.: The Library of Congress.

Schowengerdt, R. A. (1997). Remote sensing models and methods for image processing (2 ed.). San Diego.

Schut, A. G. T., Stephens, D. J., Stovold, R. G. H., Adams, M., & Craig, R. L. (2009). Improved wheat yield and production forecasting with a moisture stress index, AVHRR and MODIS data. Crop & Pasture Science, 60(1), 60-70.

Seager, R., Liu, H. B., Henderson, N., Simpson, I., Kelley, C., Shaw, T., Ting, M. F. (2014). Causes of Increasing Aridification of the Mediterranean Region in Response to Rising Greenhouse Gases. Journal of Climate, 27(12), 4655-4676.

Seager, R., Ting, M., Held, I., Kushnir, Y., Lu, J., Vecchi, G., Naik, N. (2007). Model projections of an imminent transition to a more arid climate in southwestern North America. Science, 316(5828), 1181-1184.

Seelan, S. K., Laguette, S., Casady, G. M., & Seielstad, G. A. (2003). Remote sensing applications for precision agriculture: A learning community approach. Remote Sensing of Environment, 88(1-2), 157-169.

Seneviratne, S. I. (2012). Climate science, historical drought trends revisited. Nature, 491(7424), 338-339.

Shao, Y., & Lunetta, R. S. (2012). Comparison of support vector machine, neural network, and CART algorithms for the land-cover classification using limited training data points. Isprs Journal of Photogrammetry and Remote Sensing, 70, 78-87.

Shaw, D. J. 2007. World food security: a history since 1945, New York, Palgrave MacMillan.

Sheffield, J., Andreadis, K. M., Wood, E. F., & Lettenmaier, D. P. (2009). Global and Continental Drought in the Second Half of the Twentieth Century: Severity-Area-Duration Analysis and Temporal Variability of Large-Scale Events. Journal of Climate, 22(8), 1962-1981.

Sheffield, J., Wood, E. F., & Roderick, M. L. (2012). Little change in global drought over the past 60 years. Nature, 491(7424), 435.

Shuai, Y., Schaaf, C., Zhang, X., Strahler, A., Roy, D., Morisette, J., Davies, J. E. (2013). Daily MODIS 500 m reflectance anisotropy direct broadcast (DB) products for monitoring vegetation phenology dynamics. International Journal of Remote Sensing, 34(16), 5997-6016.

Singh, N., & Glenn, N. F. (2009). Multitemporal spectral analysis for cheatgrass (Bromus tectorum) classification. International Journal of Remote Sensing, 30(13), 3441-3462.

Singh, R., Semwal, D. P., Rai, A., & Chhikara, R. S. (2002). Small area estimation of crop yield using remote sensing satellite data. International Journal of Remote Sensing, 23(1), 49-56.

Sitch, S., Brovkin, V., von Bloh, W., van Vuuren, D., Assessment, B., & Ganopolski, A. (2005). Impacts of future land cover changes on atmospheric CO2 and climate. Global Biogeochemical Cycles, 19(2).

Sivakumar, M. V. K. (2005). Impacts of natural disasters in agriculture, rangeland and forestry: An overview. Berlin: Springer-Verlag Berlin.

Siyuan, W., Bing, Z., Cunjian, Y., Yan, Z., & Hui, W. (2012). Temporal change and suitability assessment of cropland in the yellow river basin during 1990-2005. International Journal of Geographical Information Science, 26(3), 519-539.

Sobrino, J. A. (2015). Fourth International Symposium on Recent Advances in Quantitative Remote Sensing PREFACE. International Journal of Remote Sensing, 36(19-20), 4775-4778.

Son, N. T., Chen, C. F., Chen, C. R., Chang, L. Y., Duc, H. N., & Nguyen, L. D. (2013). Prediction of rice crop yield using MODIS EVI-LAI data in the Mekong Delta, Vietnam. International Journal of Remote Sensing, 34(20), 7275-7292.

Son, N. T., Chen, C. F., Chen, C. R., Duc, H. N., & Chang, L. Y. (2014). A Phenology-Based Classification of Time-Series MODIS Data for Rice Crop Monitoring in Mekong Delta, Vietnam. Remote Sensing, 6(1), 135-156.

Song, C. H., & Woodcock, C. E. (2003). Monitoring forest succession with multitemporal Landsat images: Factors of uncertainty. IEEE Transactions on Geoscience and Remote Sensing, 41(11), 2557-2567.

Soudani, K., Maire, G. l., Dufrêne, E., François, C., Delpierre, N., Ulrich, E., & Cecchini, S. (2008). Evaluation of the onset of green-up in temperate deciduous broadleaf forests derived from Moderate Resolution Imaging Spectroradiometer (MODIS) data. Remote Sensing of Environment, 112(5), 2643–2655.

Sparks, T. H., & Carey, P. D. (1995). The response of species to climate over 2 centuries - an analysis of the marsham phenological record, 1736-1947. Journal of Ecology, 83(2), 321-329.

Srikanth, P., Ramana, K. V., Shankar Prsad, T., KK Choudhary, K. K., Chandrasekhar, K., Seshasai, M., & Behera, G. (2011). nventory of irrigated

Rice Ecosystem using Polarimetric SAR dat. ISPRS Archives Vol. XXXVIII-8/W20, p 46-49.

Stehman, S. V., & Czaplewski, R. L. (1998). Design and analysis for thematic map accuracy assessment: Fundamental principles. Remote Sensing of Environment, 64(3), 331-344.

Stehman, S. V., & Milliken, J. A. (2007). Estimating the effect of crop classification error on evapotranspiration derived from remote sensing in the lower Colorado River basin, USA. Remote Sensing of Environment, 106(2), 217-227.

Strahler, A., Boschetti, L., Foody, G. M., Fiedl, M. A., Hansen, M. C., Herold, M., Mayaux, P., Morisette, J. T., Stehman, S. V. & C. Woodcock (2006): Global Land Cover Validation: Recommendations for Evaluation and Accuracy Assessment Of Global Land Cover Maps, Report of Committee of Earth Observation Satellites (CEOS) - Working Group on Calibration and Validation (WGCV).

Tan, B., Woodcock, C. E., Hu, J., Zhang, P., Ozdogan, M., Huang, D., Myneni, R. B. (2006). The impact of gridding artifacts on the local spatial properties of MODIS data: Implications for validation, compositing, and band-to-band registration across resolutions. Remote Sensing of Environment, 105(2), 98-114.

Tavakkoli, S. M., Lohmann, P., & Soergel, U. (2006.). Multi-temporal segment based classification of ASAR images of an agricultural area. Paper presented at the Proceeding of the 2nd Gottingen GIS and remote sensing days 2006, Germany.

Teillet, P. M., Staenz, K., & William, D. J. (1997). Effects of spectral, spatial, and radiometric characteristics on remote sensing vegetation indices of forested regions. Remote Sensing of Environment, 61(1), 139–149.

Teixeira, A., Bastiaanssen, W. G. M., Ahmad, M. D., & Bos, M. G. (2009). Reviewing SEBAL input parameters for assessing evapotranspiration and water productivity for the Low-Middle Sao Francisco River basin, Brazil Part B: Application to the regional scale. Agricultural and Forest Meteorology, 149(3-4), 477-490.

Tennakoon, S. B., Murty, V. V. N., & Eiumnoh, A. (1992). Estimation of cropped area and grian-yield of rice using remote sensing data. International Journal of Remote Sensing, 13(3), 427-439.

Thenkabail, P. S., Biradar, C. M., Noojipady, P., Dheeravath, V., Li, Y. J., Velpuri, M., Dutta, R. (2009). Global irrigated area map (GIAM), derived from remote sensing, for the end of the last millennium. International Journal of Remote Sensing, 30(14), 3679-3733.

Thiruvengadachari, S. (1981). Satellite sensing of irrigation patterns in semiarid areas—An Indian study. Photogrammetric Engineering & Remote Sensing, 47, 1493-1499.

Thu, P. M., & Populus, J. (2007). Status and changes of mangrove forest in Mekong Delta: Case study in Tra Vinh, Vietnam. Estuarine Coastal and Shelf Science, 71(1-2), 98-109.

Tilman, D., Balzer, C., Hill, J., & Befort, B. L. (2011). Global food demand and the sustainable intensification of agriculture. Proceedings of the National Academy of Sciences of the United States of America, 108(50), 20260-20264.

Tilman, D., Fargione, J., Wolff, B., DÕAntonio, C., Dobson, A., Howarth, R., Swackhamer, D. (2001). Forecasting Agriculturally Driven Global Environmental Change. Science, 292.

Tucker, C. J., & Choudhury, B. J. (1987). Satellite remote sensing of drought conditions. Remote Sensing of Environment, 23(2), 243-251.

Tucker, C. J., Holben, B. N., Elgin, J. H., & McMurtrey, J. E. (1980). Relationship of spectral data to grain-yield variation. Photogrammetric Engineering and Remote Sensing, 46(5), 657-666.

UNDP 2014. Sustainable land management. http://www.undp.org/drylands.

UNDP/UNSO (1997). Aridity zones and dryland populations: An assessment of population levels in the world's drylands with particular reference to Africa. UNDP Office to Combat Desertification and Drought (UNSO), New York.

United Nations Environment Programme (UNEP 1992). World Atlas of Desertification. Edward Arnold. London.

United Nations Environment Programme (UNEP) 2007. UNEP in Iraq (Post-Conflict Assessment, Clean up and reconstruction). Nairobi, Kenya.

United Nations Food and Agriculture Organization (UN FAO), 2012. Crop Production Statistics for Iraq. URL: http://faostat.fao.org (access date: 16/10/2014).

United Nations Food and Agriculture Organization (UN FAO), 2012. Crop Production Statistics for Iraq. URL: http://faostat.fao.org (access date: 16/10/2014).

United Nations Information Center (UNIC) 2011. Arid lands too degraded to provide subsistence are home to one billion of the world's poorest, hungriest people. Washington, DC. http://www.unicwash.org (12/01/2015).

United States Department of Agriculture Foreign Agricultural Service (USDA FAS) (2008). MIDDLE EAST & CENTRAL ASIA: Continued Drought in 2009/10 Threatens Greater Food Grain Shortages. Commodity intelligent report. (20/01/2015) http://www.pecad.fas.usda.gov/highlights/2008/09/mideast_cenasia_drought/.

United States Department of Agriculture Foreign Agricultural Service (USDA FAS) (2008). MIDDLE EAST & CENTRAL ASIA: Continued Drought in 2009/10 Threatens Greater Food Grain Shortages. Commodity intelligent report. (20/01/2015) http://www.pecad.fas.usda.gov/highlights/2008/09/mideast_cenasia_drought/.

United States Department of Agriculture Foreign Agricultural Service (USDA FAS) 2008. Drought reduces 2008/09 winter grain production, URL: http://www.pecad.fas.usda.gov/highlights/2008/05/Iraq_may2008.htm (last date accessed: 7 December 2011).

Van Evert, F. K., & Campbell, G. S. (1994). CROPSYST - A COLLECTION OF OBJECT-ORIENTED SIMULATION-MODELS OF AGRICULTURAL SYSTEMS. Agronomy Journal, 86(2), 325-331.

Vandiepen, C. A., Wolf, J., Vankeulen, H., & Rappoldt, C. (1989). WOFOST - A SIMULATION-MODEL OF CROP PRODUCTION. Soil Use and Management, 5(1), 16-24.

Vicente-Serrano, S. M., Cuadrat-Prats, J. M., & Romo, A. (2006). Early prediction of crop production using drought indices at different time-scales and remote sensing data: application in the Ebro valley (North-East Spain). International Journal of Remote Sensing, 27(3), 511-518.

Vicente-Serrano, S. M., Cuadrat-Prats, J. M., & Romo, A. (2006). Early prediction of crop production using drought indices at different time-scales and remote sensing data: application in the Ebro valley (North-East Spain). International Journal of Remote Sensing, 27(3), 511-518.

Viovy, N., Arino, O., & Belward, A. S. (1992). The best index slope extraction (BISE)- a method for reducing noise in NDVI time-series. International Journal of Remote Sensing, 13(8), 1585-1590.

Viovy, N., Arino, O., & Belward, A. S. (1992). The Best Index Slope Extraction (BISE): A method for reducing noise in NDVI time-series. International Journal of Remote Sensing, 13(8), 1585-1590.

Vogelmann, J. E., Sohl, T., & Howard, S. M. (1998). Regional characterization of land cover using multiple. Photogrammetric Engineering and Remote Sensing, 64(1), 45-57.

Wagenseil, H., & Samimi, C. (2006). Assessing spatio-temporal variations in plant phenology using Fourier analysis on NDVI time series: results from a dry savannah environment in Namibia. International Journal of Remote Sensing, 27(16), 3455-3471.

Wall, L., Larocque, D., & Leger, P.-M. (2008). The early explanatory power of NDVI in crop yield modelling. International Journal of Remote Sensing, 29(8), 2211-2225.

Wang, B. F., Meng, J. H., & Li, Q. Z. (2010). An integrated crop condition monitoring system with remote sensing. Transactions of the Asabe, 53(3), 971-979.

Wang, C., Liu, H. Y., Zhang, Y., & Li, Y. F. (2014). Classification of land-cover types in muddy tidal flat wetlands using remote sensing data. Journal of Applied Remote Sensing, 7.

Wang, Y (1991). Using Remote Sensing Technology for Rice Growth Monitoring and Yield Estimating in South Rice Region of China. Remote Sensing Technology and Application, 6(3), 1-6

Wardlow, B. D., & Egbert, S. L. (2008). Large-area crop mapping using time-series MODIS 250 m NDVI data: An assessment for the US Central Great Plains. Remote Sensing of Environment, 112(3), 1096-1116.

Wardlow, B. D., Egbert, S. L., & Kastens, J. H. (2007). Analysis of time-series MODIS 250 m vegetation index data for crop classification in the US Central Great Plains. Remote Sensing of Environment, 108(3), 290-310.

Wessels, K., Steenkamp, K., von Maltitz, G., & Archibald, S. (2011). Remotely sensed vegetation phenology for describing and predicting the biomes of South Africa. Applied Vegetation Science, 14(1), 49-66.

Wetherald, R. T., & Manabe, S. (2002). Simulation of hydrologic changes associated with global warming. Journal of Geophysical Research-Atmospheres, 107(D19), 15.

Wheeler, T., & von Braun, J. (2013). Climate Change Impacts on Global Food Security. Science, 341(6145), 508-513.

Whitcraft, A. K., Becker-Reshef, I., & Justice, C. O. (2015). A Framework for Defining Spatially Explicit Earth Observation Requirements for a Global Agricultural Monitoring Initiative (GEOGLAM). Remote Sensing, 7(2), 1461-1481.

White, M. A., Hoffman, F., Hargrove, W. W., & Nemani, R. R. (2005). A global framework for monitoring phenological responses to climate change. Geophysical Research Letters, 32(4).

White, M. A., Thornton, P. E., & Running, S. W. (1997). A continental phenology model for monitoring vegetation responses to interannual climatic variability. Global Biogeochemical Cycles, 11(2), 217-234.

Wilhite, D. A., & Glantz, M. H. (1985). Understanding: the Drought Phenomenon: The Role of Difinitions. Water International, 10(3), 111-120.

Wilkinson, G. G. (2005). Results and implications of a study of fifteen years of satellite image classification experiments. IEEE Transactions on Geoscience and Remote Sensing, 43(3), 433-440.

World Bank (2006). Drought, management and mitigation assessment for central Asia and the Caucasus. Europe and Central Asia Region, Environmentally and Socially Sustainable Development Department.

World Bank, Dorte Verner and Mme. Fatma El-Mallah (League of Arab States) (2011). Adaptation to a Changing Climate in the Arab Countries MNA Flagship report, Sustainable Development Department, Middle East and North Africa Region, Oct. 2011.

World Bank, World Development Report 2008: Agriculture for Development (World Bank, Washington, DC, 2008).

World Disaster Report, 2001. "International Federation of Red Cross and Red Crescent Societies". Geneva.

World Food Program (WFP) 2011. Food Insecurity and Violent Conflict: Causes, Consequences, and Addressing the Challenges. Occasional paper n°24. (21/01/2015) http://documents.wfp.org/stellent/groups/public/documents/newsroom/wfp238358.pdf.

Wu, Z. T., Thenkabail, P. S., Mueller, R., Zakzeski, A., Melton, F., Johnson, L., Verdin, J. P. (2014). Seasonal cultivated and fallow cropland mapping using MODIS-based automated cropland classification algorithm. Journal of Applied Remote Sensing, 8, 17.

Xia, C., Li, J., Liu, Q., & Ieee. (2012). Monitoring vegetation phenology in China using time-series MODIS LAI data 2012 IEEE International Geoscience and Remote Sensing Symposium (pp. 48-51).

Xiao, W., Sun, Z., Wang, Q., & Yang, Y. (2013). Evaluating MODIS phenology product for rotating croplands through ground observations. Journal of Applied Remote Sensing, 7.

Xie, H., Tian, Y. Q., Granillo, J. A., & Keller, G. R. (2007). Suitable remote sensing method and data for mapping and measuring active crop fields. International Journal of Remote Sensing, 28(1-2), 395-411.

Xie, Y. & Kiniry J R. A (2002). Review on the Development of Crop Modelling and its Application. Acta Agronomica Sinica, 28(2), 190-195.

Yan, E. P., Wang, G. X., Lin, H., Xia, C. Z., & Sun, H. (2015). Phenology-based classification of vegetation cover types in Northeast China using MODIS NDVI and EVI time series. International Journal of Remote Sensing, 36(2), 489-512.

Yau, S. K., & Ryan, J. (2013). Differential impacts of climate variability on yields of rainfed barley and legumes in semi-arid Mediterranean conditions. Archives of Agronomy and Soil Science, 59(12), 1659-1674.

Yi, Y. H., Yang, D. W., Chen, D. Y., & Huang, J. F. (2007). Retrieving crop physiological parameters and assessing water deficiency using MODIS data during the winter wheat growing period. Canadian Journal of Remote Sensing, 33(3), 189-202.

You, X. Z., Meng, J. H., Zhang, M., & Dong, T. F. (2013). Remote Sensing Based Detection of Crop Phenology for Agricultural Zones in China Using a New Threshold Method. Remote Sensing, 5(7), 3190-3211.

Zakaria, S., Al-Ansari, N., & Knutsson, S. (2013). Historical and Future Climatic Change Scenarios for Temperature and Rainfall for Iraq. Journal of Civil Engineering and Architecture, 7(12).

Zhang, B., Di, L. P., Yu, G. N., Shao, Y. Z., Shrestha, R., Kang, L. J., & Ieee. (2013). A Web Service Based Application Serving Vegetation Condition Indices for Flood Crop Loss Assessment. 2013 Second International Conference on Agro-Geoinformatics (Agro-Geoinformatics), 214-219.

Zhang, F. & Wu, B, (2004). A Method for Extract Regional Crop Growth Information with Time Series of NDVI Data. Journal of Remote Sensing, 8(6), 515-528.

Zhang, M. W., Zhou, Q. B., Chen, Z. X., Liu, J., Zhou, Y., & Cai, C. F. (2008). Crop discrimination in Northern China with double cropping systems using Fourier analysis of time-series MODIS data. International Journal of Applied Earth Observation and Geoinformation, 10(4), 476-485.

Zhang, S., & Liu, L. (2014). The potential of the MERIS Terrestrial Chlorophyll Index for crop yield prediction. Remote Sensing Letters, 5(8), 733-742.

Zhang, X. Y., Friedl, M. A., Schaaf, C. B., & Strahler, A. H. (2004). Climate controls on vegetation phenological patterns in northern mid- and high latitudes inferred from MODIS data. Global Change Biology, 10(7), 1133-1145.

Zhang, X. Y., Friedl, M. A., Schaaf, C. B., & Strahler, A. H. (2004). Climate controls on vegetation phenological patterns in northern mid- and high latitudes inferred from MODIS data. Global Change Biology, 10(7), 1133-1145.

Zhang, X. Y., Friedl, M. A., Schaaf, C. B., Strahler, A. H., Hodges, J. C. F., Gao, F., Huete, A. (2003). Monitoring vegetation phenology using MODIS. Remote Sensing of Environment, 84(3), 471-475.

Zhang, X., Friedl, M. A., & Schaaf, C. B. (2006). Global vegetation phenology from Moderate Resolution Imaging Spectroradiometer (MODIS): evaluation of global patterns and comparison with in situ measurements. Journal of Geophysical Research-Part G-Biogeosciences, 111(G4), G04017-04011-04014.

Zhang, X., Hodges, J. C. F., Schaaf, C. B., Friedl, M. A., Strahler, A. H., & Feng, G. (2001). Global vegetation phenology from AVHRR and MODIS data. IGARSS 2001. Scanning the Present and Resolving the Future. Proceedings. IEEE 2001 International Geoscience and Remote Sensing Symposium (Cat. No.01CH37217), 2262-2264 vol.2265.

Zhao, T. B., & Dai, A. G. (2015). The Magnitude and Causes of Global Drought Changes in the Twenty-First Century under a Low-Moderate Emissions Scenario. Journal of Climate, 28(11), 4490-4512.

Zhao, Y. & Tang J. (2002). A Discussion on Growing State Survey and Yield Estimation of Paddy in Jiangsu Province by Means of Remote Sensing. Remote Sensing For Land & Resources, (53), 9 – 11.

Zheng, B. J., Myint, S. W., Thenkabail, P. S., & Aggarwal, R. M. (2015). A support vector machine to identify irrigated crop types using time-series Landsat NDVI data. International Journal of Applied Earth Observation and Geoinformation, 34, 103-112.

Zhong, L., Hawkins, T., Biging, G., & Gong, P. (2011). A phenology-based approach to map crop types in the San Joaquin Valley, California. International Journal of Remote Sensing, 32(22), 7777-7804.

Zhu, X. L., Chen, J., Gao, F., Chen, X. H., & Masek, J. G. (2010). An enhanced spatial and temporal adaptive reflectance fusion model for complex heterogeneous regions. Remote Sensing of Environment, 114(11), 2610-2623.

Zurita-Milla, R., Kaiser, G., Clevers, J. G. P. W., Schneider, W., & Schaepman, M. E. (2009). Downscaling time series of MERIS full resolution data to monitor vegetation seasonal dynamics. Remote Sensing of Environment, 113(9), 1874-1885.